nagra
National Cooperative for
the Disposal of Radioactive Waste

TECHNICAL REPORT 90-09

TRANSMISSIVITIES AND HEADS DERIVED FROM DETAILED ANALYSIS OF SIBLINGEN 1989 FLUID LOGGING DATA

V.A. KELLEY [1)]
J.M. LAVANCHY [2)]
S. LÖW [2)]

DECEMBER 1991

Untergruppe für IN-SITU-Versuche (UGIV)
Gruppe für Hydrodynamische Modellierung (GHM)

[1)] INTERA Inc., Austin, Texas
[2)] Colenco Power Consulting LTD, Baden

Hardstrasse 73, CH-5430 Wettingen/Switzerland, Telephone + 41-56-37 11 11

nagra National Cooperative for the Disposal of Radioactive Waste

TECHNICAL REPORT 90-09

TRANSMISSIVITIES AND HEADS DERIVED FROM DETAILED ANALYSIS OF SIBLINGEN 1989 FLUID LOGGING DATA

V.A. KELLEY [1)]
J.M. LAVANCHY [2)]
S. LÖW [2)]

DECEMBER 1991

Untergruppe für IN-SITU-Versuche (UGIV)
Gruppe für Hydrodynamische Modellierung (GHM)

[1)] INTERA Inc., Austin, Texas
[2)] Colenco Power Consulting LTD, Baden

Hardstrasse 73, CH-5430 Wettingen/Switzerland, Telephone + 41-56-37 11 11

This report was prepared as an account of work sponsored by Nagra. The viewpoints presented and conclusions reached are those of the author(s) and do not necessarily represent those of Nagra.

ZUSAMMENFASSUNG

Die Tiefbohrung Siblingen wurde durch die Nationale Genossenschaft für die Lagerung radioaktiver Abfälle (NAGRA) abgeteuft, um die hydraulischen Eigenschaften des Grundgebirges in der Nordschweiz zu beschreiben und dessen Eignung für die sichere Endlagerung hochaktiver Abfälle zu beurteilen. Der kristalline Abschnitt der Tiefbohrung wurde mit umfassenden hydraulischen Packertests und mit geophysikalischen Methoden untersucht. Zusätzlich wurde das Bohrprofil im Abschnitt zwischen 490 m und 1522 m unter Terrain mit neuentwickelten Fluid Logging Techniken getestet.

Die in Siblingen angewandten Fluid Logging Methoden umfassten das Spinner Flowmeter (SF), das Spinner-Packer Flowmeter (SPF), das Heat-Pulse-Packer-Flowmeter (HPPF) sowie Temperatur- und elektrische Leitfähigkeitsmessungen (T/LF). Der vorliegende Bericht beschreibt die detaillierte Analyse dieser verschiedenen Fluid Logging Methoden. Die Analyse ermöglicht die quantitative Bestimmung der einzelnen diskreten Zuflüsse zum Bohrloch unter statischen und gepumpten Bedingungen. Ausserdem ermöglicht die elektrische Leitfähigkeitsmessung Zonen mit Zuströmung exakt zu lokalisieren. Mit klassischen Hydraulikgesetzen können diese Messungen zur Bestimmung der Transmissivitäten und in besonderen Fällen zur Erfassung der hydraulischen Potentialen herangezogen werden. Diese Berechnungen wurden für alle geeigneten Datensätze durchgeführt. Vorgängig zur Auswertung der einzelnen Fluidlogging Datensätze werden die entsprechenden Test-und Analysenmethoden diskutiert.

Ein Vergleich zwischen den verschiedenen Testmethoden wurde mittels einer Zusammenstellung der Resultate (Transmissivitäten, hydraulische Potentiale) vorgenommen. Ebenfalls wurden die Resultate aus dem Fluid Logging mit denjenigen aus den hydraulischen Tests verglichen. Im allgemeinen werden die Transmissivitäten mit den Fluid Logging Techniken und den hydraulischen Tests gleich geschätzt. Für die vorherrschenden Bedingungen in Siblingen waren die elektrische Leitfähigkeitsmessmethode und die Heat-Pulse-Packer-Flowmeter Methode die zwei genauesten Fluid Logging Methoden. Das Fluid Logging ergab hydraulische Potentiale, welche mit denjenigen aus den hydraulischen Tests nicht völlig übereinstimmten, jedoch innerhalb der Variationsbreite der Beobachtungen lagen.

Die Anwendung der Fluid Logging Methoden zur Beschreibung des kristallinen Gesteins in Siblingen war für die Bestimmung der bedeutensten Transmissivitätszonen (definiert als Zonen mit einer Transmissivität grösser als 10^{-9}m/s) sehr erfolgreich . Zudem konnten mit Hilfe dieser Methoden 13 individuelle Fliesszonen innerhalb des Unteren Kristallins (1'000 bis 1'522 m unter Terrain) mit einer Genauigkeit von ±1 m identifiziert werden. Die Fluid Logging Methoden stellen eine konkurrenzfähige Untersuchungsmethode gegenüber den hydraulischen Packertests dar. Sie erlauben eine Minderung der Packertestanzahl. Ausserdem ermöglichen die elektrische Leitfähigkeitsmessungen, den gemessenen Transmissivitäten diskrete Zuflussstellen zuzuordnen.

RÉSUMÉ

Le forage de Siblingen a été effectué par la Société coopérative nationale pour l'entreposage de déchets radioactifs afin de déterminer les caractéristiques hydrauliques du socle (Cédra) dans le nord de la Suisse, dans la perspective d'un stockage sûr des déchets hautement radioactifs. Dans le forage de Siblingen, le socle cristallin a été étudié par de nombreux tests hydrauliques entre obturateurs et par des méthodes géophysiques. De plus, la section comprise entre 490 et 1522 m de profondeur a été étudiée à l'aide de nouvelles techniques d'analyse par diagraphie de fluide.

Les méthodes de diagraphie de fluide utilisées à Siblingen sont le débitmètre à moulinet simple SF (Spinner Flowmeter), le débitmètre à moulinet avec obturateur SPF (Spinner-Packer Flowmeter), le débitmètre a impulsion thermique avec obturateur HPPF (Heat-Pulse-Packer Flowmeter) et les logs combinés de conductivité électrique et de température (T/LF). Ce rapport présente les résultats détaillés des analyses de ces différentes méthodes indirectes. En premier lieu, ces méthodes permettent de déterminer les flux verticaux présents dans le forage en fonction de la profondeur. En outre le profil de conductivité électrique et de température permet la localisation individuelle des zones productives. Ces données sont ensuite analysées à l'aide d'équations hydrauliques fondamentales afin de déterminer les valeurs de transmissivité et de charge hydraulique des zones productives. Ces analyses ont été effectuées pour toutes les diagraphies adéquates. Chaque étape de l'analyse a été précédée d'une description complète de la méthode utilisée.

Un résumé des résultats obtenus (transmissivité et charge hydraulique) permet de comparer les différentes méthodes de diagraphie utilisées. Les résultats des méthodes de diagraphie sont ensuite comparées à ceux des essais hydrauliques entre obturateurs. En général les diagraphies ont reproduit les valeurs de transmissivités determinées par essais hydrauliques avec des écarts inférieurs à un facteur 2. Les deux méthodes les plus performantes pour les conditions rencontrées dans le forage de Siblingen ont été la diagraphie de conductivité électrique et le débitmètre à impulsion thermique avec obturateur. Les méthodes de diagraphie n'ont pu reproduire avec exactitude les valeurs de charge hydraulique déterminées par les essais hydrauliques. Cependant les résultats se situent dans le domaine de variation des résultats obtenus par les essais hydrauliques.

L'utilisation des méthodes de diagraphie pour la caractérisation du socle cristallin a permis de définir avec satisfaction les principales zones perméables dans le forage de Siblingen (zones définies comme des formations ayant une transmissivité supérieure à 1E-9 m^2/s). De plus ces méthodes ont permis la localisation, avec une précision de ± 1 m, de 13 zones productives différentes dans la section inférieur du cristallin (1000 à 1522 m). Les méthodes de diagraphie des fluides représentent une excellente alternative aux essais hydrauliques et permettent d'en optimiser l'usage. Enfin, la diagraphie de conductivité électrique permet d'identifier l' intervalle précis correspondant à chaque transmissivité calculée.

SUMMARY

The Siblingen borehole was drilled by the Swiss National Cooperative for Radioactive Waste Disposal (NAGRA) to hydraulically characterize granitic basement rocks of northern Switzerland for their potential for the safe storage of high-level radioactive waste. The Siblingen crystalline section of the borehole was tested with an extensive set of hydraulic packer tests and geophysical methods. In addition, the borehole was tested from the interval 525 to 1522 m below ground (b.g.) with non-standard fluid logging techniques.

The fluid logging methods used in Siblingen were the spinner flowmeter (SF), the spinner-packer flowmeter (SPF), the heat-pulse packer flowmeter (HPPF), and temperature and electrical conductivity logging (T/LF). This report presents the detailed analysis of these various fluid logging methods. The result from each fluid logging method is the estimation of the borehole volumetric flow rate as a function of depth. In addition, through electrical conductivity logging discrete isolation of inflowing features is possible. Through fundamental hydraulic analysis these measurements can be used to estimate interval transmissivity and in certain cases interval head. These calculations were performed for all suitable logs. A complete description of analysis methods is included prior to each step of analysis.

A comparison between the various fluid logging methods is made through a review of the analysis results (transmissivities and heads). A comparison between the transmissivities and heads calculated by fluid logging and measured by hydraulic tests is made. In general the fluid logging techniques predicted transmissivity to within a factor of two when compared to hydraulic tests. The two most accurate fluid logging methods, as defined by hydraulic tests, were conductivity logging and the heat-pulse packer flowmeter for the conditions prevailing in Siblingen during testing. The fluid logging methods gave head estimates which were not in strict agreement with hydraulic test results but are within the variation in observed measurements.

The application of fluid logging methods for the characterization of the Siblingen crystalline has been successful in determination of major transmissive areas (defined as rock having a transmissivity greater than 1E-9 m^2/s). In addition, these methods have identified (to within ± 1 m) 13 individual inflow regions within the lower crystalline (1000 to 1522 m b.g.). Fluid logging methods represent a compatible borehole testing method to hydraulic packer tests in allowing for a focused use of hydraulic packer tests. In addition, conductivity logging can be used to attribute discrete intervals to transmissivity measurements.

TABLE OF CONTENTS

TABLE OF CONTENTS (continued

TABLE OF CONTENTS (continued)

TABLE OF CONTENTS

LIST OF TABLES

LIST OF TABLES (continued)

LIST OF TABLES (continued)

LIST OF FIGURES

LIST OF FIGURES (continued)

LIST OF FIGURES (continued)

LIST OF FIGURES (continued)

1 INTRODUCTION

1.1 Background Information

In fractured rocks of low primary porosity, the bulk of the water flux occurs in discrete fractures or shear zones. The characterization of such media for transport potential requires a conceptual fracture framework from which appropriate models can be proposed. This requires not only an estimate of transmissivity but also discrete fracture locations, and if possible some knowledge of fracture geometry. Determining the exact location of the most transmissive fractures in a crystalline rock from standard geophysical logs and cores is far from trivial. PAILLET et al. (1987) found that highly transmissive fractures did not differ from significantly less transmissive fractures when evaluated by televiewer and resistivity logs. Standard packer hydraulic tests can provide a vertical distribution of transmissivity, but attributing discrete features to the transmissivity is indirect and resolution is limited to the packer separation. In addition, these methods are time- and budget-intensive.

Fluid logging techniques offer a less expensive way to characterize fractured, or non-fractured media (HUFSCHMIED, 1983; REHFELDT et al., 1989; MOLZ et al., 1989; and TSANG et al., 1990). Fluid logging techniques can be very useful in fractured media in the localization of the fractures which make up the bulk of the interval transmissivity. In addition, fluid logging techniques offer an alternative method for the determination of fracture transmissivity.

The Swiss National Cooperative for Radioactive Waste Disposal (NAGRA, Nationale Genossenschaft fuer die Lagerung Radioaktiver Abfaelle) has committed significant energy in the application and development of fluid logging methods for the location and quantification of permeable features in a deep borehole completed in crystalline rocks. NAGRA has consciously and strategically incorporated fluid logging into their deep crystalline borehole characterization program. NAGRA recognizes that fluid logging methods do not replace hydraulic packer tests but instead offer a means to optimize and economize their use. Fluid logging can identify important features in the borehole and allow for the design of a focused packer test campaign. Fluid logging methods also allow for an independent estimation of transmissivity.

The Siblingen borehole is located at coordinates 680'090.2/286'693.7 in northern Switzerland (Figure 1.1) and was drilled to characterize granitic basement rocks for their potential as a radioactive waste repository host medium. The borehole was drilled beginning on September 2, 1988 and ending on April 2, 1989 at a total apparent depth of 1522 m b.g. (below ground). The ground surface is 574.35 m a.s.l. The true vertical depth of the borehole is 1502.5 m b.g. The borehole is cased to the apparent depth of 490.5 m b.g. and from this depth the borehole is open hole with a diameter of 96 mm. Two sections were cemented during the drilling phase, from 490.5 to 536 m and from 668.0 to 850.6 m. A schematic of the borehole geometry and the borehole lithology can be found in Figure 1.2.

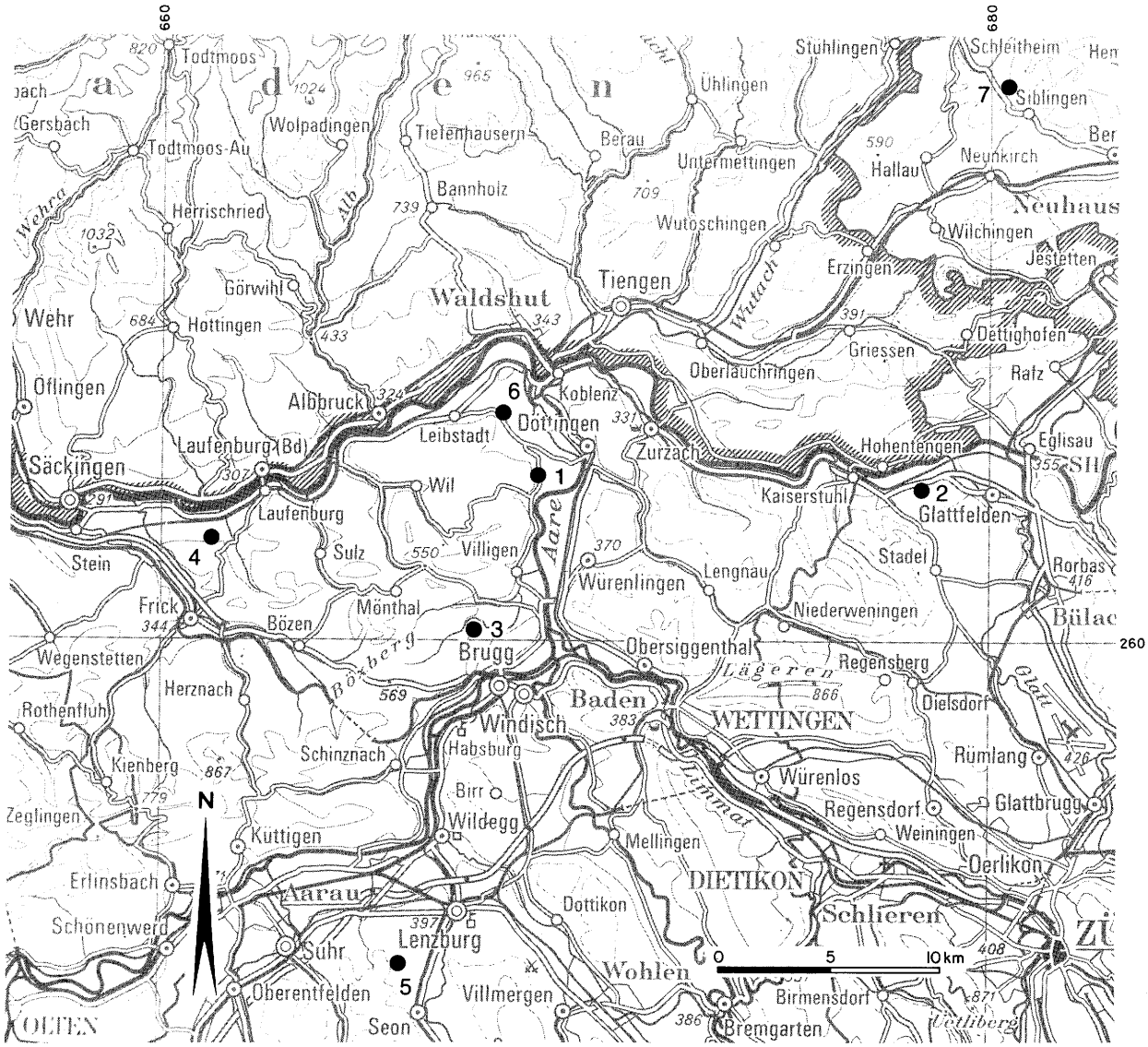

	BOREHOLE	DEPTH
1	Böttstein	1501 m
2	Weiach	2482 m
3	Riniken	1801 m
4	Kaisten	1306 m
5	Schafisheim	2006 m
6	Leuggern	1689 m
7	**Siblingen**	**1522 m**

Figure 1.1: Location of NAGRA Deep Boreholes in Northern Switzerland

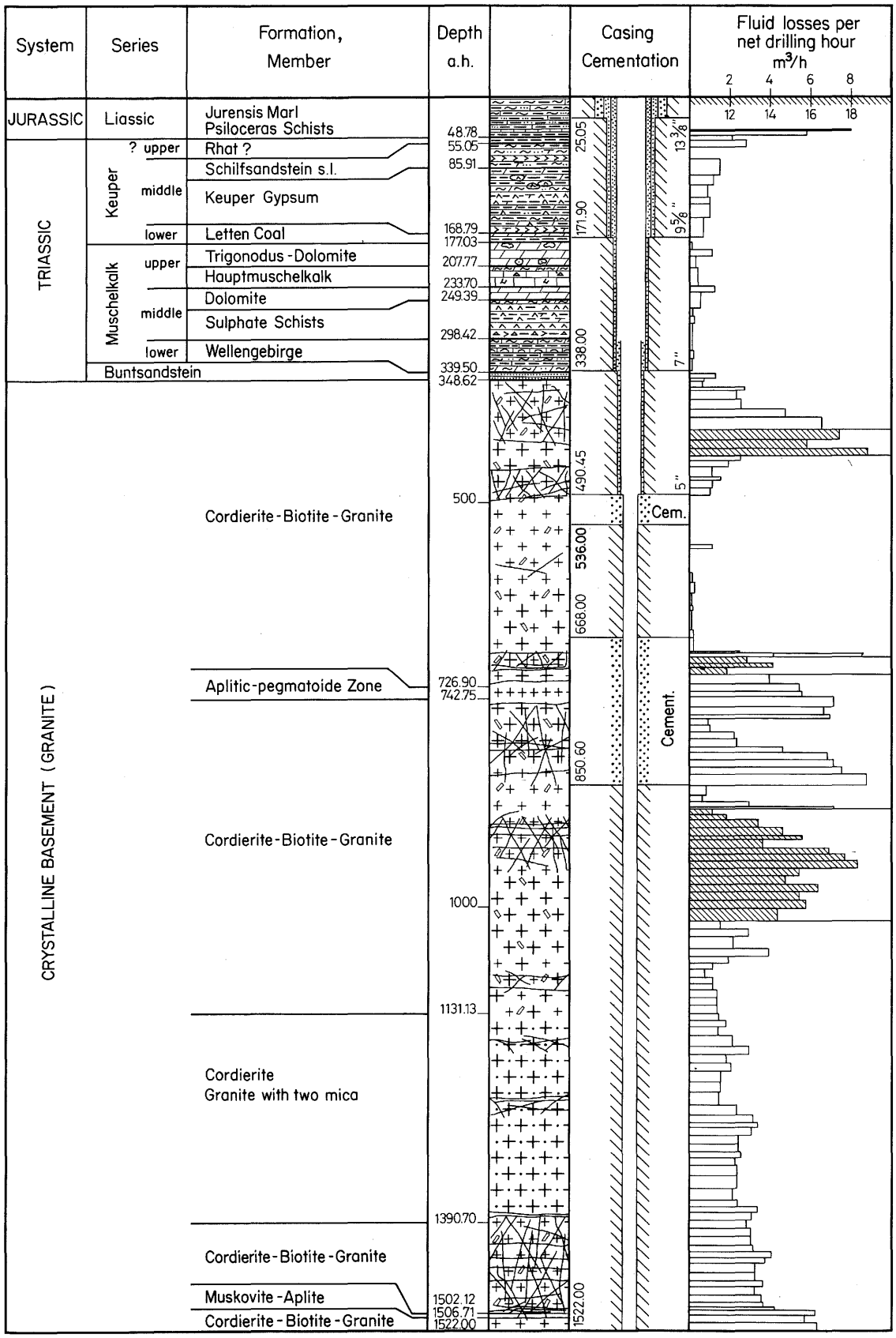

Figure 1.2: Siblingen Borehole Characteristics (from Ostrowski & Kloska, 1990)

In the Siblingen borehole, NAGRA has characterized the crystalline section of the borehole through traditional packer tests (OSTROWSKI and KLOSKA, 1990), several geophysical methods (SATTEL and BLUMLING, 1989), and through several fluid logging methods (GEOTEST/GEMAG, 1989 and PAILLET et al., 1990).

Fluid logging and packer tests were performed in the Siblingen borehole both during drilling operations and after drilling during the designated *Test Phase.* In addition, the heat pulse packer flowmeter was experimentally applied after the *Test Phase.* The fluid logging methods employed in Siblingen were the spinner flowmeter (SF), the spinner packer flowmeter (SPF), the heat-pulse packer flowmeter (HPPF), and temperature and electrical conductivity logging (T/LF). The governing principle behind all of the fluid logging methods employed in the Siblingen borehole consists of determining, either directly or indirectly, the borehole fluid velocity as a function of depth and time in response to production or injection. The methods can be broadly divided into direct and indirect methods. Direct methods include the spinner flowmeters and the heat-pulse flowmeters. They are classified as direct methods because they record as raw data a response signal which is directly related to the borehole velocity (flow rate). Temperature and electrical conductivity logging is classified as indirect because borehole fluid velocity must be derived from the raw data and multiple logs must be run.

The activities for both the flowmeter logging and the conductivity logging will be covered in detail in the analysis sections, Sections 2 and 3 respectively. For purposes of introduction Table 1.1 summarizes the fluid logging events performed in the Siblingen borehole during the drilling and testing phases. All flowmeter logging events are designated FL with a number representing chronology of testing. The electrical conductivity logging events are listed chronologically and are designated SF, OH-RW, and PIP-RW, followed by a number. These labels represent static fluid logging, open hole constant rate withdrawal, and production-injection packer constant rate withdrawal events, respectively. The term *static* is used in the context that the borehole has no external stresses (production or injection) put on it. This does not imply that borehole conditions are hydrostatic. All depth measurements are measured in the borehole in meters below ground surface (hereafter m b.g.) making all depths apparent. The reference point is the ground surface at an elevation of 574.35 m above seal level (hereafter m a.s.l.). The first two flowmeter campaigns were performed during the drilling phase because of severe fluid losses and the need to characterize these zones before plugging. All flowmeter measurements have one static run followed by at least one run measured under injection conditions. The heat-pulse flowmeter was applied experimentally at Siblingen to assess its applicability and to compare the results with other proven fluid logging techniques and packer hydraulic tests. These measurements were performed by the U.S. Geological Survey (USGS) and documentation of the raw data and an interpretation report can be found in PAILLET et al. (1990). The electrical conductivity logging was aimed primarily at characterizing the borehole from 1000 to 1522 m b.g. There were five separate analyzable events, including two static measurements, one open-hole constant-rate withdrawal measurement, and two constant-rate withdrawal events where the zone 1000 to 1522 m b.g. was isolated by a production-injection packer (PIP).

Table 1.1: Summary of Fluid Logging Events Performed in Siblingen and Analyzed in this Report

EVENT	LOGGING METHOD	DATE (1989)	INTERVAL (m b.g.)	TESTING CONDITION
FL1	SPF	Dec. 20/21 (1988)	490.9 - 50.6	• Static • Injection 21.5 l/min
FL2	SF	Jan. 23/24	490.9 - 1017.8	• Static • Injection 51 l/min
FL3	SPF	April 5/7	490.9 - 1522	• Static • Injection 80 l/min
SF1	T/LF	April 15	900 - 1522	• Static
SF2	T/LF	April 16	900 - 1522	• Static
OH-RW1	T/LF	April 16/17	850 - 1522	• Open-hole production 32 l/min
PIP-RW1	T/LF	April 18/21	1000 - 1522	• PIP production 3 l/min
PIP-RW2	T/LF	April 23/25	1000 - 1522	• PIP production 1.5 l/min
FL4	HPPF	June 6/8	490.0 - 1522	• Static • Injection 8 l/min • Injection 57 l/min

1.2 Summary of Hydraulic Packer Tests

A full suite of double- and single-packer tests was performed in the Siblingen borehole. OSTROWSKI and KLOSKA (1990) report a complete interpretation of these tests and the hydraulic parameters derived. Because this report will ultimately compare the fluid logging transmissivity distribution with the transmissivities derived from hydraulic tests, a summary of the hydraulic test results is included in Table 1.2. Again, all depths are apparent and measured within the borehole. From a review of Table 1.2, it can be said that transmissivity generally decreases as a function of depth. The range of transmissivities within the crystalline section of the Siblingen borehole is greater than four orders of magnitude. Heads in the borehole also have a trend of magnitude decreasing with depth. With some exceptions, heads measured during the *testing phase* in the crystalline from 442 to 1000 m b.g. are approximately 441 to 442 m a.s.l., which is consistent with water levels taken after the drilling and testing phase during long-term monitoring, i.e., around 441.8 m a.s.l. (VOMVORIS et al., 1989). In the lower 500 m of the borehole, heads tend to decrease to a minimum measured of 436 m a.s.l.

Table 1.2: Selected Summary of Hydraulic Parameter Tests Performed in the Crystalline of the Siblingen Borehole (after OSTROWSKI and KLOSKA, 1990)

TEST	INTERVAL TOP (m b.g.)	INTERVAL BOTTOM (m b.g.)	FRESHWATER HEAD (m a.s.l.)	TRANSMISSIVITY X 10^{-7} (m^2/sec)
CR3	442.4	490.9	442	48.5 - 97.0
CR7	505.3	686.1	438	110.3
CR8	564.3	686.1	439	95.0
CR9	651.7	686.1	439	110.1
CR10	678.0	712.9	440	2094 - 3839
CR11	717.4	767.3	442	59.9
CR13	841.0	850.6	443	89.3
CR16	924.5	1017.8	441	475.8
CR17	856.8	1017.8	441	193.2 - 418.6
CR18	1154.0	1163.9	439	1.3
CR20	1062.0	1270.3	441	22.9
CR22	490.9	1061.0	442	119.7
CR24	1270.3	1522.0	437	6.8 - 9.3
CR25	1392.0	1426.3	436	0.65
CR26	1358.0	1392.0	436	2.8
CR27	1222.0	1256.3	437	3.4 - 4.8
CR28	1056.0	1090.3	440	8.6 - 13.4

1.3 Report Objectives and Report Organization

The primary objective of this report is to present a final interpretation of all the fluid logging events which were performed to characterize the crystalline section of the Siblingen borehole. This analysis will yield a vertical transmissivity distribution for the Siblingen borehole which will augment standard hydraulic packer tests. In addition, the discrete location of the features which significantly contribute to the crystalline transmissivity can be determined for portions of the borehole logged by conductivity methods. The vertical distribution of transmissivity determined through the analysis of each fluid logging event and a comparison between these results will be presented. This report also allows for a comparison between the various fluid logging methods employed and a comparison to the transmissivity distribution determined from packer tests.

Sections 2 and 3 are interpretation chapters for all fluid logging events. Section 2 is the interpretation of the flowmeter measurements and Section 3 presents the interpretation of the electrical conductivity measurements. The fundamental result from these analyses is borehole flow rate as a function of depth. Measurement of internal open borehole flow rates (flow rates from one part of the borehole to another) was performed by all fluid logging methods employed in Siblingen.

Section 4 presents a comparison between the various fluid logging methods and the internal open borehole flow rates measured by each. Section 5 presents the methodology by which transmissivities were calculated from flow rates determined from fluid logging and lists assumptions for these calculations. In Section 5, the vertical transmissivity distribution derived for each logging event is presented. The last part of Section 5 compares the transmissivity distributions derived from each fluid logging method. Section 6 presents the calculation of hydraulic heads from the various fluid logging methods. Finally, in Section 7, the transmissivity and head distributions derived from fluid logging are compared to the results from hydraulic testing. Section 8 presents the study conclusions along with a summary on the performance of the various fluid logging methods at the Siblingen borehole.

2 FLOWMETER MEASUREMENTS

2.1 Field Activities

2.1.1 Summary of Field Activities

Four flowmeter logging campaigns were performed from December 1988 to June 1989 (see Table 1.1). The test objectives were to detect and characterize hydraulically flowing fractures during the drilling phase (December and January) and during the testing phase (April). In addition, after the completion of the testing phase, test tool evaluation for the heat pulse flow meter was accomplished (June 1989). A detailed description of the field data collection is provided in GEOTEST/GEMAG (1989) and PAILLET et al. (1990).

The flowmeter logging campaign of December 20 to 21, 1988 was conducted in the section between the casing shoe (at 490.9 m b.g.) and the bottom of the hole (850.6 m b.g.). This campaign was not foreseen initially but had to be performed because of the unexpected presence of very transmissive zones in the upper part of the crystalline. For technical reasons, this section, which had been partly plugged already (i.e. from the casing shoe down to 686.1 m b.g.), had to be plugged again (down to 850.6 m), before continuing the drilling, and therefore it was of primary importance to test this section before starting the plugging operations. Two flowmeter logs were conducted with the prototype (not yet tested) spinner packer flowmeter (SPF). The first log was obtained under static conditions and the second one during injection at a rate of 21.5 l/min. A total of 16 measurements were successfully collected below the casing shoe at 9 depth stations before encountering technical problems. A leakage at the engine of the pump ultimately prevented the inflation of the packer, which led to the decision to stop the logging.

The second flowmeter logging campaign was conducted from January 23 to 24, 1989 prior to another borehole plugging operation down to 1017.8 m. In addition of the first plugging already conducted down to 850.6 m bg., sections 490.3 (casing shoe) to 536.3 m and from 668 to 850 m b.g. had even been cemented in order to reduce the fluid losses during drilling. The same problems that were encountered in December again prevented the use of the spinner packer flowmeter. It was decided to conduct trolling spinner flowmeter (SF) measurements instead of the stationary packer flowmeter measurements. Two logs were performed continuously from the casing shoe (490.9 m b.g.) to the bottom of the borehole (at this time 1017.8 m b.g.) and then upwards. One log was run under static conditions and the second one with an injection rate of about 51 l/min.

The flowmeter log campaign of April 5 to 7, 1989, was conducted from 180 m b.g. (within the casing) to the total depth of the borehole at 1522 m b.g. A total of 22 measurements were successfully collected at 14 depth stations below the casing shoe (490 m b.g.) and the upper plugged section (~526 m b.g.) using the spinner packer flowmeter method (SPF). Again technical problems occurred, leading first to use of the backup packer flowmeter and then, when it also failed, to stopping the flowmeter logs. The successful logging runs were conducted first under static conditions and then with an injection of about 80 l/min.

The fourth flowmeter log campaign was conducted from June 6 to 8, 1989, in order to evaluate the heat pulse packer flowmeter (HPPF) recently built and tested by the U.S. Geological Survey. Three logs were performed. The first log was obtained under static conditions, the second with an injection rate of 8 l/min, and the last with an injection rate of 57 l/min. Sixty-four measurements were collected at 35 particular depths.

2.1.2 Spinner Flowmeter Technique (SF)

The flowmeter tool allows direct measurement of the vertical flow rate occurring within a borehole. The measured parameter is the speed of rotation of an impeller, which is proportional to the vertical speed of the flux. In the case of Siblingen, the flowmeter was used in January for dynamic measurements. Besides the speed and continuous data capture of the method, an advantage of the moving flowmeter technique is that the impeller is already activated by the movement of the tool, which lowers the sensitivity threshold. The disadvantage is that it is difficult to maintain a constant speed of the probe. Furthermore, the measurement of the vertical flux is dependent on the well diameter. Thus, irregularities along the wall of the borehole will cause variations in the measured flux.

The flowmeter was calibrated at the GEOTEST laboratory in a tubing of 96 mm, the same diameter as the Siblingen borehole. Calibration was performed with fluxes between 3.6 and 120 l/min, oriented upwards and downwards, and for particular temperatures ranging from 10 to 45 °C. The calibration results are presented in GEOTEST/GEMAG (1989) in the form of equations providing the conversion from the measured speed of rotation of the impeller to the derived vertical flow rate. The flowmeter's sensitivity threshold for a diameter of 96 mm is about 3 l/min.

2.1.3 Spinner Packer Flowmeter Technique (SPF)

The packer flowmeter represents a further development of the flowmeter concept initiated by NAGRA for the field campaign at Siblingen. The two advantages of this tool are to reduce the sensitivity threshold and to eliminate the dependence of the measurement on the borehole diameter. When the probe is located at a selected depth, the packer is inflated by injecting borehole fluid into the packer element with a small pump. This channels the borehole vertical flux through an internal pipe of defined diameter. As for the flowmeter presented above, the packer flowmeter determines the vertical flow rate by measuring the speed of rotation of the impeller. This tool was calibrated by GEOTEST in the same conditions that were used for the flowmeter. The sensitivity threshold of the packer flowmeter is about 0.3 to 0.4 l/min.

2.1.4 Heat Pulse Packer Flowmeter Technique (HPPF)

This tool differs from the packer flowmeter described above in that, rather than measuring the rotation of an impeller, it measures the time taken for a heat pulse to travel from a heater grid to temperature sensors. The reciprocal travel time is a direct function of the flow velocity. The heat pulse packer flowmeter used was developed and calibrated by the U.S. Geological Survey and allows the

determination of upward and downward fluxes down to 0.1 to 0.05 l/min.

2.2 Flowmeter Method Analysis

The basic concept behind the flowmeter method is that, if one assumes horizontal laminar (Darcy) flow from particular layers to a well, the flux from each layer is proportional in particular to the product of layer hydraulic conductivity and layer thickness, and to the head difference between the formation and the borehole.

By measuring the variation of the vertical flow velocity during pumping or injection, one can identify flowing zones along a borehole and quantify the radial flow rate from each of these zones. In the case of the packer flowmeter, a permeable feature is defined by two stations showing significant variations of the vertical flow rate. The choice of the stations can be guided initially by the results of other logs (moving flowmeter, temperature, or electrical conductivity logs) and are then adapted continuously to focus on the effective flowing features. The measurements are collected during multiple logging runs (minimum of two), the first under static conditions in the borehole (natural flows), and the remainder during injection or pumping. Knowing for each layer the radial flow rate occurring during the different logs and the borehole head variations induced by injection or pumping, one can then calculate layer transmissivity and head.

The flowmeter logs conducted at Siblingen were analyzed with the code KPFLOW. Initially developed by Dr. P. Hufschmied to analyze and interpret flowmeter measurements in shallow boreholes (HUFSCHMIED, 1983, and REHFELDT et al., 1988), the program was modified and adapted to allow the interpretation of flowmeter and packer flowmeter measurements performed in deep boreholes (LAVANCHY and THOMPSON, in preparation).

The theory behind the code is quite general. Assuming the flow to the well is horizontal, a simple equation derived from the Cooper-Jacob approximation is used to calculate the hydraulic conductivity of each layer identified by the measurements. The hydraulic conductivity is calculated iteratively by solving the equation using data collected during the static run and during injection (or pumping). The formation head can be back-calculated from the determination of the hydraulic conductivity, using the flux measured under static conditions in the borehole (i.e., before injecting).

Among other capabilities, the modified version of KPFLOW can accomplish or consider:

- analysis of data from deep boreholes in low permeability media;
- a complex calibration file;
- an external caliper log file;

- analysis of data from stationary (with or without packer) and trolling flowmeters;
- calculation of head losses due to friction;
- statistical processing to determine statistical significance of flowmeter readings;
- propagation of uncertainty in flowmeter measurements on the calculated hydraulic conductivities; and
- analysis of flowmeter measurements taken during injection and pumping periods.

The aim of the statistical significance test is to decide whether or not a given flowmeter measurement is statistically different from the adjacent measurements. This is performed by providing in the input file the mean and the variance of the measured value at each station of reading. The values that are not significantly different are then corrected either to the value at the adjacent station or to an interpolated value using the measurements at the two adjacent stations.

The study of the propagation of the measurement uncertainties is very useful because it allows to report these uncertainties, under the form of the variance for each mean value, on the calculated hydraulic conductivity. The results are provided in the form of a table indicating for each layer the extreme, within 95 % of confidence, and the mean values of the hydraulic conductivity.

Some basic assumptions used in KPFLOW for the analysis of flowmeter data are summarized below.

- The code considers transient conditions but assumes that all the measurements for the same run were collected in the same time.
- The pressure change induced by the injection or the pumping is assumed to be the same at a given time all along the borehole. No pressure disturbance due to temperature density changes can be considered.
- The storage coefficient considered in the analysis corresponds to the lenght of total logged section. This value is then combined with the total section transmissivity, which assumes that the diffusivity ratio is the same for all layers (i.e. T/S = constant).
- The potential pre-test borehole pressure history is not taken into account. The radial flow rate determined during the logging run under static conditions is assumed to reflect the undisturbed layer head.

- To calculate the layer undisturbed head, KPFLOW assumes, for the transient analysis, a time equivalent to the period of pumping.

2.3 SPF Campaign FL1, December 20 to 21, 1988

2.3.1 Test events

The drilling was interrupted on December 19, 1988, at a depth of 850.6 m b.g. after having detected significant fluid losses in the well. Caliper and temperature/ conductivity logs were first conducted in the borehole until 16:00 on December 20. The packer flowmeter logs were then initiated in order to locate the zones where the major fluid losses occurred and to estimate the hydraulic characteristics of these permeable features. A total of about 20 hours was allowed after drilling for the water level to recover before starting the flowmeter measurements below the casing. When starting the tests, the depth to the water level corresponded to an elevation of 442.4 m a.s.l.

The first log, the reference Run 1 under static conditions, started at 16:00 on December 20 and was completed at 03:00 on December 21. A total of 12 packer flowmeter measurements were collected between 250 and 840 m b.g. During this run, the water level wsa situated at 132 m b.g.

The injection of around 21.5 l/min of cold water (about 7°C) started at 03:20 (December 21, 1988) and the water level was estimated to approach steady state conditions, at a depth of 118 m b.g., after 1.0 hours.

The second log, Run 2, started at 04:30 and had to be interrupted at 08:50 due to a leakage at the pump preventing the inflation of the packer. A total of 9 packer flowmeter measurements were collected at depths ranging from 182 to 840 m b.g. prior to pump failure.

A third log, Run 3, using an injection rate of 33.5 l/min was attempted in the afternoon, but had to be abandoned at the second measurement because of leakage that occurred in the backup packer flowmeter.

2.3.2 Model Assumptions

The static water level was determined from the first logging run to be at 132 m b.g. This is the depth where the impeller of the flowmeter first started to rotate in water. The measurements using the electrical tape were fairly uncertain, ranging from 134 to 138 m b.g., and were not taken into account. The other way to determine the water level is to use the pressure transducer of the packer flowmeter. Table 2.1 presents the measured pressures and the derived depths to water obtained at each station of flowmeter reading (assuming a constant density of the fluid column above the transducer). Although the results are affected by the precision of the transducer, one can note that the water level increased slightly

during Run 2. Before the Run 2 logging started at about 04:30, the water level was measured at about 132.0 m b.g. By 09:45, the water level had increased to 117.5 m b.g. However, the most important borehole section was logged between about 07:00 and 08:30 (675 to 840 m b.g.). During this period, the depth to water was around 118 m b.g. This corresponds to an increase in the water level of 14.0 m between Run 1 and Run 2.

Table 2.1: Measured Pressures and Calculated Depths to Water Level (Runs 1 and 2, December 1987)

STATION (m b.g.)	RUN 1		RUN 2	
	PRESSURE (bar)	DEPTH TO WATER LEVEL (m b.g.)	PRESSURE (bar)	DEPTH TO WATER LEVEL (m b.g.)
131.9	1.28	out of water		
182.0	6.02	133.5	6.77	125.9
350.0	22.51	133.2	-----	-----
480.0	35.51	132.4	36.20	123.2
525.0	39.73	132.3	40.79	121.4
575.0	44.65	132.0	45.85	119.8
625.0	49.53	132.2	-----	-----
675.0	54.43	132.1	55.72	118.9
698.0	56.70	131.9	-----	-----
725.0	59.37	131.7	60.69	118.2
775.0	64.25	131.8	65.61	117.9
825.0	69.09	132.4	70.50	118.0
840.0	75.01 (?)	86.9 (?)	72.02	117.5
182.0	6.08	133.0	7.77	115.7

For this campaign, the packer flowmeter had been set up for fluxes up to 20 l/min. The measurements collected during log 2 between 182 m b.g. (in the casing) and 675 m b.g. concern a zone where no significant flow occurs into the formation. For this section the measurements are very close to the upper limit of the calibration and may be affect by errors (see Table 2.2). As a consequence, for in the analyses, all these values have been set to 21.5 l/min which is the rate of injection measured at surface.

The calibration performed later in laboratory showed that the temperature of the water is a factor influencing the speed of rotation of the spinner. GEOTEST/ GEMAG (1989) reports calibration equations valid at given temperatures to convert the speed of rotation to a derived flow rate. However the calibration file that is used for the conversion in KPFLOW can not take into account the temperature

changes along the borehole and thus the equations chosen for the analysis of this test correspond to the calibration for water of around 30°C, which is the average temperature measured during logging. As the change in pressure between the two logs was directly measured with the pressure sensor at each station of flowmeter reading, injecting cold water did not present an obstacle for the interpretation.

In the calculations, KPFLOW considers an unique value of storage coefficient, which corresponds to the total length of the logged section (see explanations in section 2.2). A value of 2.6E-6 was estimated according to the results provided by the hydrotests (OSTROWSKI and KLOSKA, 1990).

2.3.3 Test Results

As presented in Table 2.2, a significant inflow zone (into the borehole) was detected during Run 1 between 675 and 725 m b.g., inducing a vertical, downward, flow rate of about 1.6 l/min at 725 m b.g. Further down, the main outflow must occur between 840 and 850.6 m b.g. (bottom of borehole). From the statistical check, all the vertical fluxes were determined to be significantly different from the others. Thus, no corrections had to be made to the measured values.

As presented in Table 2.2, the major outflow zones detected during Run 2, under the conditions of overpressure applied to the borehole, are located within three sections (layers):

- from 675 to 725 m b.g. (about 9.6 l/min of radial flow);
- from 775 to 840 m b.g. (about 4.4 l/min of radial flow); and
- from 840 to 850.6 m b.g. (about 5.6 l/min of radial flow)

The results of the vertical and radial flux distributions along the borehole during both logs are also represented in Figures 2.1 and 2.2. The radial fluxes represent mean values per meter of borehole section between stations with significant vertical flux differences.

It should be pointed out that the main inflows occured from and below the foot of the section previously plugged (i.e. from the casing shoe down to 686.1 m).

Table 2.2: Measured Vertical Flow Rates in l/min (Runs 1 and 2, December 1987)

Q inj. (l/min)	Run 1 0.0	Run 2 21.5
Tool # Start End	2 17:00 03:00	2 04:30 08:30
Depth (m)	Rate (l/min)	Rate (l/min)
182	-----	(-18.7)
250	0.0	-----
350	0.0	-----
480	0.0	(-19.5)
525	0.0	(-20.2)
575	0.0	(-19.2)
625	0.0	-----
675	0.0	(-19.2)
698	-1.1	-----
725	-1.6	-11.9
775	-1.6	-11.5
825	-1.4	-7.1
840	-1.3	-5.6

note: values between parentheses affected by calibration limits, corrected to injection flow rate (21.5 l/min) in the analyses.

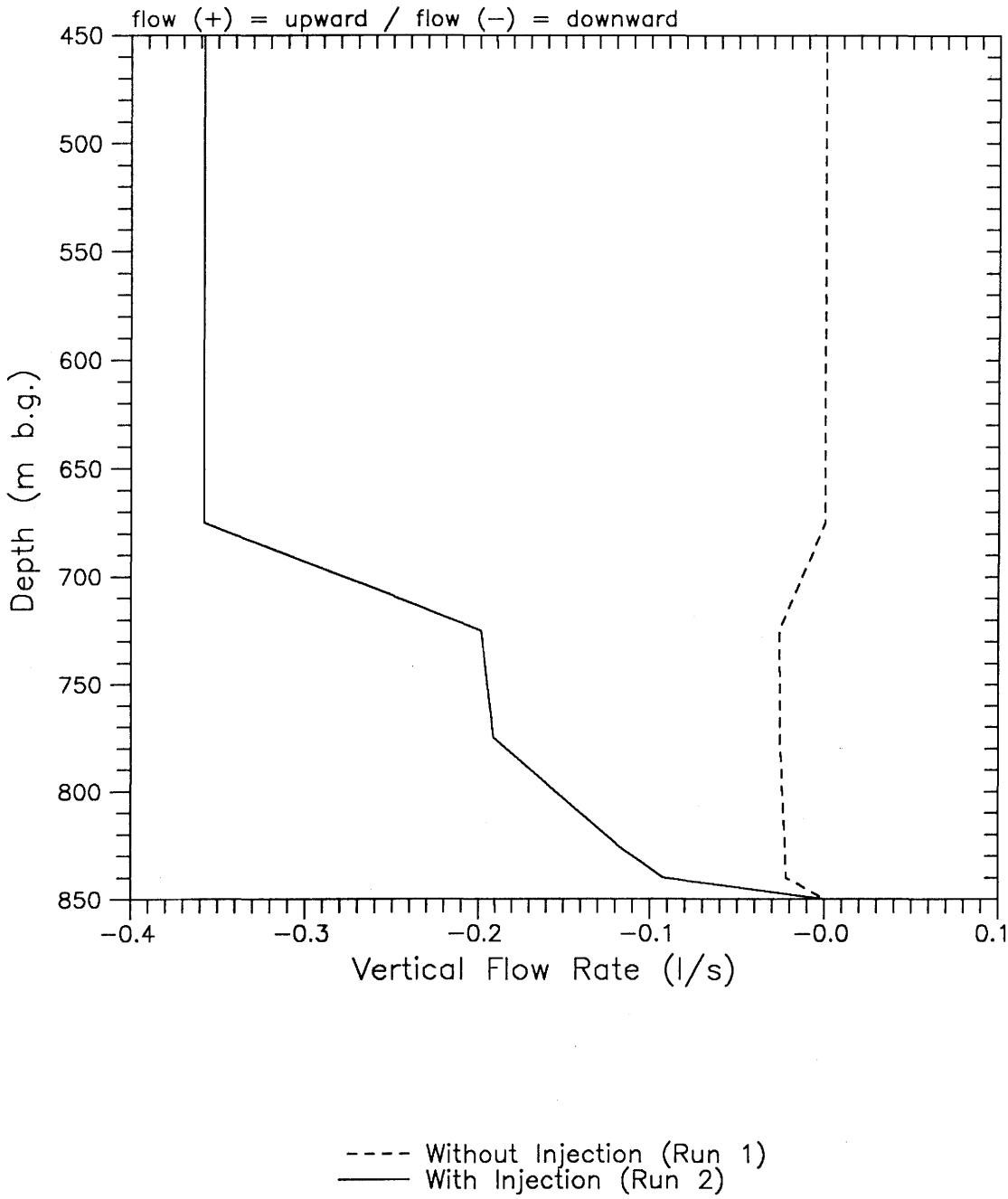

Figure 2.1: Vertical Flow Rate During Campaign FL1, 20-21.12.1988
Packer Flowmeter Interpretation, Siblingen Borehole

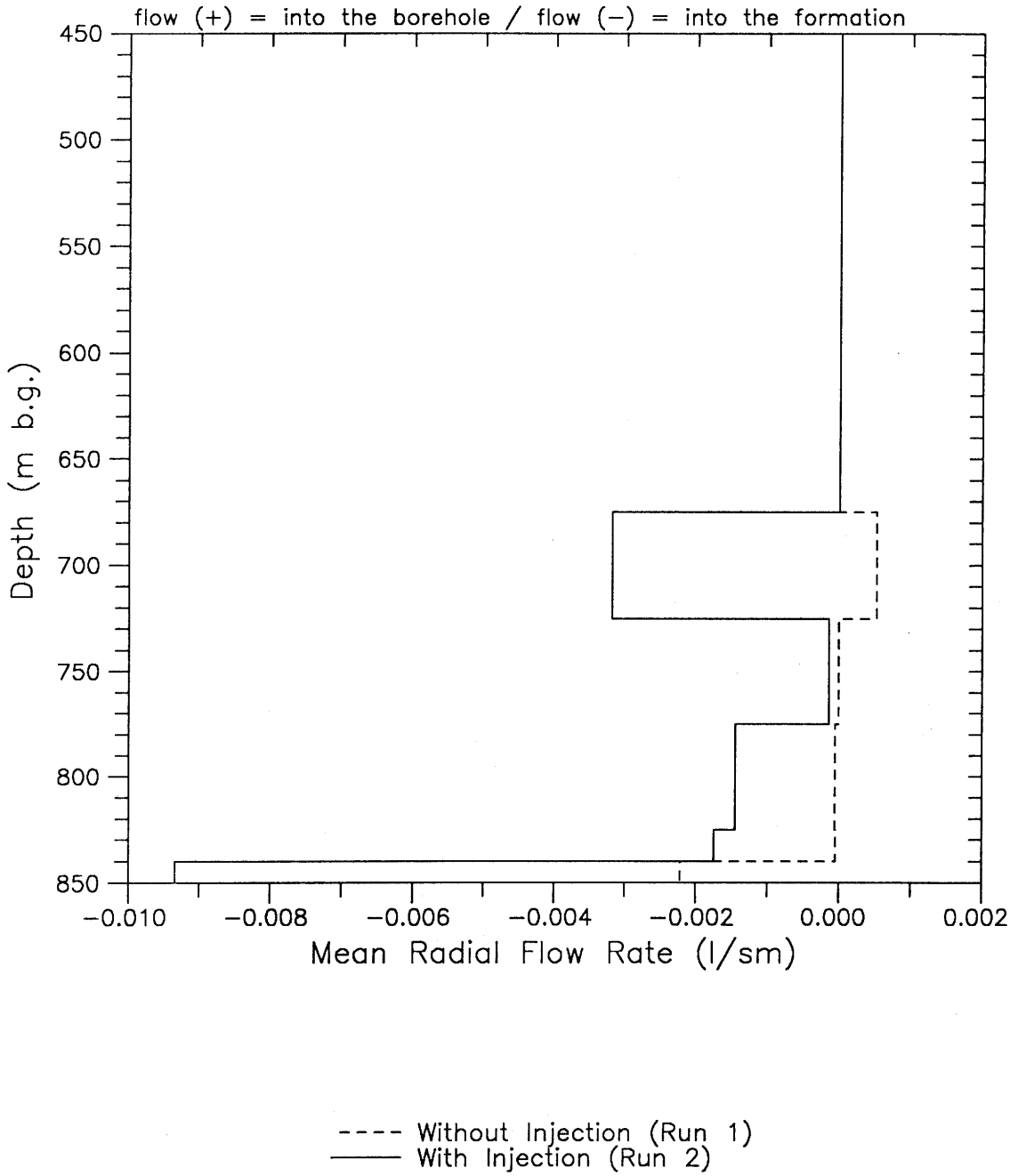

Figure 2.2: Radial Flow Rate During Campaign FL1, 20-21.12.1988 Packer Flowmeter Interpretation, Siblingen Borehole

2.4 SF campaign FL2, January 23 to 24, 1989

2.4.1 Test events

After FL1, the borehole was cemented from 675 to 851 m. The drilling was interrupted again on January 20, 1989, at a depth of 1017.8 m b.g. because of significant fluid losses. Caliper and temperature/conductivity logs and attempts with the flowmeter and packer flowmeter were conducted until January 23, 1989. Leakage at the pump of the packer flowmeter limited operations to trolling flowmeter logging. The water level had been allowed to stabilize for about 72 hours following the termination of drilling before starting the flowmeter measurements. At the beginning of the flowmeter measurements, the water level was stabilized at 132.0 m b.g.

The first log, the reference Run 1 (down and up) under static conditions, started at 18:00 from 480 m b.g., moving down to 1015 m b.g. at a mean speed of about 10 m/min. The Run 1 (up) was conducted between 18:55 and 20:00 at the same speed.

Before initiating the injection, a downhole pressure transducer was installed at a depth of 150 m b.g. in order to monitor the variation of the water level during the injection. The injection of cold water started at 02:30 on January 24, and stabilized at 51 l/min at about 04:30. According to the pressure transducer, the water level first raised by around 2.5 to 3.0 m after 1 hour of injection and then dropped by about 3.3 to 3.5 m. This phenomenon is assumed to be due to the effect of injecting cold water, which increased the density of water. At early time when the front of cold water was above the pressure transducer, the measured pressure reflected the change in head resulting from the combined effect of both variations of borehole fluid density and piezometric level of the water. When the front of cold water moved below the pressure transducer, the density of the column of water above the transducer stayed constant, but the water level continued to drop according to the increase of the average density of water within the whole borehole. A major consequence is that the variation of pressure induced by the injection at a given time was not the same along the borehole. For example, at 150 m b.g., at the elevation of the pressure transducer, the pressure effectively decreased after 1 hour of injection, but did not stop increasing at the bottom of the hole.

The second log, Run 2, started at 05:10. It was performed by moving the flowmeter from 190 m b.g. to 1012 m b.g at a speed of around 9.5 m/min, and then upward at a speed of 9.7 to 10.0 m/min. The log was completed at 07:43.

2.4.2 Model Assumptions

The water level during the first log was determined to be at 132 m b.g. with the flowmeter. As presented above, both the density and the piezometric level of water varied with time during the injection period because of the cold water used for the test. However, in the analysis of the tests, KPFLOW assumes that the density is constant and therefore the change of pressure induced by the injection must be introduced as an equivalent variation of the piezometric level. When estimating an equivalent rise in the water level, we considered the following phenomena:

- during the first hour of injection, the piezometric level rose from about 2.5 to 3.0 m
- when considering a constant water level, the pressure change induced by a modification of the borehole fluid temperature from the natural conditions to the temperature of the injected water could be estimated in an ideal case (closed system) to be 0.5 m at 700 m b.g. and 2.5 m at the bottom of the borehole.

Thus, a water level increase of 5 m was assumed in the analysis with KPFLOW, which is considered to be representative of the average borehole conditions in the logged section.

The tool was calibrated after the tests in the GEOTEST laboratory, using the same procedure as previously discussed for the packer flowmeter. The KPFLOW analyses included the calibration equations provided in GEOTEST/ GEMAG (1989). Although these equations were determined for a temperature of 10°C, GEOTEST reported no significant dependence of the temperature on the flowmeter readings.

Detailed analysis of the data showed that the flowmeter readings were affected by a variety of factors (temperature, elasticity of the cable, irregularities of the walls, solids suspended in the borehole fluid, etc.). This prevented an analysis that would consider only the effect of the mean speed of the tool on the calculated vertical fluxes. For instance, while the speed of the tool increased during the upward logging under stationary conditions (Run 1 up), the speed of rotation decreased regularly, even in sections considered to be tight from the previous investigations. Further, the range of uncertainty of the measurements was quite large, substantially reducing the amount of zones used to consider significantly different measurements.

These comments led to the conclusion that only a semi-quantitative analysis could be conducted for the interpretation of these trolling flowmeter data. For the analysis of Runs 1 down and up, it was assumed that the measured values collected above 685 m b.g. and below 938 m b.g. did not correspond to real vertical fluxes (Qvert = 0, see Figures 2.3 and 2.4). The apparent flux measured at these two depths, even though corresponding to different values, was considered to be the effect of tool noise. The speed of rotation to be attributed to a real vertical flow between these two depths was then obtained by substracting linearly the noise

(speed of the tool, disturbances) extrapolated between 685 and 938 m b.g.

Concerning analysis of Runs 2 down and up, it was assumed, for "anchoring" both ends of the logged section (pseudo-calibration), that:

- the measured values collected above 685 m b.g. (i.e. where no flow was detected during run 1) correspond to the injection rate of 51 l/min; and
- the measured values collected below 938 m correspond to zero flow as observed in Run 1.

The speed of rotation to be attributed to a real vertical flow was then calculated using the same approximation as for Runs 1 down and up. Based on a specific storage of 8.6E-8 m^{-1} and a mean distance of around 10 m between the flowmeter measurements in the zones of interest, a storage coefficient of 8.6E-7 was assumed in the KPFLOW analysis.

2.4.3 Test Results

During Run 1, a major inflow zone was detected at about 690 - 715 m b.g. (within a section previously cemented) inducing a vertical flux along the borehole down to about 925 - 938 m b.g., which corresponds to a major outflow zone.

Two major outflow zones were detected during Run 2, the first from 875 to 880 m b.g., and the second from 925 to 938 m b.g. On the contrary to the expectation, no inflow was detected from zone 690-715 m, where the major inflow from run 1 took place. This may indicate that the head in the borehole, during run 2, coincided with the formation head within this zone, thus preventing any flow by lack of pressure gradient. The results of both runs are reported in Table 2.3. Figures 2.3 to 2.6 provide illustrations of the vertical and radial fluxes during this test.

As explained above, the flowmeter readings were influenced by several effects, primarily the movements of the tool, and had to be conditioned before being converted to vertical flux for stationary measurements. Due to the complex nature of the uncertainties and the semiquantitative approach used for the analysis, no significant checking could be performed on the measurements of this flowmeter campaign.

Table 2.3: Measured Vertical Flow Rates in l/min (Runs 1 and 2, January 1989)

Q inj. (l/min)	Run 1 0.00	Run 2 51.0
Tool # Start End Depth (m)	2 17:00 03:00 Rate (l/min)	2 04:30 08:30 Rate (l/min)
Logging upwards:		
690.7	0.0	-51.0
715.2	-7.8	-51.0
878.1	-10.1	-51.0
878.3	-10.5	-42.6
925.1	-9.4	-32.2
930.6	0.0	0.0
Logging downward:		
684.9		
691.4	0.0	-51.0
875.0	-6.1	-51.0
880.0	-11.3	-51.0
925.4	-12.0	-42.8
938.1	-12.9	-37.6
	0.0	0.0

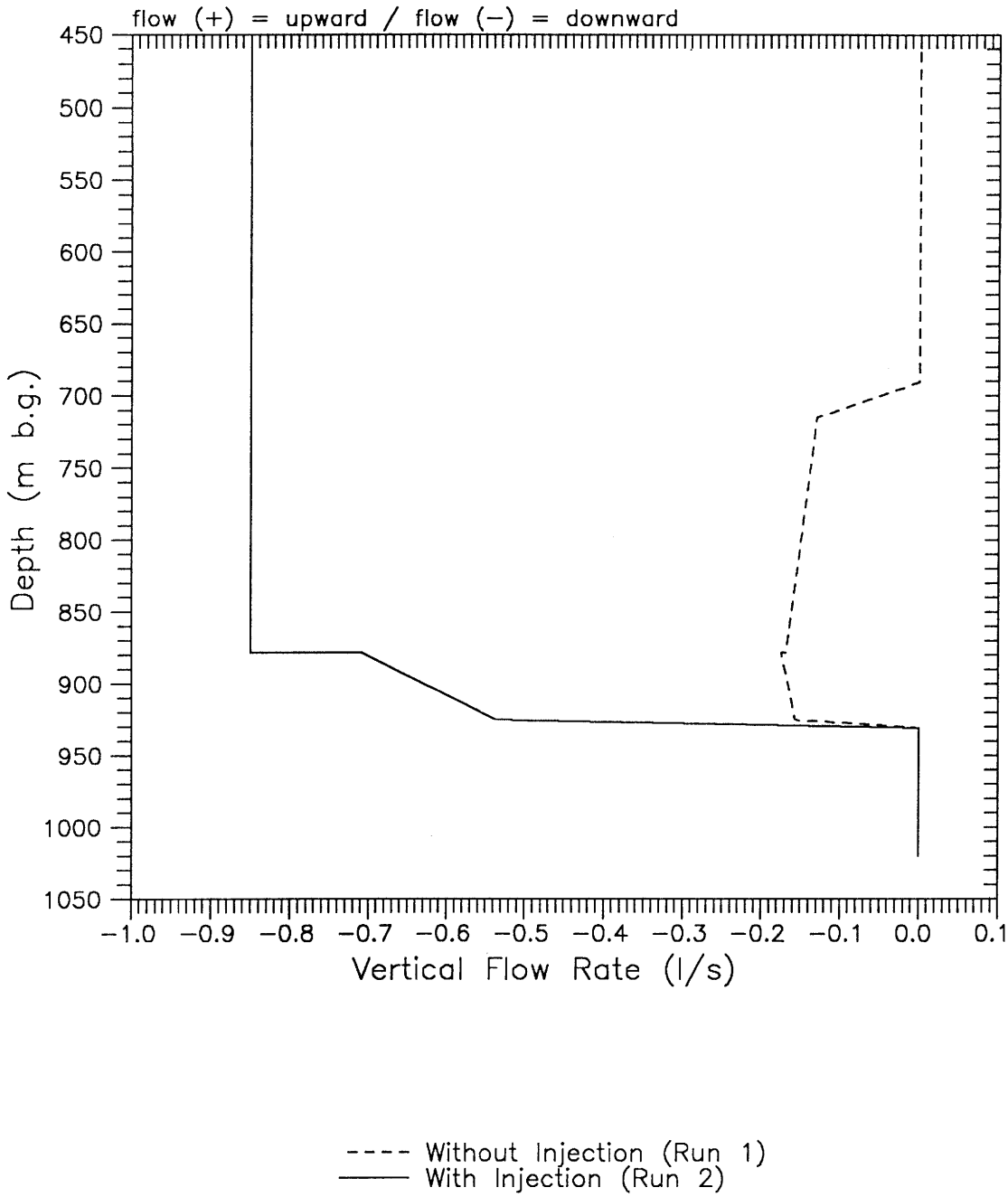

Figure 2.3: Vertical Flow Rate During Campaign FL2, 23-24.01.1989 Flowmeter Interpretation Runs upwards, Siblingen Borehole

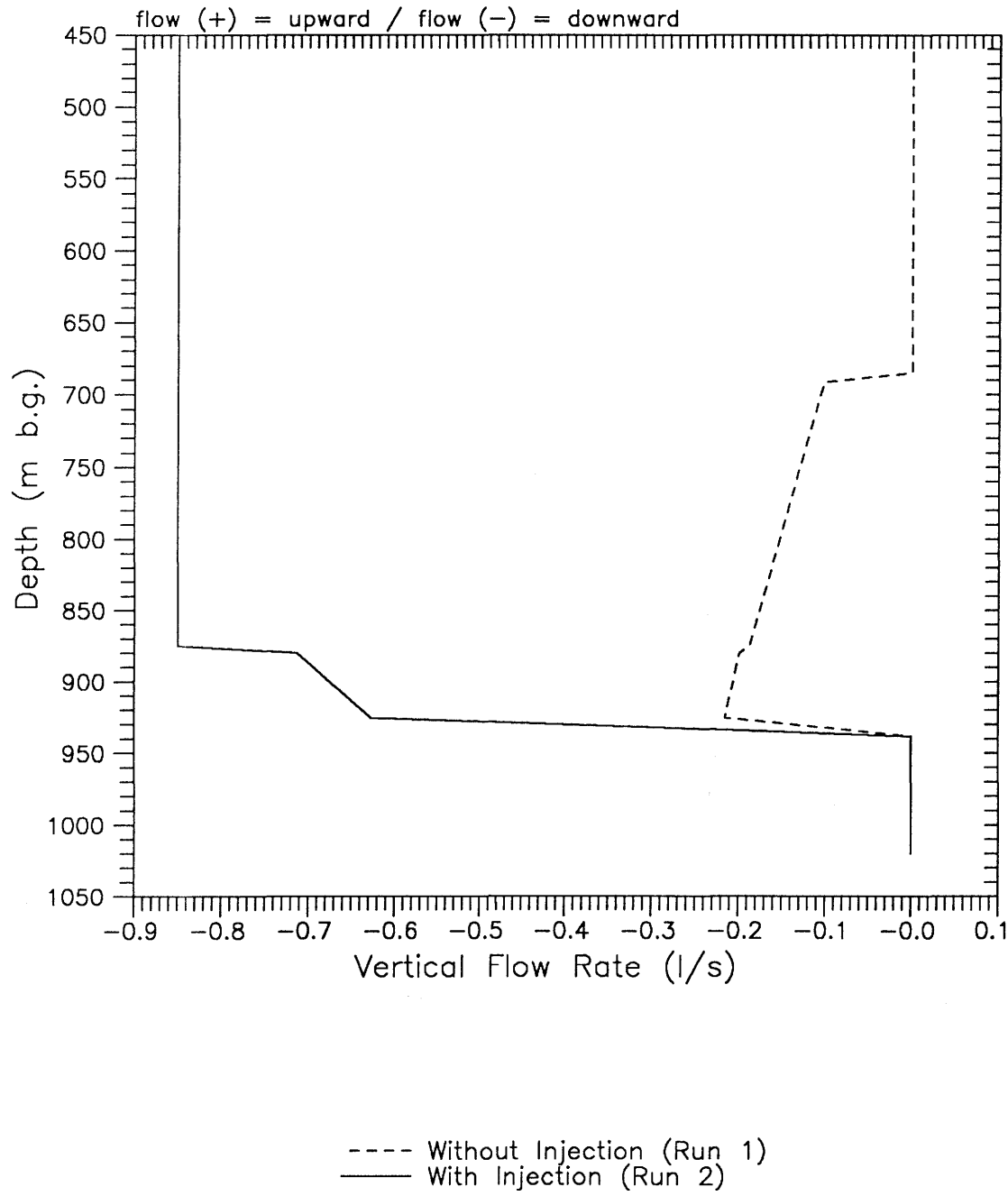

Figure 2.4: Vertical Flow Rate During Campaign FL2, 23-24.01.1989 Flowmeter Interpretation Runs downwards, Siblingen Borehole

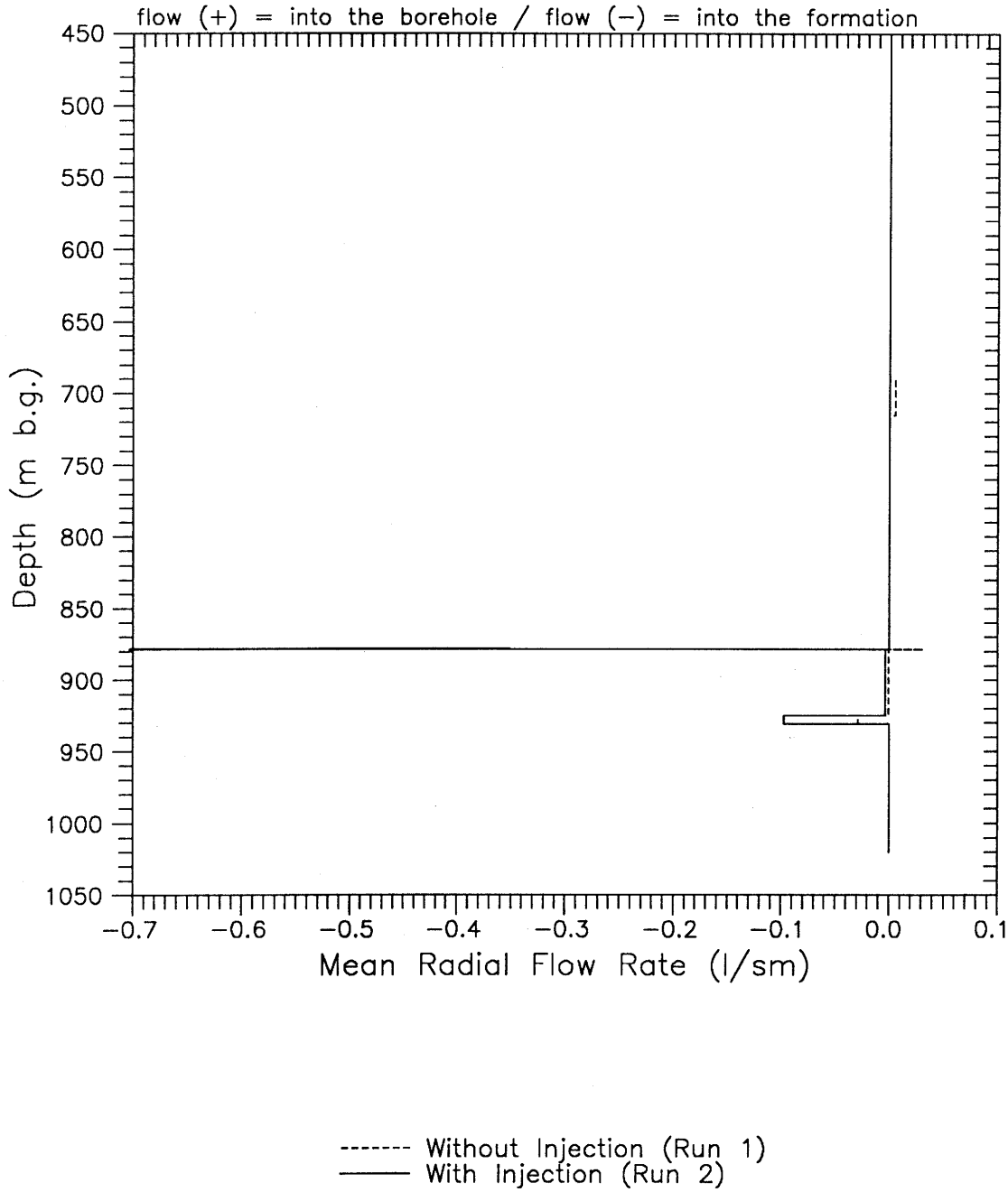

Figure 2.5: Radial Flow Rate During Campaign FL2, 23-24.01.1989, Flowmeter Interpretation Runs upwards, Siblingen Borehole

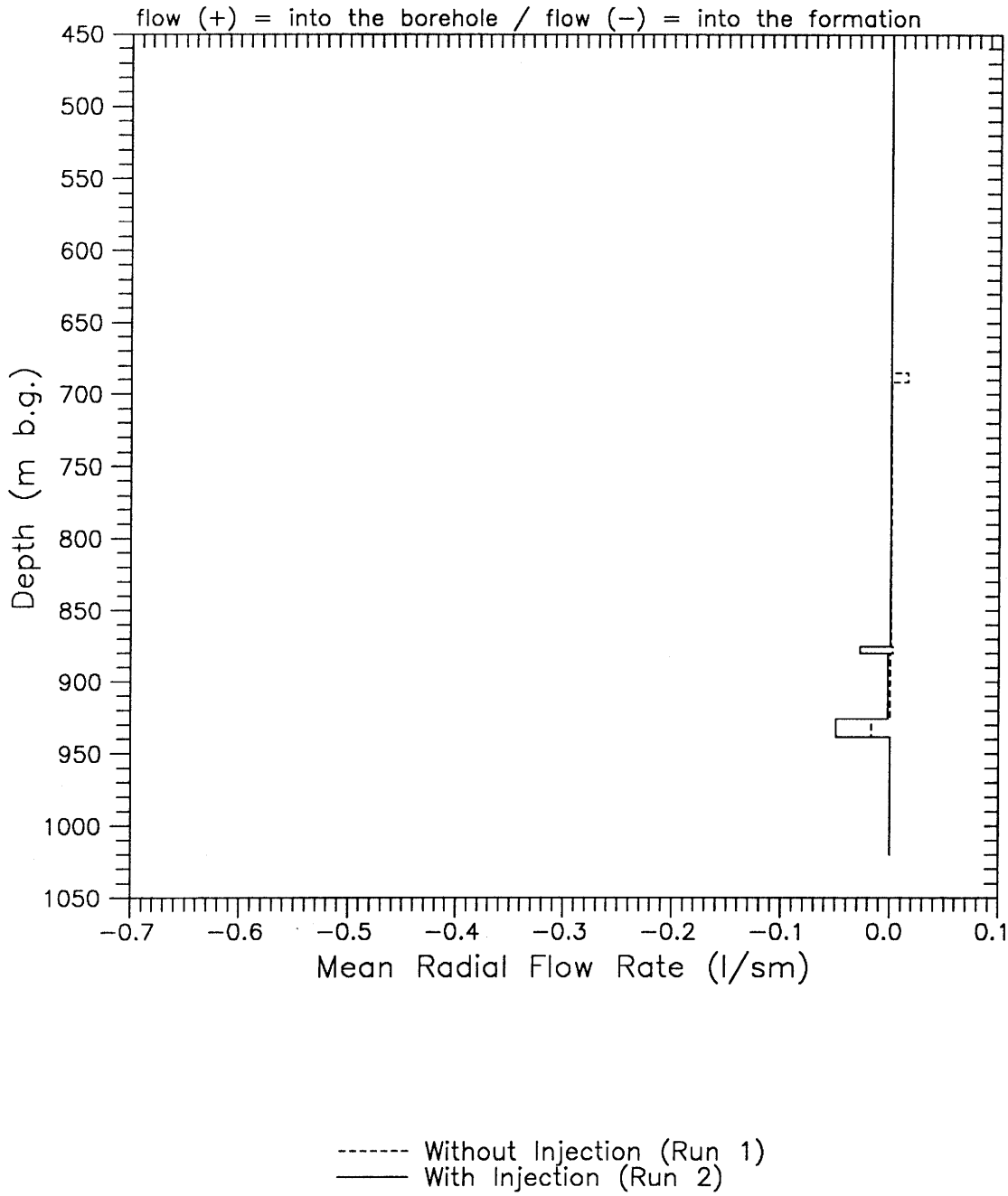

Figure 2.6: Radial Flow Rate During Campaign FL2, 23-24.01.1989, Flowmeter Interpretation Runs downwards, Siblingen Borehole

2.5 SPF Campaign FL3, April 5 to 7, 1989

2.5.1 Test Events

On April 2, 1989, drilling was completed down to 1522 m. The following days were used to perform the hydraulic packer test Cr24, temperature/conductivity logs, and a trolling flowmeter log. This resulted in a total of about 86 hours for the borehole pressures to stabilize before starting the packer flowmeter measurements. When starting the logs, the depth to the water level was 132.3 m b.g. The primary objective of this third flowmeter campaign was to determine the hydraulic characteristics of permeable layers for the section below 1062 m b.g. (i.e. the section not yet hydraulically tested. Nevertheless the measurements were conducted from the casing shoe down the bottom hole, including zones previously plugged (down to 1061.8 m) and cemented, from 490.3 to 536.3 m b.g. and from 668 to 850 m b.g.

The first log, the reference Run 1 under static conditions, was performed between 01:30 and 12:15 on April 5, 1989. The backup packer flowmeter was used at 11 stations of measurements (Run 1a) and then was removed due to leakage problems in the packer inflation pump. After correcting the problem, the same tool was used to complete the logging (Run 1b). Three further measurements were collected during Run 1b.

The injection of around 81.4 l/min started at 14:52, on April 6. The increase in the water level was monitored with a pressure transducer located at 182.3 m b.g. When Run 2 was initiated, after more than 3 hours of injection, the water level had increased about 24.5 m.

The measurements of the second log, Run 2, started at 18:08. Initially, the backup packer flowmeter was used, but logging was interrupted after about 1 hour (3 measurements collected) because of a leakage at the packer inflation pump. Run 2 was restarted with the primary packer flowmeter (Run 2b) and resulted in the measurement of the vertical flow rate at 5 depths (between 03:59 and 05:09 on April 1989). The injection rate had dropped to about 79 l/min during the Run 2b.

2.5.2 Model Assumptions

The water level before starting the injection was determined in Run 1 to be 132 m b.g. After conducting logging under static conditions, a pressure transducer was installed at a depth of 182.3 m to continuously monitor the pressure change during injection.

When performing Run 2a, the pressure had increased to about 241 kPa, which corresponds to a rise in the water level of about 24.5 m. The temperatures measured by the packer flowmeter during Runs 1a, 1b, and 2a did not vary significantly during the injection:

- from 18 to 11.5°C at 182.3 m (pressure transducer)
- from 40 to 39°C at 1062 m b.g.

- no change (43°C) at 1154 m b.g.

Therefore, the pressure change induced by the temperature variation of the water was not taken into account in this analysis.

Neither the temperature nor the pressure were measured during Run 2b.

Based on the temperatures measured during Runs 1a, 1b, and 2a, the calibration equations valid for water at 50°C were applied (conversion parameters).

In accordance with the approach used for the previous flowmeter analyses, a storage coefficient of 8.6E-6 was assumed in the KPFLOW analysis.

2.5.3 Test Results

As presented in Table 2.4, a significant inflow zone was detected during Run 1a between 660 and 708 m b.g. (within the cemented section) which induced a vertical flow rate of about 2.0 l/min down to 770 m b.g. Two outflow zones were detected at the following depths:

- from 770 to 910 m b.g. (about 0.8 l/min of radial flow)
- from 910 to 955 m b.g.(about 1.3 l/min of radial flow)

The major outflow zone detected during Run 2, under injection conditions of about 80 l/min, is located above 1062 m b.g., in a section of the borehole that had been unsuccessfully plugged several times. As presented in Table 2.4, the vertical flow rate measured at 1062 m b.g. was only 2.9 to 3.6 l/min. Below this depth, some secondary outflow zones were detected at the following depths (see Figures 2.7 to 2.10):

- from 1062 to 1100 m b.g. (0.3 to 1.2 l/min)
- from 1163 to 1210 m b.g. (about 0.6 l/min)
- below 1210 m b.g. (about 2.1 l/min)

The significance checking indicated that, during Run 2a, the measured frequency at 1100 m b.g. corresponding to 2.4 l/min was not statistically different from the measurement at 1154 m b.g. corresponding to 2.3 l/min. The value at 1100 m b.g. was then corrected internally in the code KPFLOW to the same value than measured at 1154 m b.g.

Table 2.4: Measured Vertical Flow Rate in l/min (Runs of April 1989)

Q inj. (l/min)	Run 1a 0.0	Run 1b 0.0	Run 2a 81.5	Run 2b 79.0
Tool #	2	2	2	1
Start	01:45	10:15	18:10	04:00
End	04:45	12:15	19:00	05:10
Depth (m)	Rate (l/min)	Rate (l/min)	Rate (l/min)	Rate (l/min)
180	0.0	---	-81.4*	-79.0*
660	0.0	---	---	---
708	-2.0	-1.9	---	---
770	---	-2.1	---	---
910	---	-1.3	---	---
955	0.0	---	---	---
1062	0.0	---	-3.6	-2.9
1100	---	---	-2.4	-2.6
1154	0.0	---	-2.3	-2.6
1163	0.0	---	---	-2.7
1210	---	---	---	-2.1
1276	0.0	---	---	---
1350	0.0	---	---	---
1490	0.0	---	---	---
104	0.0	---	---	---

* Injection values (measured at surface)

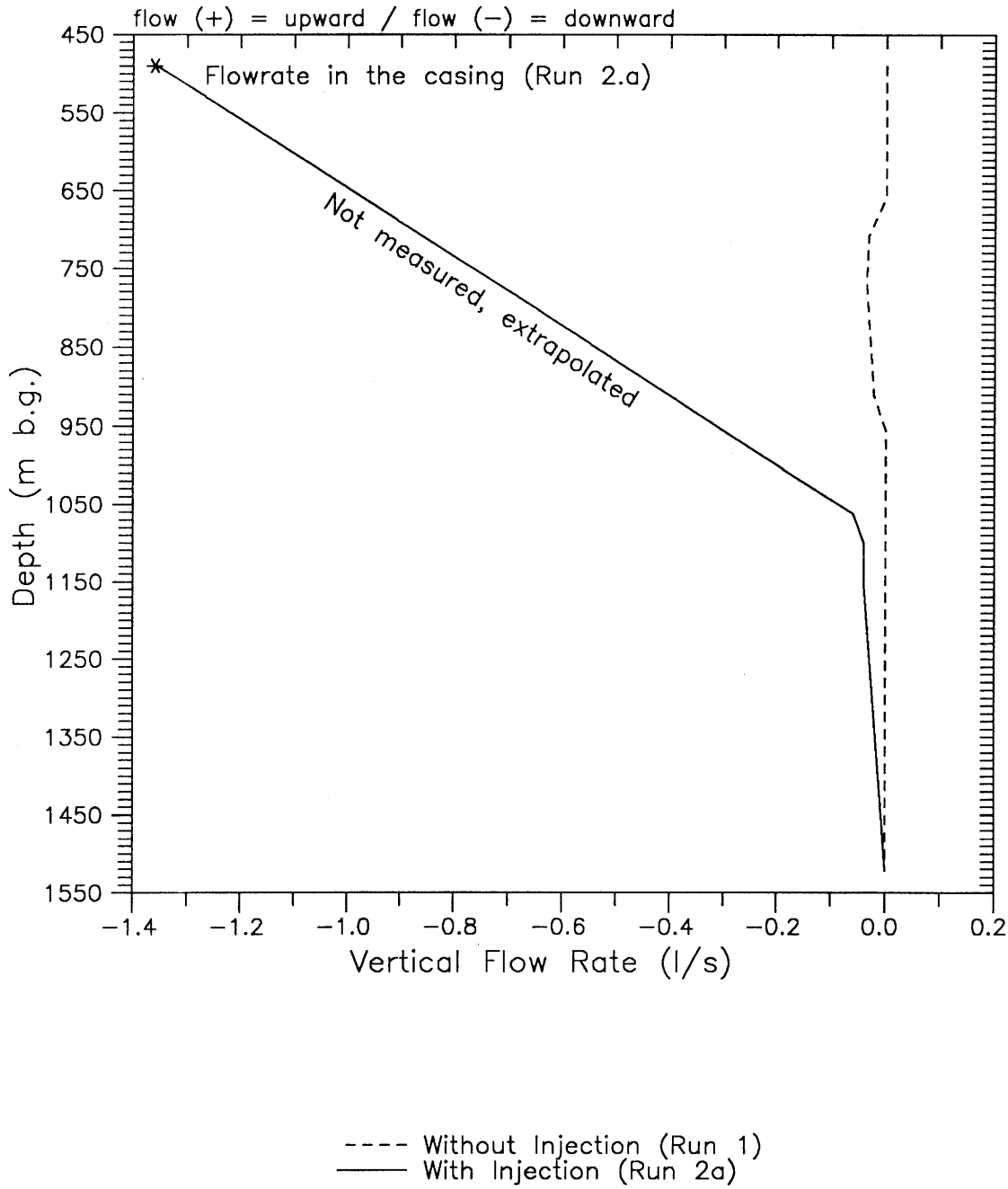

Figure 2.7: Vertical Flow Rate During Campaign FL3, 5-7.04.1989
Packer Flowmeter Interpretation (Runs 1-2a), Siblingen Borehole

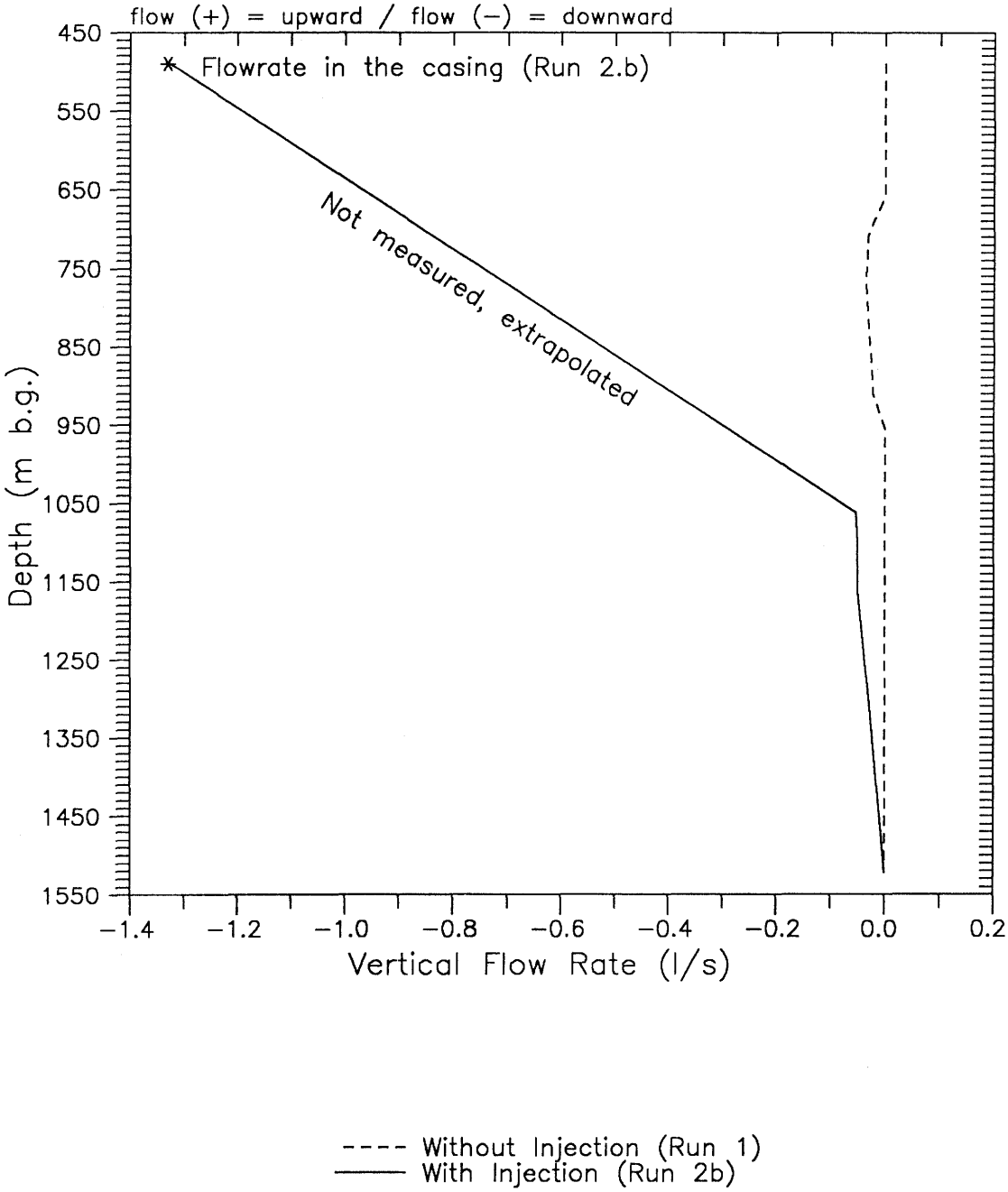

Figure 2.8: Vertical Flow Rate During Campaign FL3, 5-7.04.1989
Packer Flowmeter Interpretation (Runs 1-2b), Siblingen Borehole

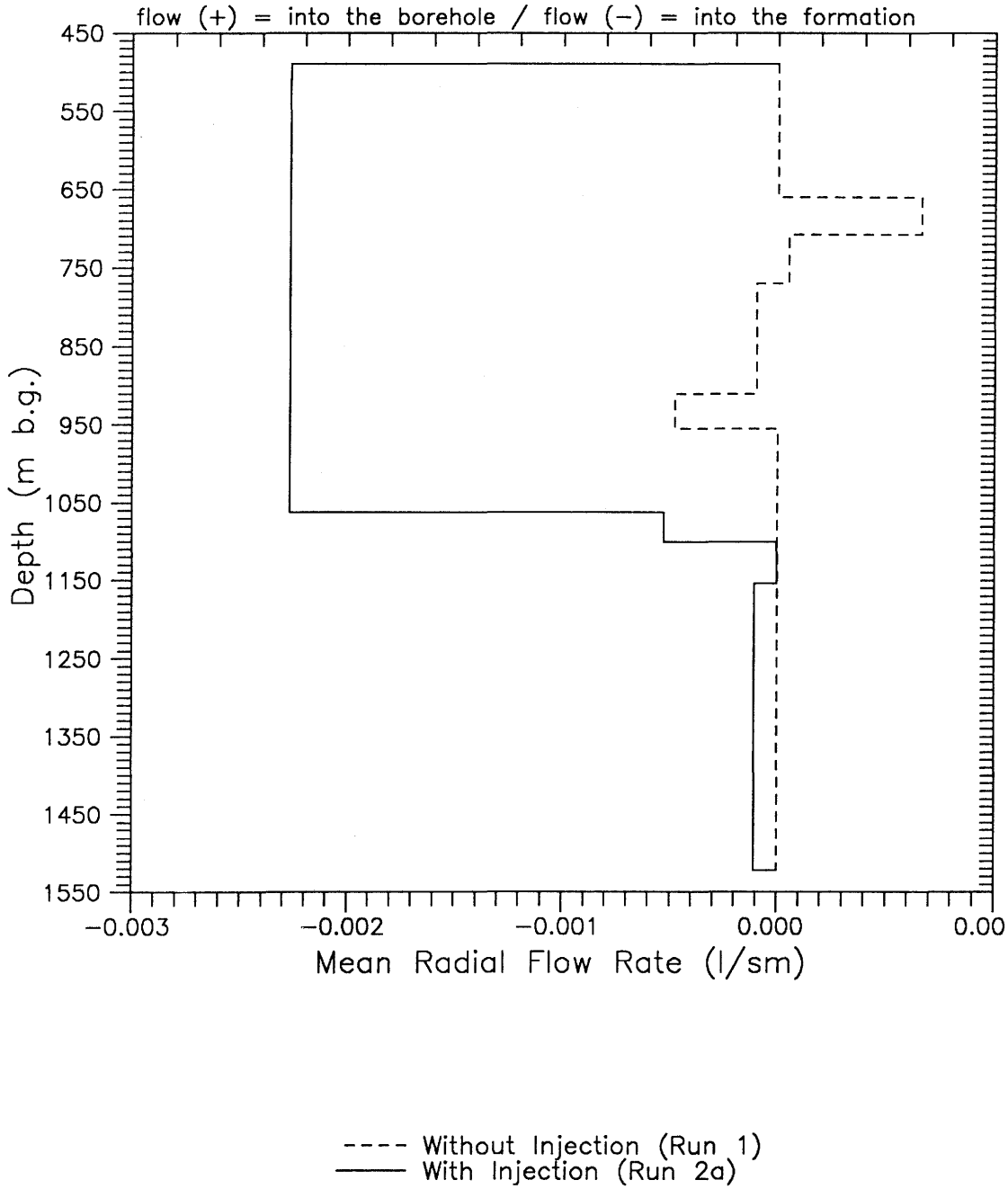

Figure 2.9: Radial Flow Rate During Campaign FL3, 5-7.04.1989
Packer Flowmeter Interpretation (Runs 1-2a), Siblingen Borehole

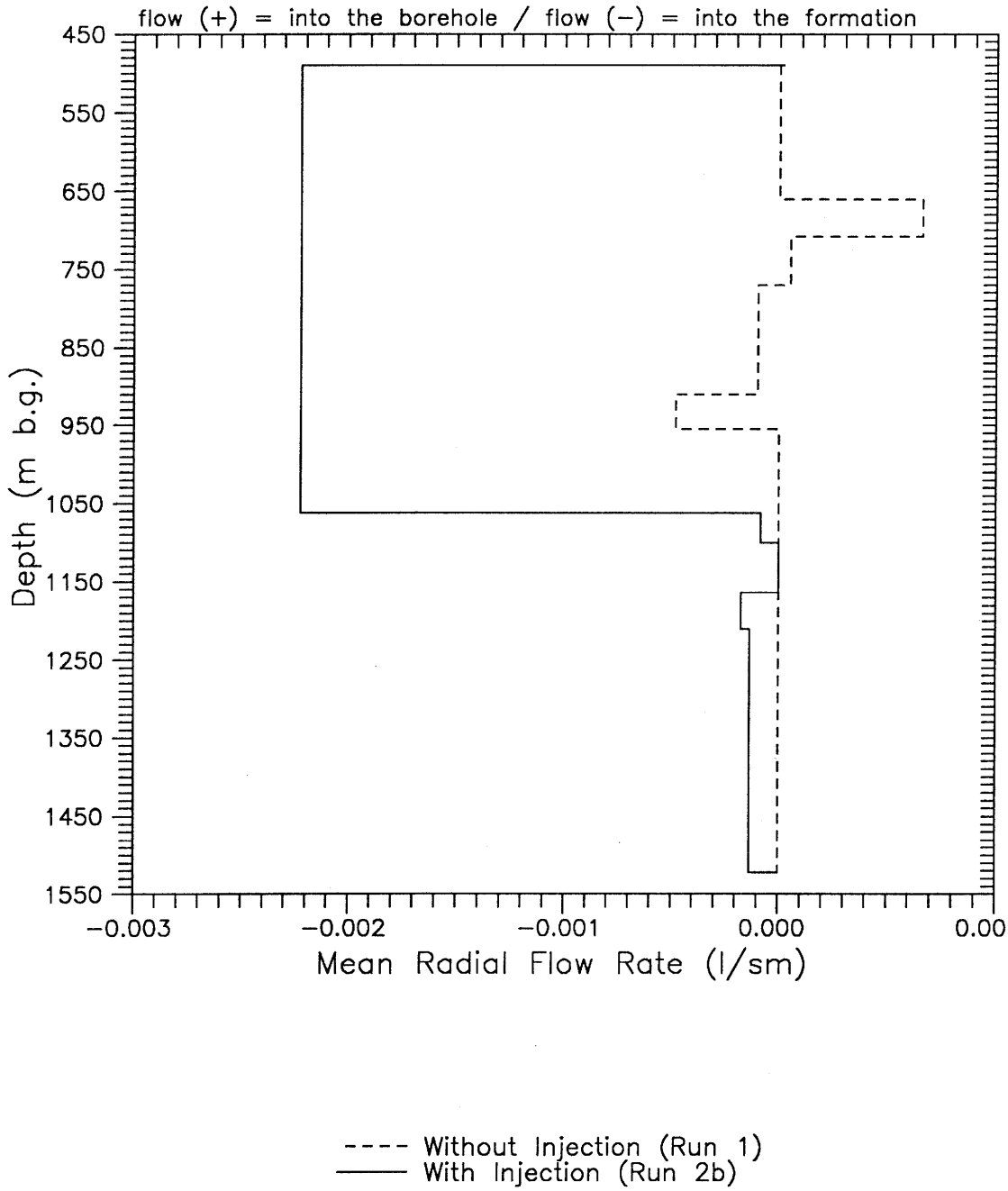

Figure 2.10: Radial Flow Rate During Campaign FL3, 5-7.04.1989
Packer Flowmeter Interpretation (Runs 1-2b), Siblingen Borehole

2.6 HPPF Campaign FL4, June 6 to 8, 1989

2.6.1 Test events

A heat pulse packer flowmeter campaign was performed in the borehole from June 6 to 8, 1989. The objectives of this supplementary test were first, to evaluate the applicability of the heat pulse flowmeter developed by the U.S. Geological Survey (USGS), and second, to compare the results of this method with other methods (electrical conductivity, packer tests and packer flowmeter). The borehole flow profile was determined with three successive logs.

The first log, the reference Run 1 under static conditions, was performed with the large diamter HPPF tool, between 15:30 and 19:45 on June 6, 1989, and collected a total of 26 measurements.

The first injection test, at 8 l/min, started at 11:45 on June 7. The measurements of the second log, Run 2, started at 14:20 and was completed within 4 hours. A total of 29 measurements were collected (packer either inflated or not), using the large diameter HPPF tool, at progressively greater depths starting from 700 m.

The next day, on June 8, an injection at 8 l/min was conducted from 08:35 to 10:25 without conducting flowmeter measurements, and then the rate was increased to 57 l/min.

During this second injection test, the measurements were performed using two runs, Run 3a with the large diameter tool between 13:45 and 15:47, and Run 3b using the small diameter tool from 18:45 to 20:00. However, due to apparent changes in the conditions of testing (water level, flow rate) during the afternoon, only the results from Run 3a were used for the analyses.

2.6.2 Model Assumptions

2During the test at 8 l/min, the change in water level was monitored by a pressure cell at 200 m b.g. and checked by some electrical tape measurements. According to the pressure cell, the water level rose about 0.5 m before declining after a few minutes. From the electrical tape the water level had stabilized at 0.8 m above the static level at 14:15. This value of 0.8 m was assumed in our analyses.

For the second injection test, the pressure, measured with a transducer located at 180 m, indicated that the water level had stabilized at about 10 m above static at 12:30. Another measurement made using the heat pulse flowmeter tool at the end of testing (20:00) indicated the water level at about 17 m above the static value.

Because of the apparent variations in the stabilized water level and also because of some apparent increase in the flow rate with time, only the first part of Run 3a, including the downward measurements from 980 to 1505 m b.g., was considered in the KPFLOW analyses. In accordance with the approach used for the previous flowmeter analyses, a storage coefficient of 2.6E-6 was assumed in the KPFLOW

analysis.

2.6.3 Test Results

As illustrated in Tables 2.5 and 2.6, and in Figures 2.11 to 2.14, Run 1 allowed the identification of three main flow zones:

- from 700 to 708 m b.g. (inflow about 1.1 l/min)
- from 935 to 938 m b.g. (outflow about 0.8 l/min)
- from 1210 to 1276 m b.g. (inflow about 0.3 l/min)

At the depth of 700 m, the vertical flow rate during Run 2 was 3.6 l/min. This log allowed the identification of three main outflow zones:

- from 835 to 840 m b.g. (1.1 l/min)
- from 920 to 929 m b.g. (2.1 l/min)
- below 1100 m b.g (0.3 l/min)

At the first flowmeter location of Run 3a (980 m b.g.), the vertical flow rate was 2.5 l/min. This value decreased continuously with depth, indicating the presence of several inflow zones. The primary inflow zones are located at the following depths:

- from 1062 to 1090 m b.g. (0.7 l/min)
- from 1210 to 1276 m b.g. (0.5 l/min)
- from 1500 to 1522 m b.g. (0.5 l(min)

As the purpose of the heat pulse flowmeter campaign was to test this new tool in a deep borehole, only the interpreted results were presented in the USGS final report. Since the raw data (travel time, size of sampling, variance) were not documented in this report, no significant checking could be applied to the FL4 analysis.

Table 2.5: Summary of the Measured Vertical Flow Rate in l/min (Runs of June 1989)

Q inj. (l/min)	Run 1 no	Run 2 8.0	Run 3a 57	Run 3b 57
Tool #	Large	Large	Large	Small
Start	15:25	14:30	13:45	18:45
End	19:38	18:25	15:47	19:55
Depth (m)	Rate (l/min)	Rate (l/min)	Rate (l/min)	Rate (l/min)
200	---	-8.7	---	---
320	---	-9.1	---	---
520	0.0	---	---	---
660	0.0	---	---	---
700	---	-3.6	---	---
704	---	-3.6	---	---
708	-1.1	-3.5	---	---
770	-1.1	-3.5	---	---
840	-1.1	-2.4	---	---
860	-0.9	-2.4	---	---
910	-1.0	-2.6	---	---
920	-1.1	-2.4	---	---
925	-1.1	-2.0	---	---
929	---	-0.3	---	---
938	-0.3	-0.4	---	---
950	---	-0.3	---	---
980	-0.3	-0.3	-2.5	---
1062	-0.3	-0.3	-2.5	---
1090	---	---	-1.8	---
1100	-0.2	-0.3	---	---
1210	-0.3	---	-1.7	---
1240	---	---	---	-2.3
1276	0.0	---	-1.2	-1.2
1320	---	---	---	-1.6
1350	0.0	---	-1.0	-1.5
1400	---	---	-0.8	-1.1
1490	---	---	-0.5	---
1500	---	---	-0.5	---
1505	---	---	-0.2	---
1470	---	-0.6	---	---
1450	---	---	-0.6	---
1390	---	---	-1.1	---
1375	---	---	-1.4	---
1240	---	---	-2.1	---
1100	-0.4	---	---	---
935	-1.4	---	---	-3.7
840	---	-2.5	---	---
835	---	-3.5	---	---
700	0.0	---	---	-3.2
704	-0.6	---	---	-3.2
708	-1.2	---	---	-3.3

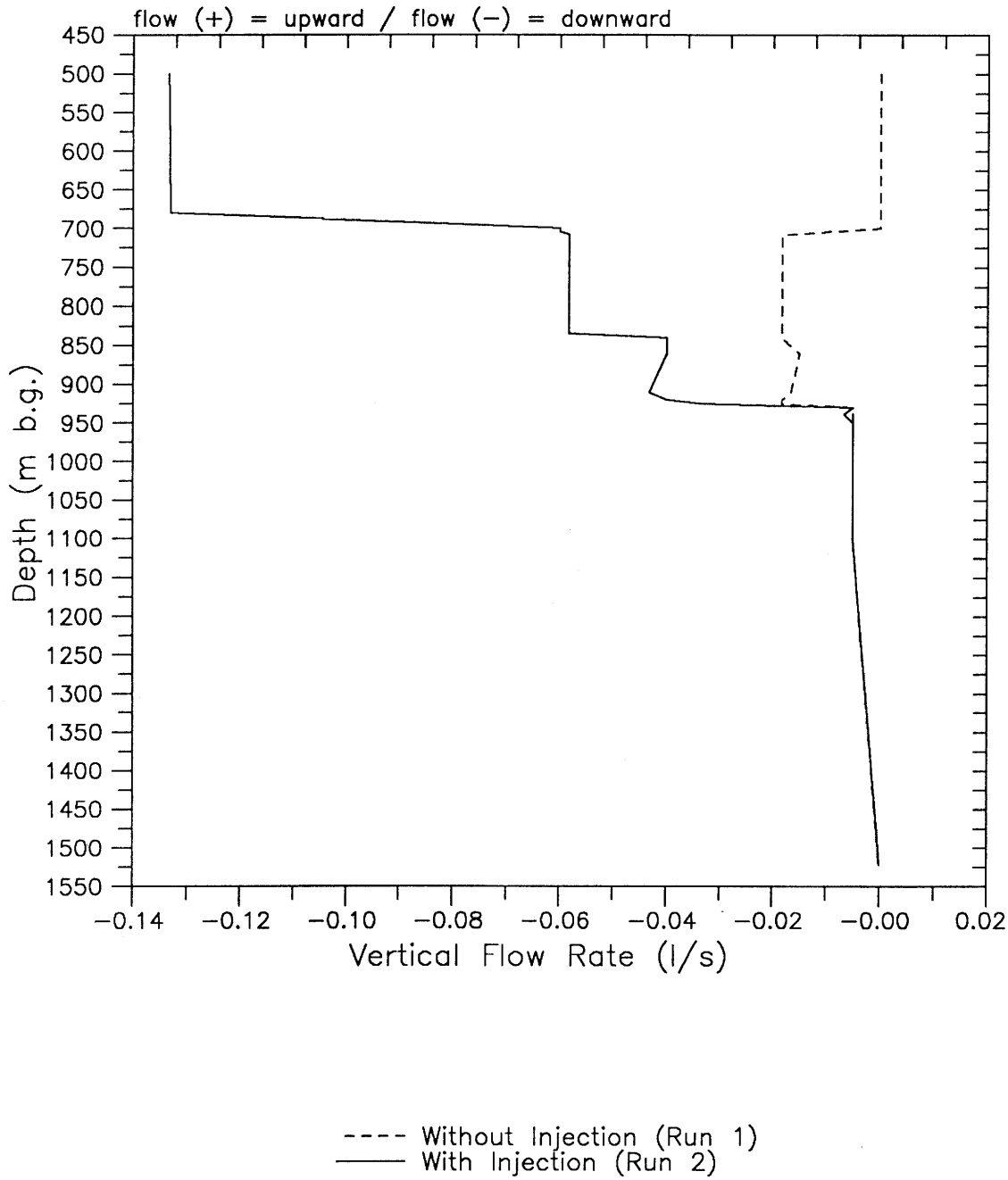

Figure 2.11: Vertical Flow Rate During Campaign FL4, 6-8.06.1989 Heat Pulse Flowmeter Interpretation (Runs 1-2), Siblingen Borehole

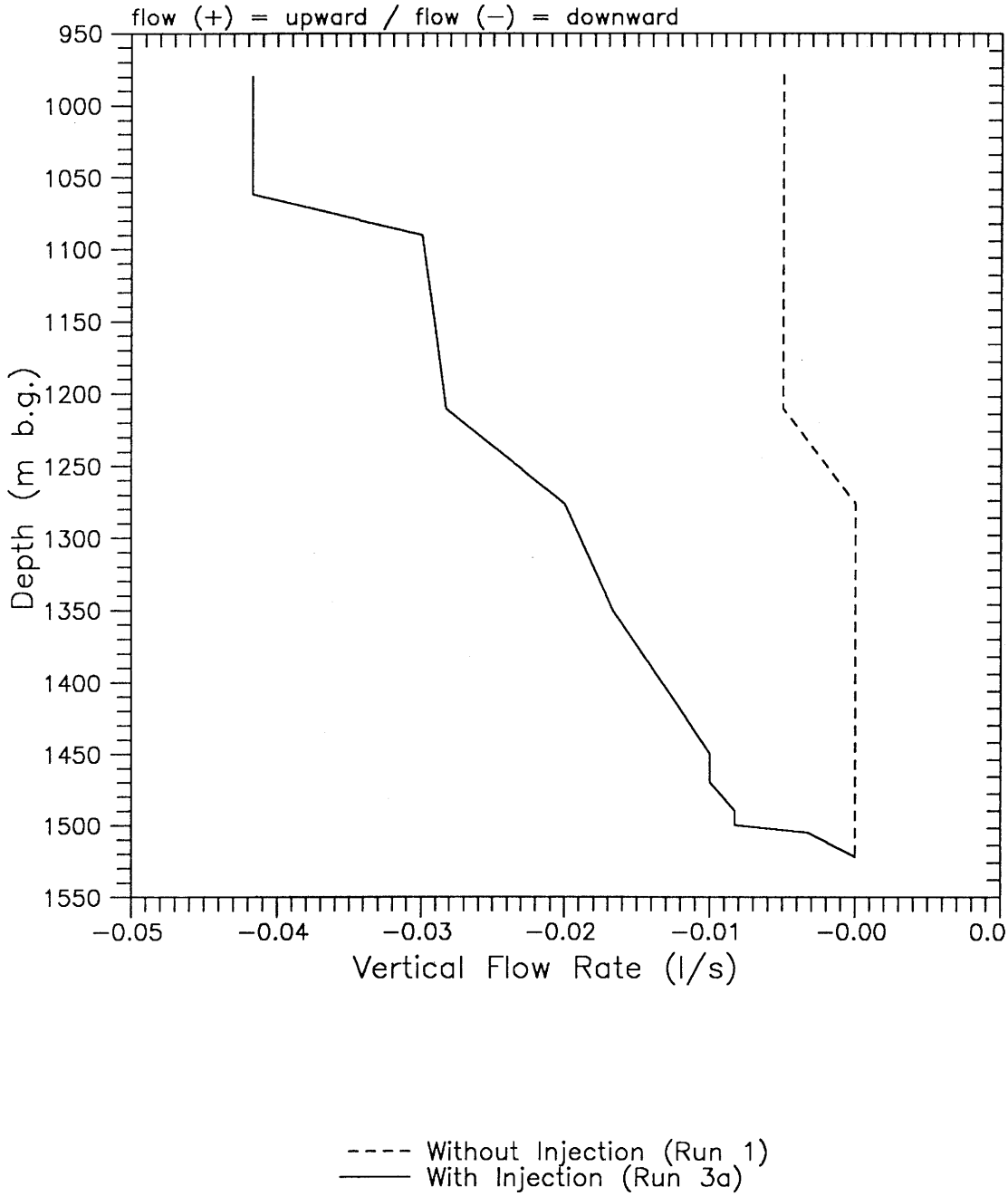

Figure 2.12: Vertical Flow Rate During Campaign FL4, 6-8.06.1989
Heat Pulse Flowmeter Interpretation (Runs 1-3a),
Siblingen Borehole

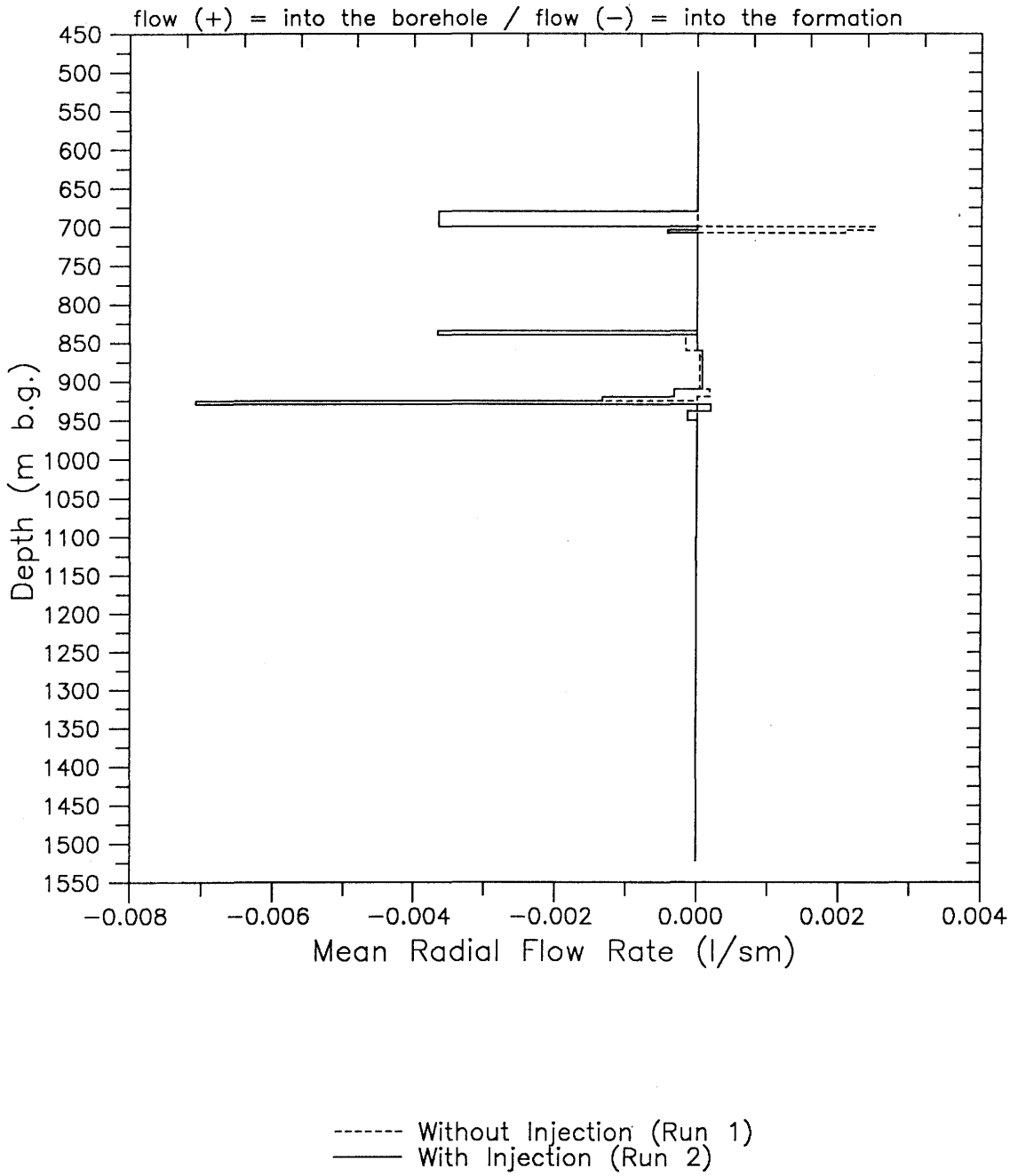

Figure 2.13: Radial Flow Rate During Campaign FL4, 6-8.06.1989
Heat Pulse Flowmeter Interpretation (Runs 1-2),
Siblingen Borehole

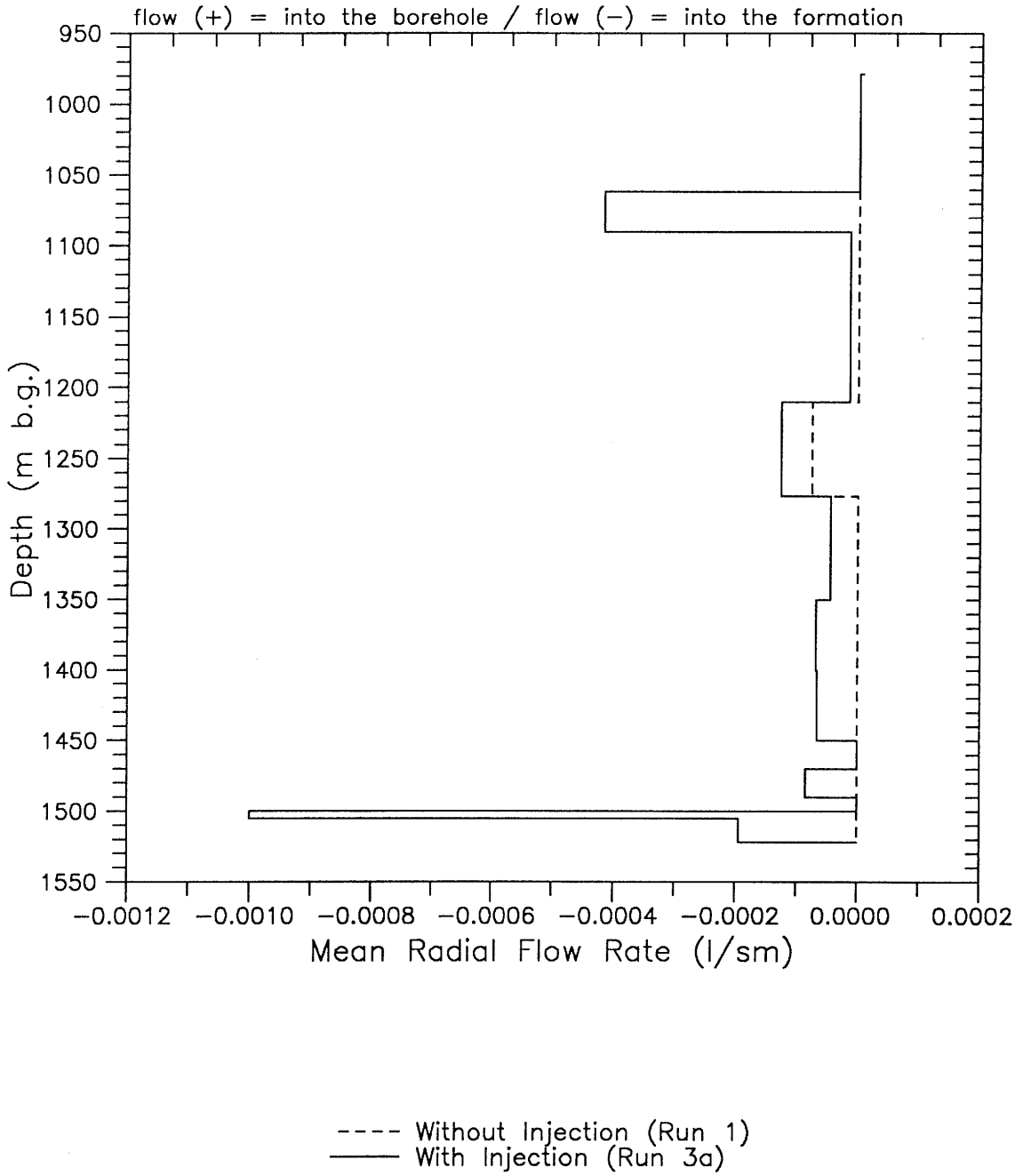

Figure 2.14: Radial Flow Rate During Campaign FL4, 6-8.06.1989
Heat Pulse Flowmeter Interpretation (Runs 1-3a),
Siblingen Borehole

3 ELECTRICAL CONDUCTIVITY MEASUREMENTS

3.1 Summary of Field Activities and Calibration

3.1.1 Introduction

From April 14 to April 25, 1989, an electrical conductivity fluid logging campaign was performed in the Siblingen borehole with the objective of characterizing the fracture inflows in the uncased crystalline section ranging 1000 to 1522 m b.g. The fluid logging technique is described in detail by TSANG et al. (1990). The method of partial moments has been used as the primary method to interpret the data and this method is documented in detail by LOEW et al. (1990). In addition, the borehole transport simulator BORE (HALE and TSANG, 1988) has been used to augment the method of moments. The use of BORE is well documented in TSANG et al. (1990). A brief explanation of the methods used to interpret the electrical conductivity logs is included in Section 3.2. The electrical conductivity logs were measured by GEOTEST AG. A detailed description of the field data collection and borehole configuration is presented in GEOTEST/GEMAG (1989).

The response of the formation to the various stresses incurred during conductivity logging was complex. For example, vertical flow within the borehole was seen in times of static conditions (i.e., no pumping/injection). This vertical flow is a result of high fracture permeabilities and variable fracture heads. In addition to these problems, there were substantial problems in the borehole flushing events. The primary objective of a flushing event is to create an initial salinity profile which is simple in structure and different from the inflowing fluid salinity. The best initial condition is a constant salinity over the entire interval to be logged. When flushing the borehole it is desirable to minimize the loss of flushing fluid to the formation. Unfortunately the mean formation head of the logged interval is approximately 132 m b.g. This caused injection of the flushing fluid to occur, which creates a condition where the concentration of the inflowing (flow to the borehole) fluid during the pumping phase is transient and non-representative of the formation fluids.

Because of the high total transmissivity in the zone between the casing shoe at 490.45 and the beginning of the logged section at 1000 m b.g., the pumping sequences were designed to be performed under the presence of an isolating system consisting of a tubing connected on each end to a production-injection-packer (PIP). The upper packer was located within the casing at 278.45 m b.g. (lower seal) and the lower packer was located at 988 m b.g. (lower seal) within open hole. This system effectively hydraulically isolated the borehole from the casing to a depth of 988 m b.g. As a result of a small well-bore radius (96 mm), the emplacement of this PIP system caused substantial problems and these problems manifested themselves in design changes in the initial test program.

A summary of test events is presented in Table 3.1. These will be discussed in chronological order in Section 3.1.2.

Table 3.1: Summary of Electrical Conductivity Logging Events

EVENT	FLU 1	SF 1	FLU 2	SF 2	OH-RW1	FLU 3	SF 3	PIP-RW1	FLU 4	SF 4	PIP-RW2	RWR
Starting date	14.04	15.04	16.04	16.04	16.04	17.04	18.04	18.04	22.04	22.04	23.04	25.04
Starting time	15:19	00:16	01:30	09:03	20:09	14:25	00:02	22:40	18:03	21:56	05:40	07:12
Duration (hrs)	9	25	7.5	11.0	14	10	22	60	4	8	50	6
Flow R. (l/min)[1]	-20[2]	-0.4	80/30	-0.4	32	80/30		3	-33		1.5	
Volume (m^3)	10.4	0.6	11.0	0.26	26.8	8.9		10.8	8		4.5	
Press. change (kPa)					7			200	< 600		130	(75)
Total # of logs		3		2	4		2	12		1	9	

(1) In case of flushing event: Flushing Fluid Injection Rate.
In case of static flow event: Flow Rate at 1,000 m b.g.
In case of pumping event: Net Outflow at Surface

(2) Negative sign means flow direction is down the borehole.

Legend:

FLU: Flushing Event (Constant Rate Injection)
SF: Static Fluid Logging Event
OH-RW: Open Hole Constant Rate Withdrawal Event
PIP-RW: PIP Constant Rate Withdrawal Event
RWR: Pressure Recovery after Constant Rate Withdrawal Event

3.1.2 Test Events

All depths used in this section are measured in the borehole from surface. Thus, the initials for *below ground* will be dropped in the text. The first event (FLU 1, Table 3.1) was a borehole flushing event in which the borehole fluid was replaced with deionized water. The flushing was carried out in 90 m displacement steps down the borehole. After the flushing with deionized water (event FLU 1 in Table 3.1), the double-PIP system could not be emplaced due to restrictive clearance between the borehole wall and the packer elements. The conductivity logs measured after flushing showed that flushing in steps caused an irregular initial salinity distribution and borehole flow was occurring in the down-well direction from 910 m to the borehole total depth during the static fluid logging event SF I.

Because the PIP system could not be emplaced, it was decided to try to run the next fluid logging test under open-hole conditions and pumping at a large rate. First the borehole was re-flushed in a two-step displacement procedure with deionized water (FLU 2). After a second static fluid logging event (SF 2) which lasted 11 hours, the open borehole was pumped at a rate of 32 l/min for 14 hours (OH RW1). Four conductivity logs were run during this open-hole flow event. A major inflow zone at approximately 940 m produced the bulk of the outflowing 32 l/min, while the borehole flow direction was still down in the borehole below 1000 m.

After a third flushing with deionized water (FLU 3), the PIP system could be installed successfully. The pre-pumping conductivity logs (SF 3) showed a good flushing in the intervals 1000-1250 m and 1450-1520 m and a zone of higher salinity (up to 250 µS/cm) fluid in the interval 1250-1450 m. This saline slug was the result of formation inflow having occurred above the logged section and then having been displaced into the logged section during emplacement of the PIP configuration. The section between 988 and 1522 m was then pumped through the PIP at a constant rate of 3.0 l/min for approximately 60 hours (event PIP-RW1). The saline slug mass migrated upward and out of the system during logging, allowing a direct measurement of borehole velocities. In total, twelve electrical conductivity logs were measured.

In an effort to establish a better conductivity contrast between the inflowing and flushing fluids, the fourth flushing event (FLU 4) used a saline water (density: 1.003 g/cm^3) as the well-bore flushing fluid. The flushing (FLU 4) was performed through the double PIP system by using 1" coil tubing. The initial concentration in the isolated section was very constant at a conductivity of 4700 µS/cm. Again, the isolated section was pumped from above the PIP in the cased section (event PIP-RW2). The flow rate, as measured at the surface, was 1.5 l/min. A series of nine conductivity logs were run under constant pumping conditions over 48 hours. The conductivity logging test was accomplished with a six-hour recovery event (RWR).

3.1.3 Calibration and Data Conversion

After test completion, the depth readings of the electrical conductivity and temperature measurements were recalibrated to account for the observed drift in the depth measurement during the 10-day logging operation. The final accuracy in fracture location associated with depth errors can be estimated to be smaller than ±1 m.

The temperature-conductivity probes ST1 and ST2 were calibrated by GEOTEST using NaCl-solutions of different electrical conductivities (59, 145, 413, 507, 994, 2009, 5256, and 8077 μS/cm) and temperatures (5-80°C). The reduction of the measured conductivities to 20°C was performed directly in the field by interpolation from the existing laboratory calibration curves. The reader is referred to the field report GEOTEST/GEMAG (1989) for more details.

The electrical conductivity measurements are reported in units of μS/cm. The methods used to analyze the fluid logging data require that the conductivity measurements be converted to units of mass per unit volume. A sample fit between electrical conductivity and NaCl concentration has been presented by HALE and TSANG (1988), based on published data. For NaCl-solutions at 20°C, TSANG et al. (1990) derive the following quadratic relationship:

$$\sigma = 1870C - 40C^2 \qquad (3.1)$$

where σ is electrical conductivity in μS/cm and C is NaCl concentration in kg/m^3. This relationship has been used throughout this report to relate conductivity to concentration and *vice versa.*

3.1.4 Geochemical Sampling of Logged Section

Four hydraulic tests were performed with the primary or secondary purpose of characterizing the formation fluid within the section of the borehole defined between 1000 and 1522 m. Properties that are important to a conductivity log interpretation are formation fluid conductivity and formation fluid density. The formation fluid electrical conductivity gives us an expected value for the concentration of the inflowing formation water. The formation fluid density allows a better estimation of formation heads. The four tests are summarized below as to type and the cumulative fluid removed. The information comes from STEIGER and STEFFEN (1989).

Table 3.2: Summary of Tests Performed to Sample the Formation Fluid in the Interval 1000 to 1522 m b.g.

TEST NAME	TEST TYPE	APPARENT DEPTH (m b.g.)	FLUID REMOVED (m^3)
CR15	SW	1005.3 - 1017.8	NR
CR18	SW	1154 - 1163.9	2.15
CR19	RW	1154 - 1163.9	6.705
CR23	SW	1493.3 - 1498.6	26.441

SW = Slug Withdrawal
RW = Rate Withdrawal
NR = Not Reported

The test CR15 was a slug withdrawal test, but the transmissivity was so small (0.6 to 4.2E-9 m^2/sec) that effective sampling was not considered possible and therefore no results were reported. The second test (CR18) was again a slug withdrawal that did yield formation fluid parameters. The formation fluid electrical conductivity leveled off at 700 to 712 µS/cm with the drilling water tracer Uranin ending at a concentration of 1-4% of the initial concentration before testing. No density was reported. Test CR19 was a constant rate withdrawal of approximately 0.9 l/min for 131 hours. The electrical conductivity levelled off at 755 µS/cm and the Uranin was at a concentration of 1.5% of the initial level. The density leveled off at 995 kg/m^3. Test CR23 was a slug withdrawal where the electrical conductivity leveled off at 734 µS/cm and the Uranin concentration was present at 2.18% of initial concentrations at the end of the test. The density leveled off at 998 kg/m^3. The following table summarizes the characteristic formation fluid conductivities and densities.

Table 3.3: Summary of Characteristic Formation Fluid Properties from Tests Performed in the Interval 1000 to 1522 m b.g.

TEST NAME	FLUID CONDUCTIVITY (µS/cm)	FLUID DENSITY (kg/m^3)	URANIN CONCENTRATION (% Co)
CR18	700 - 712	NR	1 - 4
CR19	755	995	1.5
CR23	734	998	2.18

3.2 Conceptual Model and Analysis Approach

Electrical conductivity logs can be used to determine borehole flow rates, assuming there is volumetric inflow into the borehole and that volumetric inflow is of a different electrical conductivity, or concentration, than the background borehole fluid. Thus, the basic procedure is first to ensure that the background borehole concentration is different than the inflowing concentration. This is generally done by replacing the borehole fluid with a fluid of significantly greater or lesser concentration than that of the inflowing fluid. It is important for the background concentration to be as constant and monotonic in magnitude as possible. The next step is to produce the borehole with a constant flow rate that will create significant drawdown relative to suspected, or known, head differences within the logged interval. Before producing the borehole, a background or baseline conductivity log should be measured to define initial conditions. After production has begun, a time series of logs are measured over the depth interval of interest, and these logs are analyzed to determine inflow parameters.

Figure 3.1 shows a schematic diagram of a borehole which intersects three inflowing features. The logged interval is defined by the length AB. Each inflowing feature can be characterized as having a mass flux which is composed of volumetric flow rate (q_i) and inflowing concentration (C_i). In Figure 3.1, three conductivity logs have been measured at times $t_1 > t_2 > t_3$. The electrical conductivity peak is a product of the mass flux which flows into the borehole from the intersected permeable feature. When two such peaks overlap in space, they are said to interfere. For this model, we will assume that all features are producing to the borehole, and therefore it can be said that

$$\sum_{i=1}^{n} q_i = Q_A - Q_B \qquad (3.2)$$

and is constant. The parameters known prior to the analysis are Q_A, C_A, Q_B, and C_B, where Q_A and C_A are the volumetric flow rate and concentration measured at the top of the logged interval, boundary B, and Q_B and C_B are the same, measured at the interval bottom, boundary B. If the boundary B is defined as occurring at the bottom of the borehole, then Q_B and C_B are probably zero and need not be considered as system parameters.

The parameter which can be determined immediately after logging through inspection of the conductivity logs is the individual inflow locations (x_i). The parameters which characterize the mass flux from each inflow, the inflowing volumetric rate (q_i) and inflowing concentration (C_i), are not known prior to the analysis. The determination of q_i and C_i are not the analysis endpoint, as the desired final quantities are the individual inflowing feature transmissivities (T_i). The individual inflowing flow rates are used to calculate T_i. However, the discussion of this last analysis step will be put off until Section 5.

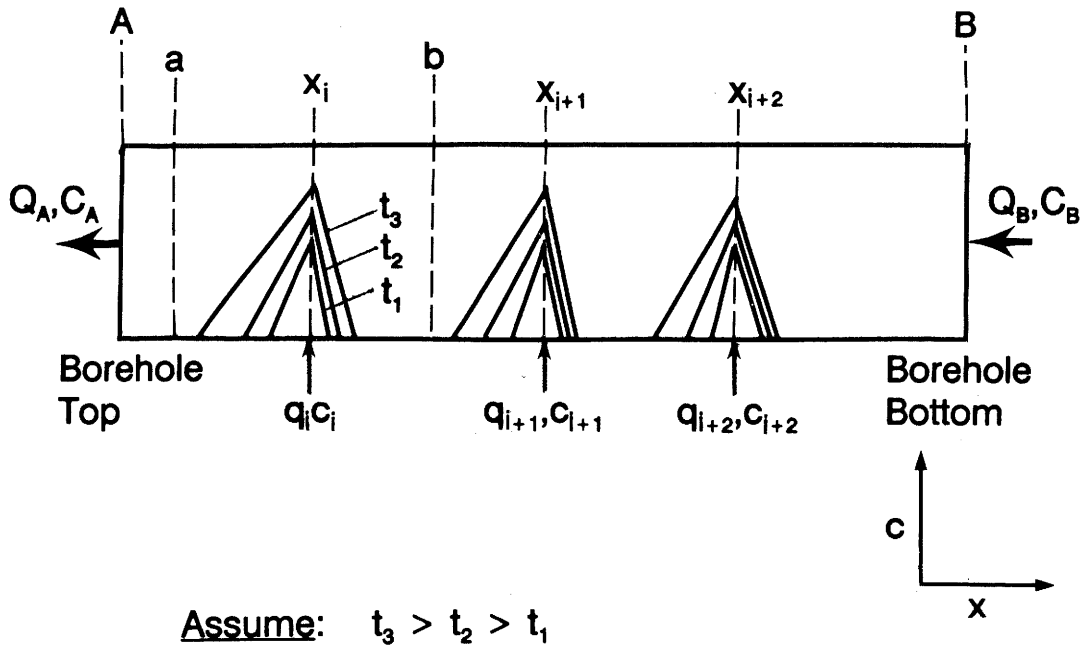

Assume: $t_3 > t_2 > t_1$

$$\sum_{i=1}^{n} q_i \text{ is constant}$$

$$\sum_{i=1}^{n} q_i = Q_A - Q_B$$

Parameters known prior to analysis:

Q_A, C_A, Q_B, C_B

Parameters determined through analysis:

x_i, q_i, C_i, T_i, H_i

Figure 3.1: Borehole Conceptual Model

Two major assumptions commonly applied when interpreting electrical conductivity logs are (1) that the volumetric flow rates from the outflowing fractures are constant as a function of time (as specified by Equation 2), and (2) that the concentration of the outflowing fluid is constant as a function of time and equal to that of the formation fluid. In many cases, these assumptions are not met. Because the flow rate produced from the logged interval is held constant by design, it is generally safe to assume that the individual inflow rates are also constant. However, because of non-artesian conditions in the logged interval, it is often the case that replacement fluid injected into the interval prior to logging gets mixed with formation waters in the individual inflows. In this case, the inflowing concentration will exhibit time dependence.

The primary variables of interest in electrical conductivity logs analysis are the location of the inflowing features (x_i) and the volumetric flow rate of each inflowing feature (q_i). Of secondary importance is the inflowing fluid concentration (C_i). The general procedure for analysis of the Siblingen electrical conductivity logs is outlined in Figure 3.2. The fundamental elements of this analysis methodology are reproduced from LOEW et al. (1990). This procedure, which is new compared to the previous analysis of electrical conductivity data (e.g., TSANG et al., 1990), allows the parameters of interest to be calculated through various methods. The decision of which method is best to use is made based on the character of the conductivity logs and the time dependence of inflowing volumetric rates and concentrations.

The first step (not considered in Figure 3.2) is to locate inflowing features through inspection of the logs. This step takes place in the field and is later refined by a more detailed analysis. From Figure 3.2, it can be seen that the first computational step is to determine the time dependence, if any, of the average inflowing concentration denoted C_{AB}. Once the function $C_{AB}(t)$ is defined, the next analysis step is to estimate the volumetric inflow rate for individual intervals (q_i) for non-interfering concentration peaks. By *non-interfering* it is meant that the individual concentration does not overlap another concentration peak emanating from a different inflow (as in Figure 3.2). This generally limits the analysis to early time logs. The two methods by which q_i can be estimated are (1) Zero Moment relationships with the assumed knowledge of C_i, or (2) Zero and First Moment relationships where C_i need not be assumed. Finally, a detailed parameter set (q_i,C_i) can be calculated for both interfering and non-interfering peaks, either through the Method of Partial Moments (LOEW et al., 1990) or by using the numerical borehole simulator, BORE (TSANG et al., 1990). This study used the Method of Moments as the primary detailed analysis tool, and BORE was used as a validation tool.

The basis behind the various interpretation methodologies is discussed in limited detail in the following sections. For a complete description of the application of MOMENT methods, and particularly the application of the Method of Partial Moments to electrical conductivity logs, the reader is referred to LOEW et al. (1990). For detailed information on the borehole simulator BORE, please refer to HALE and TSANG (1988) and TSANG et al. (1990). The Direct Integral Approach for the analysis of a detailed parameter set was not applied in this report.

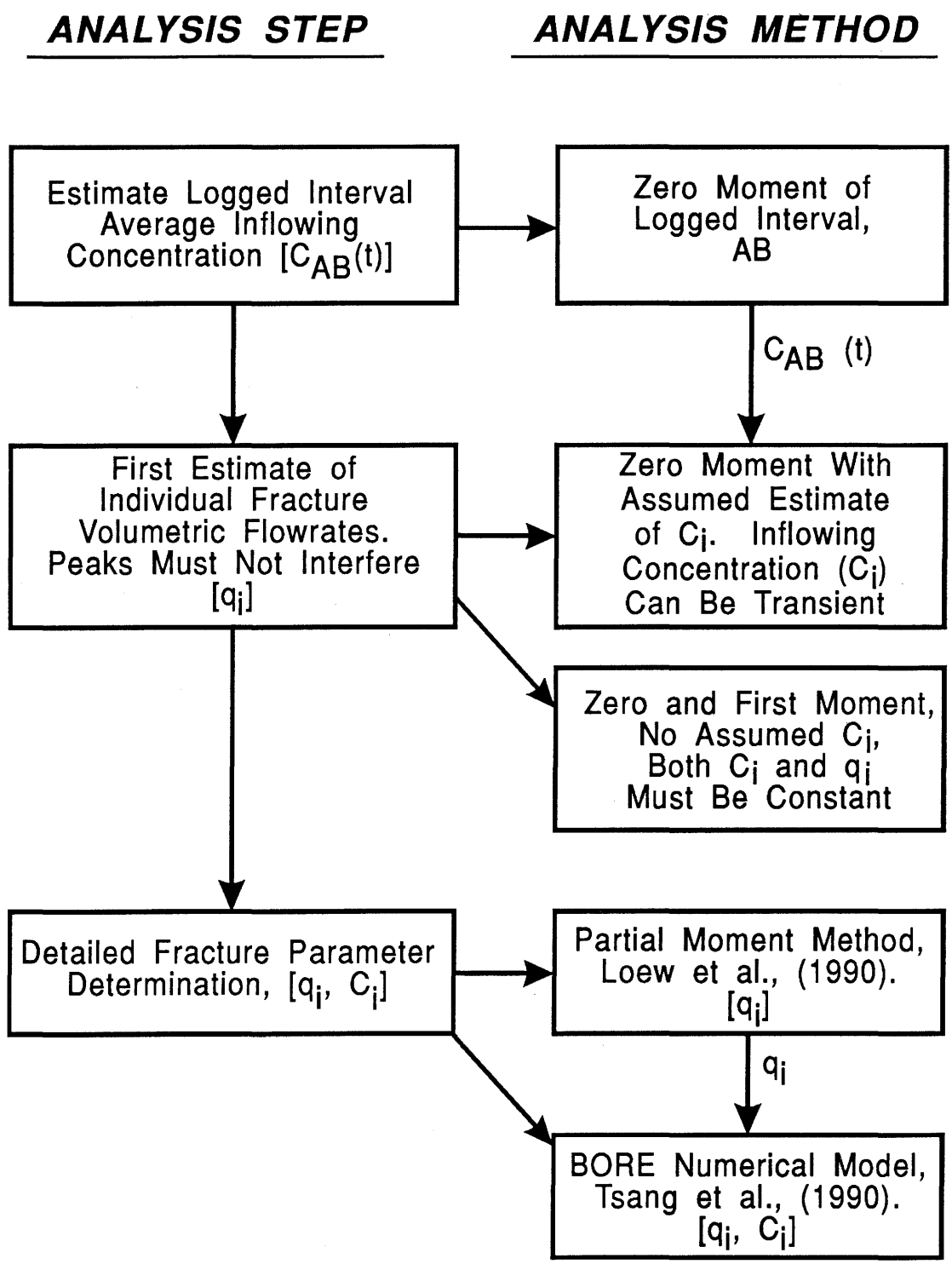

Figure 3.2: Steps to Analysis and Methodologies Applied

3.2.1 Classical Definition of the Moment

Before discussing the analysis methods in detail, it is necessary to define in general terms the meaning of the moment. The classical n_{th} moment of a concentration distribution in (x,C) space is

$$M_n = \int_{-\infty}^{\infty} x^n \, C(x,t) \, dx \tag{3.3}$$

where M_n is the moment of order (n), x is distance, and C is concentration (FISCHER et al., 1979). The classical zero moment is related to the area under a concentration distribution (mass), the classical first moment is a measure of the location of the center of mass of the concentration distribution (mean), and the classical second moment is a measure of the spread about the center of mass (variance). Therefore, for the normal distribution, M_0 is equal to 1, M_1 would be equal to 0.0, and M_2 would be equal to the distribution variance ($\sigma^2 = 2Dt$), where D is a Fickian dispersion coefficient. For a concentration slug moving in a tube, the zero, first, and second moments have likewise been associated with the mass, velocity, and the dispersion constant of the slug as it moves through the tube.

3.2.2 Determination of Average Inflowing Concentration

The desired flow boundary condition during most fluid logging tests is to pump the logged interval at a constant rate where the total volume produced comes from this logged interval. For this case, the total (summed) volumetric fracture outflow rate as a function of time, $\Sigma \, q_i \, (t)$, corresponds directly to the surface readings of the total pumping rate of the well (Q_w), assuming Q_B is zero. In this case, the steadiness of the total measured flow rate can be used as an estimation of the steadiness of the individual fracture outflow rates q_i. In the case of fracture outflows above the logged section, the time dependence of total flux can still be derived, although the absolute fluxes are no longer deducible. Where major outflowing zones exist with substantially different transmissivities than the remaining outflows, these zones may generate constant head conditions in the borehole, which in turn induce non-constant fracture outflows. Such major outflows can be found either in the logging section itself or above it. As previously stated, here Q_w is assumed to be constant.

The mass balance of a given logging interval AB (Figure 3.1) can be expressed (LOEW et al., 1990) as:

$$M_0(t)\pi r_w^2 = C_0(B-A)\pi r_w^2 - \sum_{i=1}^{n} q_i + Q_A \int_{t_o}^{t} C_A(t)\,dt + Q_B \int_{t_o}^{t} C_B(t)\,dt + \sum_{i=1}^{n} q_i \int_{t_o}^{t} C_i(t)\,dt \qquad (3.4)$$

where time (t) is the time the mass balance is evaluated (equal to some logging time), t_o is the time when production from the well starts, C_0 is the initial concentration evaluated at t_o, and $M_0(t)$ is equal to the zero moment of the logged interval AB equated at time t and defined as

$$M_0(t) = \int_{A}^{B} [C(x,t) - C_0(x)]\,dx \qquad (3.5)$$

where concentration has units of mass per unit volume. From this equation, it can be seen that the zero moment when multiplied by the area of the borehole is equal to the mass under the conductivity curve evaluated from A to B. The left-hand side of Equation 3.4 represents the mass in the logged interval (defined by AB) at time t, the first term on the right-hand side represents the initial mass in place, the second term represents the mass exiting the upper boundary A, the third term represents the mass entering the interval A-B from inflowing features, and the last term represents the mass entering interval A-B from the bottom boundary B. The sum mass flux of all inflowing features between A and B can be equated to an average inflowing mass flux for the interval A to B, and is written

$$\sum_{i=1}^{n} q_i \int_{t_o}^{t} C_i(t)\,dt = \sum_{i=1}^{n} q_i \int_{t_o}^{t} C_{AB}(t)\,dt \qquad (3.6)$$

where C_{AB} is equal to the average inflowing concentration over the logging interval AB. If we can assume that Q_B and C_B are zero, the mass balance equation (3.4) can be rewritten in terms of the average mass flux entering the borehole over interval A to B and appears as

$$M_0(t)\pi r_w^2 = C_0(B-A)\pi r_w^2 + \sum_{i=1}^{n} q_i + Q_A \int_{t_o}^{t} C_A(t)\,dt + \sum_{i=1}^{n} q_i \int_{t_o}^{t} C_{AB}(t)\,dt \qquad (3.7)$$

The zero moment as a function of time is calculated numerically by MOMENT (LOEW and CALMBACH, 1990). The only unknown in Equation 3.7 is $C_{AB}(t)$, which can be approximated by the following equation.

$$C_{AB}(t) = \frac{\left[M_0(t+1)\pi r_w^2 + \sum_{i=1}^{n} q_i \int_{t_o}^{t+1} C_A(t)\,dt\right] - \left[M_0(t-1)\pi r_w^2 + \sum_{i=1}^{n} q_i \int_{t_o}^{t-1} C_A(t)\,dt\right]}{\sum_{i=1}^{n} q_i[(t+1) - (t-1)]}$$

Through the estimation of the average inflowing concentration over the logged interval as a function of time, one can determine if it is transient and also if it is representative of the formation fluid. This helps in deciding what methods should be used in further analysis steps.

3.2.3 First Guess Fracture Outflow Parameters

This report uses two different approaches to estimate the first guess volumetric inflow rate from individual peaks. Both methods require that the conductivity peaks are not interfered with. These two methods are described briefly in the following discussion.

The first method requires calculation of the zero moment of a non-interfered peak such as the peak located at x_i in Figure 3.1. The zero moment of this peak can be defined as

$$M_0(t) = \int_{b}^{a} [C(x,t) - C_0(x)]\,dx \qquad (3.9)$$

Because the zero moment measured between points a and b is related to the mass under the conductivity log by the constant borehole area, and because the peak is considered to be non-interfered with, the zero moment is composed of the product of peak volumetric inflow rate (q_i) and the peak inflow concentration (C_i). If one assumes that the average inflow concentration calculated for the entire logged interval C_{AB} is equal to the individual inflowing peak concentrations C_i as a function of time, then the individual peak volumetric inflow rates can be estimated through classical zero moment analysis of the individual peaks. As Equation 3.4 is a mass balance for the entire logged interval AB, the following equation is a mass balance equation for the interval straddling the interval ab and containing the inflow i (see Figure 3.1):

$$M_0(t)\pi r_w^2 = C_0(b-a)\pi r_w^2 + q_i \int_{t_o}^{t} C_{AB}(t)\,dt + \int_{t_o}^{t} q_i(t)C_{AB}(t)\,dt - C_0 \int_{t_o}^{t} q_i(t)\,dt \qquad (3.10)$$

The zero moment can be evaluated numerically by MOMENT, leaving the only unknown in Equation 3.10 to be q_i, which is solved for. With this method, one can solve for q_i even under conditions where the inflowing concentration is time dependent.

A second method can be used to estimate an individual inflow volumetric rate. This method assumes that both q_i and C_i are constant with respect to time. However, this method does not require *a priori* knowledge of C_i. This method does require that C_0 is constant, or nearly constant, over the moment integration intervals (i.e., a to b).

Figure 3.3 shows a time series of electric conductivity logs which are defined by an inflow at x_i. This method requires the calculation of the first moment centered about the fracture outflow x_i, which can be written

$$M_1(t) = \int_{b}^{a} (x-x_i)\,[C(x,t) - C_0(x,t)]\,dx \qquad (3.11)$$

where a and b define the integration boundaries and C_a and C_b are equal to C_0. The method also requires evaluation of the zero moment upstream and downstream of the inflow at x_i. These zero moments can be written explicitly as

$$M_{0+}(t) = \int_{x_i}^{b} [C(x,t) - C_0(x)]\, dx \qquad (3.12a)$$

$$M_{0-}(t) = \int_{a}^{x_i} [C(x,t) - C_0(x)]\, dx \qquad (3.12b)$$

These moment quantities can be numerically evaluated by MOMENT. With these moment quantities calculated, one can estimate the downstream well-bore velocity with the relationship taken from LOEW et al. (1990)

$$M_{1t} = V_+ M_{0+} + V_- M_{0-} \qquad (3.13)$$

where M_{1t} is defined as the time derivative of the first moment, V_+ and V_- are the upstream and downstream borehole velocities, and M_{0+} and M_{0-} are the upstream and downstream zero moments. If one had a series of non-interfered peaks as in Figure 3.1, then one could start such an analysis at the bottom peak located at x_{i+2}. If one could assume that the velocity upstream to x_{i+2} is zero, then Equation 3.12 simplifies to having one unknown, the downstream flow velocity (V_-). Once this is known, the analysis can move upstream to the peak located at x_{i+1} where the upstream velocity has just been calculated. Again, there is only one unknown, the downstream velocity.

With the individual peak volumetric flow rates defined (q_i) and the average inflowing concentration (C_{AB}) defined, one has a first guess parameter set to guide the detailed analysis.

3.2.4 Detailed Fracture Outflow Parameter Determination

Very often, the electrical conductivity peaks interfere even at early times. In this case, determination of q_i is not possible by the techniques described above. It may be that some percentage of the peaks observed can be analyzed by the methods described above, whereas the rest of the peaks interfere too badly for these methods to be applicable. For this case, two methods have been used to determine each peak's volumetric flux (q_i). The first method is the Method of Partial Moments (LOEW et al., 1990), and the second method is through the use of the numerical borehole simulator BORE (TSANG et al., 1990). A comparison between the approaches is listed in Table 3.4.

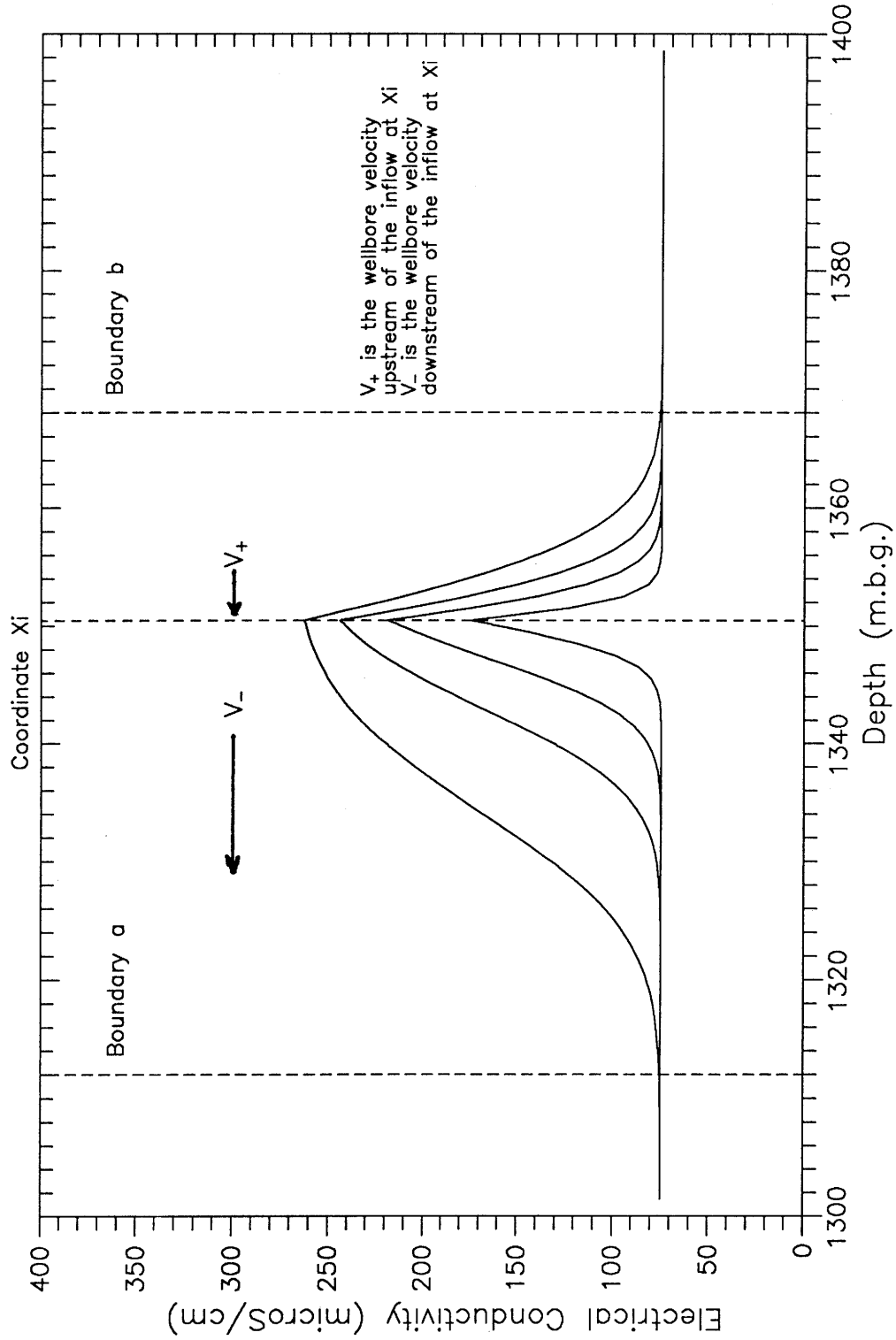

Figure 3.3: Example of Classical First Moment Application on an Inflow Centered at Coordinate Xi

Table 3.4: Methods and Tools for the Detailed Analysis of Electrical Conductivity Logs

METHOD	CODE	ASSUMPTIONS	REFERENCE
Partial Moment	MOMENT	• 1D Advective diffusive transport	LOEW et al. (1990) LOEW and CALMBACH (1990)
Numerical Simulation	BORE	• 1D Advective diffusive transport • Constant outflow concentration • Constant volumetric outflow	TSANG et al. (1990) HALE and TSANG (1988)

The primary method used to analyze the Siblingen conductivity logs is the Partial Moment Method, which is well presented in LOEW et al. (1990). This method will not be explained in this report. This is a direct analysis method and therefore relatively quick compared to the trial and error approach with the numerical simulator, BORE. Unlike classical moments defined thus far, the integration boundaries for evaluation of the partial moments must not straddle an inflow. The method does not require that the concentrations at the integration boundaries be equal to C_0. Therefore, it can also handle data from interfering peaks. The borehole velocity is calculated based on the derivative of the partial moment quantities. The assumptions of the method are that of constant volumetric flux and constant dispersivity within the integration interval over the time interval defining the time derivatives. Theoretically, this means that the method will yield approximately valid results if the parameters q_i and C_i are not changing significantly on a time scale less than or equal to the time series of the measurement of logs.

The Method of Partial Moments can have problems due to numerical problems associated with measurement "noise" and the derivation of proper time derivatives of the partial moment quantities. However, in practice these problems can be overcome by weighting the individual fracture outflow values based on criteria derived in LOEW et al. (1990). These criteria are the magnitude and slope of the partial moments as a function of time.

BORE is a finite-difference code that can simulate borehole electrical conductivity logs. Through trial and error conditional simulations, one can adjust input parameters q_i and C_i until a satisfactory calibration to the measured logs is obtained. Unlike the Method of Partial Moments, BORE can yield individual inflowing concentrations in addition to individual volumetric flow rates.

In this report, the individual volumetric flow rates were derived by applying the Method of Partial Moments for the two full logging suites (PIP-RW1 and PIP-RW2).

Then, with these individual flow rates and the logging interval average inflowing concentration ($C_{AB}(t)$), BORE was used to cross-validate the MOMENT results through a pseudo-transient restart method.

All fluid logging events were analyzed in the chronological order of their execution, with the exception of events PIP-RW1 and PIP-RW2. The complete analysis of PIP-RW1 was enhanced by prior knowledge of results from PIP-RW2. Therefore, the order of the analyses as presented in this report is non-chronological. The complete analysis approach, as outlined in Figure 3.2, could only be performed on PIP-RW2. All other events either had insufficient logs or model assumption/ boundary condition conflicts with the various methods. For these events, shortened or modified analysis strategies were applied.

3.3 Analysis of the First Static Fluid Logging Event, SF-1

3.3.1 Initial Conditions

Prior to the first fluid logging event, the borehole was flushed from bottom to top with deionized water (event FLU 1). The objective was to establish a good background concentration in the borehole that was of a lesser electrical conductivity than the formation fluid. After flushing, an attempt was made to install a production-injection packer system (PIP) which would isolate the lower crystalline section (1000 to 1520 m) from the highly transmissive upper crystalline section (536 to 1000 m). The attempt was unsuccessful because the PIP could not be installed.

Three electrical conductivity logs were measured in the borehole at times 4.37, 6.57, and 8.45 hours after the end of flushing. These logs measured conductivity over the depths 900 to 1518 m, 1000 to 1518 m, and 930 to 1020 m respectively. Figure 3.4 plots the three conductivity logs measured as a function of depth. Before further discussion of the logs a brief explanation of the flushing procedure is in order.

The borehole flushing was performed by displacing the borehole fluid in the logged interval with deionized water. First a 3-inch-diameter injection tubing was lowered to the bottom of the borehole (approximately 1520 m). At this point, borehole water filled the tubing. Next, the volume of deionized water required to fully displace the inside volume of the tubing was injected into the tubing from the surface (6.9 m^3). At this point the tubing was filled with deionized water to the total depth of the borehole. From here, the tubing was moved up the borehole from the bottom (1520 m) to the top (900 m) of the logged section in 90-m steps. Enough water was injected at each station to displace the annular volume (0.24 m^3) between stations. A total of 5.74 m^3 of deionized water was injected into the borehole. Assuming that none of the injected fluid is lost to the formation, this should allow for full displacement of the borehole volume from 1520 m to 728 m.

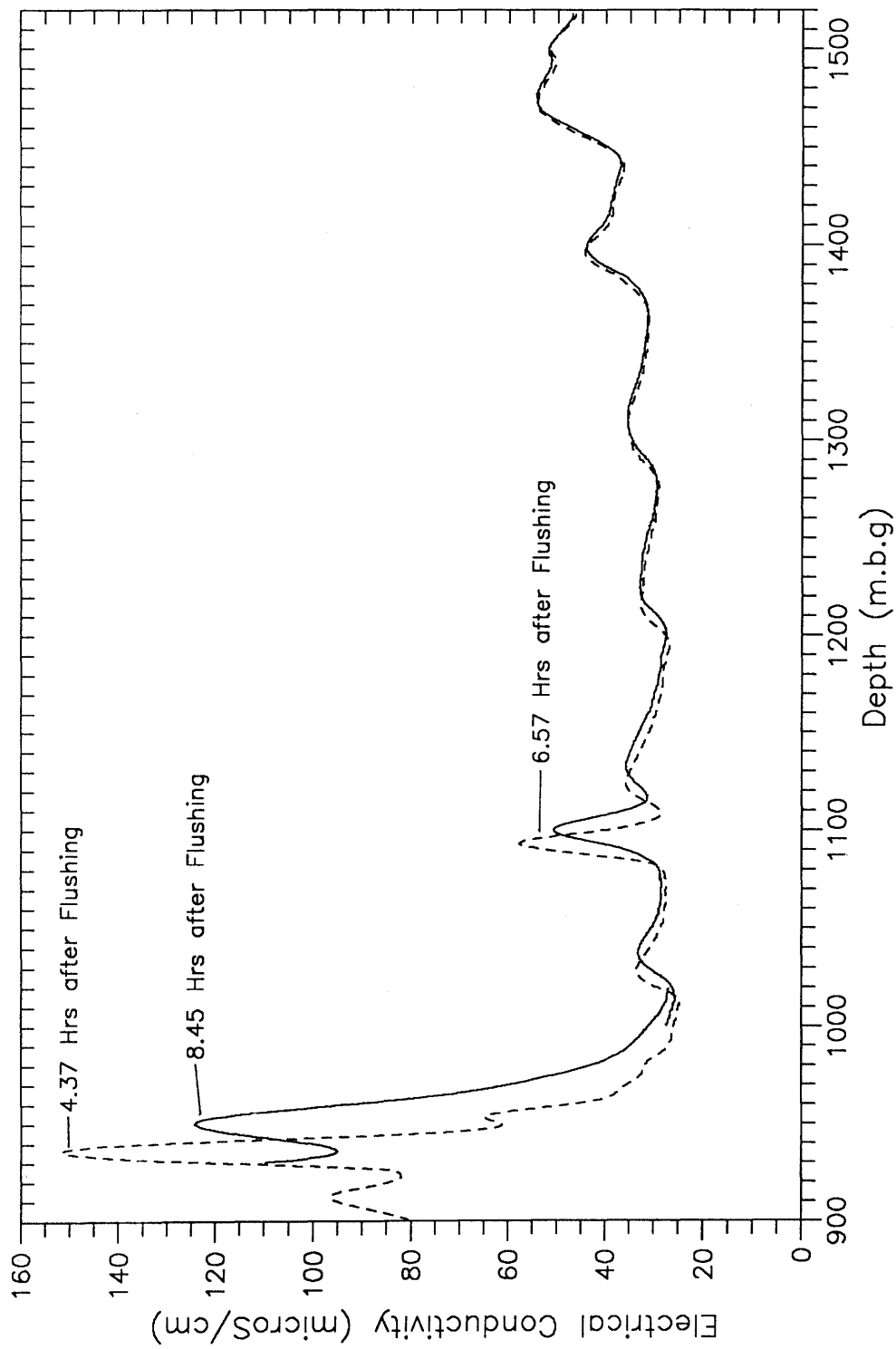

Figure 3.4: Conductivity Logs Measured During the First Static Flow Period, Fluid Logging Event SF-1, Siblingen Borehole

Examination of the measured logs reveals conductivity peaks (maximums) throughout the length of the logged section which coincide roughly with the midpoint elevation between two flushing displacement stations. This is interpreted to mean that flushing was inefficient between stations and that some percentage of the injected fluid was lost to the formation. From inspection of the logs one would expect that the flushing procedure was most inefficient between the depths 900 and 1000 m. The two largest salinity maximums (between 936 m and 950 m and between 1093 m and 1100 m) coincide with known breakouts in the borehole. These areas are not flushed well because of decreased circulation due to expanded borehole diameter. The area from 900 to 950 m is uneven, and there is a small breakout (100 mm) in the borehole wall at approximately 1085 m (SATTEL and BLUMLING, 1990).

Another possible reason for the observance of salinity peaks between 900 and 1000 m is the production of formation water into the borehole at these depths. This is not supported by the data, for two reasons. First, the mass present under the salinity peaks does not increase with time, which it should if mass flux was occurring. Also, internal borehole flow rates measured during various flowmeter logging events do not support inflows in this interval. Packer-flowmeter tests performed one week prior to SF-1 (see Section 2.5.3) revealed that the portion of the borehole between depths 660 to 955 m is very complicated hydraulically under static conditions. The spinner-packer flowmeter found evidence of internal borehole flow where formation fluid entered the borehole from 690 to 708 m (borehole flow rate -2.0 l/min) and exited the borehole from depths 770 to 955 m. The observed borehole flow rate below 930 m was below detection, implying that nearly all the inflowing fluid entering from 690 to 708 exited between 708 and 930 m. The spinner-packer flow meter detection limit is around 0.3 l/min with an error of $\pm$0.2 l/min. The Heat-Pulse flowmeter results measured at a later time also indicated internal flow under no-stress or static conditions. In this log, the downward flow was again entering the borehole above 708 m (-1.1 l/min) and this was exiting between 925 and 930 m, except for -0.3 l/min that was detected between the depths of 1210 and 1276 m. The Heat-Pulse Flowmeter detection limit is 0.1 l/min, with an error of 0.05 l/min. The implications of the observed internal borehole flow rates measured during open borehole, static conditions are discussed in detail in Section 4.

3.3.2 Internal Borehole Flow Rates, SF-1

The only quantitative analysis possible with these logs is to use the salinity slugs present due to poor flushing to determine the internal borehole flow rates as a function of borehole depth. By monitoring the peak movement for a given peak between logs, one has a direct measurement of borehole velocity and direction over the logged section under static conditions. Inspection of the conductivity logs measured at 4.37, 6.57, and 8.45 hours after flushing shows that there was internal borehole flow down the borehole during this static event, and thus the permeable features present below 960 m were taking in fluid from the borehole. The peaks in the upper portion of the borehole travel a larger distance down the borehole than those in the lower portion, implying that the borehole fluid velocity decreases with depth.

For analysis, the distance traveled by each peak is divided by the time between measurements to get a borehole velocity. This velocity can then be divided by the borehole area to get a borehole flow rate. Table 3.5 summarizes the borehole flow rates as determined by this method.

Table 3.5: Estimated Internal Borehole Flow Rates as Determined for Fluid Logging Event SF-1

Borehole Interval (m)	Borehole Flow Rate (l/min)	Estimated Error Range (l/min)
936 - 950	-0.42	-0.39 - 0.45
1027 - 1040	-0.54	-0.49 - 0.60
1093 - 1100	-0.40	-0.36 - 0.42
1123 - 1131	-0.45	-0.37 - 0.53
1219 - 1225	-0.35	-0.24 - 0.46
1397 - 1400	-0.17	-0.12 - 0.23

The estimated error is subjective and based upon the degree of uncertainty in identifying the peak concentration location (z). Generally the broader the peak, and the smaller the magnitude of the peak, the more uncertain the estimate. For this reason, the estimated error is not constant between measurements. Peaks located between depths 1300 and 1330 and between 1460 and 1480 m could not be identified with enough certainty to make the measurements meaningful.

As can be seen, the borehole flow rates do decrease with depth as would be expected. An anomalous apparent increase in borehole flow rate occurs over the interval 1027 to 1040. This estimate is considered suspect. It is possible that the static flow rates measured in this event are in fact transient and that the measurement of flow rate for the interval 936 to 950 is lower because of the larger time period over which it was measured. It is also possible that, because of breakout, the borehole is of a larger diameter in the interval 936 to 950 m. This would result in the observed velocity distribution, calculated assuming borehole diameters were constant. Given the error estimates, the flow rates are in the order of -0.4 to -0.45 l/min until below a depth of 1131 m. It appears that some decrease of downward borehole flow occurs between 1131 and 1219 m. It appears that approximately 0.05 to 0.1 l/min is exiting the borehole through the permeable fracture at 1163.5 m (peak 10). By the interval 1397 to 1400, the downward borehole flow rate has decreased by approximately 50 to 70% of that flowing past a depth of 1130 m.

3.4 Analysis of the Second Static Fluid Logging Event, SF-2

3.4.1 Initial Conditions

Prior to the second static fluid logging event, the borehole was again flushed from bottom to top with deionized water but in a slightly different method than was used in SF-1. Again, the objective was to establish a good background concentration in the borehole which was of a lesser electrical conductivity than the formation fluid. Because installation of a double production injection packer (PIP) failed in the first attempt, in this exercise it was decided to measure logs under production conditions in an open borehole. Before this event there was an approximate 11-hour static fluid logging event (SF-2) where two conductivity logs were measured.

Two electrical conductivity logs were measured in the borehole at times 5.08 and 7.23 hours after the end of flushing. These logs measured conductivity over the depths 900 to 1516 m, and 900 to 1120 m respectively. Figure 3.5 plots the two conductivity logs measured as a function of depth. Before further discussion of the logs a brief explanation of the flushing procedure is in order.

As in FLU 1, the borehole flushing was performed by displacing the borehole fluid in the logged interval with deionized water. First a 3-inch-diameter injection tubing was lowered to a depth of 800 m. Next the volume of deionized water required to fully displace the borehole from 0 to 800 m was injected into the tubing from the surface (5.7 m^3). From here the tubing was moved down the borehole to the bottom (1522 m) and here 5.41 m^3 of distilled water was injected which was slightly more than enough to fill the borehole volume from 800 to 1522 m. This assumes that none of the injected fluid is lost to the formation. This one step displacement of the logging section was thought to be advantageous over the stepped approach in that it would not leave a regular pattern of salinity peaks in the borehole.

As it turned out, some peaks were still apparent after this flushing event and salinity steadily increased as you went up the borehole. Two areas of increased salinity were at the depths of 900 to 950 m and 1089 which is almost exactly where these peaks were in the first flushing and flow event. This again is thought to be the result of borehole breakouts in these intervals. Further, the conductivity log measured 5.06 hours after flushing detected four additional salinity peaks at depths 1252 m, 1389 m, 1423 m, and 1502 m. The presence of the peaks is again not thought to be the result of inflow, but rather is the result of poor flushing near breakouts. From knowledge gained in logging event PIP-RW2 (presented later in Section 3.6, Table 3.9), it can be seen that each of these peaks closely coincides with a transmissive feature. The displacement of the concentration peaks observed with discrete transmissive zones decreases from a maximum of 8 m at 1260 m to a minimum of 2 m at 1502 m. This trend supports internal borehole flow in a down borehole direction.

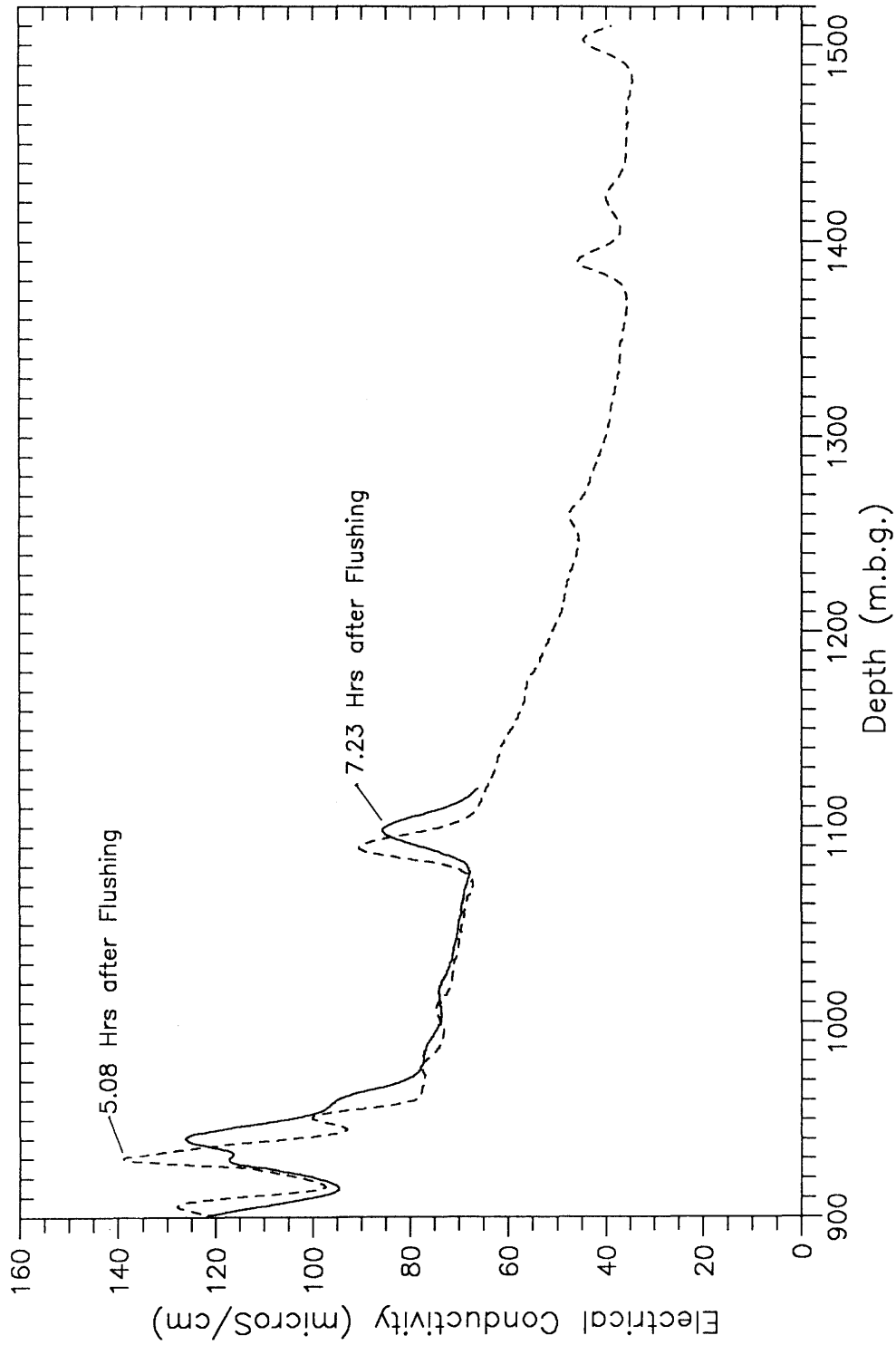

Figure 3.5: Conductivity Logs Measured During the Second Static Flow Period, Fluid Logging Event SF-2, Siblingen Borehole

3.4.2 Internal Borehole Flow Rates, SF-2

The only quantitative analysis which is possible with these logs is to use the salinity slugs present to determine the static borehole flow rates as a function of borehole depth. Monitoring the peak movement for a given peak between logs provides a direct measurement of borehole velocity and direction over the logged section under static conditions. From inspection of the two conductivity logs measured at 4.08 and 7.23 hours after flushing, it is evident that during this static event the borehole flow was down the borehole. For analysis, the distance traveled by each peak is divided by the time between measurements to get a borehole velocity. This velocity can then be divided by the borehole area to get a borehole flow rate. Table 3.6 summarizes the borehole flow rates as determined by this method.
2

Table 3.6: Estimated Internal Borehole Flow Rates as Determined for Fluid Logging Event SF-2

BOREHOLE INTERVAL (m)	BOREHOLE FLOW RATE (l/min)	ESTIMATED ERROR RANGE (l/min)
930 - 940	-0.56	-0.5 - 0.64
1089 - 1098	-0.48	-0.38 - 0.58

The estimated error is based on the degree of certainty in identifying the peak concentration location (z). For broad peaks at low peak concentrations, the definition of this maximum is more uncertain than for more definite (sharp) peaks. For this reason the estimated error is not constant between measurements.

As can be seen, the borehole flow rates appear to decrease with depth as would be expected in the case of down borehole flow. The flow rate does appear to decrease slightly between the two peaks but because of the uncertainty in the measurements this cannot be determined for sure. Estimates of transmissivity using Dupuit's Formula will be performed in Section 5.

3.5 Open Hole Constant-Rate Withdrawal Test, OH-RW1

3.5.1 Initial Conditions

After the second static flow event, the borehole was pumped at a constant production rate of 32 l/min for approximately 13.58 hours. The event was performed under open hole conditions as a result of problems installing a PIP. The pumping started on April 16, 1989 at 20:02 and ended on April 17, 1989 at 9:37. Figure 3.6 is a plot of the flow rate as measured at the surface (GEOTEST/GEMAG, 1989).

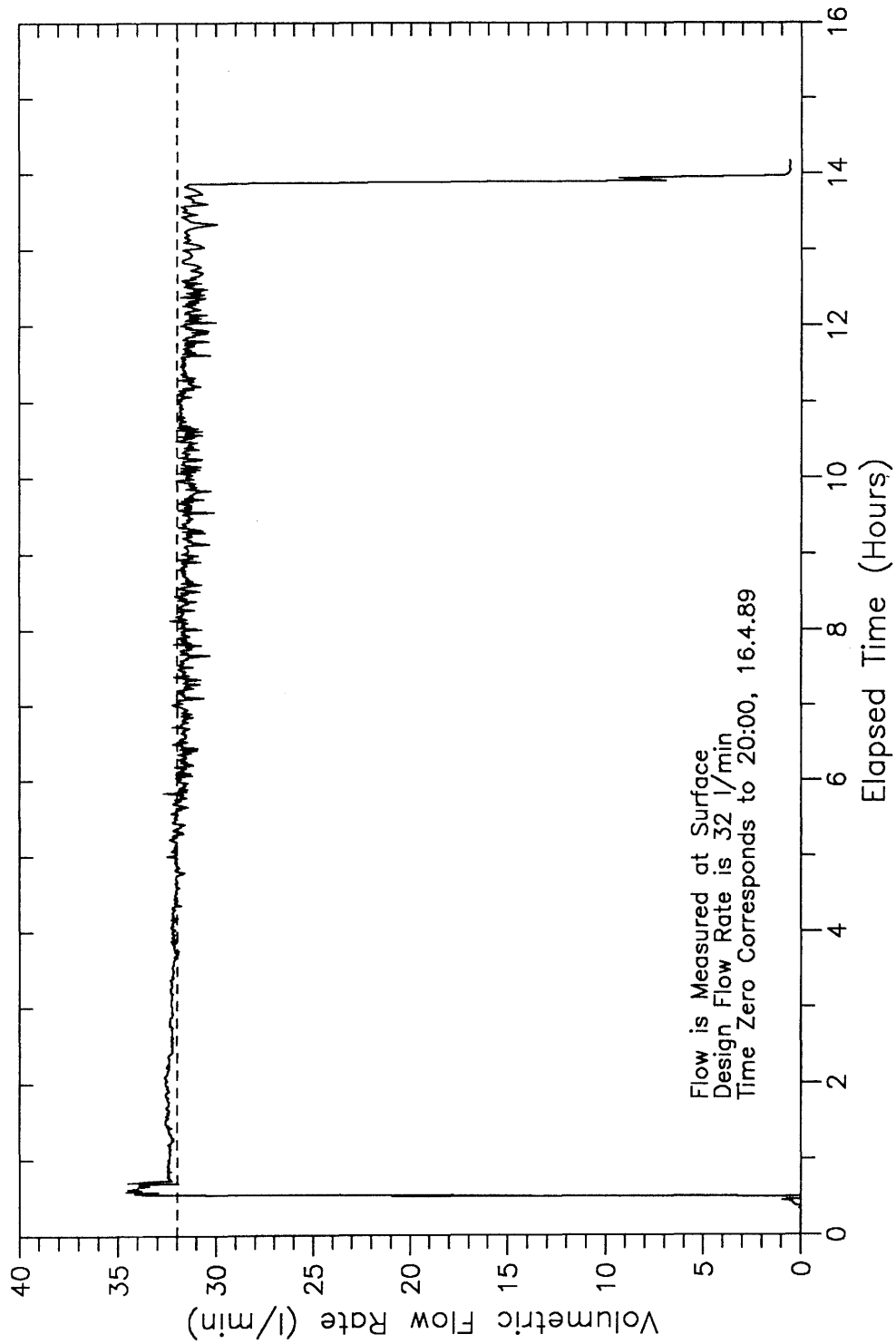

Figure 3.6: Flow Rate Measured at the Surface During the Open Hole Rate Withdrawal Test, Event OH-RW1, Siblingen Borehole

As can be seen, the flow rate is maintained at a relatively constant design flow rate of 32 l/min for the majority of the test period, with a slightly decreasing trend. Figure 3.7 plots the pressure as measured by transducer P3 at an elevation of 375.16 m a.s.l. As can be seen in the plot, the pressure in the borehole increased prior to pumping approximately 2 kPa (0.2 m). The last pressure recorded prior to pump on was approximately 758 kPa which corresponds to an equivalent freshwater head of 442 m a.s.l. This value corresponds well with the observed open borehole head measured during long-term monitoring from May to November 1989 of between 441.73 to 442.11 m a.s.l. (VOMVORIS et al., 1990). The drawdown during pumping was approximately 0.65 m, which is extremely small for this flow rate and implies a very high transmissivity of 1.3E-3 m^2/s.

Four conductivity logs were measured in the open borehole after pumping began (Figure 3.8). These were recorded 3.08, 5.47, 8.97, and 12.13 hours after pumping began. The broken line represents the background log taken during the static flow event 2 (SF-2) and was measured 5.08 hours after flushing ended. A slight salinity maximum exists in the borehole at a depth of 1090 m after flushing and prior to pumping. As can be seen, the zone above 970 m produced fluid into the borehole during the pumping event and the produced fluid moved up the borehole. Fluid was also produced from the interval between 1060 and 1100 m (specifically at peaks 11, 12, and 13 at depths of 1083.3, 1078.7 and 1070.4 m respectively). The primary inflow appears to be at 1078.7 m. An important point to be made is that the fluid flowing from these areas is travelling down the borehole contrary to the inflows above 970 m. If we assume that the interval between 1060 and 1100 was not flowing prior to pumping, then this would imply that the head in this interval was less than 442 m.

If pumping causes a drawdown of 0.65 m and the interval begins to flow, this implies that the head in this interval is between 442 and 441.35 m a.s.l. This is slightly greater than the equivalent freshwater head estimated by hydraulic test CR28 of 440 m a.s.l. (OSTROWSKI and KLOSKA, 1990). It is not surprising that there may be a discrepancy, as the head controlling vertical flow in the borehole is the environmental head. With higher transmissive zones located above this interval controlling the head response in the borehole, the interval was probably maintained under constant head conditions and therefore we would expect the flow rate to be transient.

3.5.2 Calculation of Inflowing Volumetric Rate and Inflowing Concentration

The analysis procedure for the peaks observed in the borehole section below 1000 m is based on simple tracer slug tracking and classical zero and first moment analysis.

The zero moment calculated from each log in the interval 1040 to 1200 m represents the mass in place at the time the log was measured. If this varies as a linear function of time, one can assume that the mass flux into the interval is constant and represented by the slope of the best fit line. Figure 3.9 is a plot of the zero moment (kg/m^2) as a function of time for the borehole interval 1040 to 1200 m.

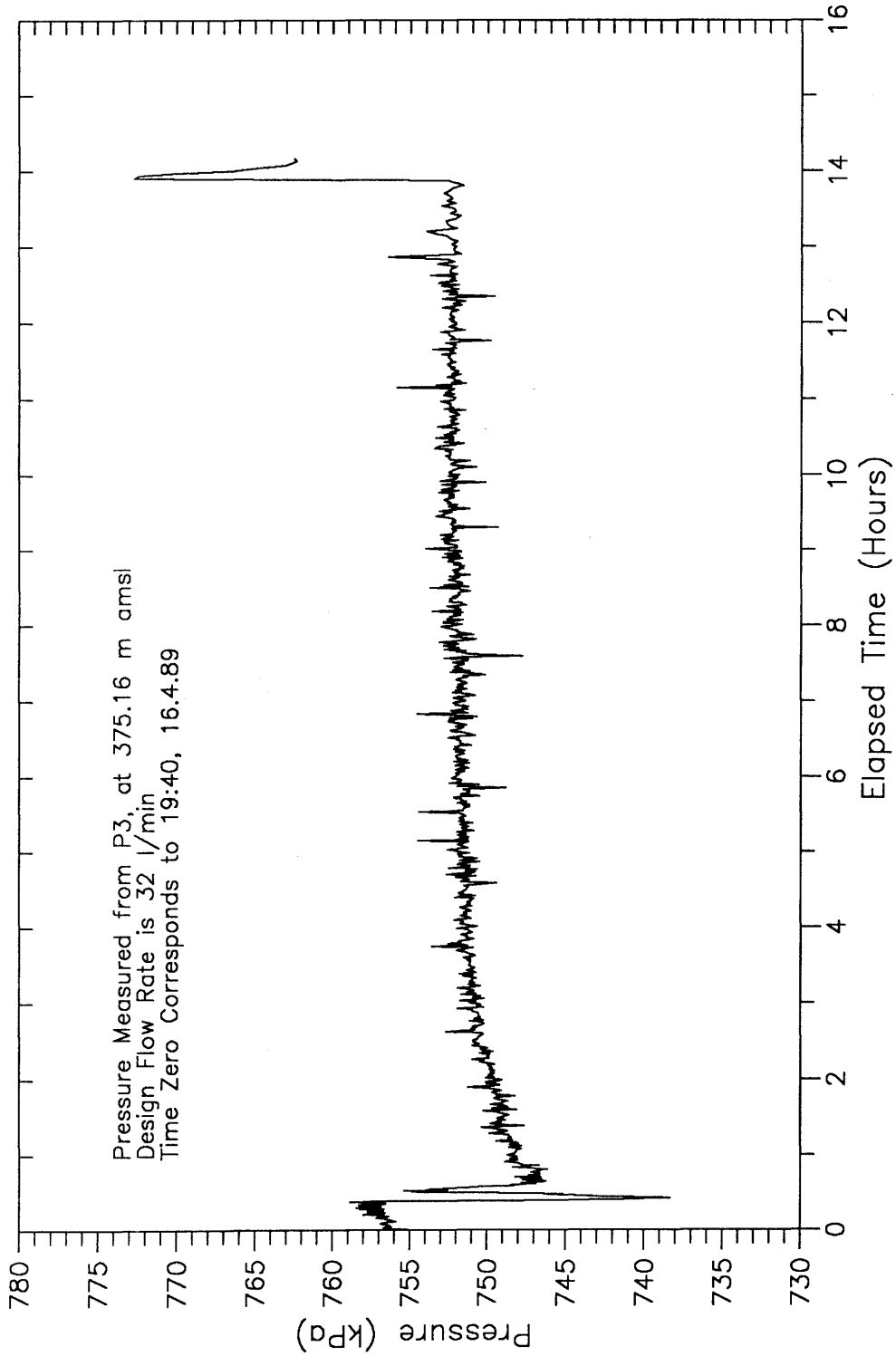

Figure 3.7: Pressure Measured at Transducer P3, 375.16 m a.s.l., Open Hole Rate Withdrawal Test, Event OH-RW1, Siblingen Borehole

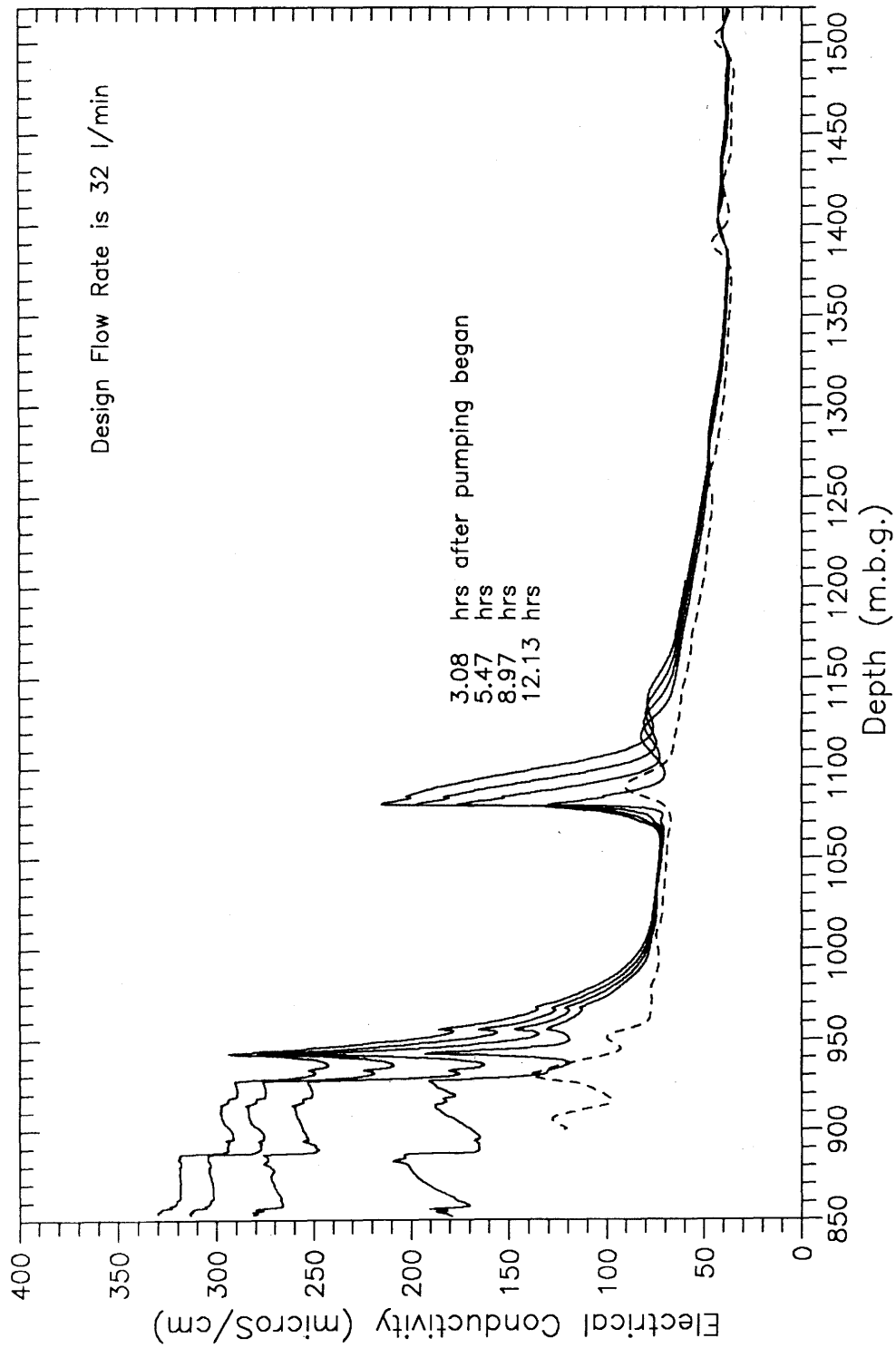

Figure 3.8: Conductivity Logs Measured During the Open Hole Pumping Period, Fluid Logging Event OH-RW1, Siblingen Borehole

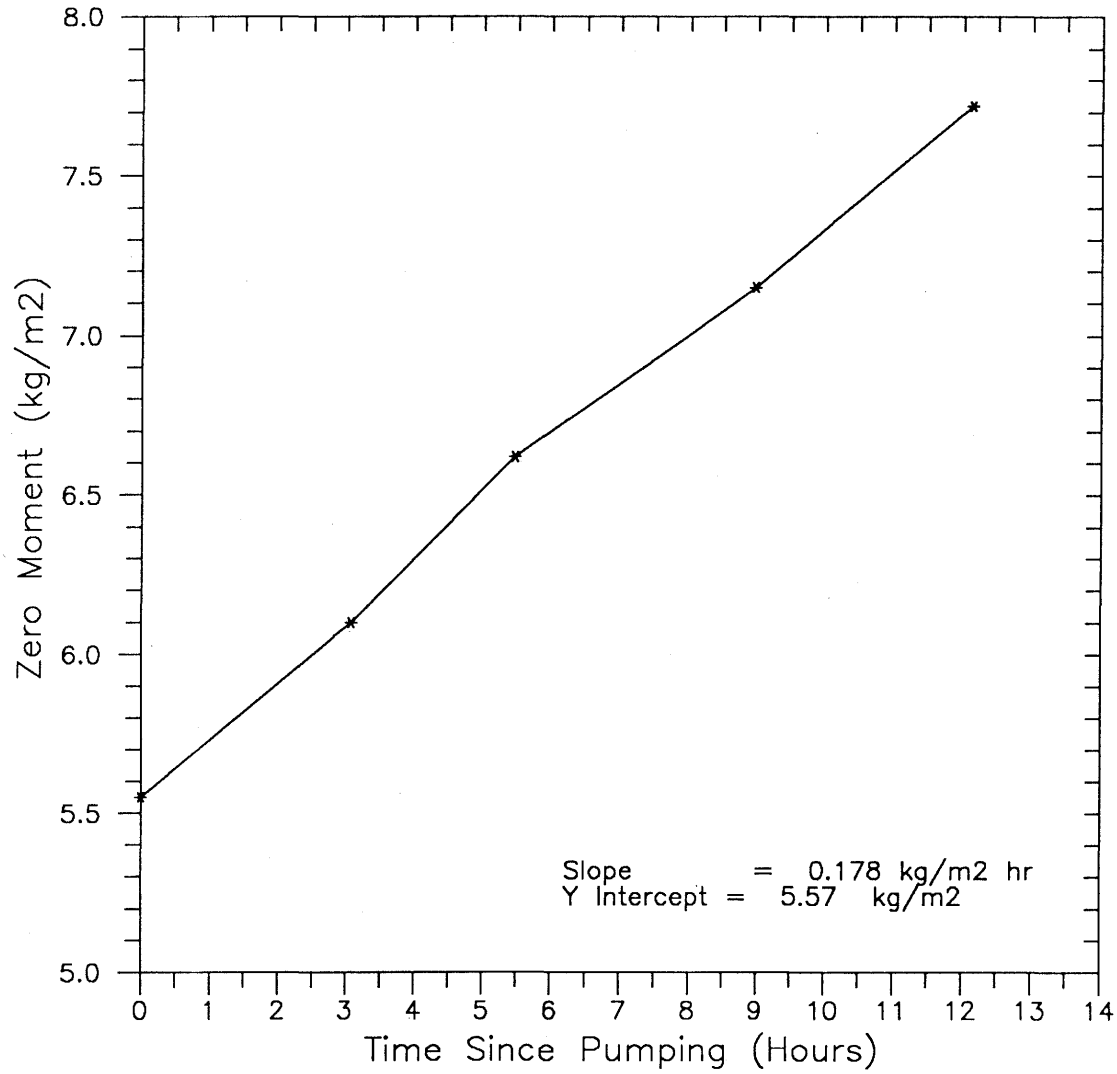

Figure 3.9: Zero Moment for Interval 1040 to 1200 m, Fluid Logging Event OH-RW1, Siblingen Borehole

The relationship is best described as a linear function of time with a best fit slope equal to a mass flux of 3.59 E-7 kg/s. The y-intercept represents the initial mass in place prior to pumping which in this case is approximately 0.04 kg. To calculate how the mass flux varies as a function of time the zero moments are simply multiplied by borehole area and the time derivative is calculated. In this case the time derivative is a simple two-point difference. The resulting fluxes appear in Table 3.7.

With the mass flux known as a function of time, the next step is to estimate the volumetric inflow rate within the interval 1040 to 1200 m. This was first done by monitoring a salinity slug which moves through the interval during pumping. The velocity of the peak is directly proportional to the borehole velocity which can be related to the borehole flow rate by the borehole cross-sectional area. This calculation has been performed and the resulting flow rates are listed in Table 3.7. The final step was to estimate the inflowing concentration as a function of time. This is done by simply dividing the mass flux by the estimated flow rate. Table 3.7 summarizes the inflowing concentration results.

Table 3.7: Calculated Mass Flux, Borehole Flow Rate, and Inflowing Conductivity for Interval 1040 to 1200 m b.g., Event OH-RW1, Determined by Pulse Analysis

TIME (hour)	FLUX RATE x 10^{-7} (kg/s)	BOREHOLE FLOW RATE (l/min)	BOREHOLE FLOW RATE (l/min)	INFLOW CONDUCTIVITY (µS/cm)
5.47	4.37	-8.34	-0.36	136
8.97	3.04	-4.29	-0.19	179
12.13	3.63	-4.74	-0.21	193

The second method to estimate borehole flow rate is the classical first moment method. For a non-interfering peak classical moment relationships can be used to estimate peak inflow rate. LOEW et al. (1990) presented an equation which related the borehole velocity on both sides of a peak to its zero and first moment quantities. This equation is presented and discussed in Section 3.2.3 (Equation 3.13).

If we assume that the upstream velocity (V_+) is equal to zero, which is a reasonable assumption, then Equation 3.13 simplifies and the downstream borehole velocity can be directly solved for by the equation

$$V_- = M_{1t} / M_{o-} \qquad (3.14)$$

This procedure was applied to the peak which developed at 1079 m during the OH-RW1, and Table 3.8 shows the results. The boundaries a and b were 1050 and 1200 m, respectively. As in the simple tracer pulse analysis, the flow rates decrease with time. The flow rate appears to stabilize to a value of approximately 0.3 l/min, which is approximately 30% greater than the estimation from the more direct tracer pulse analysis.

Table 3.8: Calculated Moments, Borehole Flow Rate, and Inflowing Conductivity for Interval 1040 to 1200 m b.g., Event OH-RW1, Determined by First Moment Analysis

TIME (hour)	M_{0-} (kg/m^2)	M_{1t} (kg/m hr)	BOREHOLE VELOCITY x 10^{-4} (m/s)	BOREHOLE FLOW RATE (l/min)	INFLOW COND. (µuS/cm)
3.08	0.42	3.56	-23.77	-1.03	
					58
5.47	0.86	3.12	-10.10	-0.44	
					79
8.97	1.32	3.40	-7.15	-0.31	
					133
12.13	1.85	4.02	-6.04	-0.26	

From the results shown in Tables 3.7 and 3.8, two intuitive results are evident. First, the flow rate into the borehole does appear to be transient at early times but stabilizes at late time. Second, the inflowing concentration increases as a function of time, which is indicative of an increasing volume of formation fluid relative to flushing fluid being produced.

The application of the classical first moment analysis to this inflow has potential problems because of model assumptions. One assumption is that prior to the inflow starting the borehole is at a constant background concentration and that boundaries a and b are at that concentration for all times. From Figure 3.8, one can see that this assumption is not met. The estimated flow rate is very sensitive to this background concentration. The concentration used for this analysis was 64 µS/cm, which is a linearly interpolated value for the midpoint of the interval a to b. As a check, the first moment was recalculated with MOMENT using a background of 70 µS/cm (9% change), which resulted in changes in the predicted flow rates by up to a factor of 1.8.

3.6 Analysis of the Second PIP Pumping Event, PIP-RW2

The last two electrical conductivity logging events were PIP-RW1 and PIP-RW2. The last event, PIP-RW2, will be analyzed prior to PIP-RW1 because knowledge gained from the PIP-RW2 analysis will be used to better quantify results from PIP-RW1.

3.6.1 Initial Conditions

As discussed in Section 3.1, the second pumping event with a PIP set above the logged section was performed with an outflow rate of 1.5 l/min (2.5 E-5 m^3/s). The logged section was flushed prior to logging (event FLU 4) with a saline solution of average concentration of 4,700 µS/cm. During the flushing phase the PIP was already in place isolating the interval from 988 to 1522 m. To flush the packed interval a coiled tubing was used which could be extended through the PIP and through which the flushing water could be injected. The total volume of the isolated interval was 3.87 m^3 . A total volume of 8.0 m^3 was injected which allows for complete plug displacement of the interval (GEOTEST/GEMAG, 1989). As the flushing fluid was injected at the bottom of the borehole, the same amount was also pumped from above the PIP in an attempt to prevent overpressuring from occurring.

To monitor overpressuring, the pressure was measured at 161 m depth in the borehole to determine the magnitude of overpressuring occurring during flushing. Figure 3.10 is a plot showing these measured pressures as converted to equivalent freshwater head. The broken line represents the average open borehole head as measured during long-term monitoring (VOMVORIS et al., 1989). Here it becomes obvious that overpressures do occur in the borehole during flushing and that it is consistent to expect flushing fluid losses to the formation. This implies that the common and simplifying assumption of constant fracture-outflow concentration versus time will probably not be met. The assumption of constant outflow concentration is not a requirement for the partial moment analysis. Currently the simulation code BORE (HALE and TSANG, 1988) will not allow for transient definition of outflow concentration or volumetric flow rate. A transient simulation can be performed by the superposition of multiple simulations. This is a time-consuming process and cannot be used in a trial-and-error mode in these analyses. BORE is used as a validation tool by performing this pseudo-transient simulation technique.

As can be seen in Figure 3.11, the flow rate did remain relatively constant at 1.5 l/min for the duration of the logging exercise. Over the first 3 hours of pumping, the flow rate varied from 1.5 to 1.3 l/min (GEOTEST/GEMAG, 1989). Because the PIP isolated the logged section from all portions of the borehole above 988 meters (GEOTEST/GEMAG, 1989), the assumption that all the flow is coming from the logged section is satisfied. For the following analysis, it will be assumed that the total flow rate from the logged section will be a constant and equal to 1.5 l/min. Figure 3.12 plots the measured pressure as a function of time during pumping.

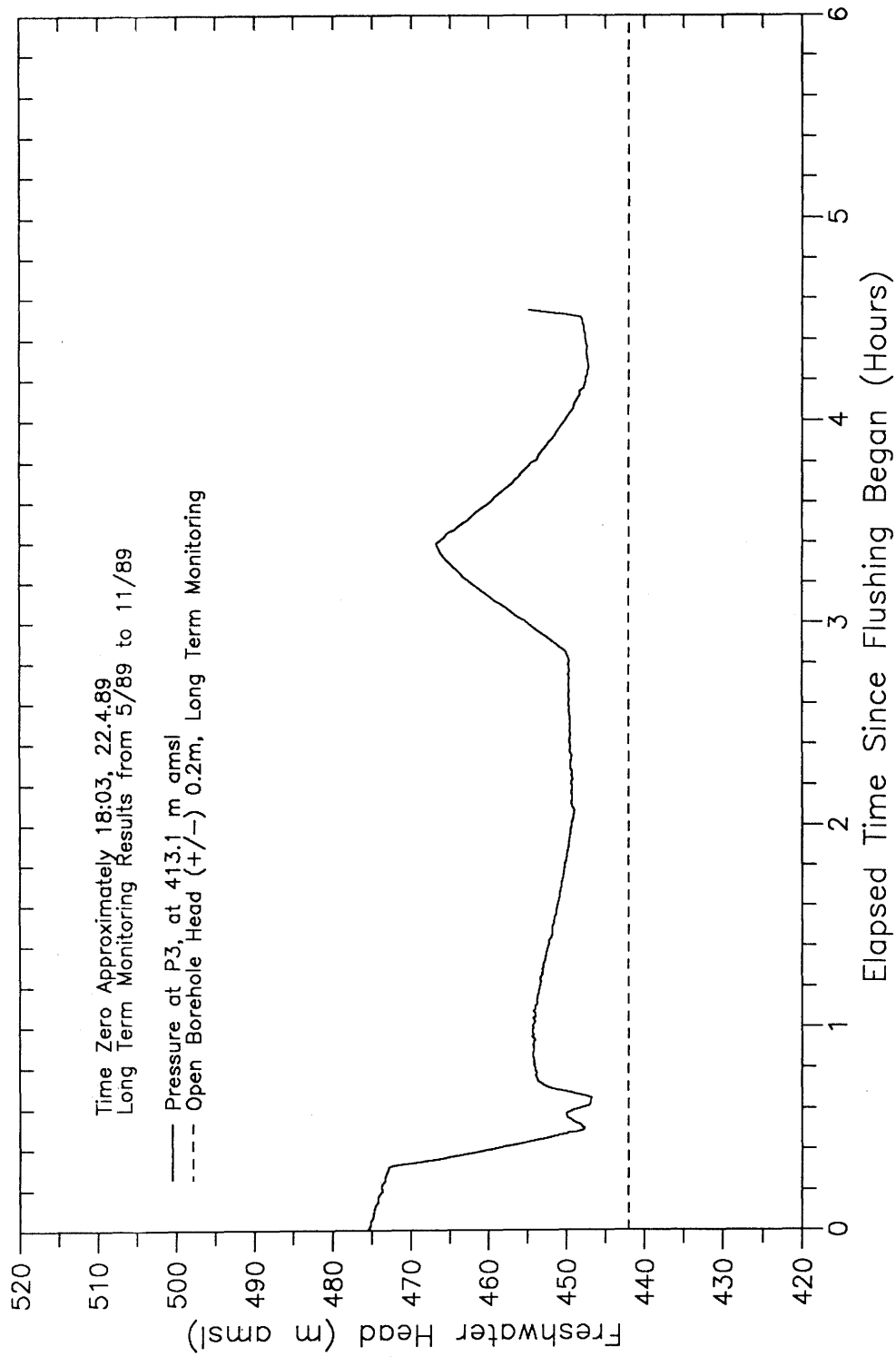

Figure 3.10: Equivalent Freshwater Head Measured in Borehole During Flushing 4, Prior to Event PIP-RW2, Siblingen Borehole

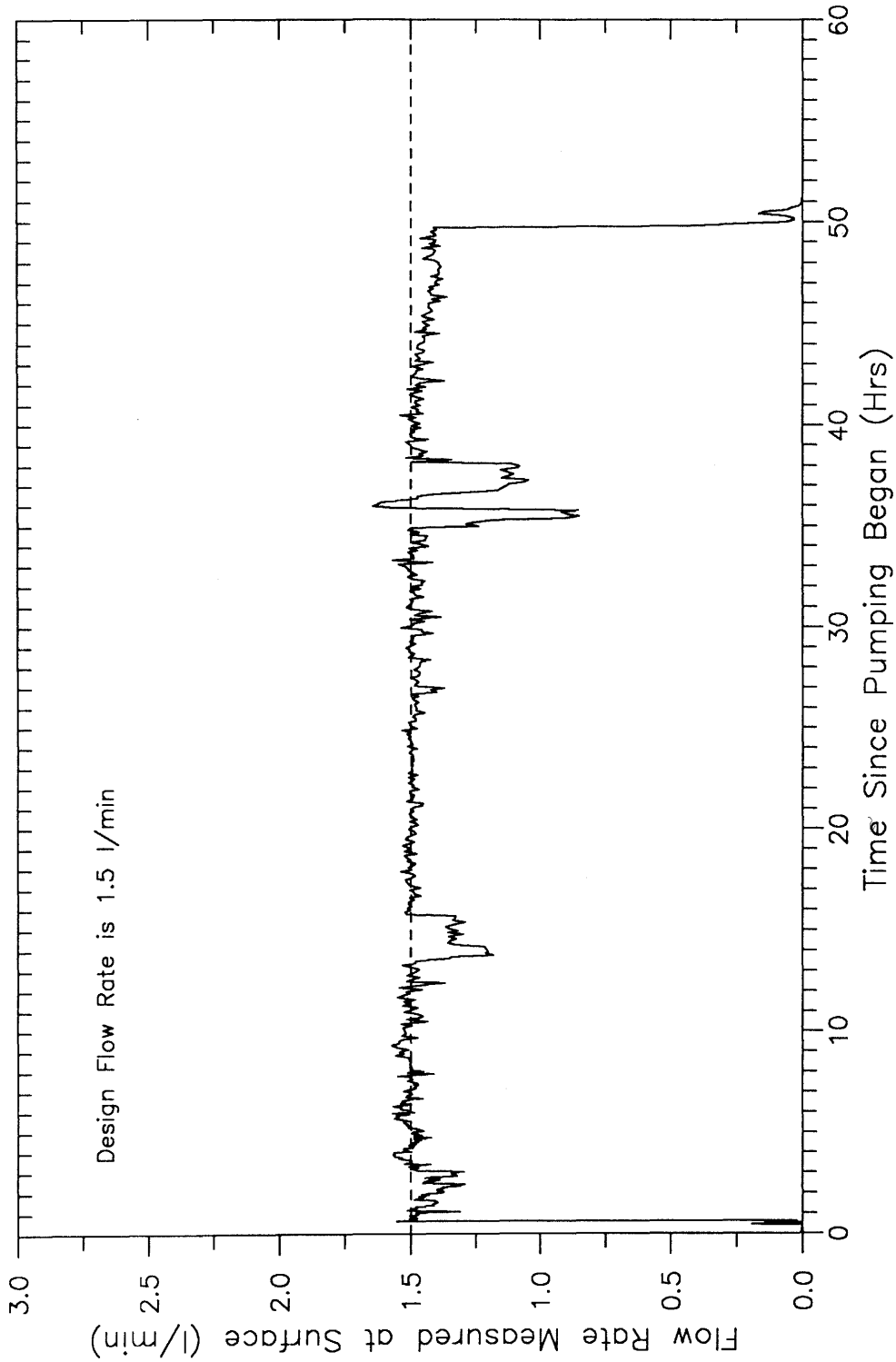

Figure 3.11: Flow Rate Measured at Surface (l/min) Fluid Logging Event PIP-RW2, Siblingen Borehole

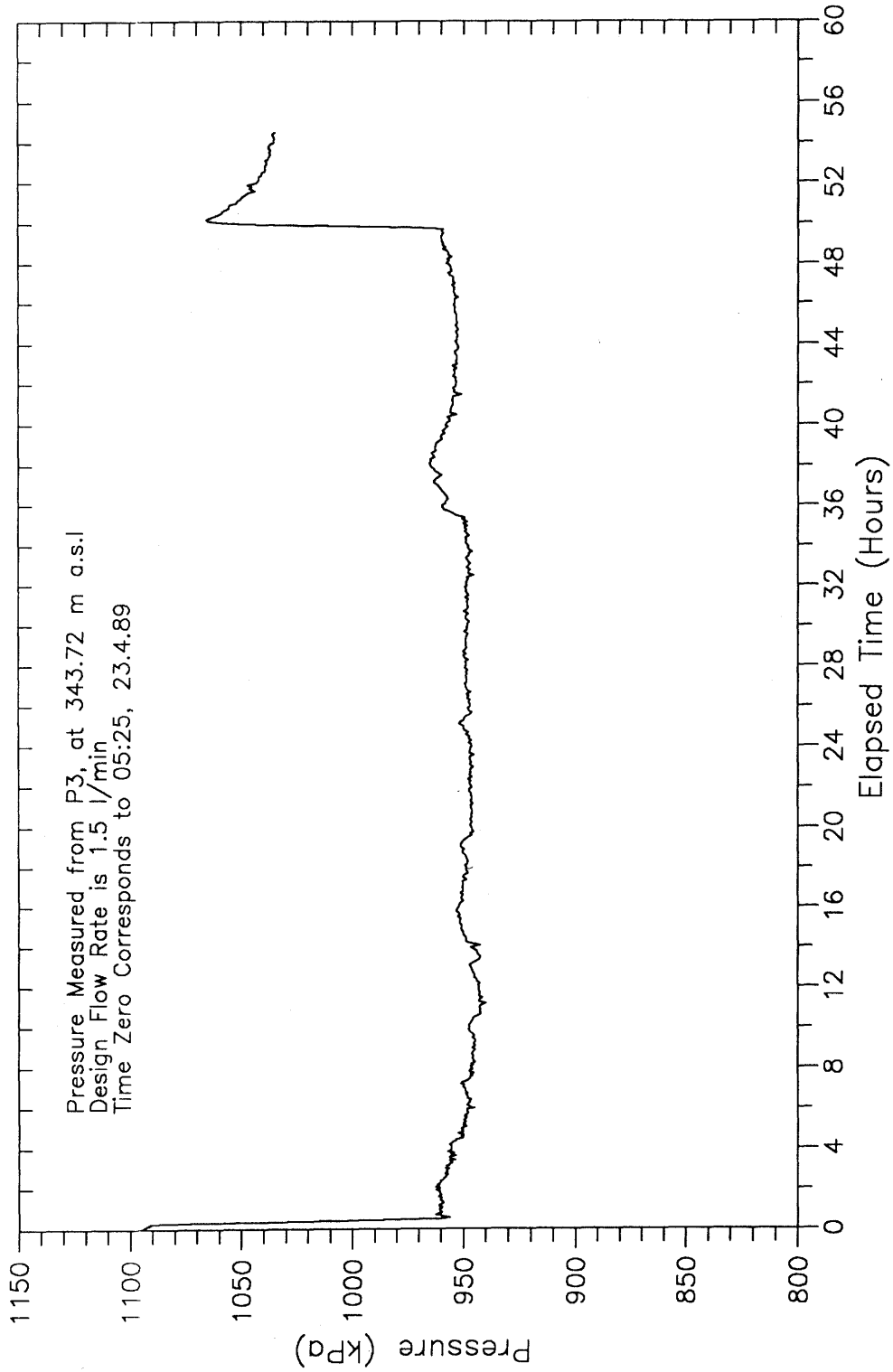

Figure 3.12: Pressure Measured at Transducer P3, 343.72 m a.s.l., Second PIP Constant-Rate Withdrawal Test, Event PIP-RW2, Siblingen Borehole

The pressures prior to pumping were falling as a result of the overpressure during flushing, with the last pressure recorded prior to pumping corresponding to a head of 444.6 m a.s.l., which is approximately 2 m above static level (VOMVORIS, et al., 1989). The stabilized drawdown is approximately 141 kPa (14.4 m) which, at 1.5 l/min, corresponds to a total section transmissivity of 2.2E-6 m^2/sec.

Figure 3.13 is a plot showing the nine conductivity logs run during PIP-RW2. The nine logs were run at times 1.0, 3.05, 6.05, 8.83, 11.95, 18.25, 24.03, 35.96, and 47.96 hours after pumping was started. Thirteen distinct inflow peaks have been identified by inspection of the fluid conductivity log profiles. Because of interference or small distance between peaks, a maximum of seven intervals and nine intervals could be defined for analysis using both classical and partial moment methods, respectively. Both Table 3.9 and Figure 3.13 show all inflow points. On Figure 3.13, the discrete inflows are marked by a dashed line. All individual inflows (peaks) or collective inflow zones used for analysis are numbered starting from the bottom of the logged section and moving up the borehole. The inflow points are considered correct within ±1.0 meter. All depths are apparent and measured in meters below ground surface (m b.g.) in the borehole.

Table 3.9: Definition of Inflow Points Identified from 1011 to 1515 m b.g. during PIP-RW2

PEAK NO.	INFLOW DEPTH (m b.g.)
1	1511.4
2	1503.6
3	1420.0
4	1410.2
5	1386.1
6	1308.5
7	1252.0
8	1237.0
9	1223.6
10	1163.5
11	1083.3
12	1078.7
13	1070.4

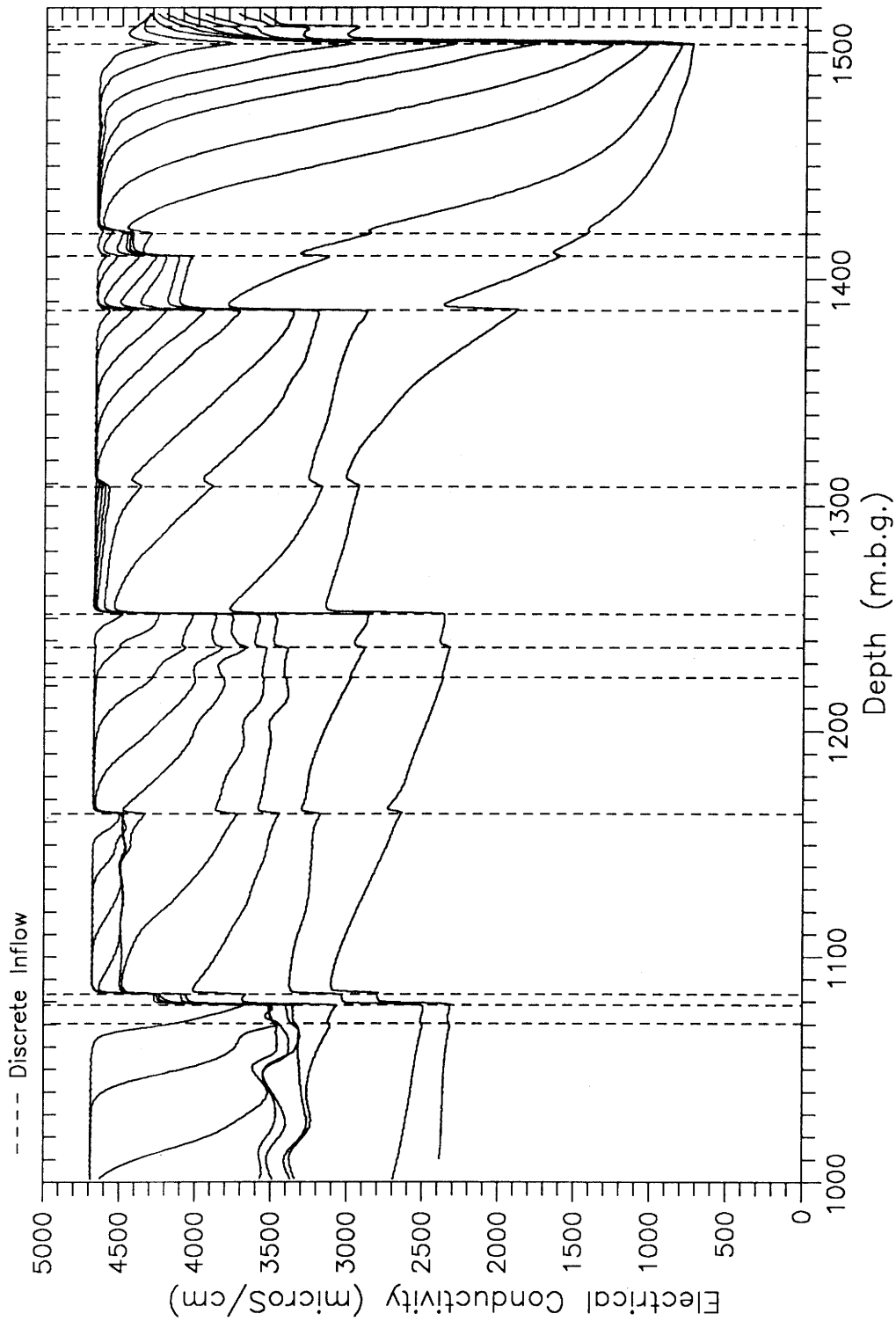

Figure 3.13: Conductivity Logs with Observed Inflows Delineated, Fluid Logging Event PIP-RW2, Siblingen Borehole, Logging Times Approximately 1, 3, 6, 12, 15, 18, 21, 27 and 36 Hours After Pumping Began

3.6.2 Estimation of Average Inflowing Concentration

The first step is to perform a MOMENT analysis to calculate the zero moment for all logging times over an integration boundary coincident with the endpoints of the logged section. The zero moment represents the amount of mass in the borehole as a function of time within the logged section divided by the cross-sectional area of the logged section. If concentration and flow rate were constant or perfectly compensating, so that their product was constant for all logging times, then the zero moment would be a linear function of time. Since mass is being lost from the upper boundary through fluid withdrawal, this loss must be estimated as a function of time.

The mass loss at the lower integration boundary should be very small relative to that leaving the upper integration boundary because the only mechanism for downward flow below the lowermost inflow point is diffusion. The sum of the mass lost through the upper boundary must always be added back to the calculated zero moment to receive a corrected zero moment, which is then representative of the mass entering the system via inflows. From Figure 3.14, which is a plot of the corrected zero moment of the entire logged section as a function of time, one can see that the zero moment for the entire logged section is curvilinear. This is indicative of non-constant inflow flow rates, concentrations, or both. The most non-linear time period is in the first 20 hours after pumping started.

With the zero moment for the entire logged section calculated by MOMENT, Equation 3.8 can be used to calculate the average inflowing concentration $C_{AB}(t)$ as a function of time over the entire logged section. Figure 3.15 is a plot of the average inflowing concentration versus time for the complete logged section as calculated by Equation 3.8. This figure shows that the average inflow concentration falls from concentrations representative of the flushing fluid concentration to a concentration representative of the formation fluid by 24 hours after the beginning of pumping. From Table 3.3 (Section 3.1.4), it can be seen that the estimated electrical conductivity of the formation fluid as derived from geochemical sampling is approximately 750 µS/cm. The relationship between concentration versus time is indicative of mixing of the flushing fluid with the formation fluid in the fractures. If one made the assumption that the inflow was constant and equal in concentration to the formation fluid, the simulation would grossly underestimate the amount of mass entering the system as a function of time. The calculated average concentration versus time is listed in Table 3.10.

At this point, the model boundary conditions or assumptions have been defined by calculating the average inflow concentration as a function of time and by assuming that the total flow from the section is equal to the surface flow rate of 1.5 l/min. The transient inflowing concentration means that the method of partial moments is the best interpretation method to follow in further analysis. Before employing partial moments, a first guess at inflowing volumetric rate can be calculated from non-interfering inflows by classical zero moment relationships.

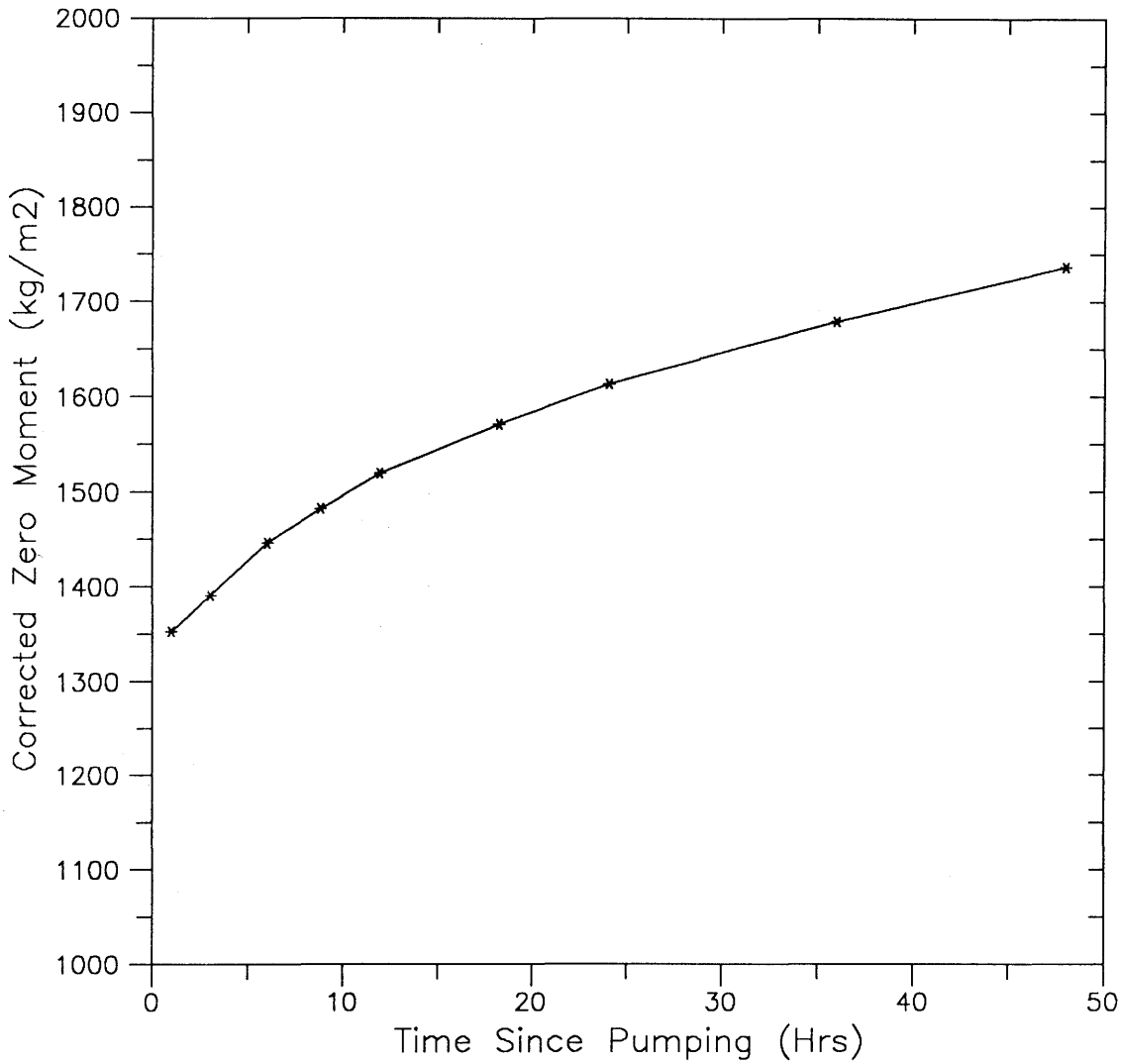

Figure 3.14: Corrected Zero Moment Calculated For the Interval 1011 to 1514 m b.g., Fluid Logging Event PIP-RW2, Siblingen Borehole

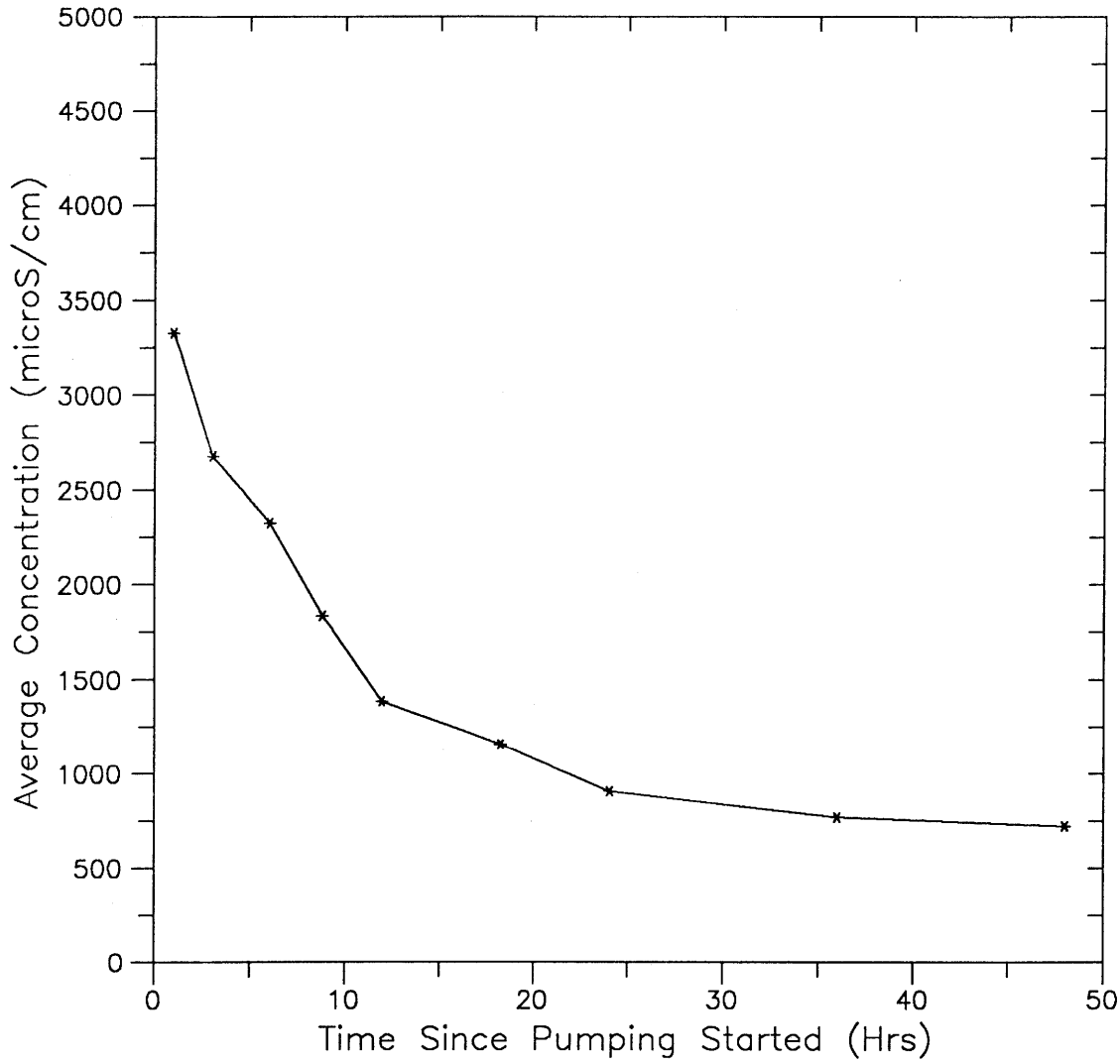

Figure 3.15: Average Inflow Concentration from 1011 to 1514 m b.g., Fluid Logging Event PIP-RW2, Siblingen Borehole

Table 3.10: Average Inflow Concentration for Section Logged during Event PIP-RW2

TIME (hours)	COND. (μS/cm)	CONC. (kg/m^3)
1.00	3328	1.853
3.05	2678	1.479
6.05	2324	1.278
8.83	1835	1.003
11.95	1387	0.754
18.25	1157	0.627
24.03	908	0.491
35.96	770	0.415
47.96	724	0.391

3.6.3 First Guess Parameter Set Through Classical Moment Analysis

Calculation of individual inflow point flow rates can be accomplished by using a classical zero moment calculated for each inflow zone and assuming that the average inflowing concentration as a function of time is constant for all inflows and equal to the logging interval average concentration (C_{AB}). Calculating the zero moment requires that integration boundaries containing a given inflow point be at background concentration for all times (i.e., uninterfered with). Since most of the peaks interfere quickly, estimates of individual peak flow rates could only be calculated for a maximum of 8.83 hours after pumping began. Some peaks (peaks 3 and 4) interfere for nearly all logs and must be combined into one analysis interval for the classical moment analysis. Because of peak-to-peak interference, only 7 analysis intervals could be selected for classical moment analysis of the 13 individual inflow points. The intervals are listed in Table 3.11.

Before presenting the individual inflow rates calculated for each interval, some semi-quantitative information can be gained through observation of the classical zero moments. The zero moment calculated for each interval is a function of C_i, q_i, πr^2, and C_0. If C_0 and the cross-sectional area of the borehole can be considered constants, then, assuming C_i is equal for all peaks, the relative magnitude of the moments reflect the relative magnitudes of the individual flow rates. Figure 3.16 plots the 7 interval boundaries along with the zero moment (M_0) calculated by MOMENT for each of the analyzed intervals. The slope of the zero moment is a measure of the interval mass flux (concentration multiplied by volumetric flow rate) and can be compared between interval. For example, peaks (11+12+13), (1+2), and (7+8+9) are the largest contributors to inflow along the logged section respectively. Interval 7 (peaks 11, 12, and 13) dominates inflow by a factor of 3 or greater. The mass flux for each analyzed interval can be calculated by taking the time derivative of the zero moment multiplied by the area of the borehole.

Table 3.11: Individual Inflow Rates Calculated by Classical Moment Analysis of Non-Interfering Intervals

FLOW RATE (l/min)	TIME (hours)				BEST ESTIMATE
INTERVAL (m)	1.0	3.05	6.05	8.83	
1002 - 1086	0.90	0.79	0.79	[0.79]	0.79 (0.71)
1087 - 1169	0.15	0.11	0.11	0.09	0.10
1170 - 1259	0.00	0.11	0.22	0.25	0.24
1260 - 1320	0.00	0.04	0.02	0.01	0.02
1350 - 1389	0.15	0.08	0.09	[0.09]	0.09
1390 - 1424	0.11	0.05	0.06	[0.06]	0.06
1425 - 1515	0.16	0.19	0.26	0.30	0.28
Total Q	1.47	1.37	1.54	1.60	1.58 (1.5)

The values in ( ) correspond to an imposed flow rate to match total flow rate Q.

The values in [ ] are taken from the previous time estimate of flow rate because peak interference did not allow a flow rate estimate.

The volumetric inflow rate for each analyzed interval can then be calculated by the use of Equation 3.10, assuming that the average concentration (Table 3.10) calculated for the whole logged interval is applicable for all inflow points. Table 3.11 summarizes the results for the seven intervals analyzed.

The results from the zero moment analysis are surprisingly consistent in reproducing the design total flow rate of 1.5 l/min. The individual flow rates vary most strongly from the 1-hour to the 3.05-hour results. At one hour, the intervals 1170 to 1260 and 1260 to 1320 did not yield flow estimates because the zero moment calculated by MOMENT for these intervals showed no change from the moment at time equal zero. The uppermost inflow zone is contributing 60% of the total interval flow at time equal to 1 hour. This percentage falls to 53% over the next two log intervals. The results from one hour suggest that the flow was dominated by the most transmissive inflow at early times and that as the drawdown stabilized the full interval contributed to flow.

The flow rate estimates taken at 6.05 and 8.83 hours are considered to be the best estimate since, by these later times, the drawdown had stabilized and the moments were changing in magnitude enough to minimize resolution errors. Three intervals could not be analyzed at 8.83 hours because of interference from other peaks.

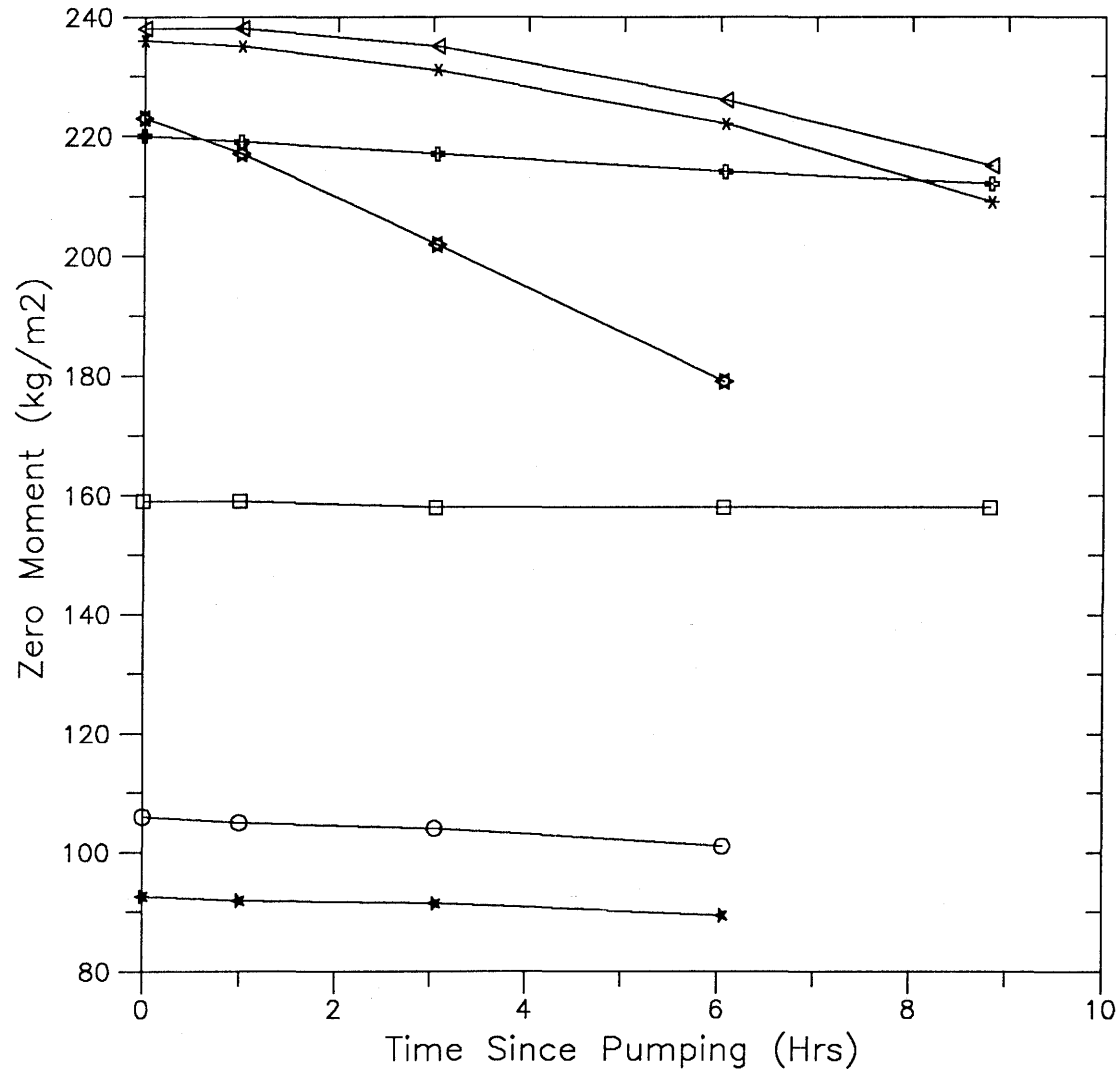

Figure 3.16: Zero Moments Calculated for Non-Interfering Peaks Fluid Logging Event PIP-RW2, Siblingen Borehole

If one uses flow estimates evaluated at 6.05 hours for the three intervals where no estimates were possible at 8.83 hours, one receives a cumulative flow rate of 1.6 l/min. In most cases, best estimates of individual flow rates were calculated as the arithmetic average between the flow rate estimated at 6.05 hours and 8.83 hours. If one sums up these flow rates, one receives a total flow from the section of 1.58 l/min. It is certainly true that the error in this cumulative flow rate is within the error in the estimation technique. The interval 1 flow rate has been decreased so that the cumulative flow equals 1.5 l/min (see values in parentheses).

3.6.4 Partial Moment Analysis

The partial moment method is a more flexible method than the zero moment method explained above in that the partial moment method allows for peak interference. A complete description of the method is given in LOEW et al. (1990). The two major constraints of the partial moment method are that over the specified integration boundaries the velocity and the dispersion terms are constant. This implies that the integration boundaries shall not surround a peak but rather must be located on one side of the peak, hence the term partial moments.

The method of partial moments can independently calculate well-bore velocity and the dispersion coefficient through the knowledge of certain parameters. These are the concentration at the integration boundaries, the concentration gradient at the integration boundaries, and the time derivative of the zero and first partial moments (see LOEW et al., 1990). The constraint listed above of constant velocity and dispersion is limited in time to the interval over which the time derivatives are taken.

Three partial moment analyses were performed using MOMENT. Only the results from the last two runs will be presented in this section. MOMENT requires as input the integration boundaries for each inflow zone analyzed, the search radius over which it calculates the boundary concentration gradients, the time interval over which it evaluates time derivatives and the polynomial degree of the line it uses to interpolate values. The 13 individual inflow points were divided into 9 integration intervals for the partial moment simulations. The parameters which have the greatest sensitivity to MOMENT results are the integration boundaries, the search radius, and the polynomial degree used to interpolate concentration to the boundaries. The two MOMENT runs presented herein are referred to as run 'B' and run 'C'. Therefore, differences in the MOMENT results presented reflect modifications in these parameters.

As stated above, well-bore velocity (well-bore flow rate) is a direct output from MOMENT and is calculated per integration interval for each logging time. Because the velocity is a function of time derivatives of the partial moments, the resulting velocity is very sensitive to the evaluation of these derivatives. Previous sensitivity and verification studies have shown that the most accurate velocities are calculated when the zero partial moment (I_o) is strongly and smoothly changing with time (LOEW et al., 1990). For this reason, plots were made showing the zero partial moment for each interval as a function of time.

From these plots we can see when the partial moment derivative might be evaluated poorly. The MOMENT code evaluates time derivatives of the partial moments numerically through a central-difference approximation. The best derivatives are evaluated when the time derivative of the partial moment quantities are (1) constant (i.e., linearly changing with time) and (2) large in magnitude. Also, any derivative evaluated when the slope of the partial moment versus time curve is very small will be in possible error due to subtraction errors.

Figure 3.17 is a plot of the zero partial moment versus time calculated in run "B" for the nine intervals analyzed. By combining this plot with a summary table (Table 3.12) of calculated well-bore flow rate, an evaluation can be made concerning which flow rate might be most representative. As an example of good and bad behavior, two intervals will be looked at in detail. Figure 3.18 shows a plot of calculated well-bore flow rate versus time for the interval 1 (1424 - 1501 m b.g.). From Figure 3.18, one can see that the flow rate stays relatively stable at approximately -0.38 l/min. The reason for this stability can in part be seen in Figure 3.16. The zero partial moment is relatively linear and shows significant change through all time so as to not cause significance problems when calculating the time derivative. Figure 3.18 also shows the calculated well-bore flow rate versus time for the interval 9 (1013 - 1075 m b.g.). Compared to interval 1, the zero partial moments do not show much change with time. Therefore, the derivative calculation shows a good deal of noise and the resulting calculated flow rates are unstable.

The calculated flow rates for the nine intervals analyzed in run 'B' are tabulated in Table 3.12. As can be seen, MOMENT estimates a flow rate for each interval at each logging time. The best estimate flow rates estimated from this analysis appear in Table 3.14. Calculated flow rates for intervals 3, 6, and 9 were too non-stable for estimation of flow rates. Because of the opportune location of interval 9, the flow rate could be estimated by subtracting the cumulative flow to that point in the borehole from the total section flow rate of 1.5 l/min.

A third analysis run was performed (run 'C') which differed from run 'B' by defining shorter integration intervals where possible and increasing the regression search distance. In addition, all interpolations were specified to be performed with lines of degree one (linear). Both intervals 7 and 9 intersected minor inflow points in run 'B'. These two integration boundaries were corrected in run 'C'. Figure 3.19 is a plot of the zero partial moment for each of the analyzed intervals as calculated in run 'C.' In general, we see a very similar behavior as was seen in the 'B' run. The two significant differences are in the zero moment curves for intervals 7 and 9. This is not surprising considering that these boundaries were corrected in run 'C.' Table 3.13 gives the calculated well-bore flow rates for each interval as calculated from MOMENT simulation 'C'. Through evaluation of the zero partial moments calculated for each interval, flow rate estimates were made for each interval. Again, intervals 3, 6, and 9 were non-stable and therefore estimates could not be made. A default flow rate was calculated for interval 9 based upon the total flow rate as in the case of run "B."

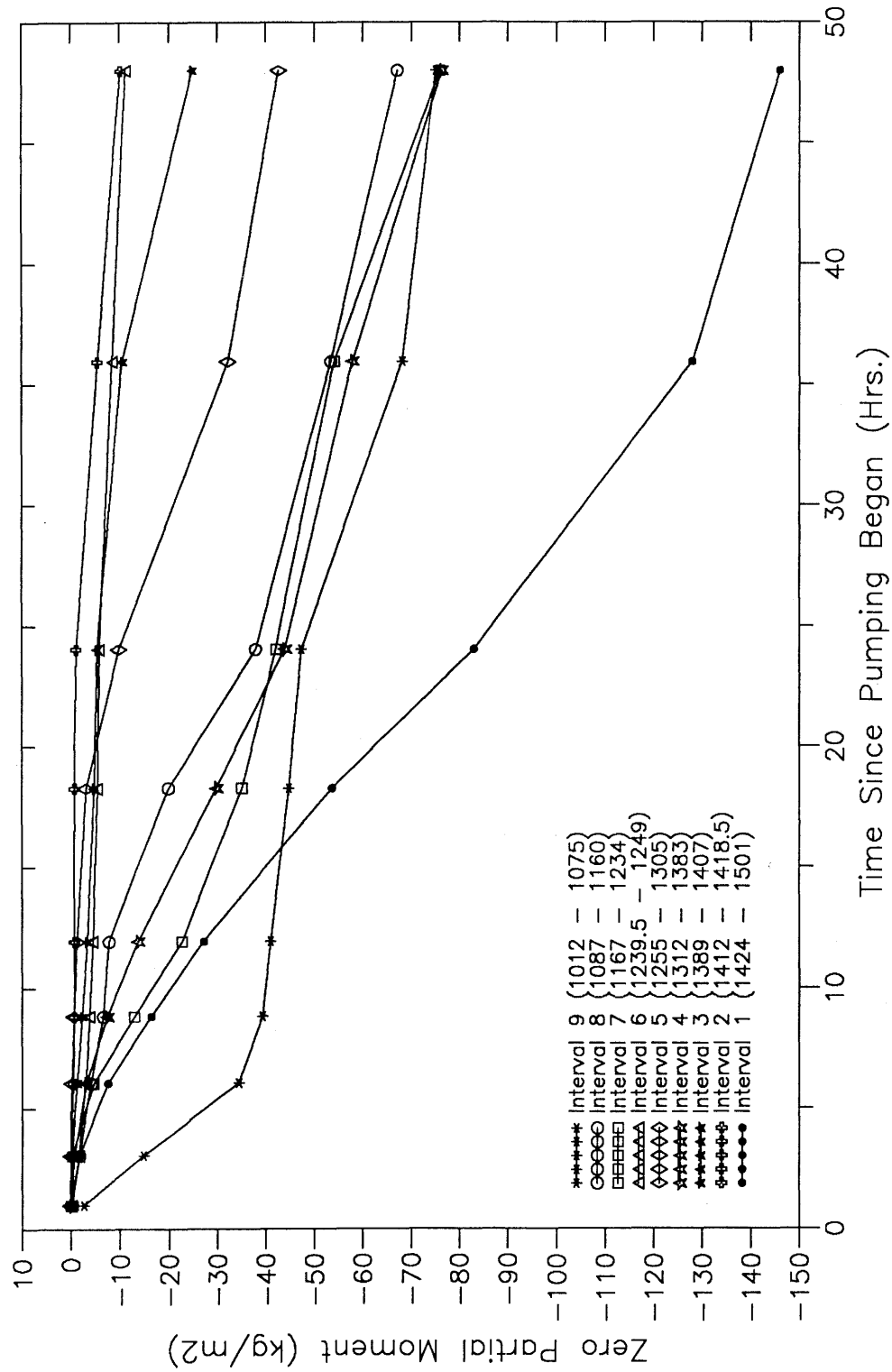

Figure 3.17: Zero Partial Moments for 'B' Simulation Fluid Logging Event PIP-RW2, Siblingen Borehole

Table 3.12: Estimated Borehole Flow Rates, Partial Moment Simulation "B"

TIME (hours)	BOREHOLE FLOW RATE (l/min)								
	Interval 9 1012-1075	Interval 8 1087-1160	Interval 7 1167-1234	Interval 6 1239.5-1249	Interval 5 1255-1305	Interval 4 1312-1383	Interval 3 1389-1407	Interval 2 1412-1418	Interval 1 1424-1501
1.00	0.98	0.61	-0.50	0.58	-4.17	1.57	0.22	0.19	0.09
3.05	1.12	0.93	0.87	0.39	0.71	0.58	0.44	0.44	0.62
6.05	-0.18	1.01	0.61	1.51	0.65	0.60	0.39	0.55	0.50
8.83	1.59	0.74	-1.35	1.40	0.63	0.58	0.38	1.12	0.42
11.95	0.50	0.17	0.71	73.17	0.91	0.54	0.33	0.44	0.45
18.25	-0.48	0.78	1.15	0.51	0.57	0.55	0.60	11.08	0.35
24.03	1.27	3.02	1.77	6.97	0.57	0.47	1.14	3.33	0.31
35.96	2.05	2.35	1.00	0.90	0.54	0.78	0.32	0.47	0.30
47.96	3.08	0.64	1.60	2.97	0.99	0.36	0.49	0.33	0.50

(-) indicates down borehole flow

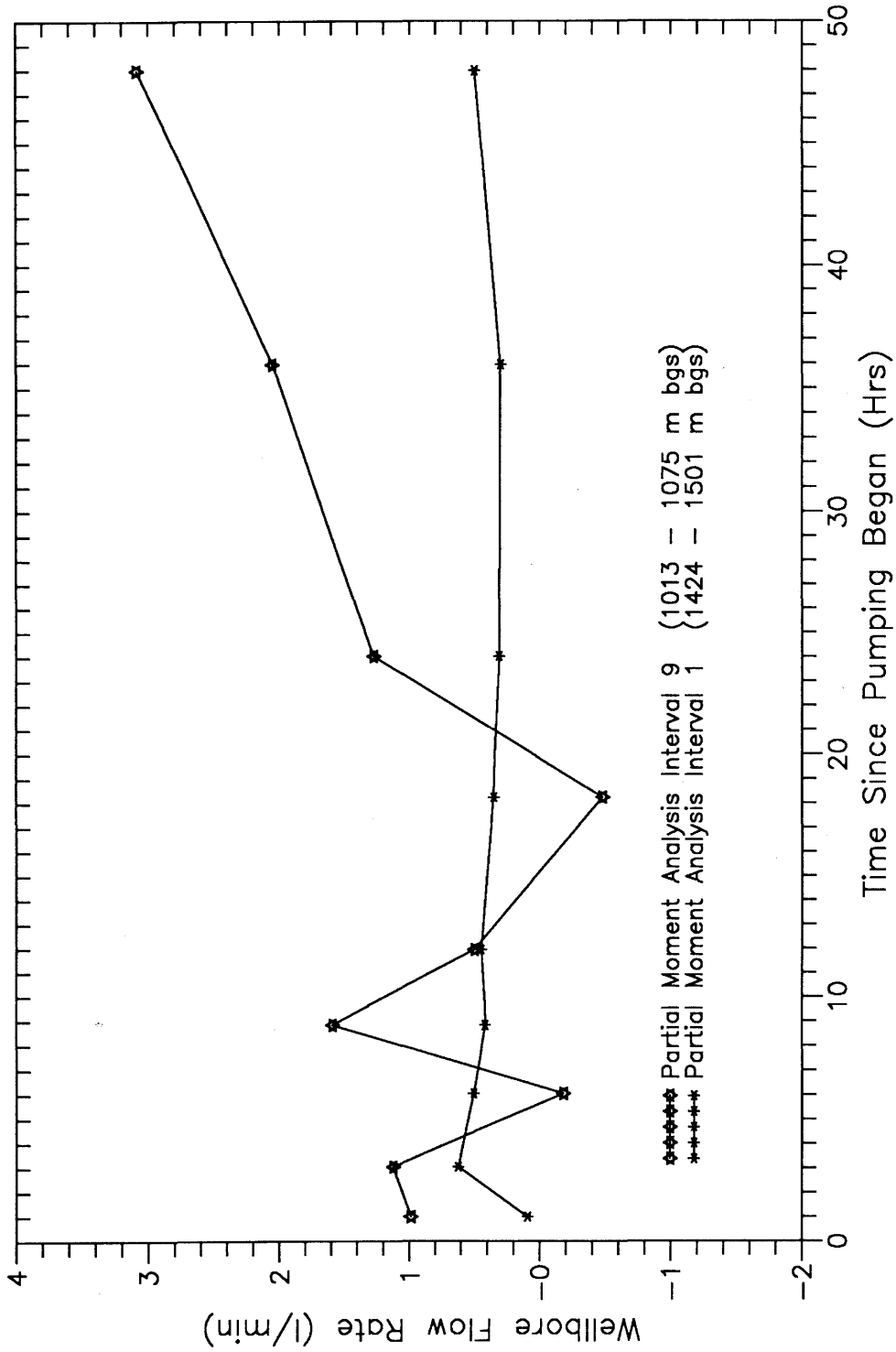

Figure 3.18: Wellbore Flow Rate Calculated from MOMENT Simulation 'B' Fluid Logging Event PIP-RW2, Siblingen Borehole

Table 3.13: Estimated Borehole Flow Rates, Partial Moment Simulation "C"

TIME (hours)	BOREHOLE FLOW RATE (l/min)								
	Interval 9 1025-1055	Interval 8 1092-1140	Interval 7 1172-1195	Interval 6 1241-1248	Interval 5 1261-1301	Interval 4 1325-1375	Interval 3 1393-1405	Interval 2 1413-1418	Interval 1 1429-1495
1.05	-27.83	-31.17	-18.67	0.48	-4.07	-14.05	0.55	0.18	0.06
3.05	0.62	-1.62	0.13	0.25	1.22	-0.32	0.32	0.48	0.13
6.05	3.42	0.86	0.17	1.18	0.53	0.46	0.42	0.54	0.27
8.83	6.35	3.80	0.66	1.18	0.64	0.57	0.39	0.97	0.36
11.95	-0.76	7.27	0.44	2.77	0.72	0.52	0.33	0.21	0.45
18.25	-1.13	0.62	1.11	0.63	1.37	0.55	0.23	3.22	0.35
24.03	6.40	1.14	0.22	-1.06	0.50	0.23	6.35	-3.03	0.29
35.96	0.86	1.42	1.75	-0.64	0.32	0.90	0.02	-0.32	0.26
47.96	1.32	0.50	1.92	2.57	-10.45	0.40	0.24	0.49	0.36

(-) indicates down borehole flow

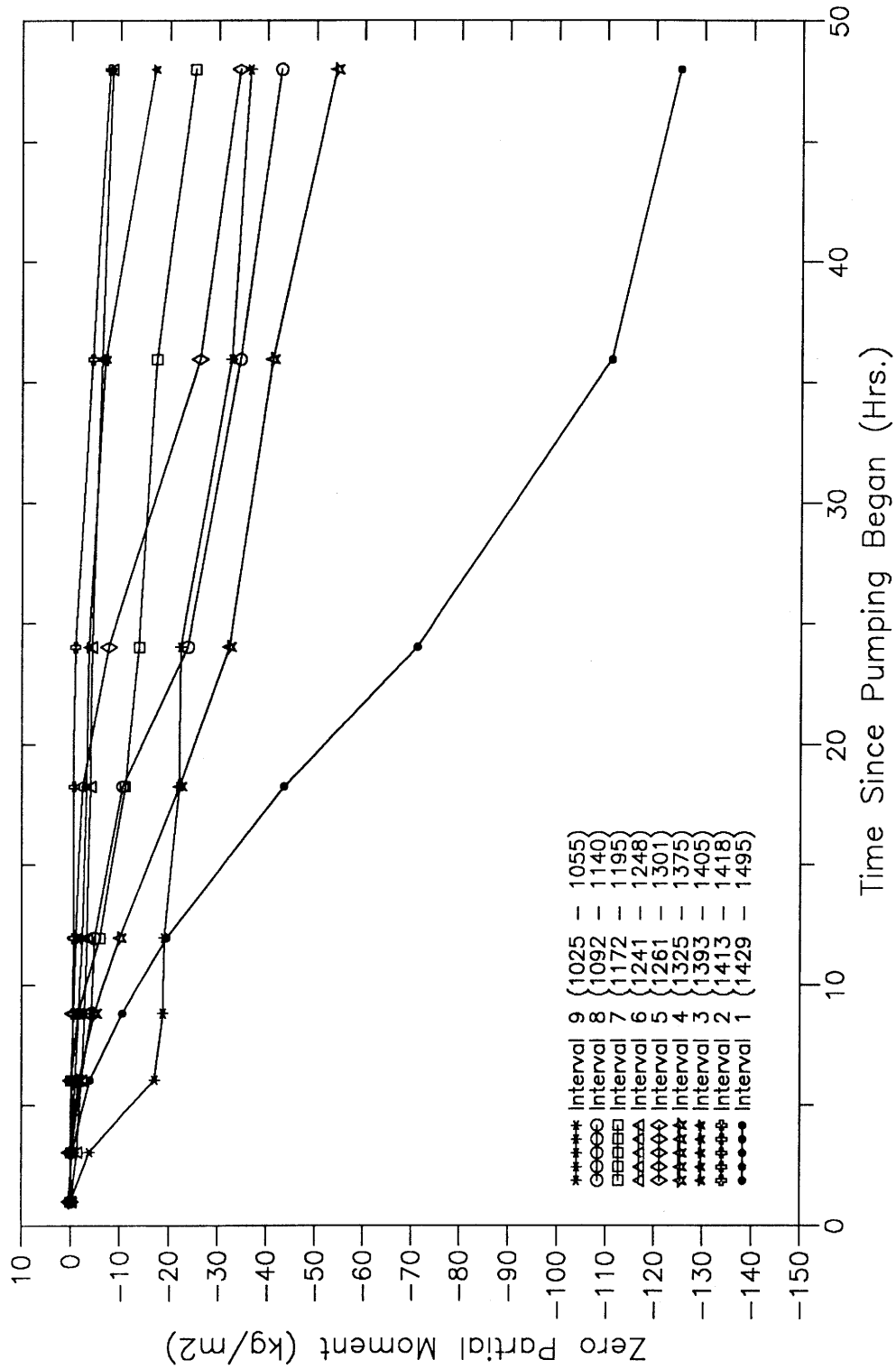

Figure 3.19: Zero Partial Moments for 'C'Simulation Fluid Logging Event PIP-RW2, Siblingen Borehole

Table 3.14: Borehole Flow Rate (l/min) as Derived from Both Classical and Partial Moment Analyses

INTERVAL (PEAK) NUMBER	INTERVAL DEPTH (m b.g.)	BOREHOLE FLOW RATE (l/min)			
		Classical Moment	Partial Moment B	Partial Moment C	Best Guess
1 (1,2)	1511-1420	0.28	0.38	0.34	0.36
2 (3)	1420-1410	0.34	0.48	0.50	0.39
3 (4)	1410-1386		(NS)	(NS)	0.42
4 (5)	1386-1308	0.43	0.57	0.55	0.52
5 (6)	1308-1252	0.45	0.59	0.63	0.54
6 (7)	1252-1224	0.69	(NS)	(NS)	0.66
7 (8,9)	1224-1164		0.73	0.66	0.74
8 (10)	1164-1070	0.79	0.87	0.74	0.84
9 (11,12,13)	1070-1011	1.50	[1.50]	[1.50]	1.50

(NS) -- The analysis was unstable

The well-bore flow rates from both partial moment runs are listed in Table 3.14. In addition to the results from the partial moment analysis, the results from the classical zero moment analysis also appear in Table 3.14. Based on these analyses, a best estimate was calculated. This best estimate represents some average value based upon the results from all analyses. This estimate is in most cases qualitative in that if a particular interval analysis showed stable results and all others were not, then the best estimate would be completely based upon that singular stable result. A discussion of the rationale behind these estimates follows.

For the first interval, both partial moment runs gave stable results. However, both were higher in magnitude than the flow rate estimate calculated by classical moment analysis. The best estimate simply represents the arithmetic average between the two partial moment runs and is 0.36 l/min. For interval 2, although a borehole flow rate estimate has been made for each partial moment analysis, these estimates are not considered sound. The partial moment analysis results for

integration interval 3 was non-stable for both simulations. Both intervals 2 and 3 have low flow rates and due to their close proximity, had to be analyzed with short integration distances. Sensitivity studies have shown that both of these factors contribute to unstable estimates of flow rate. The estimate for the borehole flow rate in interval 4 is considered more stable and is considered best for run 'B,' but the best estimate is an arithmetic average between all three analyses and is equal to 0.52 l/min. The difference between the best estimate interval 4 flow rate and the best estimate interval 1 flow rate is approximately 0.16 l/min. From a look on Figure 3.16 at the relative magnitude of the zero moments of intervals (2+3) and interval 4, it can be said that the area under intervals (3+2) (peaks 3,4,5) is approximately 60% of the area under interval 4 (peak 6) at time equal to 6.05 hours. Also, one can infer from inspection of the logs that the inflow at interval 2 (peak 3) is very similar in magnitude, after compensating for interference, to the inflow at interval 3 (peak 4). It is accepted that these arguments assume a similar inflowing concentration between peaks. From this analysis the best estimate for contribution to borehole flow from interval 2 is 0.03 l/min, for interval 3 is 0.03 l/min, and interval 4 is 0.1 l/min. This means that the borehole flow rate within interval 2 is 0.39 l/min and within interval 3 is 0.42 l/min.

For interval 5, the partial moment borehole flow rates calculated from run 'B' were more stable than for 'C'. These results were also more consistent with the flow rate derived from the classical moment analysis. Although the magnitude of the estimated borehole flow rate could be incorrect, the assumption here is that the difference in magnitude between intervals 5 and 4 of 0.02 l/min is representative. The best-estimate flow rate for interval 5 is 0.02 l/min, and added to the best estimate for interval 4, is equal to 0.54 l/min. The partial moment flow rates for interval 6 were not stable in all simulations. Again, interval 7 and interval 8 partial moment results were non-stable and open to interpretation. The difference in borehole flow rate between interval 8 and interval 5 in the case of the classical moment analysis is 0.34 l/min. The difference in borehole flow rate between intervals 8 and 5 for run 'B' is 0.28 l/min. The run 'C' results are not considered representative over this interval. Based on these differences in flow rate between intervals 8 and 5, the interval 8 flow rate was estimated to be 0.84 l/min. From the non-interfering peak zero moments, it could be determined that the mass under peaks 6 and 7 was on the average 1.9 times greater than the mass under peak 8 for the first 6 hours of logging. Therefore, based upon these facts and inspection of the logs, interval 6 was estimated to have an inflow rate of 0.12 l/min, interval 7 was estimated to have an inflow rate of 0.08 l/min, and interval 8 was estimated to have an inflow rate of 0.1 l/min. This results in interval borehole flow rates of 0.66 and 0.74 l/min for intervals 6 and 7 respectively. The final interval borehole flow rate, interval 9, was completely unstable. Therefore, the estimate for interval 9 borehole flow rate was simply set equal to the imposed outflow from the logged section during the logging event, 1.5 l/min. Table 3.15 summarizes the individual borehole flow contribution from the 9 borehole intervals analyzed. The interval lengths are arbitrarily set at ±5 m around an identified inflow. If an interval contains more than one inflow (i.e., 1 and 9), then the interval is taken to be ±5 m on either side of the end member inflows.

Table 3.15: Peak Flow Rates (l/min) Derived for the Borehole Interval from 1000 to 1522 m, Event PIP-RW2

INTERVAL NUMBER	PEAK(S) INCLUDED	INFLOW INTERVAL (m b.g.)	INFLOW RATE (l/min)
1	1, 2	1500 - 1516	0.36
2	3	1415 - 1425	0.03
3	4	1405 - 1415	0.03
4	5	1381 - 1391	0.10
5	6	1303 - 1313	0.02
6	7	1247 - 1257	0.12
7	8, 9	1219 - 1242	0.08
8	10	1158 - 1168	0.10
9	11, 12, 13	1065 - 1089	0.66

Figure 3.20 plots both borehole flow rate and individual inflowing feature flow rates as a function of depth. As can be seen, inflows at the bottom of the logged section and at the top of the logged section (peaks 1,2 and 11,12,13) contribute almost 70% of the total interval flow.

3.6.5 BORE Simulation with Best Guess Parameter Set

To see how well the best guess parameter set will match the development of the observed peaks, a direct simulation was performed with BORE. The use of BORE as a direct simulator is problematic for practical (application) reasons for event PIP-RW2. BORE assumes that both q_i and C_i are constant as a function of time and this is not the case during PIP-RW2. We have found that C_i varies as a function of time (Table 3.10). To perform the BORE simulation required a step-by-step simulation mode where each log was simulated with the appropriate C_i and then the calculated log was input as background for the next step of the simulation.

A simulation was performed for each of the nine logs measured which covers a time period of 48 hours. In all cases, the dispersion coefficient used is constant and equal to 5E-4 m^2/s. This was based on a limited early time calibration and not on theoretically significant considerations. Figure 3.21 plots the observed versus simulated logs for 11.95 hours after pumping began. Considering the transient nature of the inflowing concentration, the fit is very good. Figure 3.22 is a plot of the observe2d and the simulated conductivity log measured at 24.03 hours after pumping. The fit has deteriorated from the simulation at 11.95 hours, but not severely.

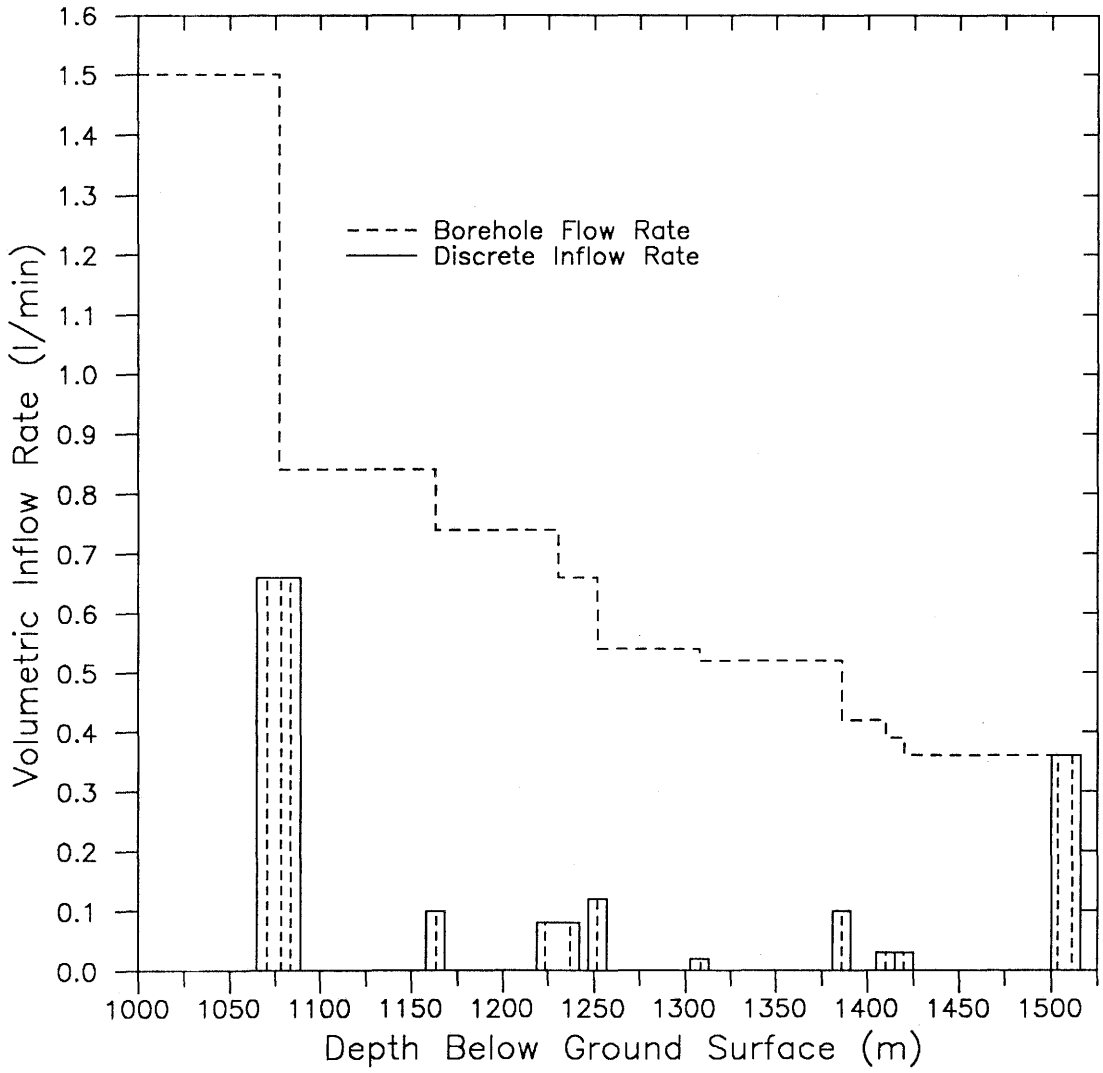

Peak 1,2	(1516 – 1500 m)
Peak 3	(1425 – 1415 m)
Peak 4	(1415 – 1405 m)
Peak 5	(1391 – 1381 m)
Peak 6	(1313 – 1303 m)
Peak 7	(1257 – 1247 m)
Peaks 9,8	(1242 – 1219 m)
Peak 10	(1168 – 1158 m)
Peaks 11,12,13	(1089 – 1065 m)

Figure 3.20: Volumetric Flow rate for 9 Intervals Analyzed Fluid Logging Event PIP-RW2, Siblingen Borehole

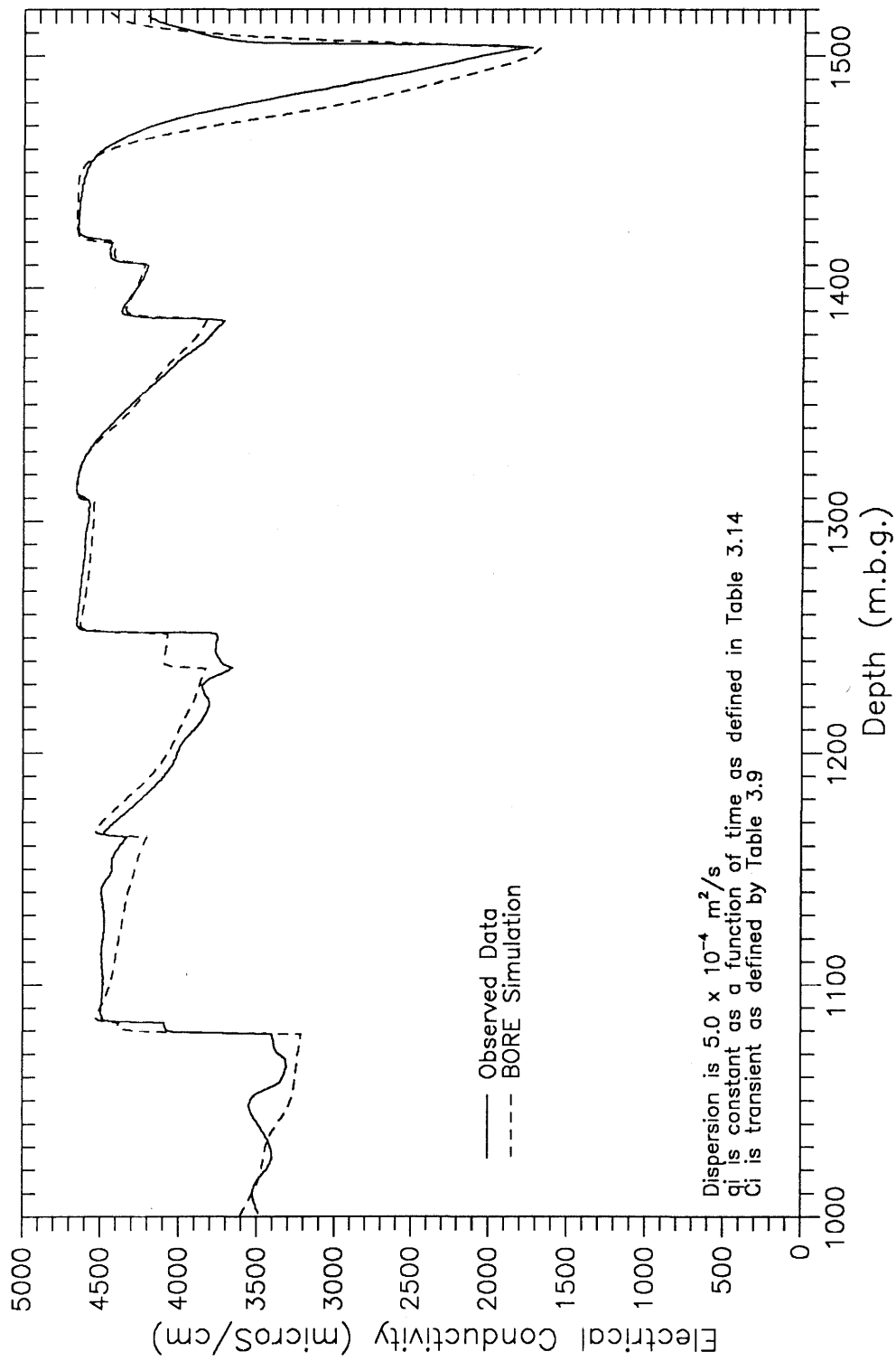

Figure 3.21: BORE Simulation of Second PIP-Pumping, PIP-RW2 Simulation Time is 11.95 Hours, Siblingen Borehole

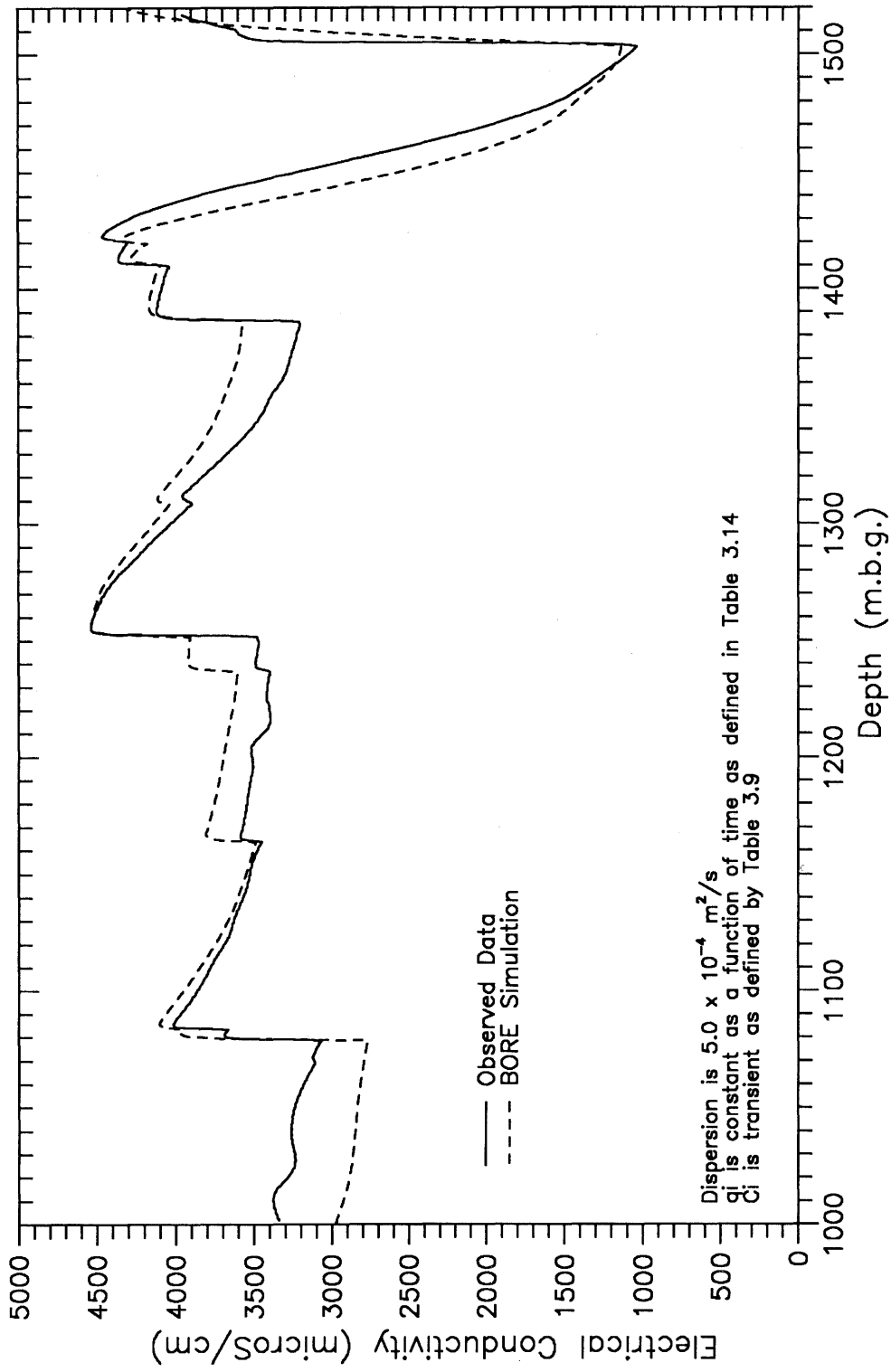

Figure 3.22: BORE Simulation of Second PIP-Pumping, PIP-RW2 Simulation Time is 24.03 Hours, Siblingen Borehole

Figure 3.23 plots all of the observed logs along with the BORE simulated logs. The fit between the observed and simulated logs are not bad considering the transient nature of the modeled system. For some peaks (i.e., peak 6 at 1308.5 m) the early time response is far in excess of observed peak, while at later times the agreement becomes very close. Other peaks (i.e., peak 12 at 1078.7 m) are under-predicted at early times and then come to close agreement at late times.

The volume of flushing fluid injected into a given unit is proportional to its transmissivity, assuming horizontal flow. The average $C_{AB}(t)$ will be in error for all inflows because all inflows will possess different pumpback concentration curves. Because the estimate of $C_{AB}(t)$ is an average over the entire logged section, this means that BORE should overpredict and underpredict flux for many individual inflows. However, the overall conservation of mass should be very close to observed. Because this concentration function is a smooth continuous function with respect to time, the discretization necessary for simulation will introduce error into the simulations.

In addition, because a high transmissivity unit is located at the top of the isolated interval, early time flow rate may be dominated or controlled by this unit. The higher transmissive units will control early time flow and can contribute a significantly larger proportion of the total flow rate at early times than when a near steady-state condition prevails. We see an indication of this behavior in Table 3.11. An additional complicating factor is the existence of significant head differences in the borehole. All such complications discussed will create error that will be cumulative in its effect. This might help explain why the early time fit is better than the late time fits.

With such complicating factors considered, the BORE simulations are pretty good, especially when it is considered that this is a direct calculation with no calibration phase. Although it might be possible to refine parameters to a degree by an intensive BORE simulation phase, this is not seen to enhance significantly the transmissivities derived.

3.7 Analysis of the First PIP Pumping Event, PIP-RW1

3.7.1 Initial Conditions

The first logging done with a PIP in place was PIP-RW1. This event preceded event PIP-RW2 analyzed in the previous section. The logged section (1000 to 1522 m) was isolated by a double PIP downhole configuration and was pumped at a constant flow rate of 3.0 l/min (5E-5 m^3/sec). Prior to the pumping period, the entire logged section of the borehole was flushed with deionized water (Event FLU III). The flushing was performed prior to installation of the PIP. The flushing fluid was deionized water and the procedure was step displacement.

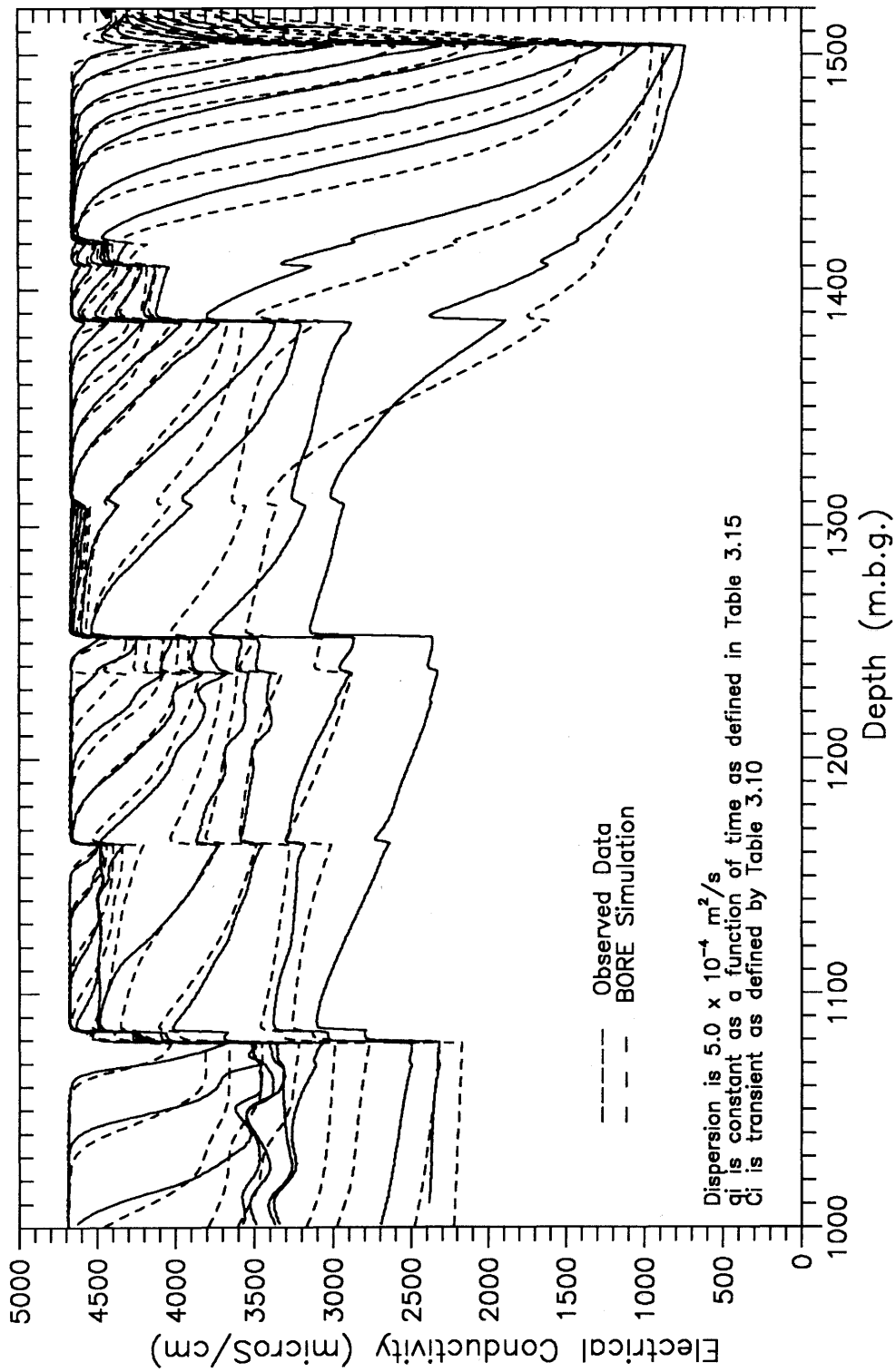

Figure 3.23: BORE Simulation of Second PIP-Pumping, PIP-RW2 All Logging Times, Siblingen Borehole

Initially, a 3-inch-diameter injection tubing was lowered to 800 m b.g. and 5.75 m^3 was injected. Next the tubing was extended to a depth of 1510 m and subsequently moved up the borehole in 90 m steps. At each step approximately 0.4 m^3 deionized water was injected. The exception was at the station at 1087 m where 0.8 m^3 was injected. The total volume injected below 800 m was 3.22 m^3 which would displace 444 m of borehole. The flushing was successful over the entire borehole length, however installation of the PIP pushed a large slug of elevated salinity into the borehole between depths 1260 and 1460 m. An additional slug, of a lesser magnitude, was present from 1000 to 1050 m b.g. before pumping. Figure 3.24 is a plot showing the background concentration in the borehole prior to the pumping phase. Also marked on the plot are the locations of the inflow points identified in the preceding analysis. The figure also shows that the tracer slugs show no correlation with the known inflow points.

Figure 3.25 plots the flow rate in l/min as measured at the surface for the duration of the test (GEOTEST/GEMAG, 1989). The flow rate varied considerably over the first 4 hours of the test but remained quite constant at 3 l/min for the remainder of the test. For this analysis it is assumed that the flow rate is constant for all times and equal in magnitude to 3.0 l/min. Figure 3.26 plots the measured pressure as a function of time during pumping (GEOTEST/GEMAG, 1989). The initial pressures prior to pumping were falling, with the last pressure corresponding to a head of 444.4 m a.m.s.l., which is approximately 2 m above static levels (VOMVORIS, et al., 1990). If the 'static' pressure is considered 1089 kPa prior to pumping, the stabilized pressure drop due to pumping was 209 kPa (21.3 m). This corresponds to a total logged section transmissivity of 3E-6 m^2/sec. The borehole pressure appeared to be falling prior to pumping. If this is not compensated for, the estimated transmissivity should be underestimated. The magnitude of underestimation should be less than 10%.

Figure 3.27 shows the 12 conductivity logs run during PIP-RW1. The logs were run at times 0.97, 2.97, 5.97, 8.97, 11.95, 14.97, 17.97, 20.97, 26.97, 35.97, 44.97, and 58.97 hours after pumping began. No new inflow points are evident from these logs that were not identified in the analysis of the PIP-RW2 logs (Table 3.9). Both peaks 9 and 13 are ill defined in this set of logs relative to the logs in PIP-RW2.

3.7.2 Estimation of Average Inflowing Concentration

As in the PIP-RW2 analysis, the first step is again to estimate the average inflowing concentration as a function of time for the total logged section. This requires calculation of the corrected zero moment for the entire logged section. The correction is required to compensate for the mass lost at the system upper boundary. Again, we can see that the zero moment is non-linear for times when there is no significant borehole pressure transience (see Figure 3.28). Figure 3.29 plots average inflow concentration as a function of time for the entire logged section (1011 to 1514 m b.g.). Again, this is taken to mean that the inflowing concentration is transient as a result of significant fluid losses to the formation during flushing.

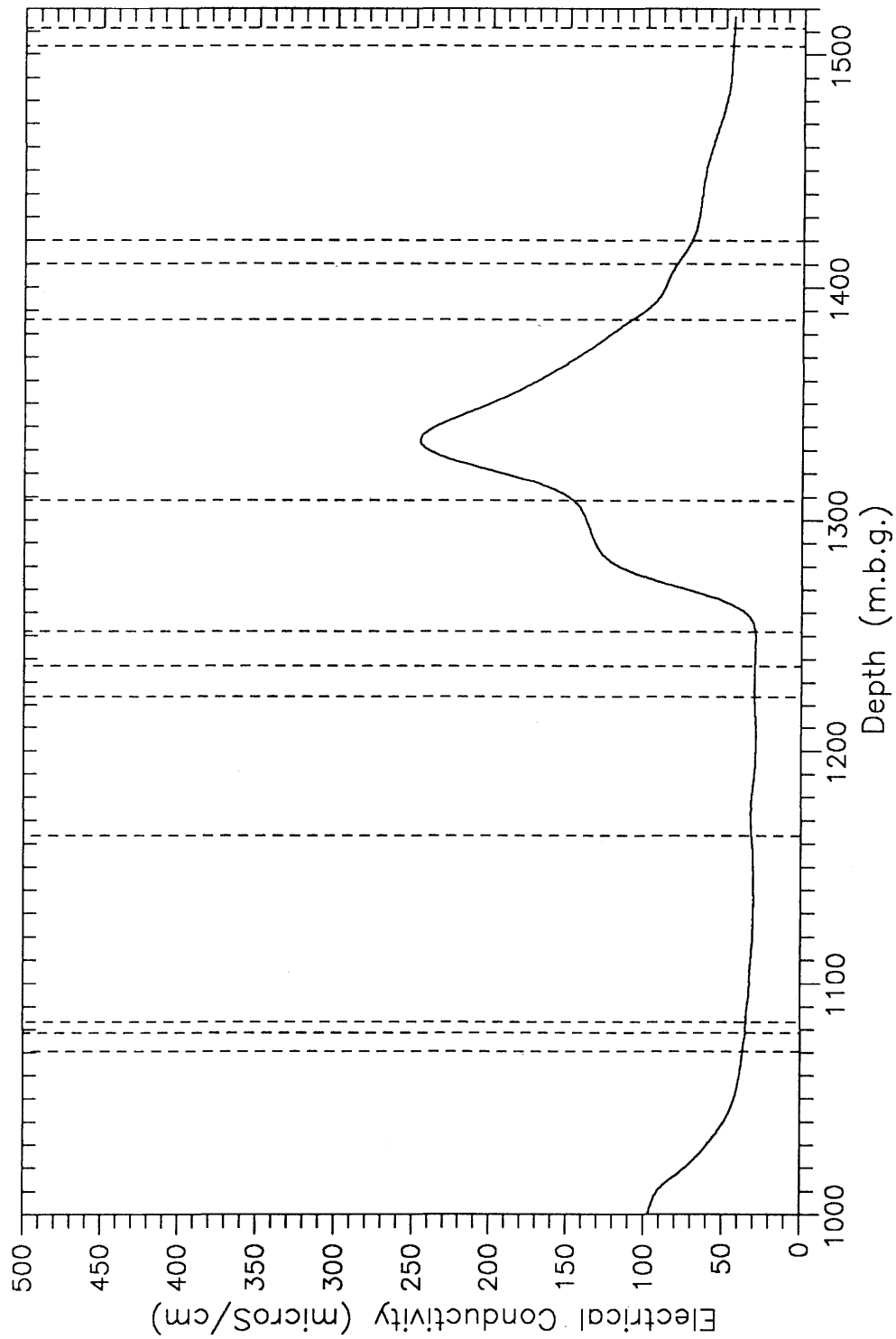

Figure 3.24: Background Conductivity (uS/cm) Prior to Fluid Logging Event PIP-RW1, Siblingen Borehole

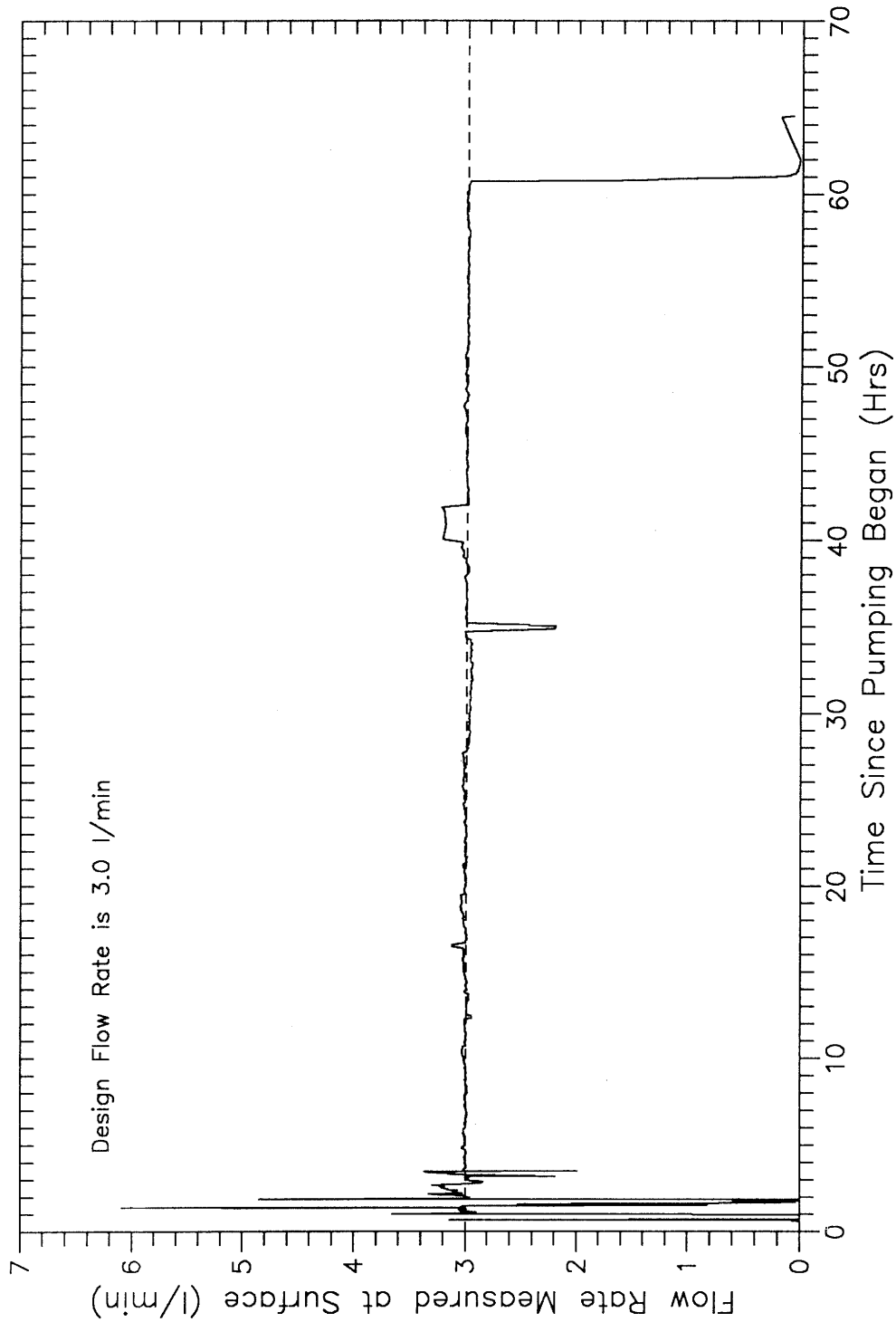

Figure 3.25: Flow Rate Measured at Surface (l/min) Fluid Logging Event PIP-RW1, Siblingen Borehole

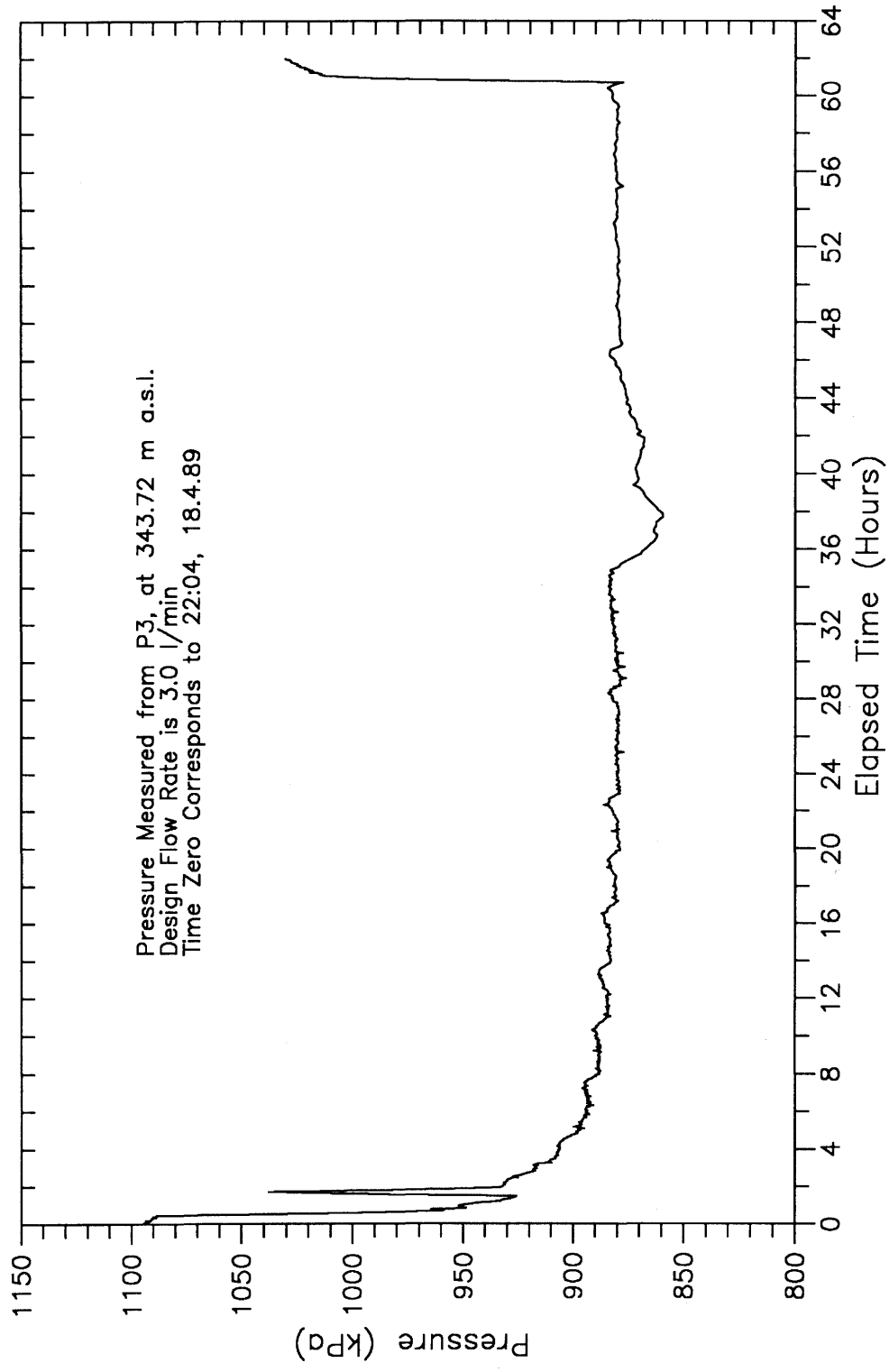

Figure 3.26: Pressure Measured at Transducer P3, 343.72 m a.s.l., First PIP Constant Rate Withdrawal Test, Event PIP-RW1, Siblingen Borehole

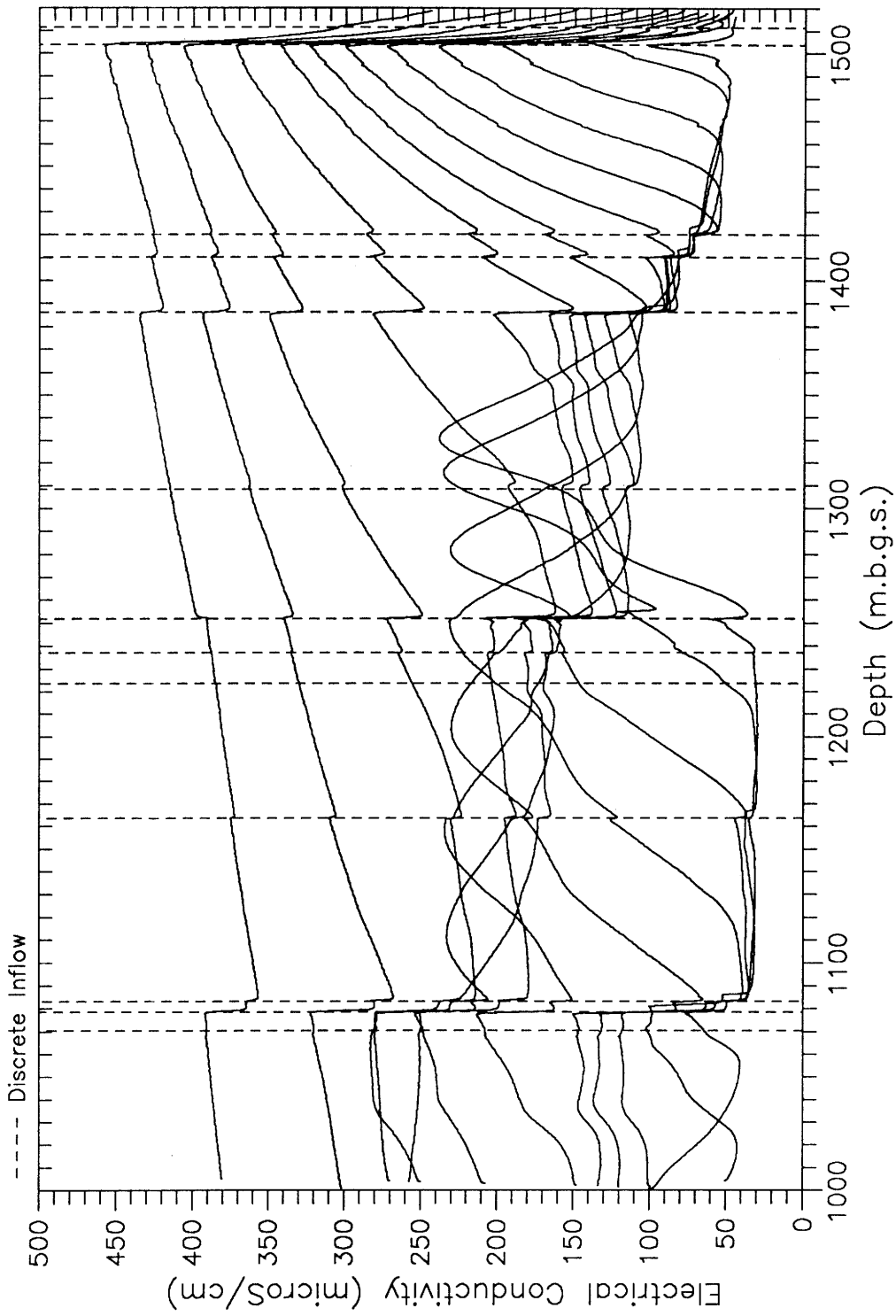

Figure 3.27: Conductivity Logs with Observed Inflows Delineated Fluid Logging Event PIP-RW1, Siblingen Borehole, Logging Times Approximately 1, 3, 6, 9, 12, 15, 18, 21, 27, 36, 45 and 59 Hours After Pumping Began

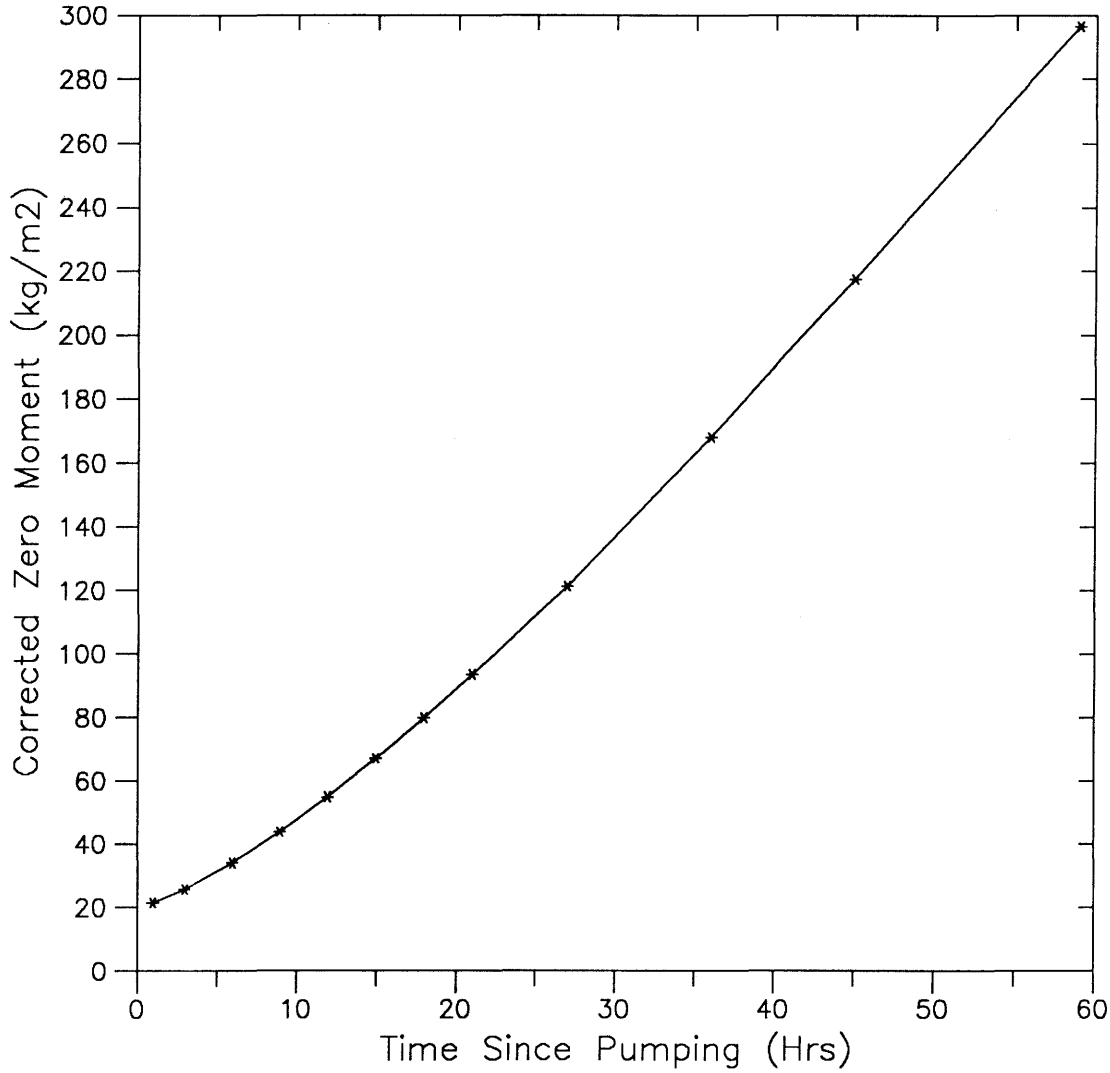

Figure 3.28: Corrected Zero Moment Claculated For the Interval 1011 to 1514 m b.g., Fluid Logging Event PIP-RW1, Siblingen Borehole

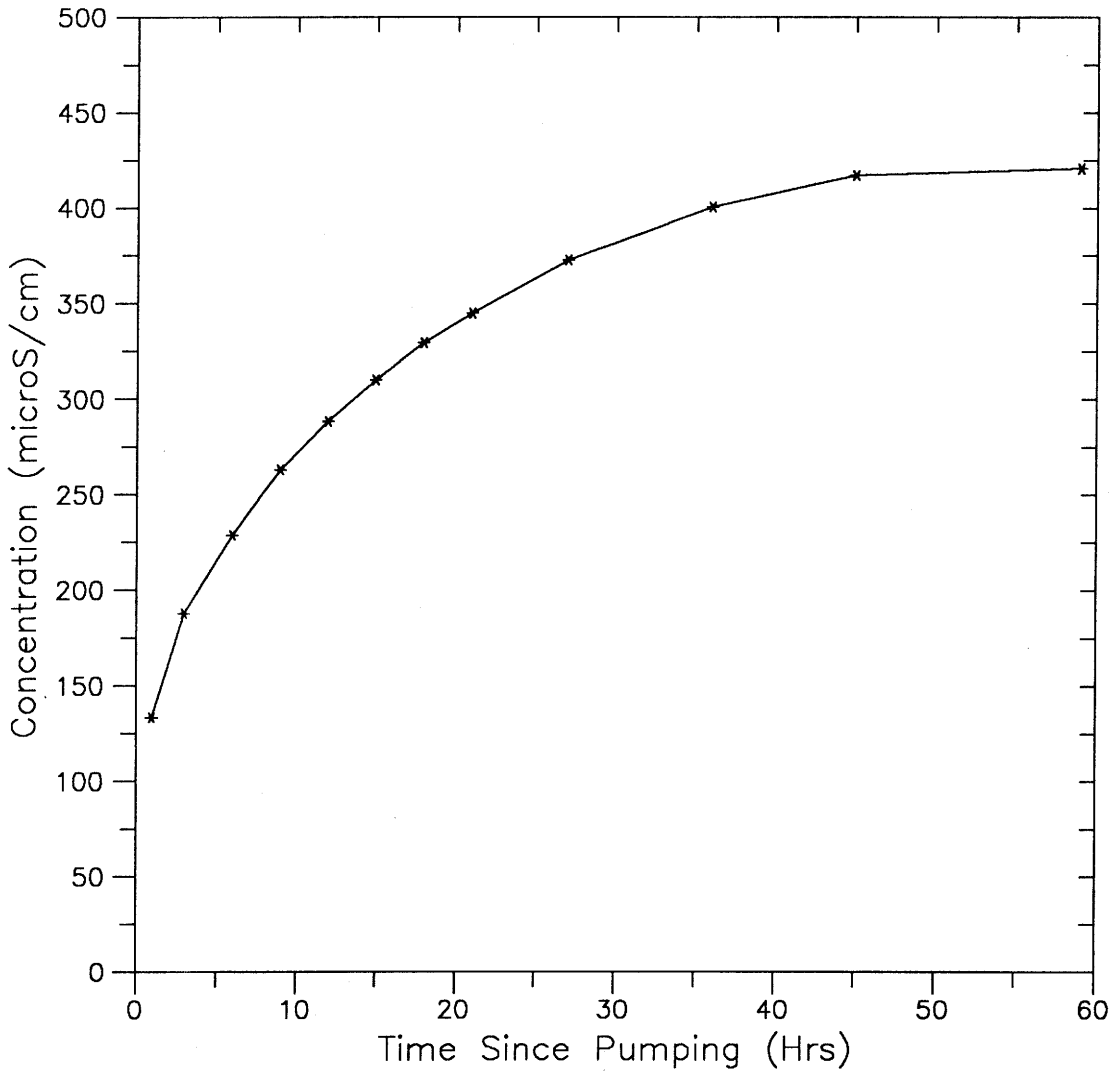

Figure 3.29: Average Inflow Concentration from 1011 to 1514 m b.g., Fluid Logging Event PIP-RW1, Siblingen Borehole

Table 3.16 lists the concentration versus time function for this logging event. Again, the calculated inflowing concentration is transient. The initial inflowing concentration is representative of the flushing fluid and slowly increases to the approximate concentration of the fracture fluid. At this point, the model boundary conditions or assumptions have been defined by calculating the average inflow concentration as a function of time and by assuming that the total outflow is constant and equal to 3.0 l/min.

Table 3.16: Average Inflow Concentration for Section Logged During Event PIP-RW1

TIME (hours)	CONDUCTIVITY (μS/cm)	CONCENTRATION (kg/m^3)
0.97	133	0.071
2.97	188	0.101
5.97	229	0.123
8.972	263	0.141
11.95	288	0.155
14.97	310	0.167
17.97	330	0.177
20.97	345	0.185
26.97	373	0.200
35.97	400	0.215
44.97	417	0.224
58.97	421	0.226

3.7.3 Estimation of Borehole Flow Rates Through the Transport of a Saline Tracer Pulse

Although a non-constant baseline concentration in the borehole prior to logging presents problems when performing the classical moment based calculations, it can allow an independent method for the estimation of borehole velocities. For example, if a slug of saline water is present in the borehole prior to pumping and logging, the logs will track the advancement of that slug up the borehole. By noting the peak location of the slug between measured logs and knowing the time elapsed between measured logs gives a direct means of calculating the borehole velocity. By multiplying this velocity by the cross-sectional area of the borehole, one receives a borehole flow rate.

As previously mentioned and shown in Figure 3.24, a large slug of saline water was present prior to pumping between the depths of 1260 and 1460 m b.g. The method of monitoring a slug or tracer pulse as it Figure 3.29 advects through the borehole is often referred to as "in-well tracing" and has proven useful in many investigations (MICHALSKI and KLEPP, 1990).

The first velocity estimate was calculated for the interval 1330 to 1314 m b.g. by analyzing the position of the slug peak for the logs taken at 0.97 and 2.97 hours. The calculated flow rate is 0.96 l/min. In the time between the logs taken at 2.97 hours and 5.97 hours the slug peak travels from 1314.4 m to 1281.5 m b.g. This segment of borehole intersects a known inflow point occurring at 1308.5 m b.g. The borehole fluid velocity calculated for the interval 1330 to 1314 m (v_1) is used to calculate the time needed for the peak to travel to the inflow point at 1308.5 m ($t_1 = x_1 / v_1$). Here x_1 is the distance between the peak location in the log taken at 2.97 hours and the location of the inflow point. At the inflow point the flow rate takes a step function increase in magnitude. The new velocity in the borehole (v_2) can then be calculated from the knowledge of the distance travelled after the intersection with the inflow zone until the log at 5.97 hours (x_2) and the time taken to travel x_2 which is t_2 ($t_2 = t_T - t_1$). Here t_T is equal to the total elapsed time between logs. The calculated borehole flow rate for the interval 1308.5 to the next known inflow at 1252 m b.g. is equal to 1.45 l/min.

The next log taken at 8.97 hours records the peak of the slug coincident with a known inflow point at 1252 m b.g. This peak was not used in the pulse velocity analysis. The next borehole flow rate estimate was calculated from the movement of the slug peak from the log taken at 5.97 hours and 11.95 hours. Between these two logs the slug peak travels across 3 known inflow points at 1252, 1237, and 1223.6 m b.g. The slug peak is located at 1281.5 m at time 5.97 hours. The borehole velocity is known between 1281.5 m and 1252 m b.g. therefore the time taken to reach the first inflow is easily calculated. The slug peak is at 1202.9 m at time 11.95 hours. Because the slug peak arrival time at the inflow zones 1237 and 1223.6 m is unknown, the individual flow rates for these inflows cannot be calculated. However, an effective borehole flow rate can be estimated for the interval 1252 to 1202.9 m b.g. The effective flow rate for this interval is 1.67 l/min. This represents the harmonic mean of the inflow from the three different regions because they act in series. Because flow in an interval must always be greater than the interval below this effective flow rate is an over-estimate for the lower most interval and an under-estimate for the upper-most interval. This value differs from all others calculated in this section because all others are discrete flow rates attributable to a discrete point in space.

The last estimate of borehole flow rate is based on the slug peak travel between logs taken at 14.97 and 17.97 hours. This gives an estimate for borehole flow rate in the interval 1164 to 1083 m b.g. The calculated flow rate is 1.83 l/min. Table 3.17 summarizes the results from the slug transport analysis.

Table 3.17: Borehole Flow Rates Calculated from Advection of a Tracer Pulse During PIP-RW1

INTERVAL NUMBER	INTERVAL DEPTH (m b.g.)	BOREHOLE FLOW RATE (l/min)
4	1330 - 1314	0.96
5	1308.5 - 1252	1.45
6, 7	1252 - 1202.9	1.67 (1)
8	1164 - 1083	1.83

(1) Represents an effective borehole flow rate for three inflows.

3.7.4 First Guess Parameter Estimation Through Zero Moment Analysis

The next step in evaluating PIP-RW1 is to estimate individual inflow rates by using the transient inflowing concentration as defined above and calculating the zero moments of the individual peaks. Classical moment analysis requires that peaks not interfere and that the integration boundaries remain at all times equal to the background concentration. This assumption could not met for any peaks except possibly for peaks 1 and 2 when analyzed collectively. For this reason it is not considered a worthwhile exercise to try individual peak analysis techniques on this set of logs because of the poor adherence to model assumptions

3.7.5 Partial Moment Analysis

As for the event PIP-RW2, the partial moment method has been used to evaluate flow velocities and therefore flow rates in the borehole. The borehole flow rate is a direct output from MOMENT. As was previously mentioned, it is important to plot the calculated zero partial moment for each analyzed section as a function of time to better define which MOMENT calculated flow rates are more representative. For this event a best estimate MOMENT input deck was constructed which relied strongly on knowledge gained from the analysis of the previous event. Again, nine integration intervals were used to derive borehole flow rates. These are numbered from the bottom of the logged section upwards from 1 to 9. The MOMENT results will be presented and compared to the direct flow rate estimates received in Section 3.7.3. From these two sets of results, a best-estimate well-bore flow rate will be derived.

Figure 3.30 is a plot of the zero partial moments versus time for the nine intervals analyzed. If the initial concentration profile were zero or equal to some non-zero constant less than the inflowing concentration, the behavior of the zero partial moment of an integration interval would increase as a function of time. The zero

partial moments for the given interval would finally plateau when all peaks below and inside the interval reach "saturation" conditions (TSANG et al, 1990). Because the well-bore velocity is a function of the time derivative of the zero partial moment, the most stable results occur when the slope of the zero partial moment as a function of time curve is both smooth and non-zero. For a complete discussion, see LOEW et al. (1990). For this event (PIP-RW1), the baseline conditions were not constant and a saline slug pulse moved through several integration intervals as a function of time. For this reason, intervals 4 through 9 do not follow a theoretical development but instead have slug-induced inflection points in the zero partial moment versus time functions. This causes problems in evaluating the borehole flow rate. The movement of this slug has a negative effect upon MOMENT calculations since it causes large variations, and even slope reversals, in the zero partial moment versus time curves. Figure 3.30 shows that the zero partial moment is affected by the movement of this tracer pulse through intervals 4 through 9.

Table 3.18 tabulates the flow rates calculated by MOMENT for simulation "A" for each integration interval for each logging time. Based upon the behavior of the zero partial moments, estimates of an appropriate borehole flow rate will be calculated from the values in Table 3.18. As in the PIP-RW2 event, the most ideal and stable interval is interval 1. The zero partial moment has a slope of a relatively high magnitude and that is relatively constant. The flow rate estimates at 11.95, 17.97, and 20.97 hours should give the most stable results so for the best estimate these three values were averaged to give a flow rate of 0.65 l/min. Interval 2 is a low magnitude inflow and the magnitude of the slope of the zero partial moment is low. This causes instability in the estimation of flow rate. The best estimate is an average between the flow rate calculated at 20.97 and 44.97 hours and is equal to 0.67 l/min. This value has a relatively high degree of uncertainty.

From review of the zero partial moment parameter space for interval 3 it is believed that the slope maximum in the zero partial moment at 20.97 hours should yield the most robust calculation of flow rate. The flow rate at this time was 0.82 l/min and this is the value adopted for the interval.

The zero partial moment for integration interval 4 initially decreases because of the movement of the saline pulse out of it. Between 5 and 10 hours, the interval reaches a mass balance, with the mass exiting the interval equaling the mass entering the interval, resulting in a constant zero partial moment. The behavior of the zero partial moment is not advantageous for the calculation of the borehole flow rates. The best estimates of flow rate should be calculated at times when the derivative of the zero partial moments are large and constant. This corresponds to times 8.97, 11.95, 14.97, and 17.97 hours. The best estimate represents an average between the flow rates calculated at 8.97, 11.95, 14.97, and 17.97 hours. The average is 1.11 l/min.

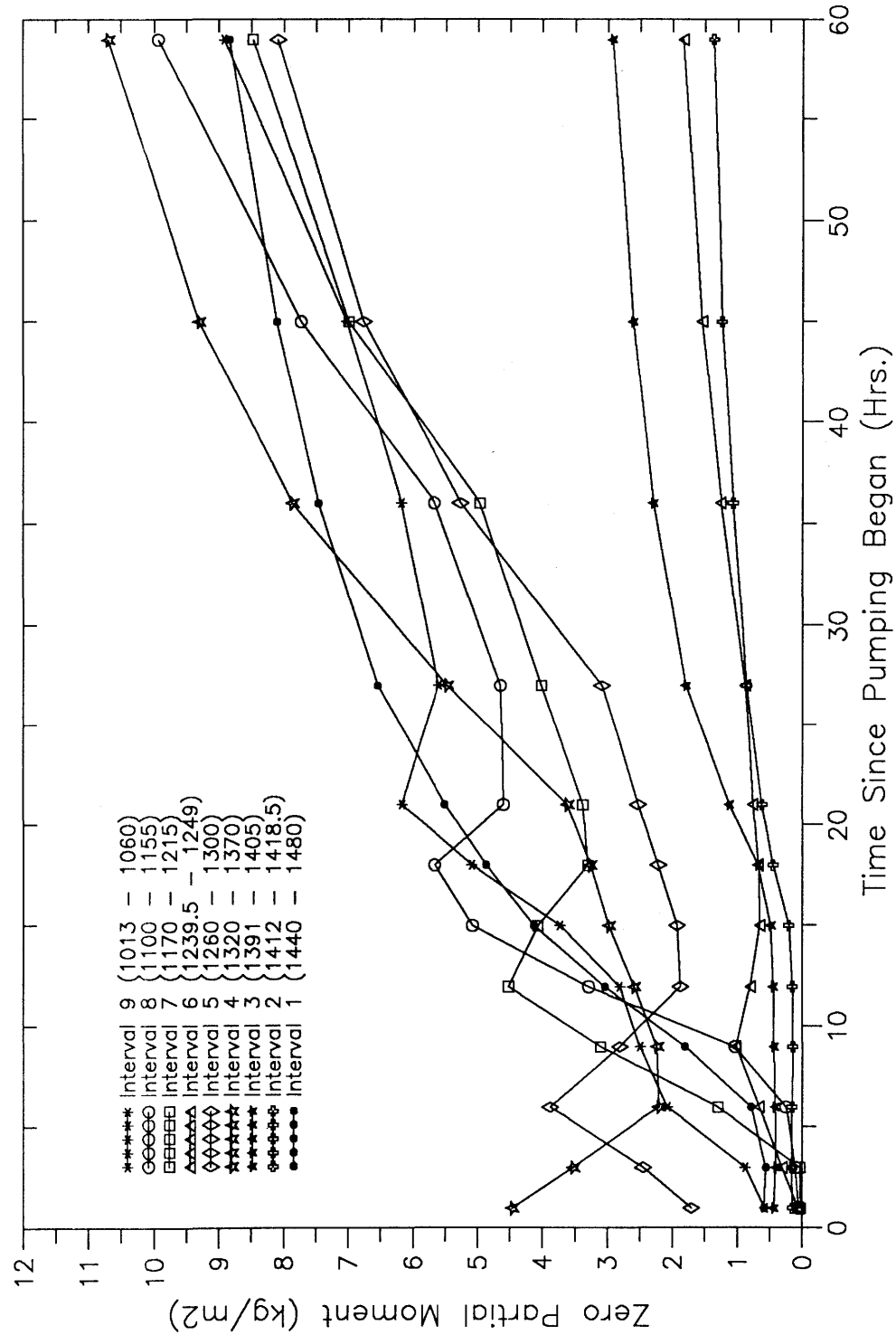

Figure 3.30: Zero Partial Moments for 'A' Simulation Fluid Logging Event PIP-RW1, Siblingen Borehole

Table 3.18: Estimated Borehole Flow Rates, Partial Moment Simulation "A"

TIME (hours)	BOREHOLE FLOW RATE (l/min)								
	Interval 9 1013-1060	Interval 8 1100-1155	Interval 7 1170-1215	Interval 6 1239.5-1249	Interval 5 1260-1300	Interval 4 1320-1370	Interval 3 1391-1405	Interval 2 1412-1418.5	Interval 1 1440-1480
0.97	-1.24	-1.83	-1.17	0.98	1.97	-0.66	-6.20	-0.40	-3.38
2.97	1.40	1.57	-8.12	1.43	1.30	0.86	-0.50	-0.00	0.22
5.97	3.73	7.25	1.26	7.55	0.40	0.53	-0.95	-0.07	-1.07
8.97	2.02	1.07	2.40	0.30	0.66	1.05	0.36	0.01	0.95
11.95	-14.75	-6.07	0.69	0.36	0.70	1.11	2.98	-0.74	0.63
14.97	2.13	1.41	0.80	0.95	1.08	1.08	0.96	0.53	0.66
17.97	5.13	0.84	1.45	-0.50	1.23	1.18	1.27	1.53	0.67
20.97	0.38	0.73	2.23	0.58	1.46	0.84	0.82	0.67	0.65
26.97	-0.53	1.30	2.40	4.55	1.98	0.88	0.64	0.46	0.56
35.97	2.67	3.40	3.20	38.17	0.94	-2.85	1.02	-1.15	0.76
44.97	-1.87	1.28	1.70	0.98	-0.16	1.65	1.02	0.67	0.95
58.97	18.83	2.55	-1.25	-0.13	1.75	6.17	0.08	0.03	0.93

(-) indicates down borehole flow

The zero partial moment for interval 5 is again affected at early times by the movement of the slug pulse through the integration interval. The derivative of the moment quantities for interval 5 is most constant and large for logging times 14.97, 17.97, and 20.97 hours. The magnitude of the derivatives of the partial moment quantities are larger for logs measured from 26.97 to 58.97 hours. However, the magnitude of the derivatives varies, causing variations in estimated flow rates. The best flow-rate estimates are thought to occur at times 14.97, 17.97, and 20.97 hours. An average of the flow rates estimated at these times yields a flow rate of 1.26 l/min. Integration interval 6 has poor moment behavior. The zero partial moment is adversely affected by the movement of the slug pulse through the integration boundaries at early times. The zero partial moment has a small slope which Table 3.18 makes evaluation of flow rates uncertain. The best flow rate is thought to be evaluated at 2.97 hours and is equal to 1.43 l/min. Because of the instability of the calculated flow rates for this interval and the estimate being based on one number, this flow rate is considered to be uncertain.

Again for integration intervals 7 and 8, the behavior of the zero partial moment as a function of time has been affected by the movement of the slug pulse through the integration intervals. Based on the derivatives of the zero partial moment, the best estimates of interval flow rate are at 5.97, 8.97, 20.97, and 26.97 hours. The average borehole flow rate for these four values is 2.07 l/min (see Table 3.18). The best flow rates are thought to be evaluated for integration interval 8 at times 35.97 and 44.97 hours. The average value for these two times is equal to 2.34 l/min. For the last integration interval, interval 9, the zero partial moment behavior suggests that the best estimates of flow rates will occur at times 14.97, 17.97, and 35.97 hours. The average flow rate for these three times is 3.31 l/min. The flow rate for this last interval should be equal to the flow rate measured at surface, 3 l/min. The flow rate estimates for the last three intervals, 7 through 9 are very unstable and consequently uncertain in magnitude.

Table 3.19 summarizes the borehole flow rates calculated both by the partial moment method and through the saline slug pulse analysis. Included in the table are the best estimate flow rates derived for each interval. For intervals 1, 2, and 3, only MOMENT results are available, so the MOMENT calculated flow rates are the best estimate flow rates. For intervals 4 and 5, results from both MOMENT and the slug pulse analysis are available. For interval 4, the two flow rate estimates by the two methods vary by only 6%. For interval 5, the two methods yield results which vary by 13%. For intervals 4 and 5, the best estimate flow rate is the arithmetic mean between the two results. For interval 6, only MOMENT results are available. For intervals 7 and 8, both MOMENT and slug pulse results are available. The pulse analysis results are considered more correct because of the instability of the flow rates calculated for these two intervals. For this reason the best estimate is solely derived from the slug pulse analysis results. The interval 9 flow rate is set equal to the pumping rate from the logged section (3 l/min.).

Table 3.19: Peak Flow Rates (l/min) Derived from Partial Moment and Saline Slug Pulse Analyses

Interval Number	Interval Depth (m b.g.)	Borehole Flow Rate (l/min)		
		Partial Moment	Pulse Analysis	Best Guess
1	1480 - 1440	0.65	NA	0.65
2	1418 - 1412	0.67	NA	0.67
3	1405 - 1391	0.82	NA	0.82
4	1370 - 1320	1.02	0.96	1.00
5	1300 - 1260	1.26	1.45	1.36
6	1249 - 1239.5	1.43	NA	1.43
7	1215 - 1170	2.07	1.67	1.67
8	1155 - 1100	2.34	1.83	1.83
9	1060 - 1013	3.00	NA	3.00

Figure 3.31 plots the borehole flow rate and the individual inflow feature flow rate as a function of depth. The box represents the interval listed in Table 3.20 and the dashed lines within the solid box represents the 13 discrete inflow zones. Table 3.20 summarizes the discrete feature inflow rates. The PIP-RW2 event was a constant-rate withdrawal event with a flow rate of 1.5 l/min which is exactly one half of the constant flow rate withdrawn during this event (PIP-RW1). For this reason, one would expect that the individual flow rates determined during this event would be approximately a factor of two higher than those determined for PIP-RW2 (see Table 3.15). This is the case for four of the intervals (Intervals 1, 4, 8, and 9).

Table 3.20: Peak Flow Rates (l/min) Derived for the Borehole Interval from 1000 to 1522 m, Event PIP-RW1

Interval Number	Peak(s) Included	Inflow Interval Depth (m b.g.)	Inflow Rate (l/min)
1	1, 2	1500 - 1516	0.65
2	3	1415 - 1425	0.02
3	4	1405 - 1415	0.15
4	5	1381 - 1391	0.18
5	6	1303 - 1313	0.36
6	7	1247 - 1257	0.07
7	8, 9	1219 - 1242	0.24
8	10	1158 - 1168	0.16
9	11, 12, 13	1065 - 1089	1.17

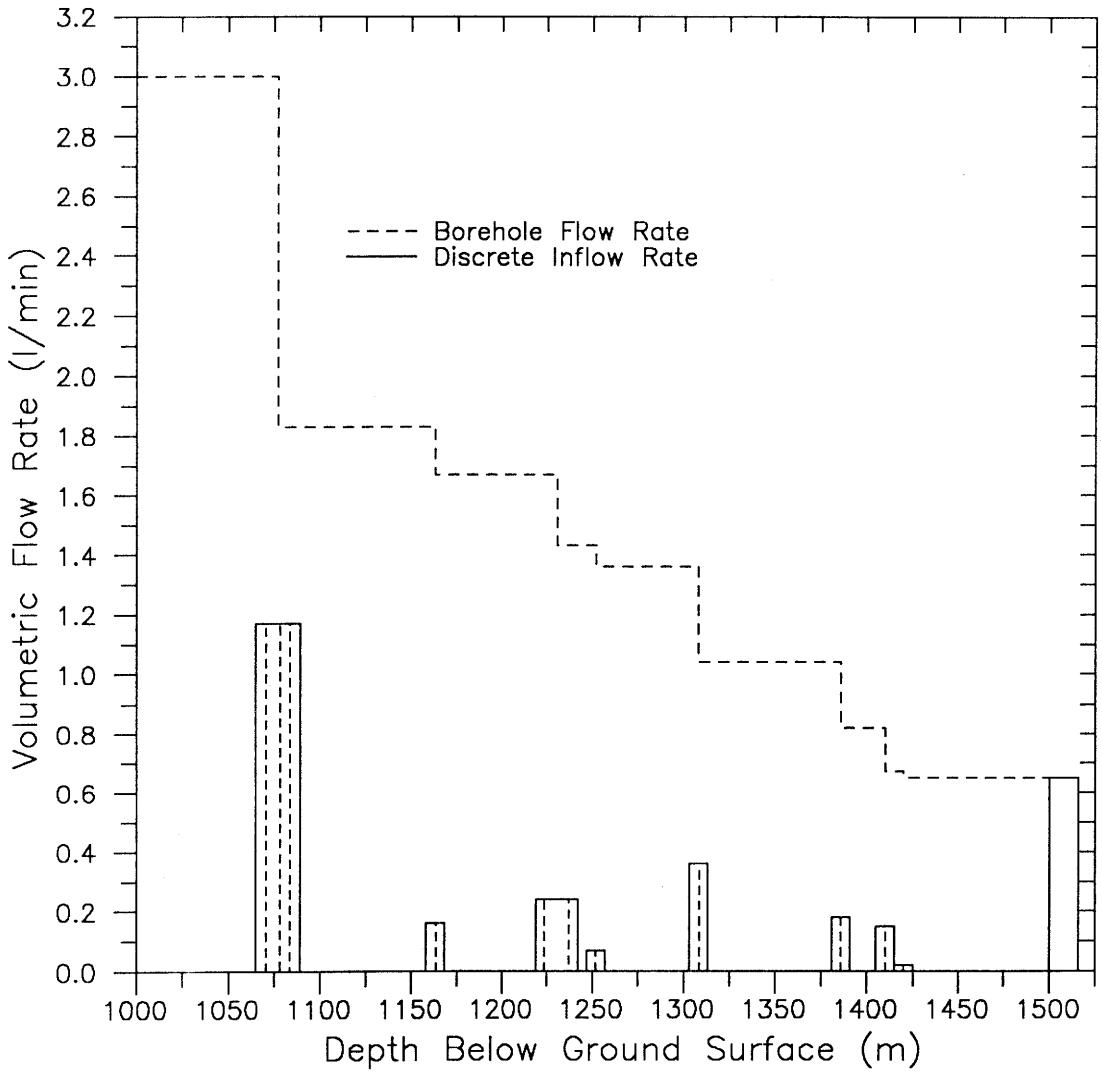

Peak 1,2	(1516 – 1500 m)
Peak 3	(1425 – 1415 m)
Peak 4	(1415 – 1405 m)
Peak 5	(1391 – 1381 m)
Peak 6	(1313 – 1303 m)
Peak 7	(1257 – 1247 m)
Peaks 9,8	(1242 – 1219 m)
Peak 10	(1168 – 1158 m)
Peaks 11,12,13	(1089 – 1065 m)

Figure 3.31: Volumetric Flow Rate for 9 Intervals Analyzed Fluid Logging Event PIP-RW1, Siblingen Borehole

The most anomalous flow rate is for interval 5 which is a factor of 18 higher than for PIP-RW2. The moment analysis is complicated by the pulse moving through the interval at early time. The pulse analysis gives an even higher flow rate for this interval. The reason for this discrepancy is not known. For intervals 2 and 6, flow rates were obtained which were less than for PIP-RW2 which again represents an inconsistency. For interval 2 this might be expected because of the low flow rate from that interval. Because there exists a vertical gradient for flow in the borehole under non-stressed conditions, some degree of this type of behavior should be expected. Also, it is felt that because PIP-RW2 was performed relatively soon after PIP-RW1, superposition of pumping events is expected and can cause nonlinear variation in fracture flow rates as a function of pumping rate. This is already evidenced in the fact that for PIP-RW1 the borehole was pumped at 3.0 l/min and stabilized at 21.3 m of drawdown and during PIP-RW2 the borehole was pumped at 1.5 l/min and stabilized at 14.4 m of drawdown.

3.7.6 BORE Simulation with Best Guess Parameter Set

As in the analysis of PIP-RW2, we again use BORE to see how well the best guess parameter set will match the development of the observed peaks. Again the parameters used as input are derived from the MOMENT analysis.

A simulation was performed for each of the nine logs measured which covers a time period of 59 hours. In all cases the dispersion coefficient used is constant and equal to 5E-4 m^2/s. This was based upon a limited early time calibration and not based upon theoretically significant considerations. Figure 3.32 plots the observed versus simulated logs for 11.95 hours after pumping began.

Considering the transient nature of the inflowing concentration, the fit is very good. The obvious exception to this is peak 6, which we have already identified as being anomalously high. Figure 3.33 is a plot of the observed and the simulated conductivity log measured at 24.03 hours after pumping. The fit has deteriorated from the simulation at 11.95 hours.

Because of the slug pulse which was advected through the section during logging, a plot showing all observed logs compared to all simulated logs is very difficult to decipher. Instead, the last log measured will be presented to show the late time fit for the transient simulation. Figure 3.34 plots the observed log measured at 58.97 hours along with the BORE simulated log. The fit between the observed and simulated logs is again not bad, considering the transient nature of the modeled system. Problems with this type of simulation have already been presented in Section 3.6.4 and will not be repeated here. Again, further calibration will not be performed and all of the flow rates derived in this chapter will be used to calculate transmissivities in Section 5.

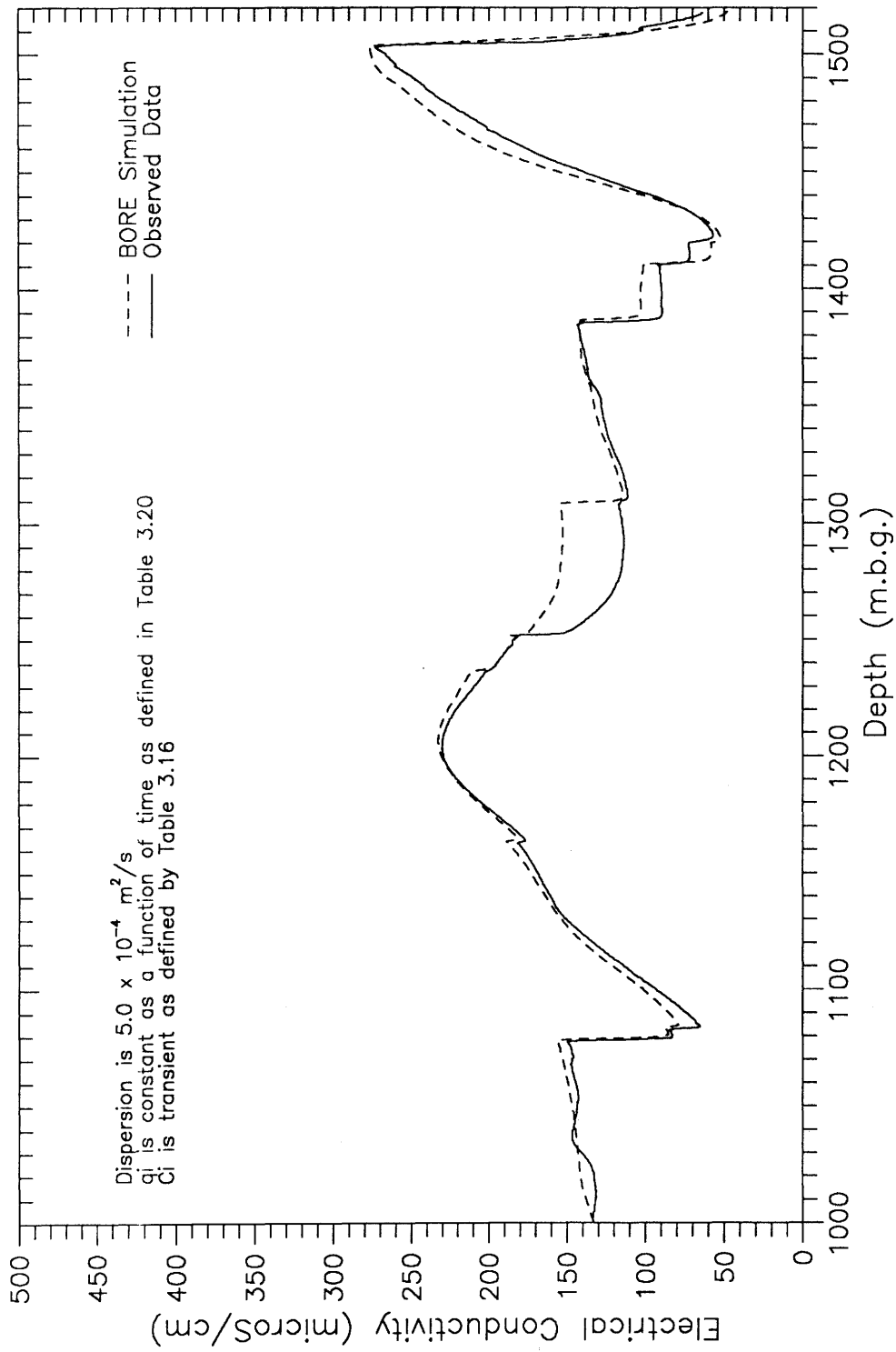

Figure 3.32: BORE Simulation of First PIP-Pumping PIP-RW1 Simulation Time is 11.95 Hours, Siblingen Borehole

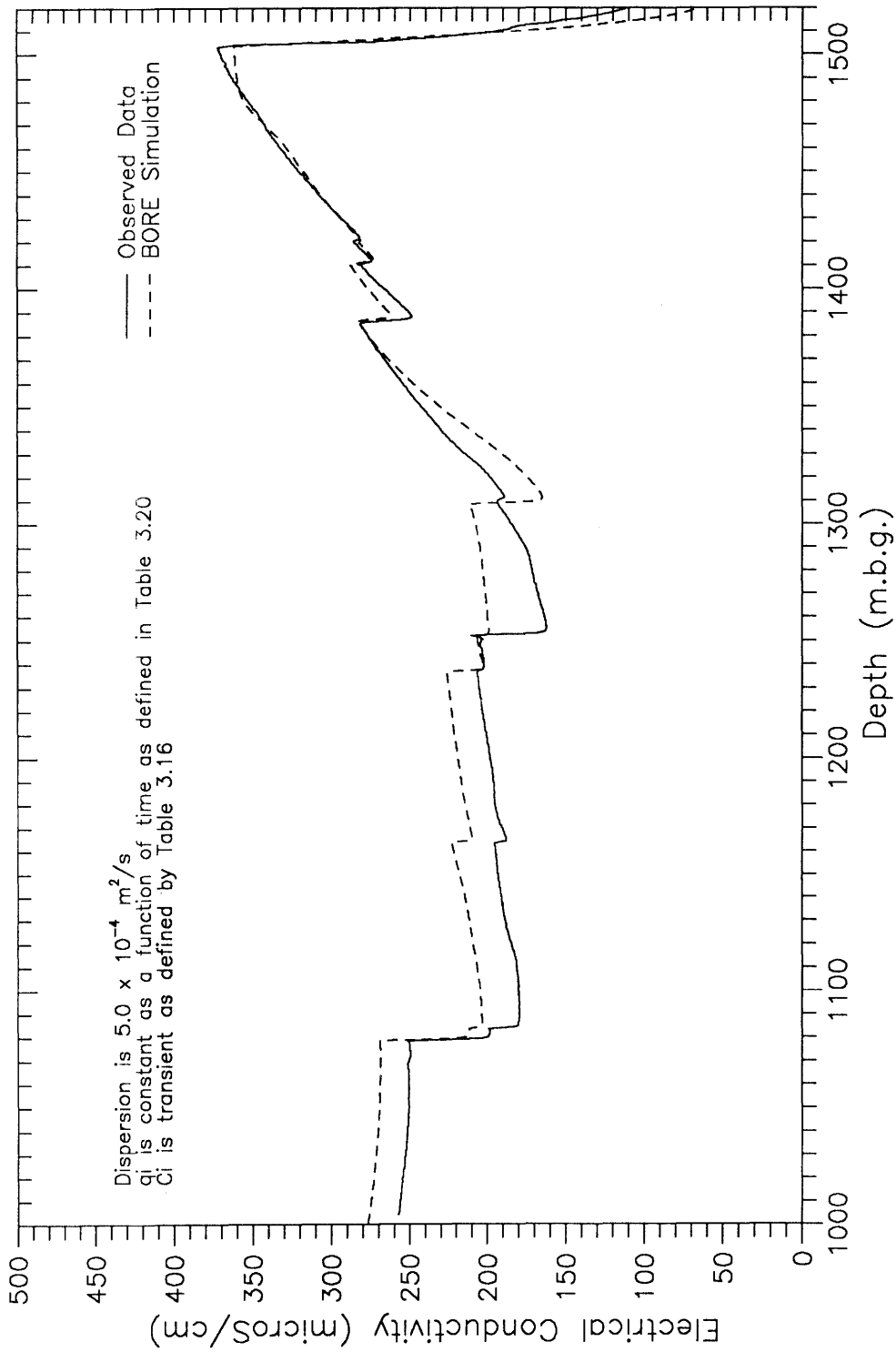

Figure 3.33: BORE Simulation of First PIP-Pumping PIP-RW1 Simulation Time is 26.97 Hours, Siblingen Borehole

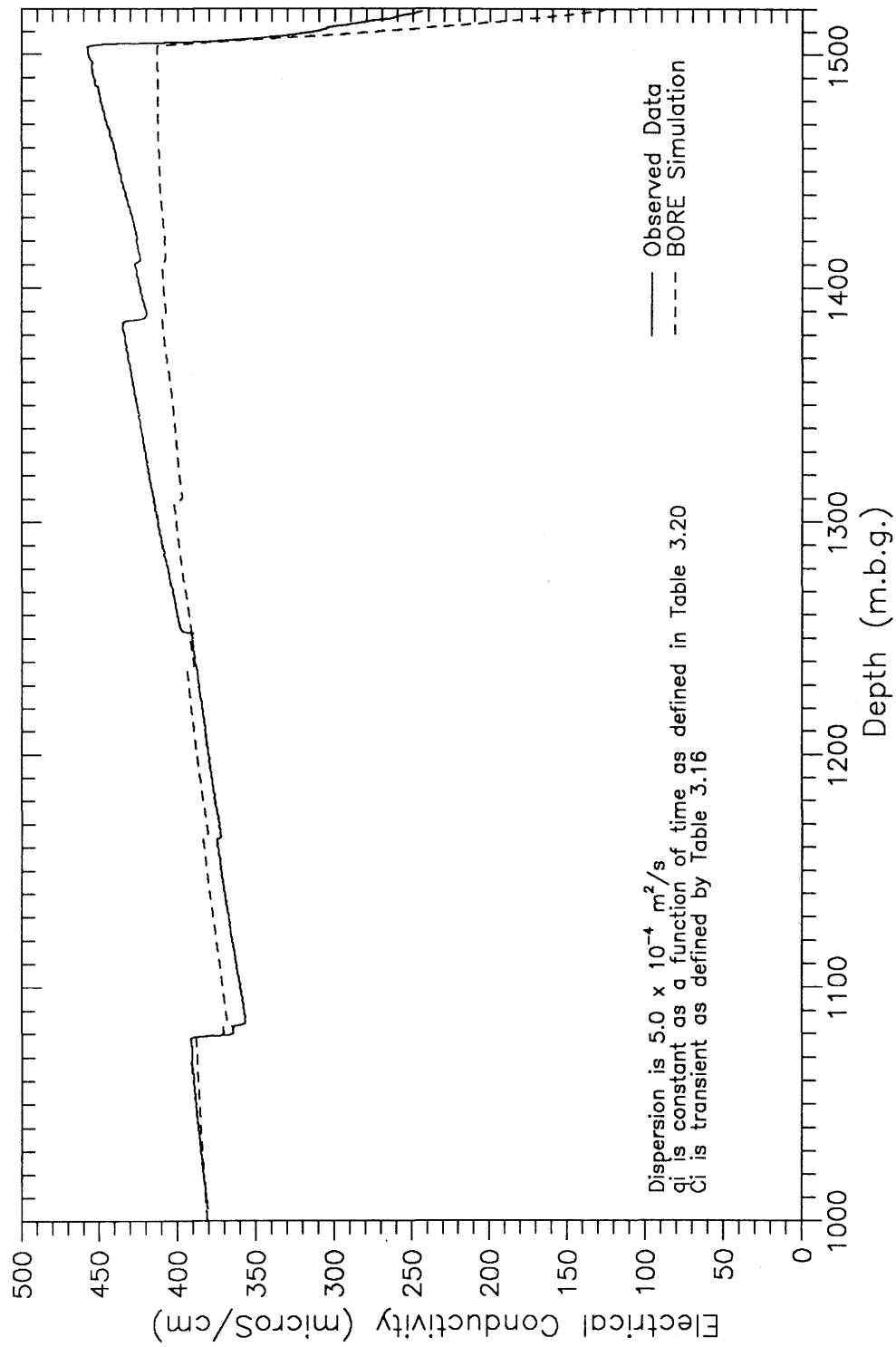

Figure 3.34: BORE Simulation of First PIP-Pumping PIP-RW1 Simulation Time is 58.97 Hours, Siblingen Borehole

4 INTERNAL BOREHOLE FLOW RATES MEASURED DURING STATIC FLUID LOGGING EVENTS

4.1 Introduction

If significant head differences exist between aquifers encountered within an open borehole section, internal borehole flow can develop. Large and structurally massive sections of fractured rock are particularly susceptible to internal flow when left hydraulically connected through an open borehole (MICHALSKI and KLEPP, 1990). The term *static* is used in this report to describe a fluid logging event where the borehole is not stressed through either production or injection. It does not imply hydrostatic conditions within the wellbore.

The Siblingen borehole crystalline section does have internal flow (VOMVORIS et al., 1990). This internal flow is the result of significant head differences within permeable features in open communication through the borehole (see Table 1.2 in this report modified from OSTROWSKI and KLOSKA, 1990). PAILLET et al. (1990) report that heat-pulse packer flowmeter results indicate that under static conditions flow enters the borehole at approximately a depth of 690 to 700 m b.g. and exits over a large interval from 930 to 1280 m b.g. These raw data are re-interpreted in this report (see Section 2.6) and indicate a similar pattern. In fact all static fluid logging events analyzed showed a similar pattern.

Static fluid logging events were analyzed from electrical conductivity logs, spinner packer flowmeter logs, spinner flowmeter logs, and heat-pulse packer flowmeter logs (see Table 1.1). This Section will compare the static flow results from each log and determine if the results are coherent and internally consistent with known borehole conditions determined through means independent of fluid logging.

4.2 Comparison of Results

For static fluid logging events where the borehole water table was measured, the head in the borehole only varied from 440.9 to 442.4 m a.s.l. Table 4.1 lists the results from the various fluid logging methods as measured during static conditions in the borehole. Figure 4.1 perhaps offers an easier medium for comparing these results. From review of these results it can be said that all measurements depict a similar pattern of borehole flow. There is however some differences in flow rate magnitudes. The extreme case is the spinner flowmeter results (FLU-2). The spinner flowmeter detected zero flow until a depth of 691.4 m, where it recorded a flow rate of -6.1 to -7.8 l/min (the minus sign signifies that the flow is down the borehole). This rate increased to a maximum of -12.9 l/min at 925.4 m and then was again below detection at a depth of 938.1 m. These results are not considered correct due to problems in interpretation (see Section 2.4). As a result, these measurements are not included in Figure 4.1 and are simply noted as plotting off the scale.

Table 4.1: Measured Internal Borehole Flow Rates as Derived from Static Fluid Logging Events

Measure-ment Depth (m b.g.)	Dec 20/21 SPF FL1 Run 1	Jan 23/24 SF FL2 Run 1 up	Jan 23/24 SF FL2 Run 1 down	Apr 5/7 SPF FL3 Run 1a	Apr 5/7 SPF FL3 Run 1b	Apr 15 T/LF SF-1	Apr 16 T/LF SF-2	June 6/8 HPPF FL4 Run 1
150		0.0	0.0					
180								
182	0.0							
350	0.0							
480	0.0							
490.45	**********	********	**********	CASING	*******	*******	*******	********
525	0.0							0.0
575	0.0							
625	0.0							
660				0.0				0.0
675	0.0							
684.9			0.0					
690		0.0						
691.4			-6.1					
698	-1.1							
708				-2.0	-1.9			-1.10
715		-7.8						
725	-1.6							
770					-2.1			-1.10
775	-1.6							
825	-1.4							
840	-1.3							-1.10
860								-0.90
875			-11.3					
878.1		-10.1						
878.3		-10.5						
880			-12.0					
910					-1.3			-1.00
920								-1.10
925.4		-9.4	-12.9					
930		0.0					-0.56	
936						-0.42		-0.30
938.1			0.0					
955				0.0				
980								-0.30
1027						-0.54		
1062				0.0				-0.30
1089							-0.48	
1093						-0.40		
1100								-0.20
1123						-0.45		
1210								-0.30
1219						-0.35		
1276								0.00
1350				0.0				0.00

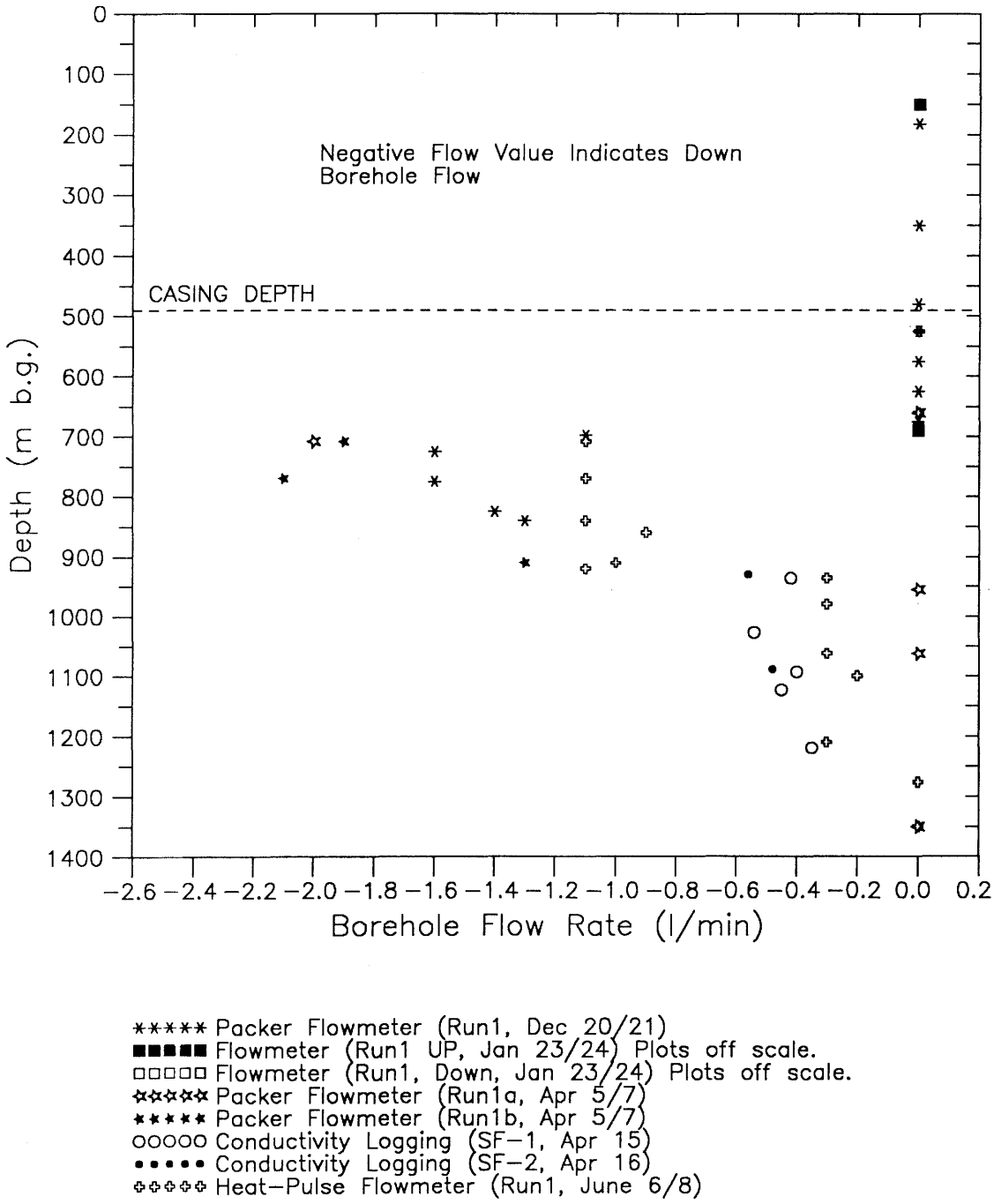

Figure 4.1: Borehole Flow Rate as Determined from all Static Fluid Logging Events, Siblingen Borehole

The first packer flowmeter results detected no flow until a depth of 698 m, where it recorded a flow rate of -1.1 l/min (Table 4.1). The maximum flow rate measured during this run was -1.6 l/min at 725 m. The last station was at 840 m and recorded a flow rate of -1.3 l/min. The next results in time were from the spinner flowmeter and are not considered. Two static runs were performed with the packer flowmeter from April 5 to 7, 1989. Run 1a detected no flow until a depth of 708 m where it recorded a downward flow rate of -2.0 l/min. The last two measurements in this run were at depths 955 and 1062 m and yielded flow rates below detection. The second run, Run 1b, was run to increase resolution and gave similar results. The first measurement was -1.9 l/min at a depth of 708 m. Two additional measurements were made at depths 770 and 910 m and were -2.1 and -1.3 l/min, respectively.

The heat-pulse packer flowmeter first detected flow at a depth of 708 m of -1.1 l/min. This flow rate was essentially constant from 708 to 920 m. From depths 936 to 1210 m, the heat-pulse packer flowmeter recorded a nearly constant flow rate of -0.3 l/min and, after a depth of 1210 m, flow was not measurable. The conductivity results showed flow rates below 930 m from -0.56 to -0.35 l/min, with a perceptible trend of decreasing flow rate with depth.

From a comparison of these results, it can be said that the results from each method concur on overall flow patterns within the borehole during static conditions. The borehole can generally be divided into three sections as defined by borehole static flow. To summarize, flow within the borehole under static conditions is negligible from the casing at 490.9 m to a depth of 675 m. Between the depths 685 and 930 m, there is significant (-2.0 to -1.0 l/min) downward flow in the borehole. Between the depths 930 and 1522 m, the downward flow is diminished but is still perceptible by fluid logging (-0.5 to -0.2 l/min) and decreases with depth. The bulk of the flow enters the borehole between 685 and 692 m. Although spinner flowmeter measurements are not considered correct in absolute magnitude, they still yield relative magnitude information concerning flow and restricted the entrance interval to between 685 and 691.4 m. A large percentage of this flow exits the borehole between the depths 920 to 930 m. The remaining percentage of the flow continues down the borehole past a depth of 930 m (-0.56 to -0.3 l/min) and the flow rate steadily decreases with depth.

The static borehole flow rates determined by the various fluid logging methods were very similar in magnitude (with the exception of the spinner flowmeter). However, the heat pulse static borehole flow rates are smaller (by a factor of 2 in some cases) in magnitude than the flow rates determined by the other methods. Tool measurement variation could be held responsible for some differences seen between the fluid logging methods, although this is not felt to be large enough to explain the difference between the heat-pulse packer flowmeter and the other methods. Other potential explanations for this difference will be discussed in the following sections.

4.3 Qualitative Analysis of Transient Borehole Flow Rates

Internal borehole flow is controlled by two primary system parameters, the head gradient between the flowing units and the transmissivity of the flowing units. The head of units communicating within the borehole can change given open borehole conditions. The transmissivity of the units would in most cases be considered constant.

The water enters the borehole between the depths 685 and 692 m. This flux is controlled by the head difference between this interval and the borehole and the transmissivity of this interval. The transmissivity of this unit was determined in hydraulic test CR10 which gave a range between 2.1 and 3.8E-4 m^2/sec. If we assume that a representative transmissivity is 3E-4 m^2/sec and use Dupuit's steady-state equation (Equation 5.1), we can calculate the drawdown needed to receive 2 l/min flow from this interval. The estimate is 0.2 m of drawdown. It is easy to see how internal flow can get started. Once the water flows out of this interval, it feels a greater head gradient downward than upward. This is consistent with hydraulic packer test estimates of head (see Table 1.2).

The distribution of where the inflowing borehole fluid will outflow is again driven by the transmissivity and borehole-to-interval head gradients for the transmissive intervals below the primary inflow interval, i.e., the portion of the borehole from 692 to 1522 m. If all head gradients were the same, then the amount of water that would flow out of a given interval would only be a function of the interval transmissivity. Therefore, high transmissivity zones get the most water and *vice versa*. From fluid logging results, it is clear that a large percentage of the flow exits the borehole between 920 and 930 m. This means that this zone has a smaller head than the borehole head. The transmissivity of this interval is 4.8E-5 m^2/sec (Test CR16) which is over an order of magnitude greater than the transmissivity of the remainder of the borehole (1013 - 1522 m, T = 3.1E-6 m^2/sec, CR20 + CR24). Using Dupuit's equation, we find that this interval between 920 to 930 m could take 1.5 l/min from the borehole, with a head difference of only 0.8 m. The remainder of the borehole fluid would be lost to the zone from 930 to 1522 m, since these zones have hydraulic heads many meters lower than the head in the borehole.

From the results summarized in Table 4.1, it can be deduced that the borehole flow rates had decreased between the static measurements performed during drilling and testing and the later heat-pulse packer flowmeter results. VOMVORIS et al. (1989) also noticed that flow measurements made early in the borehole history were greater than those measured later in the borehole history. VOMVORIS et al. (1989) cites results from a post-test phase spinner packer flowmeter campaign performed on October 3, 1989. The results from this logging event were that the vertical flow rate in the borehole was less than or equal to -0.3 l/min. They measured no flow in the entire borehole and arrived at -0.3 l/min by using the tool detection limit. Temperature logs recorded immediately before the flowmeter measurement confirm internal borehole flow in both cases (i.e., even when the packer flowmeter recorded zero flow). The explanation presented was that significant fluid losses during

drilling created an overpressure in the upper portions of the borehole. As the pressure in this section diminished, so the driving force also diminished for vertical flow.

Because a large amount of intervals of varying head and transmissivity are hydraulically connected through the borehole, the borehole head will be less than the highest head and greater than the lowest head. The head in the borehole is going to be dominated by the high transmissivity intervals. As we have seen in the calculations above, only slight head differences are required to see static flow rates on the order of what has been observed. It is certain that overpressuring could have a great effect upon the transient nature of the flow rates observed.

For inter-borehole flow to diminish, either a reduction in the participating interval's transmissivity or a reduction in the driving force, the head differences, is required. Assuming the transmissivity of the intervals is constant (see the next section), then the driving force must change. This reduction in head variations does not necessarily require an overpressure scenario. A borehole that is left open over large intervals with significant head differences will require some time to reach a steady-state flow condition. In the case of Siblingen, the high head intervals will dominate the overall head measured for the encased borehole. This effectively imposes a boundary condition at the borehole opposite the lower head intervals, which is meters above the ambient static head. At the same time, the higher head interval would tend to fall toward the mean borehole head. A final static borehole flow would occur as a result of a new borehole equilibrium condition. This flow would be significantly reduced. This model assumes that the units behave as infinite media.

The conclusion is that the internal borehole flow rates measured under open borehole conditions during static fluid logging events have decreased as a function of time from the initial drilling period. The observed flow rate at any time is a function of both the vertical head differences and the transmissivity of the flowing units. The head in the borehole has remained relatively constant. This causes the lower head found in the flow units to increase. A combination of this and the depressurization of any overpressured intervals would finally result in a steady-state flow cell which would be significantly reduced relative to early flow measurements.

The discussion above is based on the assumption that the transmissivity of the flowing units is constant through time. This should not be the case for the Siblingen borehole because sections of the borehole were sealed during the fluid logging campaigns.

4.3.1 Transmissivity Transience from Borehole Sealing

During the course of drilling the Siblingen borehole, substantial fluid losses were incurred. To prevent these fluid losses, the borehole was sealed with clay, celloflex, and mica on numerous occasions over several intervals. In addition, two zones

were cemented because of extreme fluid losses. The first interval cemented was between 490.3 m (casing shoe) and 536 m, and was done after hydraulic test CR12 (December 28, 1988). The second interval cemented was from 668 to 850 m, and was cemented after hydraulic test CR13 (January 4, 1989). Attempts were also made to plug the borehole down to 1062 m with clay, celloflex, and mica.

One would expect the transmissivity of an interval to be radically changed if that interval were cemented. The fluid logging results do not confirm intuition. The first packer flowmeter measurement was performed prior to the cementing of the interval 668 to 850 m. The maximum borehole flow rate measured during this campaign was -1.6 l/min at a depth of 725 m. The next logs run were with the spinner flowmeter and were run after cementing. However, they cannot be considered for comparison. The next static measurements were performed with the packer flowmeter (Runs 1a and 1b). These two runs measured an average borehole flow rate of -2.0 l/min from the borehole interval 708 to 770 m. This shows that the effect of cementing the highly transmissive portion of the borehole straddled from 691 to 850 m was short-lived. Reduction of transmissivity associated with cementation had been lost between cementation (January 4, 1989) and the static packer flowmeter logs measured April 5/7, 1989. It is concluded that cementation is not responsible for variation in borehole flow rates as measured at different times and through different means, especially in the case of the heat-pulse flow meter.

5 TRANSMISSIVITY AS CALCULATED FROM FLUID LOGGING FLOW RATES

5.1 Transmissivity Calculation Methodology

The primary result of all of the fluid logging analyses is borehole flow rate. In each analysis these borehole flow rates have been made attributable to intervals, or in the case of conductivity logging, to discrete inflow points. Interval transmissivities (T_i) can be estimated from the individual interval flow rates (q_i) as determined through the various fluid logging events and the head difference driving the flow rate. In the case of internal borehole flow rates measured during static fluid logging events, the driving force is the head difference between flowing intervals relative to the average borehole head, termed (D_{si}). In the case of constant-rate fluid logging events, the driving force is the head difference between the flowing interval head and the drawdown in the borehole as a result of pumping, termed (D_{Ri}). The observed drawdown in the borehole as a result of a constant-rate withdrawal event is termed D_{RW} and may or may not be equal to D_{Ri}. To calculate transmissivities from flow rates derived from electrical conductivity logs, it was assumed that, for each analyzed interval, ($D_{si} << D_{RW}$). The interval transmissivities are calculated using elementary analytical solutions to the diffusion equation.

In the methodology and equations used here to calculate transmissivity, each individual inflow zone is assumed to behave independently of the other, and responds to the borehole condition either imposed or natural. Therefore, here we assume zero hydraulic connection between zones, so that the zones are considered horizontal and the interbeds are considered to have zero hydraulic diffusivity. Explicitly stated, the assumptions are that:

(1) flow is horizontal,
(2) the medium is infinite, isotropic, and homogeneous, and
(3) the well is fully penetrating.

5.1.1 Steady Flow Solution

The steady-state solution to the diffusion equation is termed Dupuit's or Theim's formula, and, at a radius equal to the well radius ($r = r_w$), is written

$$D_w = (Q_w / 2\pi T) \ln(R/r_w) \qquad (5.1)$$

where D_w is the steady state drawdown in the well, Q_w is the steady state flow rate, T is the system transmissivity, and R is the location of the outer constant head boundary condition where the head is always constant. Although R is unknown, the solution of the equation is relatively insensitive to the evaluation of the natural log.

Because this is a steady-state equation, it is independent of both time and of a medium storage parameter, and therefore such variables must not be estimated. This equation is considered applicable for static flow events where head changes and borehole flow rates are assumed to be as a result of steady-state conditions.

5.1.2 Transient Solution

For some cases, the head changes as a function of time and is therefore classified as transient flow. The primary solution for transient drawdown in a well is the Theis solution. The Theis solution requires evaluation of the exponential integral function and is therefore not easily applied. COOPER and JACOB (1946) found that if the argument of the exponential integral met certain criteria, then a simplified logarithmic approximation could replace the exponential integral in the transient formula. The Cooper-Jacobs approximation for a constant-rate withdrawal test would be written as

$$D_{RW}(t) = (q_{Ri} / 4\pi T_i) \ln (2.25\ T_i t / S_i r_w^2) \qquad (5.2)$$

where $D_{RW}(t)$ is the drawdown in the well at time t, q_{Ri} is the flow rate of layer i in response to D_{RW}, T_i is the transmissivity of layer i, and S_i is the storage coefficient for layer i. This approximation is valid as long as the following condition holds.

$$4T_i t / S_i r_w^2 \geq 100 \qquad (5.3)$$

This condition is met within minutes for all inflows in the Siblingen analysis. Assuming that $D_{RW} >> D_{si}$ for all intervals analyzed, Equation 5.2 is appropriate for estimating transmissivity for all constant-rate injection or withdrawal events during fluid logging. By rearranging Equation 5.2 to solve for T_i outside of the log term, one can then iterate for T_i. This technique is used to estimate transmissivity for the electrical conductivity logs. This assumes that the drawdown in the well is also representative of the drawdown for each layer i. As stated, this implicitly assumes that the natural head variation between the intervals is small relative to D_{RW}.

For all flowmeter events, a measurement of static flow rates in the borehole is done prior to a constant-rate injection run. KPFLOW, which is the code used to estimate interval transmissivity, takes into consideration the static vertical flow rates in the borehole and estimates interval transmissivity by a modified Cooper-Jacobs procedure. Details of the theoretical basis behind KPFLOW calculations can be found in REHFELDT et al. (1989). This section will briefly discuss the methodology and most important equations without presenting the derivation of the methodology.

For input, KPFLOW requires flowmeter logs for the same interval during static conditions and during a constant-rate withdrawal or injection condition. From this, KPFLOW calculates interval flow rate under static conditions (q_{si}) and under constant-rate conditions (q_{Ri}), and takes as input the drawdown of the well resulting

from constant-rate withdrawal or injection conditions (D_{RW}).

The drawdown to a well can be expressed as a function of time by the Cooper-Jacobs approximation reproduced in Equation 5.2. The first step that KPFLOW performs after calculating interval flow rates is to calculate each interval hydraulic conductivity (K_i). This calculation is performed with a solution derived from the Cooper-Jacobs equation:

$$K_i = (q_{Ri} - q_{si}) \ln (R_a/r_w) / 2\pi D_{RW}(t_e)b_i \quad (5.4)$$

where r_w is the radius of the well, R_a is the radius of influence as defined for a multi-step test (REHFELDT et al., 1989), and b_i is the interval thickness. This radius of influence is defined as

$$R_a = 1.5 (K b t_e / S)^{1/2} \quad (5.5)$$

where S is the logged section storage coefficient, b is the full logged interval thickness, and t_e is the effective pumping time as defined for a multi-step pumping test. For the case where the first step of a two-step test is static (i.e., $Q_w = 0.0$), then t_e is simply taken to be equal to the second constant-rate period duration. In our case, therefore, t_e is equal to the duration of the constant-rate withdrawal/ injection phase of logging.

The radius of influence (R_a) for the multi-step test (constant-rate in our case) requires prior knowledge of the logged section hydraulic conductivity (K). The logged section hydraulic conductivity can be calculated from the following equation.

$$K = \frac{Q_{RW} \ln (R_a/r_w)}{2\pi D_{RW} b} \quad (5.6)$$

The parameters Q_{RW} and D_{RW} are defined as the borehole flow rate and drawdown during the constant-rate test. However, the unknown parameter desired (R_a) appears in both Equations 5.5 and 5.6. The radius of influence (R_a) can be iteratively solved for by first assuming a value of R_a and solving for K in Equation 5.6, which is then used to calculate R_a in Equation 5.5. Once R_a becomes constant, it can be used in Equation 5.4 to solve for K_i. The use of these equations requires estimation of logged section storage parameter, a time of measurement, and a borehole radius, all of which introduce uncertainty into the calculation. It is important to note that KPFLOW assumes all measurements were performed at the same time (t_e). With the thickness of each interval (b_i) known and the hydraulic conductivity (K_i) calculated, then simple multiplication yields the interval transmissivity (T_i).

The storage coefficient for the logged lower crystalline section is relatively uncertain. The specific storage used within this chapter is taken from the hydraulic test interpretation report by OSTROWSKI and KLOSKA (1990). They calculated a specific storage based upon the variation of in-situ fluid properties within the Siblingen borehole. The specific storage values used by OSTROWSKI and KLOSKA

(1990) varied from 8.4 to 8.6 x 10^{-8} m^{-1}, with the latter value used for most cases. The value of 8.6 x 10^{-8} m^{-1} for specific storage is adopted for this study. To calculate the appropriate storage coefficient, one must multiply the logged section thickness by the specific storage. It has been shown in BELANGER et al. (1989) that for formations with a hydraulic conductivity greater than 1.0E-10 m/s the estimation of conductivity is relatively insensitive to the estimate of specific storage.

5.1.3 Normalized Transmissivity Calculation

An alternative method of estimating individual inflow (layer) transmissivity is available under injection or withdrawal conditions. This method first gives a measure of the individual layer transmissivity as compared to the total logged section transmissivity. From knowledge of the total logged section transmissivity (T), one can then estimate the transmissivity (T_i) for each layers. This method, as well as the ones presented before, takes advantage of the fact that flow becomes horizontal at the well-bore radius (r_w) in a ideally layered aquifer even when the individual layers have relatively high contrasts in conductance (JAVENDEL and WITHERSPOON, 1969). When this condition is met, the flow from an individual inflow point or layer is proportional to that layer's transmissivity by a proportionality constant (MOLZ et al., 1989). The relationship for a layer's transmissivity can be expressed

$$q_i = \alpha T_i \tag{5.7}$$

where α is the proportionality constant and q_i is the flow rate from the layer i. MOLZ et al. (1989) report that Equation 5.7 is applicable at dimensionless times greater than 100, where dimensionless time is defined according to Equation 5.3. In Equation 5.3, T is the transmissivity, S is the storage coefficient for the entire logged section, and t is the time since production/injection has started.[1)] For the lower section of Siblingen (1000 to 1522 m), the dimensionless time equal to 100 is equivalent to the real time of 3 seconds. The proportionality constant α is equal to

$$\alpha = Q_w / T \tag{5.8}$$

where Q_w is the total injection or production rate for the logged interval. With the total production/injection rate known, and an estimate of q_i for each layer from fluid logging, one can calculate a normalized transmissivity equal to

$$T_i/T = q_i/Q_w \tag{5.9}$$

where ($1.0 \geq T_i/T > 0$). The vertical transmissivity distribution can be presented as a normalized distribution. In this case, no assumptions are made about S, s_i, t, or r_w. If one has a good estimate of T, then the individual transmissivities (T_i) can be calculated as dimensional quantities. If T can be estimated from a steady-state

---

[1)] Unless specific reasons existed (like superposition effects of two logging events), T for the entire logging section was calculated from the total production rate and drawdown during logging.

response, again estimates of s, s_i, and t are not required. Also, in the case of analyzing flowmeter data, systematic or multiplicative errors will be canceled out. Estimates of these types of errors have been reported to be as much as factors of 0.5 to 2 for spinner flowmeters (REHFELDT et al., 1989).

5.2 Transmissivity Derived from Flowmeter Measurements

Transmissivities could be estimated from the four constant-rate injection flowmeter campaigns performed in the Siblingen borehole between December 1988 and June 1989. The campaigns FL1 (December 1988) and FL2 (January 1989) were conducted during the drilling phase of the overall program at depths of 849 and 1017 m b.g., respectively. The borehole was plugged and partially cemented after the performance of FL1 and FL2. Both campaigns FL3 and FL4 were performed in the testing phase of the program, with the primary aim of characterizing the open-hole section (unplugged), ranging between 1060 and 1522 m b.g. The most extensive borehole coverage comes from campaign FL4, performed using the heat-pulse packer flowmeter. This campaign provided data from 490 to 1522 m.

5.2.1 Transmissivity Derived from the Spinner Packer Flowmeter (SPF) Campaign FL1 (December 1988)

The SPF campaign FL1 allowed for the determination of transmissivity of eight 8individual layers between 490 and 851 m b.g. It should be noted that the layers do not necessarily correspond to permeable features but represent the intervals between two flowmeter measurements. The analysis with KPFLOW was performed using data of Run 1 conducted under static conditions, and Run 2 conducted under an injection rate of about 21.5 l/min. The measured vertical flow rates during both runs have been commented in Section 2.3 and reported in Table 2.2. Prior to performing the test, the borehole had been plugged down to the borehole total depth at test time (767 m b.g.). However, even given this plugging, the most permeable layer was found to be located between 675 and 725 m b.g., with a transmissivity of 2.0E-5 m^2/s. Before plugging, this zone had been recognized by the hydraulic packer test CR10 to have a transmissivity of around 2E-4 m^2/s. All the results of the KPFLOW analyses are presented in Table 5.1 and on Figure 5.1.

Table 5.1: Transmissivities Calculated from Flow Rates Derived from Flowmeter Campaign FL1 (SPF, December 1988)

Interval Depth	Layer Numbers	TRANSMISSIVITY X 10^{-7} (m^2/s)		
		KPFLOW	NORMALIZED	
(m b.g.)		T_i	T_i/T	T_i
480 - 525	1	0.0	0.00	0.00
525 - 575	2	0.0	0.00	0.00
575 - 675	3	0.0	0.00	0.00
675 - 725	4	201.3	0.44	130.0
775 - 825	5	6.14	0.02	5.92
725 - 775	6	71.3	0.20	59.1
825 - 840	7	24.6	0.07	21.4
840 - 849	8	72.4	0.26	75.4

The KPFLOW analysis for the propagation of the measurement uncertainty generally showed very small ranges of error, corresponding to around 5 to 15% of the mean values. For instance, the hydraulic conductivity of layer 4, the most permeable layer, is between 3.91E-7 and 4.14E-7 m/s. For the less permeable layer 5 (from 725 to 775 m b.g.), the hydraulic conductivity is between 1.13 and 1.33E-8 m/s.

The "normalized" approach is another method of calculating the layer's transmissivity, based on the whole borehole transmissivity T (see Section 5.1.2). T is calculated with the Cooper-Jacob equation (Equation 5.2), using the injection rate and the pressure rise in the well, measured during Run 2 of the flowmeter measurements and a specific storage equal to 8.6 x 10^{-8} m. From the injection phase of the flowmeter campaign FL1, the value of T was calculated to be around 3E-5 m^2/s.

By comparing results between both KPFLOW and the normalized approach, it can be seen that they differ by less than a factor of 2. The differences can be attributed to the fact that KPFLOW considers for each layer the radial flow rate determined during the two logs (Run 1 = "static" and Run 2 = "dynamic"), while the normalized approach considers for each layer the ratio of the radial flow rate over the whole injection rate ($Q_i/Q = T_i/T$). In any case, the differences are considered to be small and within the range of uncertainty of the results normally estimated for the hydraulic packer tests.

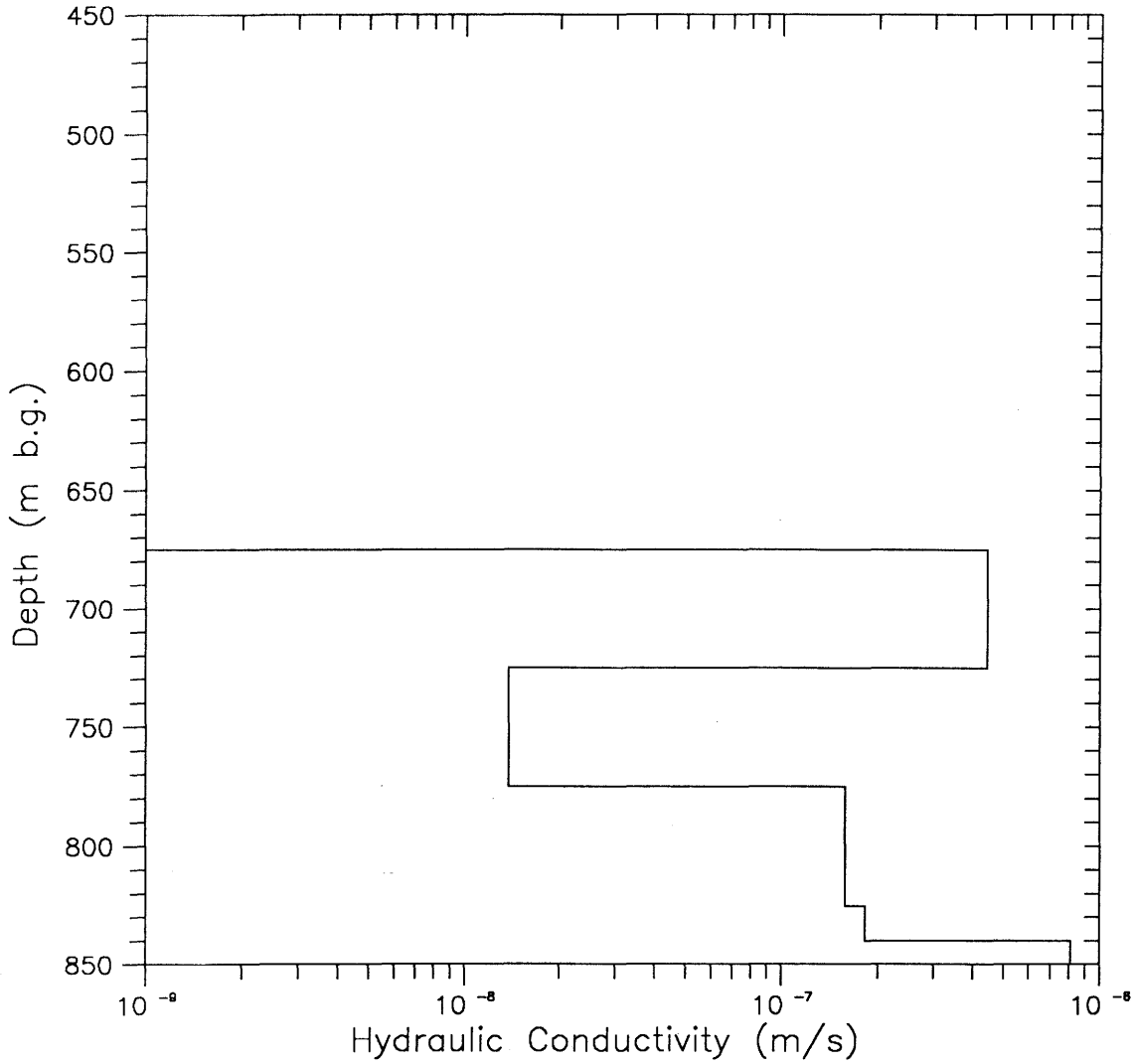

Figure 5.1: Hydraulic Conductivity Results from Campaign FL1,20-21.12.1988, Packer Flowmeter Interpretation, Siblingen Borehole

5.2.2 Transmissivity Derived from the Spinner Flowmeter (SF) Campaign FL2 (January 1990)

The trolling SF campaign FL2 allowed for a semi-quantitative analysis of the data collected from logging under static conditions (Run 1) and an injection of 51 l/min (Run 2). As explained in Section 2.4, the analysis has been treated for stationary measurements by extrapolating linearly the various disturbances affecting the data. This linear extrapolation resulted in the reconstituted vertical fluxes during both runs, as reported in Table 2.3. When conducting the test, the borehole had been partially cemented and plugged down to 850.6 m b.g.

The analysis aimed to focus on the characterization of particular flowing layers clearly identified from the continuous vertical flux profile (raw data). These layers are located at around 685-715, 875-880, and 925-938 m b.g., and correspond to layers 2, 4, and 6 identified in Table 5.2. Layer 2 (685-715 m b.g.) was identified from its flow rate occurring during Run 1. When injecting (Run 2), no significant inflow or outflow was detected at this depth. This indicates that the heads in the borehole and the layer were both at an elevation of about 447 m a.s.l. The transmissivities calculated with KPFLOW independently for the logs in both directions are fairly consistent, with 4.3E-5 m^2/s for the log in an upward direction and 3.4E-5 m^2/s for the log going downward . The results calculated for the two other layers are also consistent, with 5.0E-5 m^2/s in both directions for layer 4 (875-890 m b.g.), and 1.4E-4 m^2/s (upwards) and 1.5E-4 m^2/s (downwards) for layer 6 (925-938 m b.g.). These results are illustrated in Table 5.2 and Figures 5.2 and 5.3.

Table 5.2: Transmissivities Calculated from Flow Rates Derived from Flowmeter Campaign FL2 (SF, January 1989)

Interval Depth	Layer Numbers	TRANSMISSIVITY X 10^{-7} (m^2/s)		
		KPFLOW	NORMALIZED	
(m b.g.)		T_i	T_i/T	T_i
Logging upwards:				
490 - 691	1	0.0	0.00	0.0
691 - 715	2	432.1	0.00	0.0
715 - 878	3	121.0	0.00	0.0
878 - 879	4	497.2	0.17	345.0
879 - 925	5	526.5	0.20	436.2
925 - 931	6	1347.0	0.61	1313.0
931 - 1017	7	0.0	0.00	0.0
Logging downwards:				
490 - 685	1	0.0	0.00	0.0
685 - 691	2	337.0	0.00	0.0
691 - 875	3	279.1	0.00	0.0
875 - 880	4	502.6	0.16	344.7
880 - 925	5	338.8	0.10	215.9
925 - 938	6	1467.0	0.76	1617.0
938 - 1017	7	0.0	0.00	0.0

In the normalized approach, the transmissivity value calculated for layers 2 and 3 are zero because no flow was detected into the formation during Run 2. Aside from this inconsistency, the results are within a factor of less than 2 for both methods. The overall borehole transmissivity value T used in the normalized approach was calculated from the injection test to be equal to 2.2E-4 m^2/s. This value may be an underestimate because no flow occurred from layers 2 and 3, as stated above. Because of the poor quality of the data and the disturbances occurring during the trolling logs, no study of the uncertainty propagation could be performed for campaign FL2.

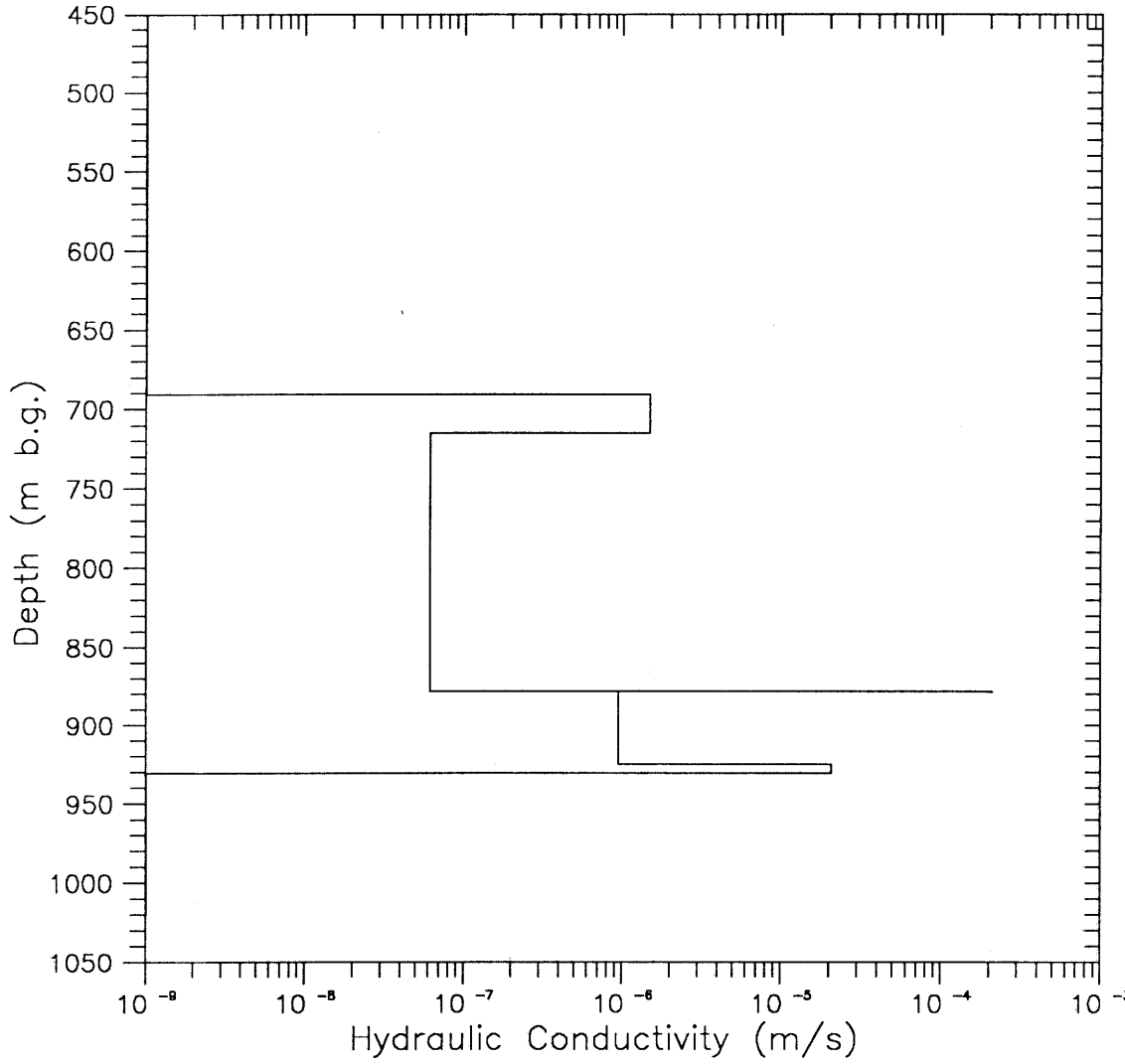

Figure 5.2: Hydraulic Conductivity Results from Campaign FL2, 22-24.01.1989, Flowmeter Interpretation Runs upwards, Siblingen Borehole

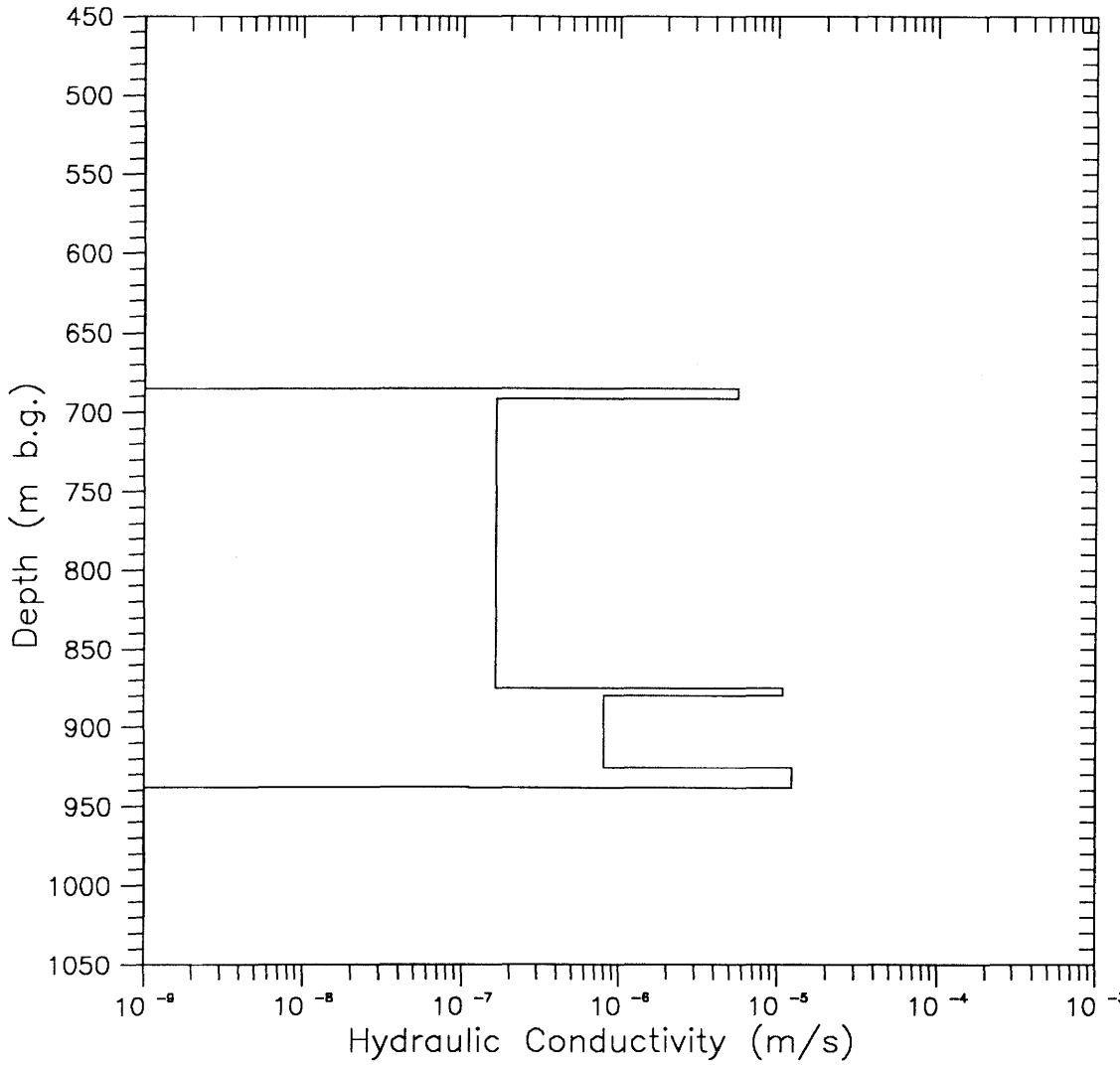

Figure 5.3: Hydraulic Conductivity Results from Campaign FL2, 22-24.01.1989, Flowmeter Interpretation Runs downwards, Siblingen Borehole

5.2.3 Transmissivity Derived from the Spinner Packer Flowmeter (SPF) Campaign FL3 (April 1990)

The SPF campaign FL3 allowed for the determination of transmissivity for six zones between 490 and 1522 m b.g. For the analysis with KPFLOW, three different logs were used. The first log was performed under static conditions in the borehole. The two last logs were conducted under an injection rate of about 81.5 - 79 l/min, but were obtained after around 3 and 13 hours of injection, respectively. The measured vertical flow rates during the logs have been discussed in Section 2.5 and are reported in Table 2.3. Even though the borehole had been cemented and plugged in several intervals between 490.3 m and 1061.8 m b.g., the most permeable zone was determined to occur in the upper section above 1060 m b.g. However, the primary aim of this campaign was to characterize hydraulically the lower, unplugged, section of the borehole. All the results of the KPFLOW analysis are presented in Table 5.3 and in Figures 5.4 and 5.5.

Table 5.3: Transmissivities Calculated from Flow Rates Derived from Flowmeter Campaign FL3 (SPF, April 1989)

Interval Depth	Layer Numbers	TRANSMISSIVITY X 10^{-7} (m^2/s)		
		KPFLOW	NORMALIZED	
(m b.g.)		T_i	T_i/T	Ti
Logging Runs 1-2a:				
490 - 1062	1	793.40	0.96	602.90
1062 - 1100	2	9.37	0.01	9.33
1100 - 1154	3	0.04	0.00	0.07
1154 - 1522	4	19.40	0.03	18.40
Logging Runs 1-2b:				
490 - 1062	1	938.80	0.92	622.00
1062 - 1100	2	2.11	0.00	1.88
1100 - 1154	3	0.03	0.00	0.04
1154 - 1163	4	0.00	0.00	0.55
1163 - 1210	5	4.48	0.07	45.10
1210 - 1522	6	20.00	0.03	18.30

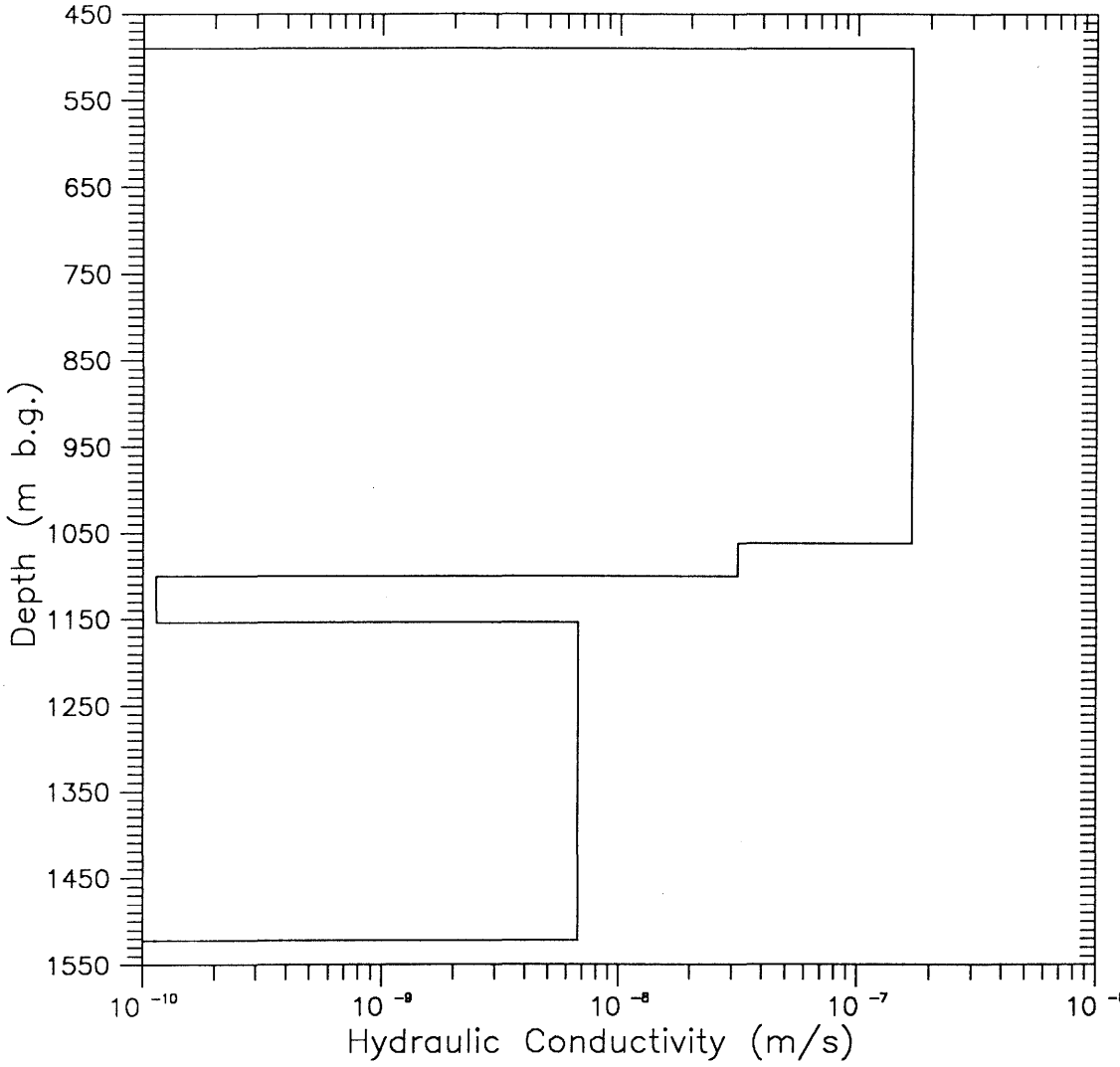

Figure 5.4: Hydraulic Conductivity Results from Campaign FL3, 5-7.04.1989Flowmeter Interpretation (Runs 1-2a), Siblingen Borehole

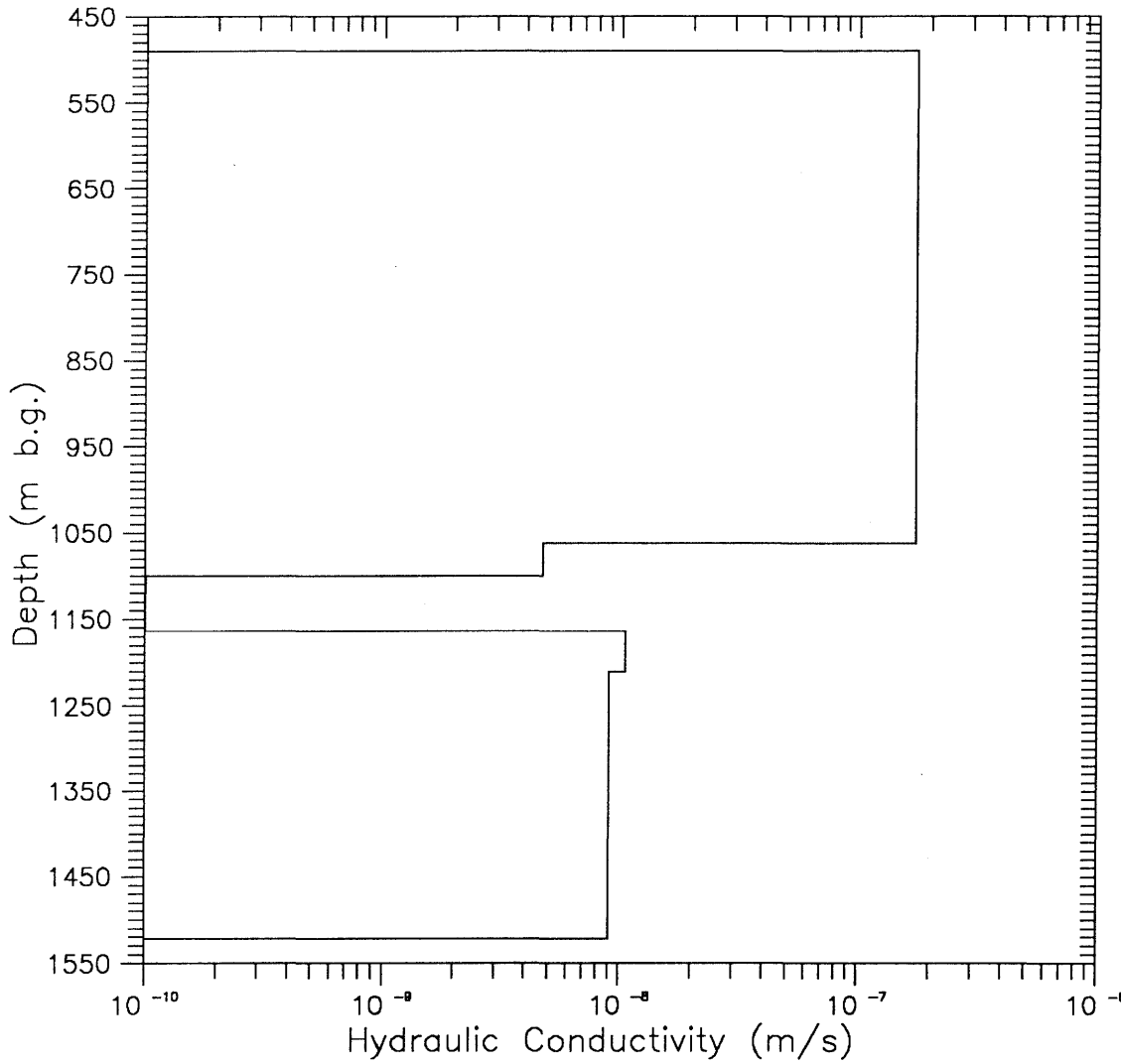

Figure 5.5: Hydraulic Conductivity Results from Campaign FL3, 5-7.04.1989Flowmeter Interpretation (Runs 1-2b), Siblingen Borehole

The overall transmissivity of the lower section is fairly low, at about 2E-6 m^2/s, which corresponds to about 6% of the total borehole transmissivity. The most permeable layers identified are situated at about 1060-1110 m b.g. (T = 2 to 9E-7 m^2/s) and below 1210 m b.g. (T = 1.9E-6 m^2/s). Due to technical problems affecting the packer flowmeter, no further measurements could be performed below 1210 m b.g.2

The study of the uncertainty propagation from the measurements to the calculated hydraulic conductivities indicated that such effects were very small, corresponding to less than 7% of the mean value. The most sensitive layer, from 1062 to 1100 m b.g., has a hydraulic conductivity ranging between 5.47 and 5.86E-9 m/s.

A comparison of the results between KPFLOW and the normalized approach shows that they give consistent results, usually within a ratio less than a factor of 2. The transmissivity value T of the entire borehole used in the normalized approach was calculated from the injection test to be around 6.5E-5 m^2/s.

5.2.4 Transmissivity Derived from the Heat Pulse Packer Flowmeter (HPPF) Campaign FL4 (June 1990)

The HPPF campaign FL4 was performed using two different flow rates of injection, 8 l/min during Run 2 and 57 l/min during Run 3. Run 2 was designed to focus on the upper section of the borehole (490-1062 m b.g.) and measured borehole flow rate over 18 intervals. Run 3 focused on the lower section of the borehole (1062-1522 m b.g.) and measured flow rates over 13 intervals, corresponding to layers 1 through 13. The measured vertical flow rates during these logging runs are discussed in Section 2.6 and reported in Table 2.4. As noted in the previous fluid logging campaigns, the most permeable zones were located in the cemented section between 650 and 850 m b.g. All the results of the KPFLOW analysis are reported in Tables 5.4 and 5.5 and Figures 5.6 and 5.7. It should be noted that due to the low injection rate applied during Run 2, no vertical flow rate could be determined below 1100 m b.g. This means that no permeable features could be identified for this interval from this first injection log.

The primary aim of this campaign was to make a demonstration of the USGS heat-pulse flowmeter tool, and the data and analyses were reported in PAILLET et al. (1990). The raw data and information about the calibration were not available, so no significant checking or study of the uncertainty propagation could be performed.

A comparison of the results from both the KPFLOW analysis and the normalized approach shows that they provide very consistent values, generally within a factor of 2. The larger differences usually can be attributed to the fact that the normalized approach does not take account of the fluxes occurring during the static log (Run 1), e.g., for layers 3, 4 and 18 in Table 5.4 and layer 5 in Table 5.5. The overall borehole transmissivity T used in the normalized approach was calculated from the injection test to be 1.4E-4 m^2/s.

Table 5.4: Transmissivities Calculated from Flow Rates Obtained from Flowmeter Campaign FL4 (HPPF 8 l/min, June 6/7, 1989)

Interval Depth	Layer Numbers	TRANSMISSIVITY X 10^{-7} (m^2/s)		
		KPFLOW	NORMALIZED	
(m b.g.)		T_i	T_i/T	T_i
Runs 1-2 (8 l/min):				
500 - 680	1	4.96	0.002	4.7
680 - 700	2	1515.0	0.55	1144.0
700 - 704	3	186.6	0.00	0.0
704 - 708	4	186.6	0.02	31.4
708 - 770	5	0.0	0.00	0.0
770 - 835	6	0.0	0.00	0.0
835 - 840	7	353.3	0.14	286.9
840 - 860	8	0.0	0.00	0.0
860 - 910	9	0.0	0.00	0.0
910 - 920	10	89.7	0.02	51.7
920 - 925	11	122.2	0.05	105.0
925 - 929	12	284.4	0.21	443.6
929 - 938	13	0.0	0.00	0.0
938 - 950	14	28.6	0.01	26.7
950 - 980	15	0.0	0.00	0.0
980 - 1062	16	0.0	0.00	0.0
1062 - 1100	17	0.0	0.00	78.4
1100 - 1522	18	0.0	0.00	0.0

Table 5.5: Transmissivities Calculated from Flow Rates Obtained from Flowmeter Campaign FL4 (HPPF 57 l/min, June 7/8, 1989)

Interval Depth	Layer Numbers	TRANSMISSIVITY X 10^{-7} (m^2/s)		
		KPFLOW	NORMALIZED	
(m b.g.)		T_i	T_i/T	T_i
Runs 1-3a (57 l/min):				
500 - 980	1	1405.00	0.96	1388.0
980 - 1062	2	0.00	0.00	0.00
1062 - 1090	3	13.90	0.01	17.1
1090 - 1210	4	1.75	0.002	2.59
1210 - 1276	5	3.58	0.01	12.7
1276 - 1350	6	3.58	0.003	5.04
1350 - 1400	7	3.70	0.003	5.20
1400 - 1450	8	3.58	0.003	5.04
1450 - 1470	9	0.00	0.00	0.00
1470 - 1490	10	1.75	0.002	2.59
1490 - 1500	11	0.00	0.00	0.00
1500 - 1505	12	5.60	0.005	7.64
1505 - 1522	13	3.58	0.003	5.04

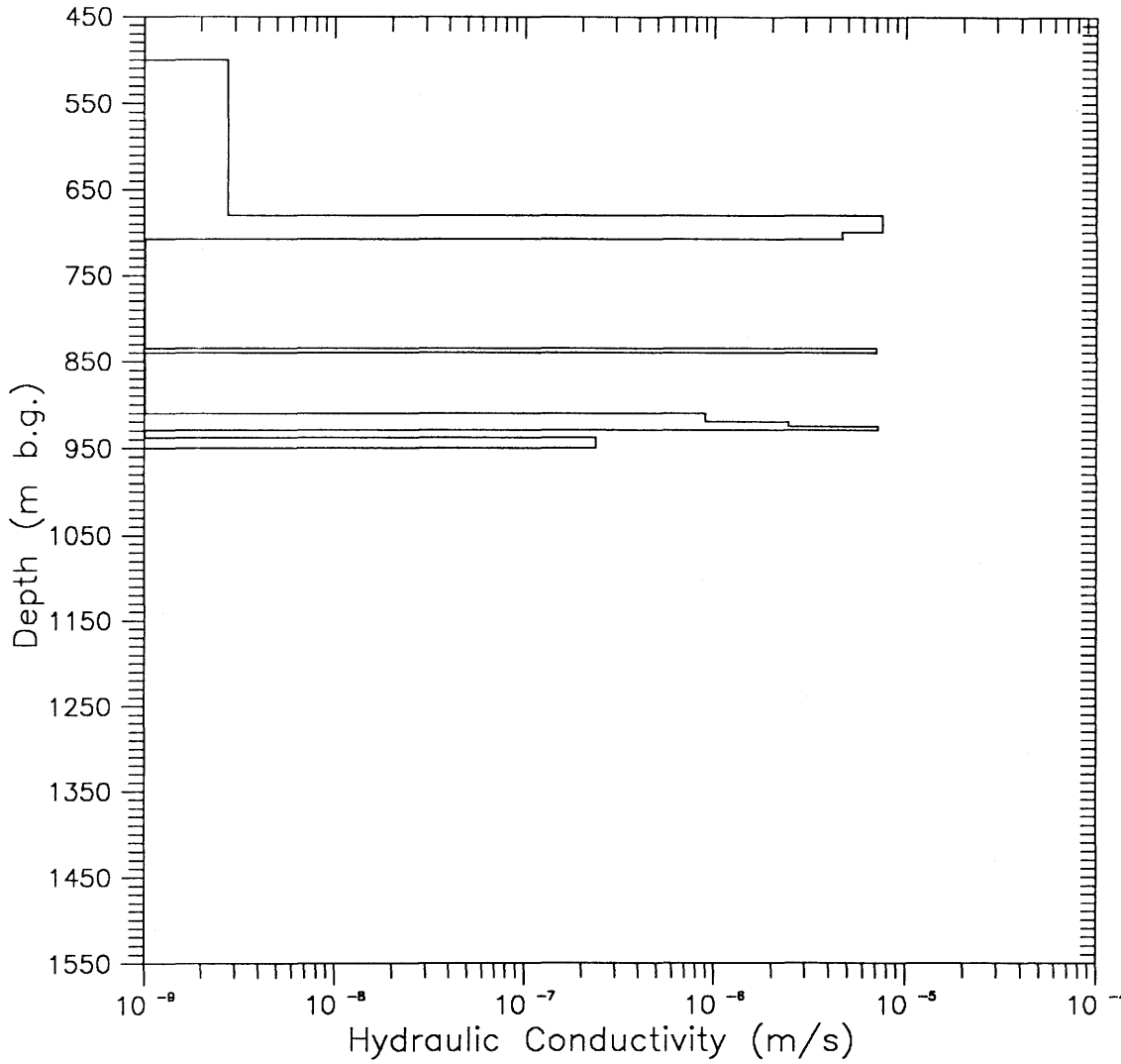

Figure 5.6: Hydraulic Conductivity Results from Campaign FL4, 6-8.06.1989 Heat Pulse Packer Flowmeter Interpretation (Runs 1-2), Siblingen Borehole

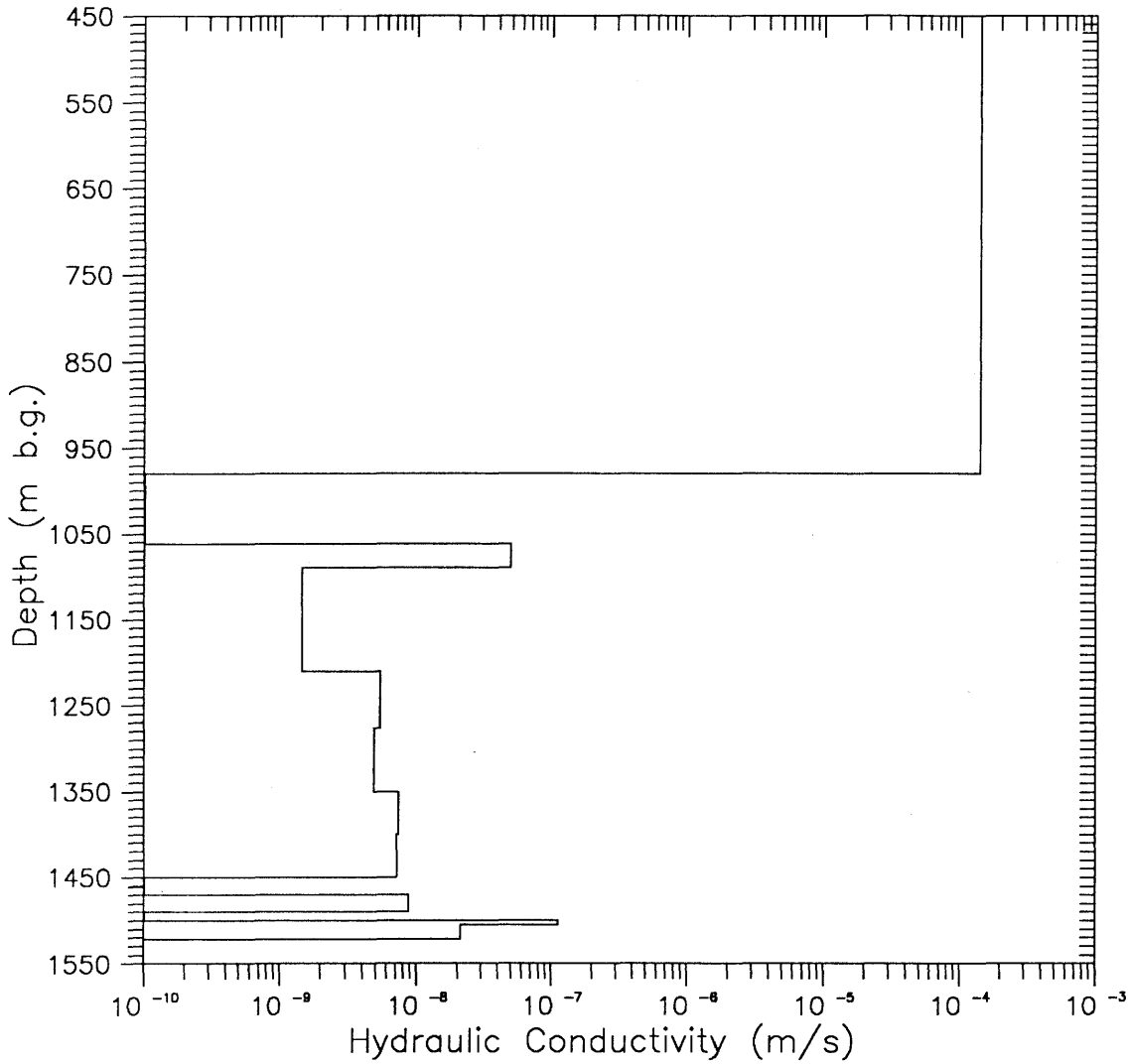

Figure 5.7: Hydraulic Conductivity Results from Campaign FL4, 6-8.06.1989 Heat Pulse Packer Flowmeter Interpretation (Runs 1-3a), Siblingen Borehole

5.3 Transmissivity Derived from Electrical Conductivity Measurements

Transmissivities could be estimated from three constant-rate withdrawal events (OH-RW1, PIP-RW1, and PIP-RW2) and two different static flow events (SF-1 and SF-2). The most extensive borehole coverage comes from both constant rate withdrawal events performed with a PIP isolating the lower crystalline section. For these two events, the section of borehole from 1000 m to 1520 m was divided into nine different intervals with nine different transmissivity estimates. For the open-hole constant rate withdrawal test (OH-RW1), only one interval yielded an estimate of transmissivity.

In the first static flow event, transmissivity is estimated for a large interval of the logged section (1158 to 1522 m). For the second static flow event, a second transmissivity estimate for the zone below 1158 m can be made. The following five subsections present transmissivity calculations for each of these fluid logging events. The discussion of fluid logging events follows in chronological order of testing.

5.3.1 Transmissivity as Derived from Calculated Internal Borehole Flow Rates, Event SF-1

As mentioned in Section 3.3.2, the decrease in downward flow rate during event Static Flow 1 (SF-1) is not considered significant until past a depth of 1131 m. This is consistent with the heads derived from hydraulic tests (OSTROWSKI and KLOSKA, 1990) since Test CR18 was the first test below 900 m to show a significantly lower head than the zones above it. Therefore, a driving force should exist for flow into the formation beginning at the fracture at 1163 m. The average head above this interval is approximately 440 to 441 m a.s.l., and the heads in this interval and below are from 439 to 436 m a.s.l., as determined from hydraulic testing. With such observed head differences and the measured flow rates, a total transmissivity can be estimated. The equation used is Dupuit's steady-state solution to the diffusion equation. Two flow rates were used to calculate transmissivity, -0.4 and -0.45 l/min. Also, two values of the radial distance to a constant head boundary (R) were used, 100 and 1000 m. As can be seen in Table 5.6, the estimated transmissivity range is from 1.6 to 4E-6 m^2/s.

Table 5.6: Calculated Transmissivity Using Dupuit's Formula for the First Static Fluid Logging Event (SF-1), for Interval 1158 - 1522 m

Transmissivity x 10^{-7} (m^2/s)	Borehole Flow Rate = -0.4 l/min		Borehole Flow Rate = -0.45 l/min	
	R = 100 m	R = 1000 m	R = 100 m	R = 1000 m
Assumed drawdown = 3 m	27	35	30	40
Assumed drawdown = 4 m	20	26	23	30
Assumed drawdown = 5 m	16	21	18	24

5.3.2 Transmissivity Derived from Static Flow Event SF-2

In Static Flow Event 2, there was one prominent peak located in the lower crystalline from which an estimate of borehole flow rate could be made. This peak was not an inflow but rather was a pulse present in the well after flushing and then advected down the borehole in response to static borehole conditions. The pulse traveled from 1089 to 1098 m in 131 min. The calculated flow rate is 0.48 l/min down the borehole. As in the previous case, Dupuit's formula is used to estimate a transmissivity for the interval 1158 to 1522 m. The results are listed in the table below.

Table 5.7: Calculated Transmissivity Using Dupuit's Formula for the Second Static Fluid Logging Event (SF-2), for Interval 1158 - 1522 m

Transmissivity x 10^{-7} (m^2/s)	Borehole Flow Rate = -0.48 l/min	
	R = 100 m	R = 1000 m
Assumed drawdown = 3 m	32	42
Assumed drawdown = 4 m	24	32
Assumed drawdown = 5 m	19	25

As can be seen in Table 5.7, the estimated transmissivity range is from 1.9 to 4.2E-6 m^2/s. The center of this range is approximately 3.1E-6 m^2/s. The similarity in results from SF-1 and SF-2 is not surprising because they are measured over the same intervals (1100 - 1522 m) of borehole under assumed static conditions. The comparability between the two can be viewed favorably as corroboration of results.

5.3.3 Transmissivity Derived from the Open Hole, Constant Rate Withdrawal Test, Event OH-RW1

During the open-hole constant-rate withdrawal test, the borehole was pumped at 32 l/min, resulting in 0.65 m of drawdown. The head in the borehole was last measured to be 442 m a.s.l. prior to pumping. Most of the 32 l/min was probably provided by the interval 678 to 712 m b.g., which has a transmissivity one full order of magnitude larger than any other interval from 490 to 1522 m b.g. A number of intervals above 1,000 m b.g. produce fluid to the borehole and up the borehole. The interval from 1070 to 1083 m b.g. produces fluid, but it flows down the borehole and eventually back into the formation.

From a review of the logs measured, it appears that the interval from 1070 to 1083 m b.g. did not flow when the borehole was not pumped. However, it did flow after 0.65 m of drawdown. This means that the head in the interval from 1070 to 1083 m b.g. is between 442 and 441.35 m a.s.l. The direction in which the volumetric flux moved once it entered the borehole was controlled by the vertical head gradients in the borehole. It is possible that the two highly transmissive zones at 678 to 712 and 924 to 1005 m b.g. bounded the interval 1070 to 1083 m b.g. from above by constant head conditions (head at 441.35 m a.s.l.). However, from below the interval 1070 to 1083 m b.g. is bounded by lower heads in the range of 441.35 to 437 m a.s.l. Therefore, the initiation of inflow for interval 1070 to 1083 m b.g. was caused by a head difference less than or equal to 0.65 m. However, the direction of this flow, and in part the magnitude, is controlled by the head difference between interval 1070 to 1083 m b.g. and the interval 1083 to 1522 m b.g. The head difference between this interval and the lower portions is highly uncertain, but OSTROWSKI AND KLOSKA (1990) measured heads as low as 437 m a.s.l., which implies head differences up to 4 m.

For the borehole interval 1065 to 1088 (peaks 11, 12, and 13), the transmissivity can be estimated using the observed borehole drawdown of 0.65 m and the estimated borehole flow rate down the borehole of -0.21 l/min measured 12 hours after pumping began. This estimate is a minimum estimate, because 0.65 m is the maximum possible drawdown.

The measured borehole flow rate of -0.21 l/min can also be used to estimate the transmissivity of the interval 1158 to 1522 m b.g. under various assumed head differences. OSTROWSKI AND KLOSKA (1990) report head differences between the interval 1065 to 1088 m b.g. and the lower portion of the borehole of up to 4 m. For this reason, drawdowns ranging from 1 to 4 m were used as the applicable driving force. The following lists the calculated transmissivities for intervals 1065 to 1088 and 1158 to 1522 m b.g.

Table 5.8: Calculated Transmissivity Using Cooper-Jacob's Formula, Constant-Rate Withdrawal Test (OH-RW1)

Interval (m b.g.)	Assumed Drawdown (m)	Borehole Flow Rate (l/min)	Transmissivity (x 10^{-7} m^2/s)
1065 - 1088	0.65	-0.21	81.2
1158 - 1522	1.0	-0.21	54.1
1158 - 1522	2.0	-0.21	25.8
1158 - 1522	3.0	-0.21	16.7
1158 - 1522	4.0	-0.21	12.3

The calculation of interval 1065 to 1088 m b.g. transmissivity assumes that none of the -0.21 l/min originates from above 1065 m b.g. If part of the downward volumetric flow rate does not originate from 1065 to 1088 m b.g., the transmissivity will be overestimated.

Because the highly transmissive zones above the interval 1065 to 1088 m b.g. are controlling the borehole response to pumping 32 l/min, it is probable that the zones below 1000 m b.g. are being held at constant head conditions at early time. Because of this, the applicability of Cooper-Jacob's formula is in doubt.

5.3.4 Transmissivity Derived from First PIP Constant Rate Withdrawal Test, Event PIP-RW1

In Table 3.20, a best-guess volumetric flow rate was estimated for the nine intervals analyzed between the depths of 1000 to 1522 m for the constant-rate withdrawal event PIP-RW1. By using the Cooper-Jacobs formula, an estimate of transmissivity for each of the nine intervals can be made. For each interval, an estimate of transmissivity requires an appropriate time of production and a storage coefficient. The time used is 12 hours and the storage coefficient used was based on an interval length of 10 m and a specific storage coefficient consistent with OSTROWSKI and KLOSKA (1990) and equal to 8.4E-8 m^{-1}. The storage coefficient is assumed constant and equal to 8.4E-7.

Another method of calculating transmissivity is through the calculation of a normalized transmissivity based on the total logged section transmissivity (see Section 5.2.3). To calculate transmissivity with this method requires an estimate of total interval transmissivity. For this value the transmissivity determined from hydraulic test CR20 (1062 to 1263.6 m b.g.) and test CR24 (1263.6 to 1522 m b.g.) were added (see Table 1.2). This gives a total transmissivity equal to 3.11E-6 m^2/s. The results from each of the calculations is presented in the table below. The first estimate is from the Cooper Jacobs approach and the second estimate is termed the normalized transmissivity.

Table 5.9: Transmissivities Calculated from Flow Rates Derived from Fluid Logging Event PIP-RW1

Interval Depth	Peak Numbers	TRANSMISSIVITY X 10^{-7} (m^2/s)		
		COOPER-JACOB	NORMALIZED	
(m b.g.)		T_i	T_i/T	T_i
1065 - 1089	13, 12, 11	12.8	0.39	12.1
1158 - 1168	10	1.55	0.05	1.66
1219 - 1242	9, 8	2.38	0.08	2.49
1247 - 1257	7	0.64	0.02	0.73
1303 - 1313	6	3.24	0.12	3.73
1381 - 1391	5	2.17	0.06	1.87
1405 - 1415	4	1.44	0.05	1.56
1415 - 1425	3	0.17	0.007	0.21
1500 - 1516	2, 1	6.88	0.22	6.74

Again, the intervals are defined as ±5 m about an inflow. In the case of multiple peaks within an analysis interval, the interval is again based upon 5 m on either side of the included peaks. The peak depths are summarized in Table 3.9.

By comparing results between the two methods, it can be seen that they give very similar results that are perhaps indistinguishable when viewed in light of the error in the method. From viewing the relative transmissivity values, we can see that approximately 40% of the transmissivity (and therefore flow) is located at the top of the interval, and that 22% is located at the bottom of the logged section. Sixty-one percent of the total interval transmissivity is present in two intervals which, when combined, add up to less than 24 m of the 500 m logged section.

The agreement between the Cooper-Jacob calculated interval transmissivities and the normalized transmissivities is very good. The total interval transmissivity calculated from the observed flow rate and the observed drawdown is in good agreement with the total interval transmissivity calculated from the results of OSTROWSKI and KLOSKA (1990). This can be explained by the fact that no super-imposition or history disturbance affected PIP-RW1. If borehole history affected the interval during PIP-RW1, one could expect these two methods to differ because the history effects would be canceled from the estimated normalized transmissivities.

5.3.5 Transmissivity Derived from Second PIP Constant Rate Withdrawal Test, Event PIP-RW2

In Table 3.15, a best-guess volumetric flow rate was estimated for the nine intervals analyzed between the depths of 1000 to 1522 m b.g. from the conductivity logs measured during the second PIP constant-rate withdrawal test. By using the Cooper-Jacobs formula, an estimate of transmissivity can be made for each of the nine intervals.

Another method of calculating transmissivity is through the calculation of a normalized transmissivity based upon the total logged section transmissivity (see Section 5.2.3). With this method, no production time is assumed. Again, we use a total logged interval transmissivity of 3.11E-6 m^2/s as explained in the previous section. The results from each of the calculations is presented in Table 5.10. The first estimate is from Cooper Jacobs and the second estimate is termed the *normalized transmissivity.*

By comparing results between the two methods, we see that they give different results, in some cases by a factor of 1.6, which is higher than the differences between the methods encountered in PIP-RW1 results. Contrary to PIP-RW1, the normalized transmissivity is larger in magnitude than the transmissivity calculated with Cooper-Jacobs. The difference is greatest for the lower transmissivity intervals and smallest for the higher transmissivity intervals. Sixty-eight percent of the total logged interval transmissivity is present in two intervals which, when combined, add up to less than 24 m of the 500 m logged section.

Table 5.10: Transmissivities Calculated from Flow Rates Derived from Fluid Logging Event PIP-RW2

Interval Depth	Peak Numbers	TRANSMISSIVITY X 10^{-7} (m^2/s)		
		COOPER-JACOB	NORMALIZED	
(m b.g.)		T_i	T_i/T	T_i
1065 - 1089	13, 12, 11	10.7	0.44	13.7
1158 - 1168	10	1.43	0.07	2.07
1219 - 1242	9, 8	1.13	0.05	1.66
1247 - 1257	7	1.75	0.08	2.49
1303 - 1313	6	0.26	0.01	0.41
1381 - 1391	5	1.44	0.07	2.07
1405 - 1415	4	0.40	0.02	0.62
1415 - 1425	3	0.40	0.02	0.62
1500 - 1516	2, 1	5.63	0.24	7.46

The fact that the Cooper-Jacob calculated transmissivity is always smaller than the normalized transmissivity can be explained by history effects from PIP-RW1. The flow rate in PIP-RW1 was 3.0 l/min and the pumping lasted almost 60 hours. The drawdown was 21.3 m which corresponds to a transmissivity of 3E-6 m^2/s. This corresponds very closely to the hydraulic test interval transmissivity of 3.1E-6 m^2/s. For PIP-RW2, the borehole was pumped for 48 hours at 1.5 l/min with a stabilized drawdown of 14.4 m, which corresponds to an interval transmissivity of 2.2E-6 m^2/s. The transmissivity of the interval from 1000 to 1500 m did not change between events. The two pumping events were separated by less than 12 hours. Apparently some intervals did not return to static conditions prior to the second PIP pumping.

Table 5.11 summarizes the transmissivities calculated from all electrical conductivity logging events. These transmissivities are calculated by Cooper-Jacobs and do not represent the noramlized values. These results were presented and discussed in the preceding sections. In the next section, the transmissivity results from conductivity logging will be compared to the results from the flowmeter logging. In Section 7, the transmissivities determined by all fluid logging methods will be compared to the results from standard hydraulic packer tests.

Table 5.11: Summary of Transmissivities Derived from Electrical Conductivity Logging, Normalized Values not shown

Interval Depth (m b.g.)	Peak Numbers	TRANSMISSIVITY X 10^{-7} (m^2/s) FLUID LOGGING EVENT				
		SF-1	SF-2	OH-RW1	PIP-RW1	PIP-RW2
Pumping Rate (l/min)		0 (-0.45)	0 (-0.48)	32 (-0.21)	3.0	1.5
1065 - 1089	13, 12, 11			81.2	12.83	10.71
1158 - 1168	10	←	←	←	1.55	1.43
1219 - 1242	9, 8				2.38	1.13
1247 - 1257	7				0.64	1.75
1303 - 1313	6	23	26	16.7	3.24	0.26
1381 - 1391	5				2.17	1.44
1405 - 1415	4				1.44	0.40
1415 - 1425	3				0.17	0.40
1500 - 1516	2, 1	←	←	←	6.88	5.63

5.4 Comparison of Results from Fluid Logging Methods

The electrical conductivity logging gave transmissivity results which were restricted to the borehole interval from 1000 to 1522 m. The heat-pulse packer flowmeter gives the most extensive coverage in this portion of the borehole. However some spinner packer flowmeter logs were also measured over this interval. Table 5.12 compares the transmissivities calculated for intervals covered by both conductivity logging and the flowmeter logging.

In general, the results are fairly consistent in relative magnitudes of the various intervals. For the interval from 1065 to 1100 m, the results between the methods compare to within a factor of 1.3. The higher the transmissivity, the better the agreement between the two types of fluid logging methods. One obvious exception to this is the interval from 1210 to 1276 (peaks 7,8, and 9), which varies by a factor of 1.2 with a relatively low transmissivity.

Table 5.12: Comparison Between Transmissivities Derived from Flowmeter and Electrical Conductivity Methods

Peak No.	Electrical Conductivity Interval (m bgs)	Flowmeter Test Interval (m bgs)	TRANSMISSIVITY X 10^{-7} (m^2/s)					
			SPF FL3 Apr 5/7 Run 2a	SPF FL3 Apr 5/7 Run 2b	HPPF FL4 June 6/7 Run 2	HPPF FL4 June 7/8 Run 3	T/LF PIP-RW1 Apr 18/19	T/LF PIP-RW2 Apr 23/25
11, 12, 13	1065 - 1089	1062 - 1090	--	--	--	13.9	12.8	10.7
11, 12, 13	1065 - 1089	1062 - 1100	9.4	2.1	28.6	--	12.8	10.7
		1100 - 1154	0.04	0.03	--	--	--	--
		1154 - 1163	--	0.0	--	--	--	--
1 - 10	1158 - 1522	1154 - 1522	19.4	--	--	--	18.5	12.4
10	1158 - 1168	1163 - 1210	--	4.5	--	--	1.6	1.4
10	1158 - 1168	1090 - 1210	--	--	--	1.8	1.6	1.4
1 - 9	1219 - 1522	1210 - 1522	--	20	--	25.4	16.9	11.0
7, 8, 9	1219 - 1257	1210 - 1276	--	--	--	3.6	3.0	2.9
6	1303 - 1313	1276 - 1350	--	--	--	3.6	3.2	0.3
5	1381 - 1391	1350 - 1400	--	--	--	3.7	2.2	1.4
3, 4	1405 - 1425	1400 - 1450	--	--	--	3.6	1.6	0.8
--	--	1450 - 1470	--	--	--	0.0	--	--
--	--	1470 - 1490	--	--	--	1.8	--	--
--	--	1490 - 1500	--	--	--	0.0	--	--
1,2	1500 - 1516	1500 - 1522	--	--	--	9.2	6.9	5.6

SPF = Spinner Packer Flowmeter
HPPF = Heat-Pulse Packer Flowmeter
T/LF = Electrical Conductivity/Temperature Logging

The resolution of the methods is best for the electrical conductivity logging and worst for the spinner packer flowmeter for this range of flow rates. The greatest discrepancy between methods occurs for the intervals 1276 to 1350 and 1400 to 1450 m, where differences are a factor of 12 and 4.5 respectively. It is important to note that the heat-pulse packer flowmeter detected transmissivity between the interval 1470 to 1490, whereas the electrical conductivity analysis did not. Review of the PIP-RW2 logs showed that there is early time evidence for an inflow of small magnitude within this interval.

The best and most complete results from the flowmeter methods for the interval 1000 to 1522 m is the heat-pulse packer flowmeter. The best full interval set of electrical conductivity logs was PIP-RW2. Figure 5.8 is a bar chart showing the comparison between the transmissivities determined by the heat-pulse packer flowmeter and the electrical conductivity analysis of PIP-RW2. This figure shows that the heat-pulse packer flowmeter consistently overpredicts the transmissivity relative to the conductivity log analysis. This figure also shows that, within the transmissivity range of 1 to 4E-7 m^2/s, the electrical conductivity analysis has greater sensitivity to variation, whereas the heat-pulse packer flowmeter shows less small-scale resolution. It is important to note that this resolution is a function of flow rates and not transmissivity. In conclusion, it can be said that the two methods reproduce transmissivity profiles in many cases to within a factor of two, which is very good for the magnitude of flow rates being measured.

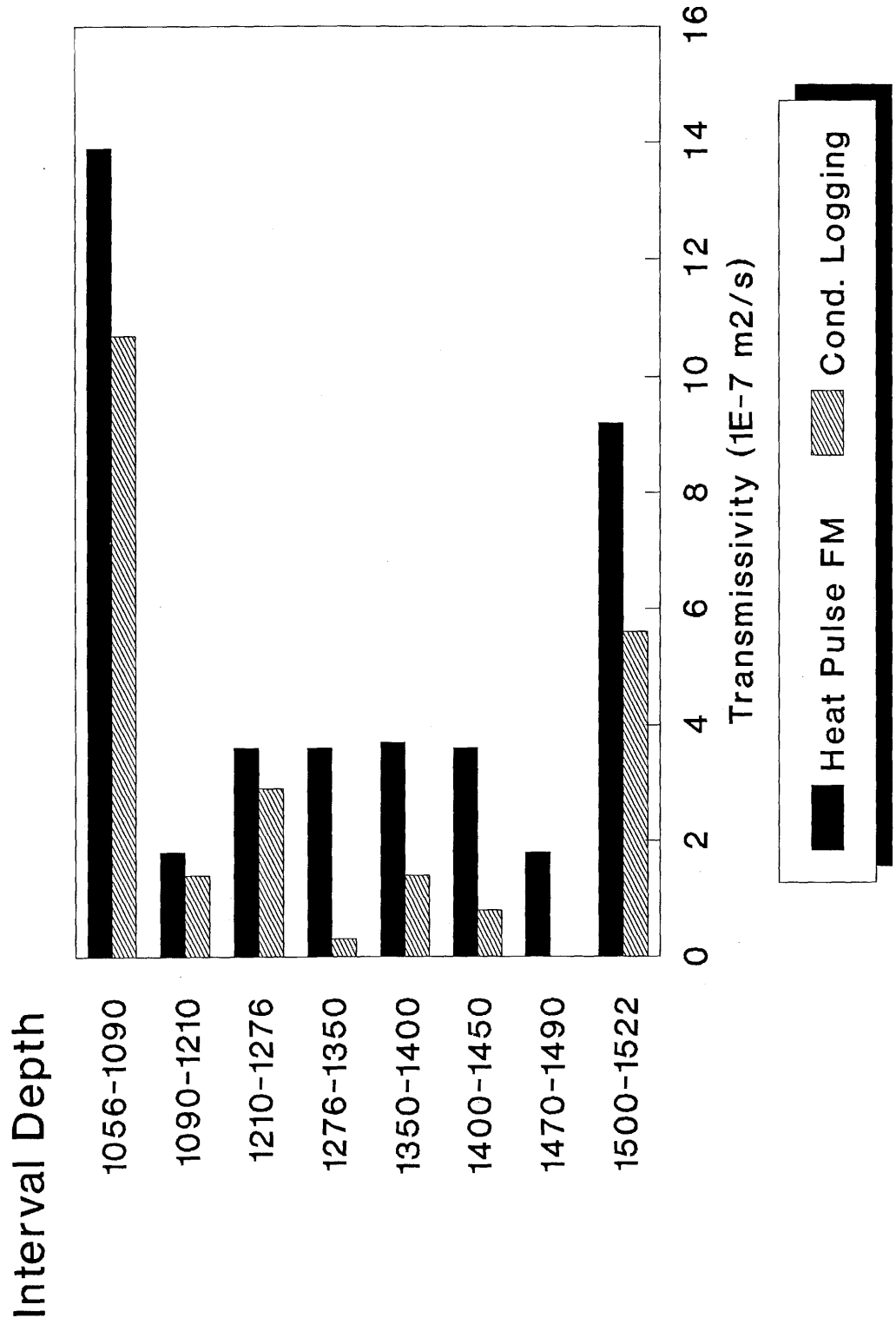

Figure 5.8: Comparison between Interval Transmissivity as Calculated from Electrical Conductivity Flow Rates and Heat Pulse Packer Flowmeter Measurements, Siblingen Borehole

6 HEAD AS CALCULATED FROM FLUID LOGGING FLOW RATES

When heads within intervals connected through an open borehole vary, vertical flow will occur within the borehole. Therefore, in some cases fluid logging measurements under static borehole conditions will measure internal borehole vertical flow rates. As discussed in detail in Section 4, this condition is known to exist in the Siblingen borehole.

The calculation of individual interval heads is theoretically possible through fluid logging methods. To estimate interval head requires interval flow rate (q_i) and borehole drawdown during two borehole conditions where at least one condition is a constant-rate withdrawal or injection test, and the difference in the borehole drawdown between events is much larger than the expected interval head variation (i.e., $D_{RW} >> D_{si}$). An ideal first run would occur under static conditions. In this case, the relative magnitude of each interval head, compared to the borehole head, is known after this first run. The flowmeter logs are analyzed with the code KPFLOW, which requires as input a flowmeter log taken under static conditions and a flowmeter log taken under constant-rate withdrawal/injection conditions. From this, KPFLOW calculates interval heads for the intervals measured. The method used is relatively simple and requires a series of important assumptions.

Because the elementary solutions used here to calculate heads are identical to the equations presented in Section 5, the assumptions are identical. That is, each individual inflow zone behaves independently of each other and responds to the borehole condition either fixed or natural. Therefore, here we assume zero hydraulic connection between zones, so that the zones are considered horizontal and the interbeds are considered to have zero hydraulic diffusivity. Explicitly stated, the assumptions are:

(1) flow is horizontal,
(2) the medium is infinite, isotropic, and homogeneous, and
(3) the well is fully penetrating.

6.1 KPFLOW Calculation of Interval Head

As discussed previously, KPFLOW estimates interval head in addition to an interval hydraulic conductivity. The theoretical basis behind KPFLOW calculations can be found in detail in REHFELDT et al. (1989). This section will briefly discuss the methodology and most important equations without presenting the derivation of the methodology.

KPFLOW requires flowmeter logs for the same interval during static conditions and during a constant-rate withdrawal or injection condition. From this, KPFLOW calculates interval flow rate under static conditions (q_{si}), interval flow rate under constant-rate conditions (q_{Ri}), and takes as input the drawdown of the well as a result constant-rate withdrawal or injection conditions (D_{RW}).

From these measurements, KPFLOW can calculate an interval hydraulic conductivity (K_i) as explained in Section 5.2.2.

Once the hydraulic conductivity K_i for each layer is calculated, then these and the static interval flow rates (q_{si}) can be used to solve for a natural drawdown for each layer which will be termed D_{si}. KPFLOW uses Equation 5.4 to calculate these head differences. The equation is changed to

$$D_{si} = q_{si} \ln(R_a/r_w) / 2\pi K_i b_i \qquad (6.1)$$

To calculate the interval head (H_i), one simply adds the drawdown for each layer (D_{si}) to the borehole stabilized head during static measurement (REHFELDT et al., 1989).

For the electrical conductivity logging, we have no good estimate of individual interval static flow rates q_{si} for all inflows. For this case, estimates of head were made in a similar procedure as presented above, except that the constant-rate withdrawal event (PIP-RW2) with the lowest flow rate was used as a static event. This means that the interval flow rates determined for PIP-RW2 were made equivalent to q_{si}, the interval flow rates determined for PIP-RW1 were made equivalent to q_{Ri}, and the quantity D_{RW} (Equation 5.4) was taken as the difference in stabilized drawdowns in the well between PIP-RW1 and PIP-RW2. With these three parameters unknown, Equation 5.2 (Cooper-Jacobs) is iterated for to solve for an intermediate interval transmissivity. In this case D_{RW} is equal to the stabilized drawdown during PIP-RW1 minus the stabilized drawdown during PIP-RW2. The term S_{Ri} in Equation 5.2 is replaced by (q_{Ri} - q_{si}). For each interval, a D_{si} was estimated using the intermediate transmissivity calculated above and the q_{si} value for each interval. Finally, each interval head is calculated by adding D_{si} to the stabilized borehole head during PP-RW2. This technique appears overly complicated, yet is identical in form to the technique KPFLOW uses on flowmeter measurements.

The calculation of interval head is based on the Cooper-Jacob approximation, and therefore the same assumptions hold as in Section 5.1. It is also important that fracture (layer) flow rates be significant in magnitude with respect to measurement uncertainty. Finally, the drawdown imposed during the constant-rate test should be significantly greater than the natural layer head variation.

6.2 Vertical Head Distribution as Calculated From Flowmeter Log Analysis

The results of the head calculations are only reported for the most complete and reliable flowmeter campaign FL4, which will later allow for further comparison with other methods. The results are presented in Table 6.1, where q_{si}, T_i, and D_{si} are, for each layer i, the radial flux under static conditions (Run 1), the transmissivity and the calculated head difference between the borehole and the layer during Run 1. These results are also graphically represented in Figures 6.1 and 6.2. The heat-pulse packer flowmeter recorded very little flow within the borehole from a depth of 1276 to 1522 m (corresponding to layers 20 through 27). From viewing Equation 6.1, it can be seen that, if q_{si} is close to zero, then D_{si} is close to zero and

the interval head (H_i) will simply be equal to the observed head in the borehole during the static flow rate measurement. This was the case for layers 20 through 27 and therefore the results from these sections are lumped together in Table 6.1

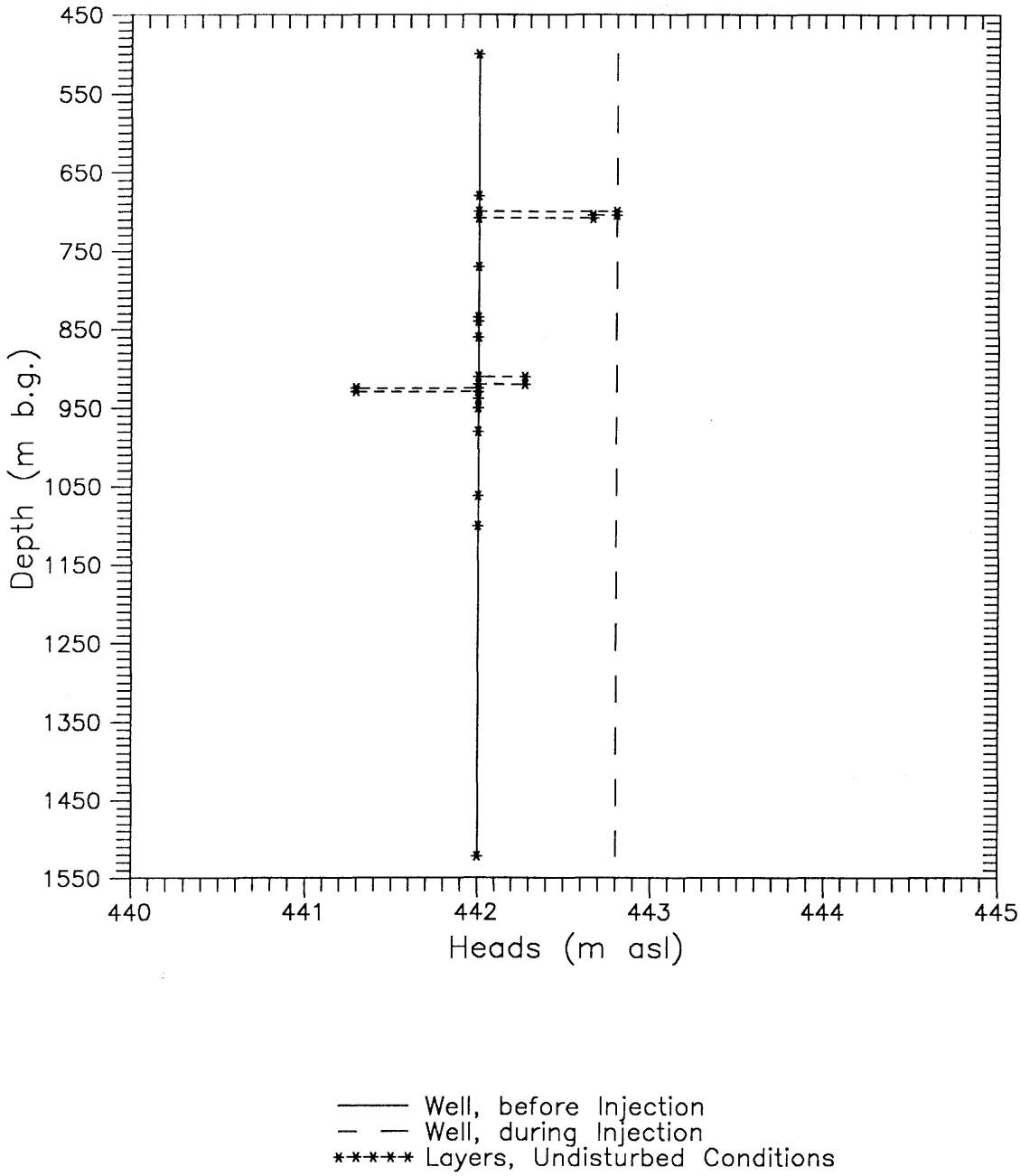

Figure 6.1: Layers Heads from Campaign 6-8.6.1989 (Runs 1-2) Heat Pulse Packer Flowmeter Interpretation, Siblingen Borehole

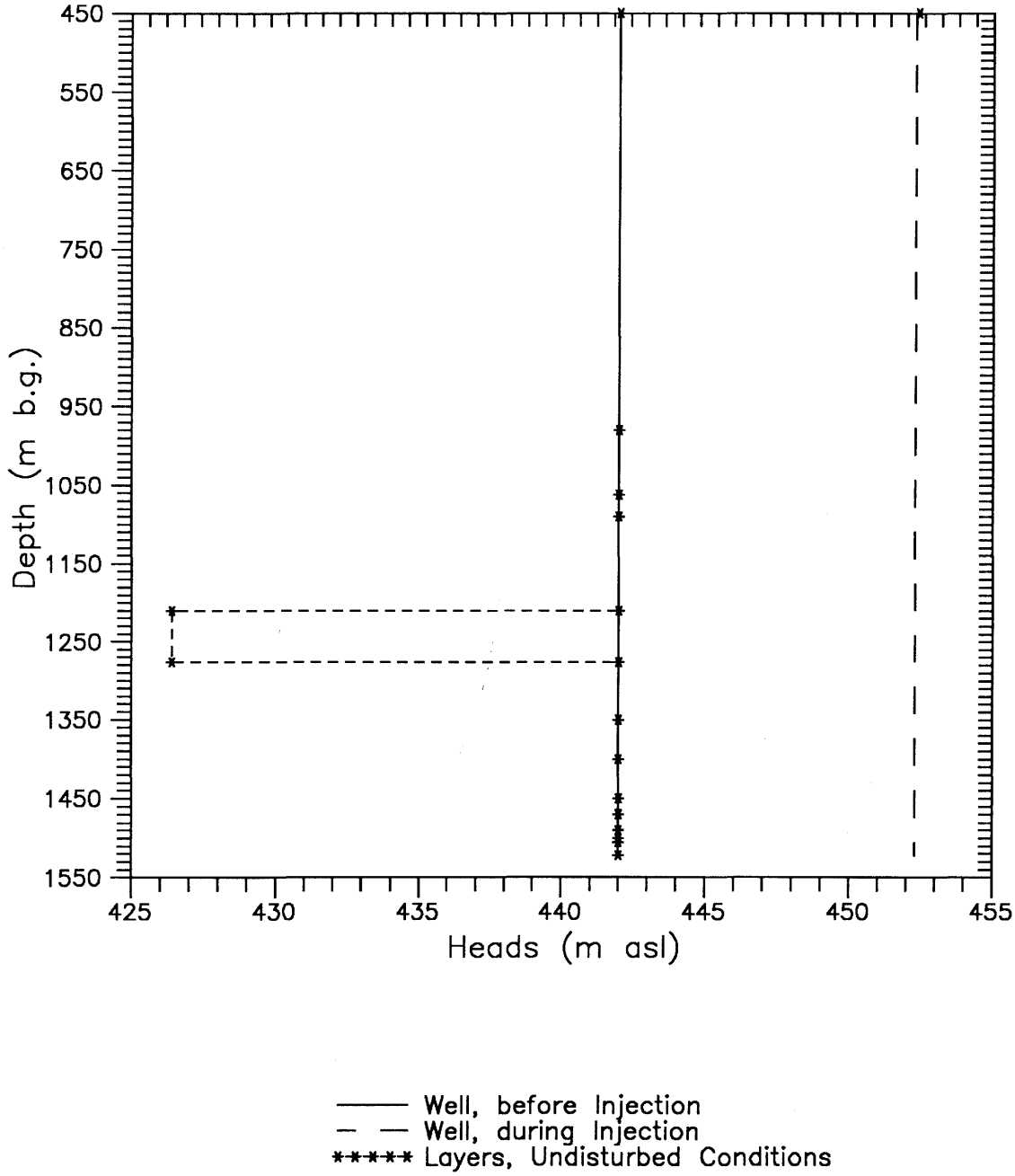

Figure 6.2: Layers Heads from Campaign 6-8.6.1989 (Runs 1-3a)
Heat Pulse Packer Flowmeter Interpretation,
Siblingen Borehole

Table 6.1: Heads Calculated from HPPF Logging

Interval Depth (m b.g.)	Layer Number	q_{si} (l/min)	T_i x 10^{-7} (m_2/s)	D_{si} (m)	Head (H_i) (m a.m.s.l.)
Logging Runs 1 and 2					
500 - 700	1.2	0.0	1520.0	0.0	442.0
700 - 704	3	0.6	186.6	0.8	442,8
704 - 708	4	0.6	186.6	0.6	442,7
708 - 925	5 to 9	0.0	70.7	0.0	442.0
910 - 920	10	0.1	89.7	0.3	442.3
920 - 925	11	0.0	122.2	0.0	442.0
925 - 929	12	-0.8	284.4	-0.7	441.3
929 -1522	13 to 18	0.0	28.6	0.0	442.0
					442.8
Logging Runs 1 and 3a					
1090 - 1210	18	0.0	142.1	0.0	442.0
1210 - 1276	19	-0.3	3.6	(-15.6)	(426.4)
1276 - 1522	20 to 27	0.0	21.8	0.0	442.0

note: HPPF measurements uncertainty is about 0.1 l/min

The variations of the flow rate during Run 1, without injecting, were generally low, more particularly in the bottom part of the borehole. This explains why most of the calculated heads are very close to the borehole head. However, layer 19 seems to have a particularly low head located about 16 m below all the other layers. We suggest that this value be considered with caution because of the uncertainties affecting the transmissivity value of this especially low permeability zone. Furthermore, according to the empirically estimated tool uncertainty (measurement plus calibration) documented in the USGS report (PAILLET et al., 1990), one could expect uncertainties on the calculated heads ranging between 0.1 to 10 m for transmissivities ranging from 1E-5 to 1E-7 m^2/s, respectively.

To summarize, one can say that a few inflow points between 450 and 1522 m b.g. were found to have static heads slightly (less than 1 meter) above the borehole head under static conditions (442.0 m asl). However two main zones were discovered which have a static head below the water level under static conditions.

They are situated at 925-929 m and at 1210-1276 m b.g., with heads of 0.7 and around 15.6 m, respectively, below the borehole water level without injection (442.0 m asl).

6.3 Vertical Head Distribution as Calculated From Electrical Conductivity Log Analysis

The most complete interval flow rate data from conductivity logging comes from the analyses of PIP-RW1 and PIP-RW2, where nine interval-specific flow rates were determined. Both events were constant-rate withdrawal events where the flow rates were 3.0 and 1.5 l/min, respectively. The drawdown which occurred in the borehole during PIP-RW1 was 21.3 m and the drawdown which occurred during PIP-RW2 was 14.4 m. To calculate interval heads for these nine intervals required the subtraction of the interval flow rate determined from PIP-RW2 from the flow rate determined from PIP-RW1. Using these individual flow rate differences and the difference in borehole drawdown between the two events, the Cooper-Jacob approximation was used to calculate intermediate interval transmissivities (T_i). Table 6.2 below shows the difference in the flow rates (q_{Ri}-q_{si}) between PIP-RW1 and PIP-RW2 with the estimated interval transmissivities T_i. As can be seen, in two instances (intervals 2 and 6), the flow rate determined from PIP-RW2 exceeded the flow rate determined for PIP-RW1. This represents error in the analysis and heads for these two intervals cannot be estimated with confidence. With the individual interval transmissivities estimated and the interval flow rates from the event PIP-RW2, the static interval drawdowns (D_{si}) are predicted for the seven appropriate intervals (see Table 6.2). These drawdowns (D_{si}) are then added to the stable drawdown head during pumping during event PIP-RW2 (430.3 m a.m.s.l.) to calculate interval heads (H_i).

Table 6.2: Heads Calculated from Electrical Conductivity Logging

Interval Depth (m b.g.)	Peak Number	$(q_{Ri} - q_{si})^{(1)}$ (l/min)	$T_i^{(2)}$ x 10^{-7} (m^2/s)	D_{si} (m)	Head (H_i) (m a.m.s.l.)
1065 - 1089	13, 12, 11	0.51	19.2	8.9	439
1158 - 1168	10	0.06	2.00	11.5	442
1219 - 1242	9, 8	0.16	5.63	3.5	434
1247 - 1257	7	-0.05	NA	NA	NA
1303 - 1313	6	0.30	10.9	0.5	431
1381 - 1391	5	0.12	4.15	5.8	436
1405 - 1415	4	0.12	4.15	.7	432
1415 - 1425	3	-0.01	NA	NA	NA
1500 - 1516	1, 2	0.29	10.6	8.6	439

(1) In this case, (q_{Ri} - q_{si}) is equal to the interval flow rate calculated for the PIP-RW1 logging minus the flow rate calculated for the PIP-RW2 event.

(2) T_i here represents an intermediate value of interval transmissivity and is not equal to the proposed interval transmissivities presented in Section 5.

Theoretically, using the flow estimates from the static flow event SF-1 and the flow estimates from PIP-RW1 would have resulted in more defendable, albeit fewer, interval head estimates. This was not done because a good estimate of the static head during SF-1 was not available.

The heads calculated above do not all fall within the range of heads presented in OSTROWSKI and KLOSKA (1990). There is no observable trend in the data. The results from this analysis should be considered only as estimates and should be viewed with care. The difference in natural heads within the borehole (up to 4 m) is very close to the head difference used to calculate these values (6.9 m). This is not desirable from a theoretical viewpoint and essentially renders these calculations very uncertain. These values will be compared to the results from hydraulic tests in Section 7 and to the head estimates derived from flowmeter methods in the following Section 6.4.

6.4 Comparison of Heads Calculated by Flowmeter and Conductivity Logging Methods

Table 6.3 summarizes the interval heads as calculated by fluid logging methods. Very little can be said in the comparison between heads determined by heat-pulse packer flowmeter results and conductivity results because the packer flowmeter gave uniform static heads for all intervals below 1090 m, with the exception of one.

Table 6.3: Comparison of Heads Calculated from Both Flowmeter and Electrical Conductivity Logging Methods

INTERVAL DEPTH (m b.g.)	PEAK NUMBER	INTERVAL HEAD (H_i) (m a.s.l.)	
		FLOWMETER HPPF JUNE 7/8 RUN 3 (BELOW 1090 m)	ELEC. COND. PIP-RW2 APRIL 23/25, 1989
1056 - 1090	13, 12, 11	442	439
1154 - 1164	10	442	442
1219 - 1256	7, 8, 9	426	434
1303 - 1313	6	442	431
1358 - 1392	5	442	436
1392 - 1426	3, 4	442	432
1471 - 1476	--	442	ND
1493 - 1499	--	442	ND
1426 - 1522	1, 2	442	439

It is perhaps better to discuss the results in light of requirements to get significant results.

For the heat-pulse packer flowmeter, it is obvious that the flow rates measured were not large enough to indicate significant head variation. PAILLET et al. (1990) report that these static measurements were correct to a value of ±0.1 l/min. This suggests that the static borehole flow rates are on the order of the measurement error and this will yield estimates which are highly uncertain and lacking in significance. With this stated, it is important to recognize that static heads are thought to be transient with time (see Section 4). The lack of substantial head differences in the lower portion of the borehole (1000 to 1522 m) could be the result of these intervals reacting equilibrium with the open borehole. The HPPF testing was performed approximately 6 weeks after the electrical conductivity logging.

Many problems occur when using the two constant-rate withdrawal events (PIP-RW1 and PIP-RW2) performed during electrical conductivity logging. The PIP-RW2 response to pumping has been shown to be affected by superimposition of the PIP-RW1 constant-rate withdrawal test which preceded it (see Section 5.3.5). This will clearly have a negative effect on the estimated heads. An additional problem exists in that the drawdown difference between events PIP-RW1 and PIP-RW2 (6.9 m) is not significantly greater than the variation in heads determined by packer tests for the section of borehole from 1000 to 1500 m. When this effect and the potential superimposition effect are combined, it can be seen that this data set should not be expected to yield accurate results. The effects of superimposition and potential errors in flow measurement would be expected to be greatest in the

lower transmissivity intervals.

In order to obtain more reliable head estimates from electrical conductivity logging, certain conditions should be insured. These are: (1) flow rates should be significant in magnitude relative to measurement error and static borehole flow rates, (2) events should be planned so that superposition effects are minimal, and (3) the head difference between the static borehole head and the borehole head during the constant-rate test should be significantly greater than expected head differences in the logged intervals.

The uncertainty of the head results presented in this report does not negate the utility of the methods, but rather underscores the importance of using data which meet the assumptions for the method.

7 COMPARISON OF FLUID LOGGING RESULTS WITH PACKER TEST RESULTS

In Sections 5 and 6, both transmissivity and head have been calculated for the various fluid logging methods employed in the Siblingen borehole. With the discussion of the results has been a comparison between the methods, where possible. In this chapter, the results presented from all fluid logging methods will be compared with independent estimates of transmissivity and head as determined through hydraulic packer testing. As described in Section 1 and summarized in Table 1.2, a complete hydraulic test campaign was performed for the Siblingen crystalline section and is fully described in OSTROWSKI and KLOSKA (1990).

7.1 Comparison Between Transmissivities Derived from Flowmeter Logging and Hydraulic Packer Tests

Table 7.1 compares the transmissivity results calculated from the packer flowmeter campaigns (December 1988, April 1989 and June 1989) with the results obtained from hydraulic packer testing. The calculations from the spinner flowmeter data were not reported in this table because the results obtained from this method are estimated to be too uncertain (higher detection limit, disturbances due to the tool movement, and suspicious estimated values of the vertical flux along the borehole). Furthermore, as the crystalline section 490 - 1060 m had been plugged and even cemented several times, only the most permeable zones having been studied by hydraulic packer tests and detected by the different flowmeter methods have been considered in our comparisons. These zones are the layers at around 680 to 700 m b.g. and 920 to 929 m b.g.

The inflow zones listed in Table 7.1 were determined from the electrical conductivity results in order to facilitate the comparison between the different intervals investigated during the various packer flowmeter campaigns and those studied during the hydraulic packer tests (OSTROWSKI and KLOSKA, 1990). The hydraulic test designation defines the hydraulic test corresponding to the inflow zone considered.

In the upper zone 490 to 1060 m b.g., the plugging of the transmissive feature at 680 - 700 m b.g. between the test CR10 and the campaign FL1 prevented a direct comparison. The plugging had reduced the transmissivity from around 2.2-2.8E-4 to 2E-5 m^2/s. However, the results derived from both campaigns FL1 and FL4 seem to indicate that the effectiveness of the plugging and cementation had degraded with time, since the transmissivity increased from 2E-5 to 1.5E-4 m^2/s between campaigns. In addition, plugging of the zone 920 - 929 m b.g. did not seem to be successful either, since the transmissivity determined during campaign FL4 was about the same as was obtained during CR17 (3.2-3.8E-5 m^2/s and 4.1E-5 m^2/s respectively).

Table 7.1: Comparison Between Transmissivities Derived from Flowmeter Logging and Hydraulic Tests

	Inflow Zone (m b.g.)	Hydraulic Test Interval (m b.g.)	Hydraulic Test Designation	Hydraulic Test Trans. $x10^{-7}$ (m^2/s)	TRANSMISSIVITY X 10^{-7} (m^2/s)						
					FL1	FL2		FL3		FL4	
					Flowmeter SPF Dec 20/21, 1988 Run 2	Flowmeter SF Jan 23/24, 1989 Run up	Flowmeter SF Jan 23/24, 1989 Run down	Flowmeter SPF Apr 15, 1989 Run 2a	Flowmeter SPF Apr 16, 1989 Run 2b	Flowmeter HPPF June 6/7, 1989 Run 3	Flowmeter HPPF June 6/8, 1989 Run 3
Upper zone partially plugged	680-700	678-713	CR10	2200-2800	201	432	337	793	938	1515	1405
	920-929	857-1018	CR17	320-380	---	1347	1467			406.6	
Lower zone open borehole	1065-1089	1056-1090	CR28	8.6-13.4	---	---	---	9.4	2.1	0.0	13.9
"	1158-1168	1154-1164	CR18; CR19	1.1-1.3	---	---	---	---	4.5	---	1.8
"	1158-1522	1154-1522	(CR20-CR28) + CR24	20	---	---	---	19,4	24.5	0.0	27.1
"	1219-1267	1222-1256	CR27	3.4-4.8	---	---	---	---	---	---	3.6
"											
"	1303-1313	---	---		---	---	---	---	---	---	3.6
"	1381-1391	1358-1392	CR26	2.8	---	---	---	---	---	---	3.7
"	1405-1425	1392-1426	CR25	0.65	---	---	---	---	---	---	3.6
"	---	1471-1476	CR21	0.04-0.06	---	---	---	---	---	---	1.8
"	1504	---	---	---	---	---	---	---	---	---	5.6
"	1511	---	---	---	---	---	---	---	---	---	3.6
"	1500-1516	1426-1522	CR24-(CR25 + CR26)	4.7	---	---	---	---	---	---	9.2

The comparison of the overall transmissivity value characterizing the entire section 490 to 1060 is not an easy task because of the plugging jobs and cementations that were performed several times within the borehole. However, campaign FL3 provides a transmissivity value around 7.9-9.4E-5 m^2/s, which is slightly below the values obtained by tests CR12 and CR17 (1.1-1.7E-4 m^2/s). Campaign FL4 generally provides higher values than campaign FL3. However, the second injection test (Run 3), which was performed under better conditions (flow rate, pressure change), provides a transmissivity of 1.4E-4 m^2/s. This value agrees well with the hydraulic packer tests. The flowmeter campaigns FL3 and FL4 clearly indicate that the plugging after performance of tests CR12 and CR17 was not successful.

The open-hole crystalline section, between 1060 and 1522 m b.g. was investigated by campaigns FL3 (partially) and FL4. During the FL3 campaign, the transmissivities derived from the spinner packer flowmeter appeared to be in a very good agreement with the results from the hydraulic packer test for the section 1154 - 1522 m b.g. (1.9 to 2.5E-6 m^2/s and 2.0 E-6 m^2/s, respectively). Two other zones (1070 - 1083 m b.g. and 1164 m b.g.) could be characterized within a reasonable range (less than a factor 4) for transmissivity values down to 1E-7 m^2/s. The discrepancy between both flowmeter results for zone 1070 - 1083 m b.g. is believed to be due to a disturbance (fluctuation of the injection rate or debris moving down the borehole) that affected the flowmeter measurement at the depth 1062 during Run 2b (see Section 2.5.3).

The comparison between the heat pulse packer flowmeter and the hydraulic packer tests in the open-hole section show excellent agreement between the methods, with variation nearly always less than a factor of two and in most cases much less.
The transmissivity values of the features at around 1410, 1420, and, more particularly, at 1475 m b.g. (6.5E-8 and 4-6E-9 m^2/s) seem to be at the lowest limit for being detected by the flowmeters under the injection conditions. The error factor is 5 for the zone 1410-1420, and more than an order of magnitude for the zone 1471-1475. It should be noted that this last zone was not detected by the electrical conductivity method.

7.2 Comparison Between Transmissivities Derived from Conductivity Logging and Hydraulic Packer Tests

Table 7.2 compares the transmissivity results calculated from conductivity logging with the results derived from traditional packer tests. The inflow interval listed in Table 7.2 2is derived from conductivity logs, and the hydraulic test interval is from OSTROWSKI and KLOSKA (1990). The hydraulic test designation defines what hydraulic test corresponds to the inflow interval as defined by conductivity logging. The transmissivities reported from fluid logging correspond to the transmissivities calculated by the Cooper-Jacobs formula (see Section 5). The agreement between the methods is excellent, with variation almost always less than a factor of two, and much less in most cases. For the two static flow events, the transmissivity for the lower portion of the borehole was estimated at between 1158 and 1522 m. The

hydraulic test transmissivity estimate was 2E-6 m^2/s, whereas events SF1 and SF2 gave a range between 1.6 and 3.2E-6 m^2/s. Event OH-RW1 estimated transmissivity for intervals 1056 to 1090 m b.g. and 1158 to 1522 m b.g. The estimate for 1050 to 1090 m b.g. grossly overestimates the transmissivity for this interval as determined by hydraulic tests. This could be due in part to the fact that some of the down borehole flow attributed to this interval came from above the interval. This overestimation could also result in incorrect use of Cooper-Jacobs, if constant head conditions prevailed in the borehole at this depth. The transmissivity estimate for the interval 1158 to 1522 m b.g. is much better and falls approximately between the two hydraulic packer test estimates for this interval. One hydraulic test transmissivity is based on large test intervals and the transmissivity in parentheses is based on short intervals.

The two PIP constant-rate logging events (PIP-RW1 and PIP-RW2) compare very closely with the hydraulic tests results. The conductivity logging identified one interval between 1303 and 1313 m (peak 6) which had not been characterized by the packer tests. The hydraulic tests measured two zones which had transmissivity which were not evaluated by the conductivity logging analysis. These are 1471 to 1476 m (Test CR21) and 1493 to 1499 (Test CR23). The omission from analysis of these two inflows could be because these relatively low flux inflows quickly get masked by the large inflow associated with peaks 1 and 2 (1500 - 1516 m). The conductivity results consistently overpredict the transmissivity of the lowest inflow intervals (peaks 1 and 2). This is interesting because the partial moment analysis was the most stable for this interval.

7.3 Selected Comparison Between Transmissivities Derived from Fluid Logging Methods and Hydraulic Packer Tests

To compare both flowmeter results and conductivity logging results to the packer test results required that all three methods be applied to the same interval of borehole. The conductivity logging was restricted to the borehole interval from 1000 to 1522 m. The best coverage of the total interval comes from both of the constant-rate withdrawal events performed with a PIP isolating the interval (Events PIP-RW1 and PIP-RW2). The best flowmeter coverage of this interval came from the heat-pulse packer flowmeter.

Table 7.2: Comparison Between Transmissivities Derived from Electrical Conductivity Logging and Hydraulic Tests

Peak No.	Inflow Interval (m b.g.)	Hydraulic Test Interval (m b.g.)	Hydraulic Test Designation	TRANSMISSIVITY X 10^{-7} (m^2/s)					
				Hydraulic Test	Event SF-1 Apr 15, 1989	Event SF-2 Apr 16, 1989	Event OH-RW1 Apr 16/17, 1989	Event PIP-RW1 Apr 18/19, 1989	Event PIP-RW2 Apr 23/25, 1989
11,12,13	1065-1089	1056-1090	CR28	8.6 - 13.4			81.2	12.8	10.7
1 - 10	1158-1522	1154-1522	(CR20-CR28) + CR24	10 (14.5)[1]	16 - 30	19 - 32	16.7	18.5	12.4
10	1158-1168	1154-1164	CR18/CR19	1.1 - 1.3				1.6	1.4
7,8,9	1219-1267	1222-1256	CR27	3.4 - 4.8				3.0	2.9
6	1303-1313	--	--					3.2	0.3
5	1381-1391	1358-1392	CR26	2.8				2.2	1.4
3,4	1405-1425	1392-1426	CR25	0.65				1.6	0.8
--	--	1471-1476	CR21	0.04 - 0.06					
--	--	1493-1499	CR23	1.0					
1,2	1500-1516	1426-1522	CR24-(CR25 + CR26)	4.7				6.9	5.6

( )[1] Sum transmissivity from tests CR18/CR19 + CR27 + CR26 + CR25 + CR21 + CR23 + CR24 - (CR25 + CR26).

Table 7.3 summarizes the transmissivities determined by these various methods in the interval from 1000 to 1522 m. A bar chart was produced with the information in this table to emphasize relative differences (Figure 7.1). The results from electrical conductivity logs depicted in Figure 7.1 are the transmissivities calculated for event PIP-RW2.

Again, it can be said that the overall agreement between the methods is good and the differences are nearly always within a factor of two. The exception is for the interval between 1471 and 1476 where the heat-pulse method overpredicts the packer test by a factor ranging from 30 to 45. The corresponding flow rate is near the resolution of the method and this could explain large errors. The discrepancy between conductivity logging and flowmeter logging is large for the interval 1303 to 1313. The electrical conductivity logging analyses presented in Section 3 suggest that the inflow is small in this interval, and therefore it is possible that there is a large error in its quantification using packer flowmeter data.

As can be seen on Figure 7.1, the electrical conductivity logging shows similar resolution for transmissivity at the lower ranges as does packer testing. The heat-pulse does not preserve the small scale transmissivity variation as well as packer testing and electrical conductivity. This is because the flow-rate resolution of the methods is probably best for the packer tests, then the conductivity logging, and finally the heat-pulse packer flowmeter. These conclusions are specific to the testing conditions at Siblingen. The resolution of these borehole logging methods is flow-rate dependent and not directly transmissivity dependent.

Table 7.3: Selected Comparison Between Transmissivities Derived from Heat Pulse, Electrical Conductivity, and Hydraulic Test Methods

Peak No.	Borehole Interval (m b.g.)	Hydraulic Test Designation	TRANSMISSIVITY X 10^{-7} (m^2/s)			
			Hydraulic Test	HPPF FL4 June 7/8, 1989 Run 3	T/LF PIP-RW1 Apr 18/19, 1989	T/LF PIP-RW2 Apr 23/25, 1989
11,12,13	1056-1090	CR28	8.6 - 13.4	13.9	12.8	10.7
10	1154-1164	CR18/CR19	1.1 - 1.3	1.8	1.6	1.4
7,8,9	1222-1256	CR27	3.4 - 4.8	3.6	3.0	2.9
6	1303-1313	--	ND	3.6	3.2	0.3
5	1358-1392	CR26	2.7	3.7	2.2	1.4
3,4	1392-1426	CR25	0.65	3.6	1.6	0.8
--	1471-1476	CR21	0.04-0.06	1.8	ND	ND
--	1493--	CR23	0.9	0.0	ND	ND
1,2	1499 1500-1516	CR24-(CR25+CR26)	4.7	11.0	6.9	5.6

HPPF = Heat-Pulse Flowmeter
T/LF = Electrical Conductivity/Temperature Logging

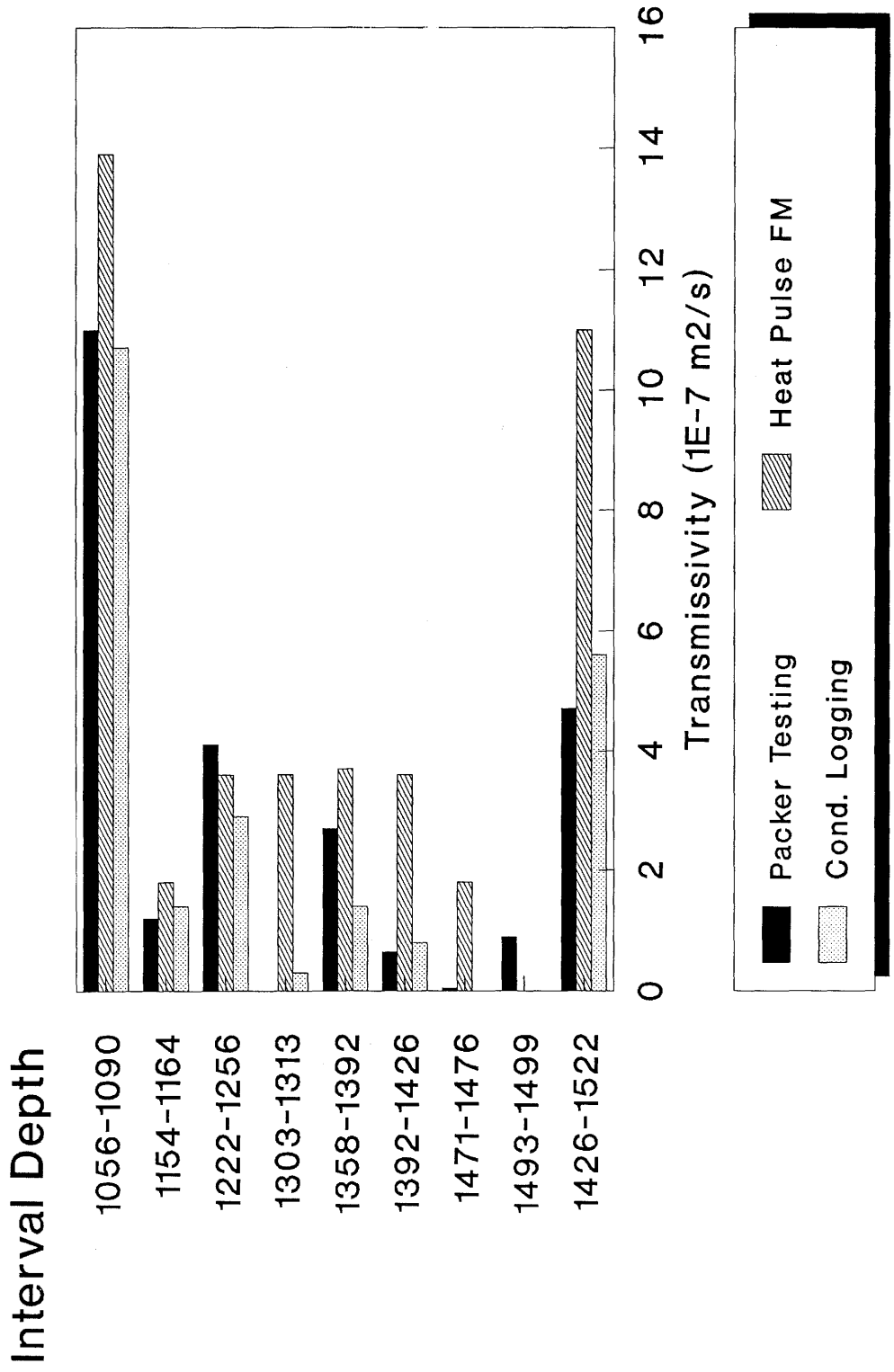

Figure 7.1: Comparison between Intervals Transmissivity as Calculated from Fluid Logging Methods and Hydraulic Packer Tests, Siblingen Borehole

7.4 Comparison Between Heads Derived from Flowmeter Logging and Hydraulic Packer Tests

The comparison between heads determined from flowmeter logs and hydraulic packer tests is presented here, using the two flowmeter campaigns FL3 and FL4 which have investigated the entire borehole from 490 to 1522 m b.g. According to the comparison of the transmissivities presented in Section 7.1, only two permeable layers, assumed to be imperfectly plugged, were considered for the comparison of heads in the upper part of the borehole. In the open borehole section of the well, this comparison could be done on eight individual flowing zones, primarily characterized by the heat pulse packer flowmeter. The comparison between these heads and the heads determined by the hydraulic packer tests (from OSTROWSKI and KLOSKA, 1990) is reported in Table 7.4.

Table 7.4: Comparison Between Heads Calculated from Selected Flowmeter Logs and by Hydraulic Packer Tests

INFLOW ZONE	BOREHOLE INTERVAL (m b.g.)	HYDRAULIC HEAD (m a.s.l.)		
		Hydraulic Test	Flowmeter FL1 (SPF)	Flowmeter FL4 (HPPF)
680 - 700	678 - 713	441	444	442
920 - 929	857 - 1018	442	---	441
1065 - 1089	1056 - 1090	440	---	443
1158 - 1168	1154 - 1164	439	---	442
1219 - 1267	1222 - 1256	437	---	426
1381 - 1391	1358 - 1392	436	---	442
1405 - 1425	1392 - 1426	436	---	442
--	1471 - 1476	438	---	442
--	1493 - 1499	436	---	442
1500 - 1516	1500 - 1516	---	---	442

From this table, one can see that the flowmeter logs did not seem to be very sensitive to the trend identified by the hydraulic packer tests. Actually no vertical flow was detected below 1276 m b.g., which leads to the conclusion that all the layers below this depth were hydraulically in equilibrium with the water level in the well. In fact, the only layer showing a significantly lower head with the flowmeter method is located at 1210-1276 m b.g. As described in Section 6.2, this value of 426 m a.s.l. is probably affected by a fairly large uncertainty because of the very low transmissivity of this layer.

However, one should remember that the borehole had been left open for at least one month between the hydraulic packer tests and the heat pulse flowmeter campaign. During this time, the borehole head did not vary significantly, which means that the layers being characterized by a relatively low head, according to the hydraulic packer tests, had been influenced over this period by the higher pressure occurring in the borehole. In conclusion, we think that the real head characterizing the layers when conducting the heat pulse flowmeter logs should probably be situated between the values reported by the hydraulic packer tests and the value of 442 m a.s.l. reported for most of the layers characterized by the heat pulse flowmeter method. Because of the high uncertainty associated with measurement of the low borehole flow rates under static conditions, it cannot be concluded whether the heads determined by flowmeter were dominated by error or truly represent near equilibrium conditions.

7.5 Comparison Between Heads Derived from Conductivity Logging and Hydraulic Packer Tests

As described in Section 6 (Table 6.2), heads could be estimated by the use of results from conductivity logging events PIP-RW1 and PIP-RW2. The comparison between these heads and the heads determined by hydraulic packer tests (from OSTROWSKI and KLOSKA, 1990) can be found in Table 7.5. From review of Table 7.5, one can see that the conductivity logging heads show a similar trend as the heads determined from hydraulic tests, that is decreasing magnitude with depth. The most obvious exception to this trend is the head calculated for the lowermost interval.

Table 7.5: Comparison Between Heads Calculated from Electrical Conductivity Logging and by Hydraulic Packer Tests

PEAK NUMBER	BOREHOLE INTERVAL (m b.g.)	HYDRAULIC HEAD (m a.s.l.)		
		Hydraulic Test Designation	Hydraulic Test	Electrical Conductivity
11, 12, 13	1056 - 1090	CR28	440	439
10	1154 - 1164	CR18/CR19	439	442
7, 8, 9	1222 - 1256	CR27	437	434
6	1303 - 1313	--	---	431
5	1358 - 1392	CR26	436	436
3, 4	1392 - 1426	CR25	436	432
--	1471 - 1476	CR21	438	---
--	1493 - 1499	CR23	436	---
1, 2	1500 - 1516	--	---	439

The heads determined by electrical conductivity logging generally are not in good agreement with heads determined by hydraulic tests. This is not surprising when we have shown that the results are potentially affected by the fact that some intervals did not fully recover from PIP-RW1 pumping before PIP-RW2 began. These effects are potentially responsible for the two anomalously low heads determined for intervals 1303 to 1313 m (peak 6) and 1392 to 1426 m (peaks 3 and 4). One would expect the effect upon interval static pressure to be strongest on the low transmissive units. In fact these two anomalous head values correspond to the two intervals which have transmissivities lower than 1E-7 m^2/s as determined by the analysis of PIP-RW2.

7.6 Comparison Between Heads Derived from Fluid Logging and Hydraulic Packer Tests

Finally, we compare how the heat-pulse packer flowmeter heads and the electrical conductivity heads compare with the heads determined by hydraulic packer tests. Because only one set of heads is presented for both types of fluid logging, the comparison between the methods and the comparison of the methods to hydraulic packer tests has been fully described. This section will only present the methods together as a summary, and since discussion would be repetitious, it will be limited.

Table 7.6 combines the heads determined from fluid logging and hydraulic packer tests. An easier method to see the differences in the heads is through a simple x-y plot, and this is done in Figure 7.2. On Figure 7.2, the head value is plotted at the interval midpoint.

Table 7.6: Comparison Between Heads Calculated from Fluid Logging and by Hydraulic Packer Tests

Peak Number	Borehole Interval (m b.g.)	HYDRAULIC HEAD (m a.s.l.)		
		Hydraulic Test	Flowmeter HPPF	Electrical Conductivity
11, 12, 13	1056 - 1090	440	442	439
10	1154 - 1164	439	442	442
7, 8, 9	1222 - 1256	437	426	434
6	1303 - 1313	---	442	431
5	1358 - 1392	436	442	436
3, 4	1392 - 1426	436	442	432
--	1471 - 1476	438	442	---
--	1493 - 1499	436	442	---
1, 2	1500 - 1516	---	442	439

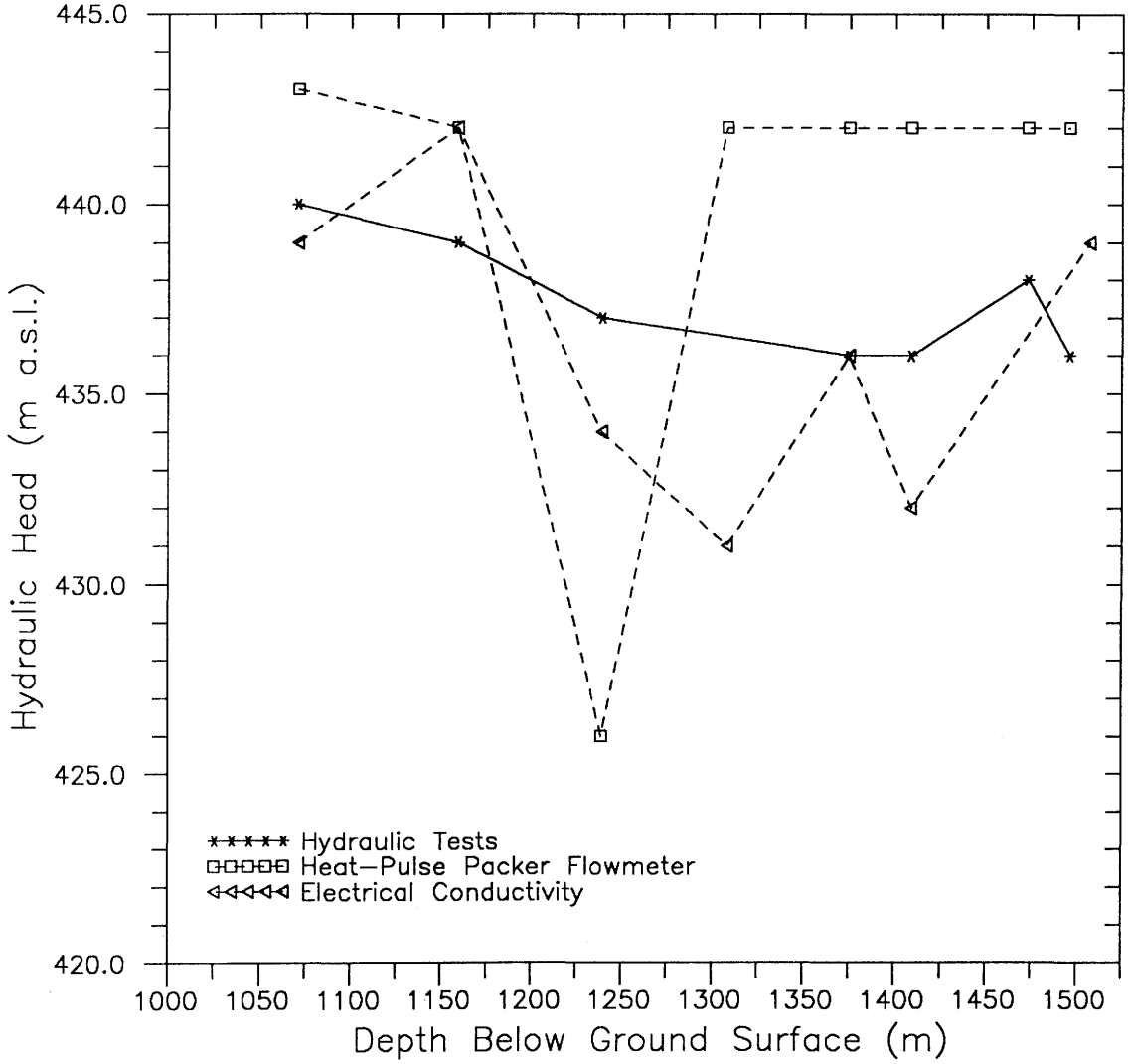

Figure 7.2: Comparison between Intervals Head as Calculated from Fluid Logging Methods and Hydraulic Packer Tests, Siblingen Borehole

Many problems arise when trying to compare the heads derived from the various methods. It has already been pointed out that the fluid logging results used to calculate heads are not ideal for such purposes and could contribute significant errors to such calculations. In addition, the validation of interval heads determined by fluid logging by their agreement to hydraulic test determined heads is problematic and should not be considered as a conclusive check.

Even for hydraulic tests, determination of interval head is not trivial and is sensitive to borehole conditions. For example, as discussed in Section 4, a major borehole flow cell exists where water enters the borehole between the depths 685 and 692 m, and exists between 920 and 930 m. However, the hydraulic head for the interval between 920 and 930 m (CR16) was estimated to be one meter higher than the head between 685 and 692 m (CR10). This represents an example of differential head transience. The concept of interval head transience undermines the concept of validation through comparison. In conclusion, it can be said that the fluid logging determined interval heads generally fall within the range of heads available from hydraulic tests. If one compares the heads determined by electrical conductivity logging to those determined by packer tests, one can say that both data sets suggest that the heads above 1200 m b.g. are larger than those measured below 1200 m b.g.

8 CONCLUSIONS

The open borehole section of crystalline rocks in the Siblingen borehole have been successfully characterized by various fluid logging methods. Characterization has included the determination of interval transmissivity, interval head, and for the section of borehole below 1000 m b.g., isolation of discrete inflow zones.

The fluid logging methods employed in the Siblingen borehole include the spinner flowmeter, the spinner packer flowmeter, the heat-pulse packer flowmeter, and electrical conductivity logging. Analysis of the flowmeter logs was performed with the code KPFLOW, and analysis of the electrical conductivity logs was performed through a combination of the codes MOMENT and BORE. From the analysis of these various fluid logging methods, the following conclusions can be drawn.

- The discrete localization of significant flowing features could be determined by electrical conductivity logging with an accuracy of ±1 m.
- The vertical transmissivity distribution determined by flowmeter and electrical conductivity logging methods were internally consistent for values of transmissivity in the lower section of the borehole (1000 to 1522 m b.g.). The range of transmissivity detected in this section was between 0.3 and 11E-7 m^2/s determined for intervals from 10 to 34 m in length.
- Both flowmeter and electrical conductivity logging methods reproduce transmissivity as determined from the hydraulic packer tests within a factor of 2 in most cases. This is below the uncertainty range commonly accepted for standard hydraulic packer tests in this transmissivity range.
- The determination of interval heads provided results which did not quantitatively reproduce heads as determined by hydraulic packer tests. The electrical conductivity logging did preserve the qualitative head trend produced by hydraulic packer tests. The differences in the calculated heads is not surprising when one considers that the vertical static flow rates within the borehole changed with time. This implies that the interval heads within the borehole changed with time. This makes comparison of heads measured at different times tenuous.
- The application of the method of moments (LOEW et al., 1990) to the analysis of electrical conductivity logs has proven this method to be very powerful.

Table 8.1 is a summary of interval transmissivities as calculated by fluid logging methods. Summarized with the interval depth and transmissivity are the type of fluid logging method used and the fluid logging event. Characterization of the borehole to a depth of 1000 m was done with flowmeter methods, and the lower borehole section 1000 to 1522 m.b.g. was characterized by flowmeter and electrical conductivity methods. The transmissivity values listed in Table 8.1 represent best estimates. All intervals of the borehole not represented in Table 8.1 are considered to have transmissivities less than the resolution ($T \leq$ 1E-9 m^2/s) of the fluid logging methods.

Table 8.1: Summary of Interval Transmissivity as Determined through Fluid Logging Methods, Siblingen Borehole

Interval Depth (m a.s.l.)	Fluid Logging Method	Fluid Logging Events	Interval Transmissivity ($m^2/s \times 10^{-7}$)
500 - 680	HPPF	FL4	5.0
680 - 700	HPPF	FL4	1515.0
700 - 704	HPPF	FL4	186.6
704 - 708	HPPF	FL4	186.6
775 - 825	SPF	FL1	71.3
835 - 840	HPPF	FL4	353.3
840 - 850	SPF	FL1	72.4
910 - 920	HPPF	FL4	89.7
920 - 925	HPPF	FL4	122.2
925 - 929	HPPF	FL4	284.4
938 - 950	HPPF	FL4	28.6
1065 - 1089	T/LF	PIP-RW2	10.7
1158 - 1168	T/LF	PIP-RW2	1.4
1219 - 1242	T/LF	PIP-RW2	1.1
1247 - 1257	T/LF	PIP-RW2	1.8
1303 - 1313	T/LF	PIP-RW2	0.3
1381 - 1391	T/LF	PIP-RW2	1.4
1405 - 1415	T/LF	PIP-RW2	0.4
1415 - 1425	T/LF	PIP-RW2	0.4
1470 - 1490	HPPF	FL4	1.75
1500 - 1516	T/LF	PIP-RW2	5.6

HPPF = Heat-Pulse Flowmeter
SPF = Spinner Packer Flowmeter
T/LF = Electrical Conductivity/Temperature Logging

Interval heads were apparently transient during the drilling and testing of the Siblingen borehole. In addition, significant transience with respect to the inflowing fluid electrolyte concentration during conductivity logging occurred as a result of losses of the flushing fluid to the transmissive intervals prior to logging. With all these non-ideal disturbances, it can still be concluded that fluid logging performed well in the quantification of interval transmissivity and, to a lesser degree, interval heads. This is an important and promising result, as we know that all field tests are initially plagued with non-ideal conditions.

In summary, fluid logging methods do not replace the standard hydraulic packer tests, but do allow for economization and optimization of their use. The use of electrical conductivity logging also allows for the isolation of discrete inflow zones which contribute to interval transmissivity.

9 ACKNOWLEDGEMENTS

The authors would like to express their appreciation for the sustaining support and constructive technical review supplied by our colleagues at NAGRA, Stratis Vomvoris, Peter Blümling, and François Paquier. We would also like to acknowledge our appreciation for the helpful comments supplied by C.F. Tsang of Lawrence Berkeley Laboratories regarding the analysis of the electrical conductivity logs.

10 REFERENCES

BELANGER, D.W., FREEZE, G.A., LOLCAMA, J.L., and PICKENS, J.F., 1989: Interpretation of Hydraulic Testing in Crystalline Rock at the Leuggern Borehole. NAGRA Technischer Bericht, 87-19, Nationale Genossenschaft für die Lagerung radioaktiver Abfälle, Baden, Switzerland.

COOPER, H.H. JR., and JACOB, C.E., 1946: A Generalized Graphical Method for Evaluating Formation Constants and Summarizing Well-field History. *AGU Transactions*, Vol. 27, No. 4, pp 526-534.

FISCHER, H.B., LIST, E.G., KOH, R.C., IMGERGER, J., AND BROOKS, N.H., 1979: Mixing in Inland and Coastal Waters, Academic Press, Inc., New York.

GEOTEST/GEMAG, 1989. SIB: Fluid-Logging Feld- und Kalibrierbericht. NAGRA Interner Bericht, Nationale Genossenschaft für die Lagerung radioaktiver Abfälle, Baden, Switzerland.

HALE, F.V. and TSANG, C.F., 1988: A Code to Compute Borehole Fluid Conductivity Profiles with Multiple Feed Points. NAGRA Technischer Bericht 88-21, Nationale Genossenschaft für die Lagerung radioaktiver Abfälle, Baden, Switzerland.

HUFSCHMIED, P., 1983: Die Ermittlung der Durchlässigkeit von Lockergesteins-Grundwasserleitern, eine vergleichende Untersuchung verschiedener Feldmethoden. Dissertation 7397, ETH, Zurich, Switzerland.

JAVANDEL, I. and WITHERSPOON, P.A., 1969: A Method of Analyzing Transient Flow in Multilayered Aquifers. *Water Resources Research*, Vol 5, pp 856-869.

LOEW, S., TSANG, C.F., HALE, F., and HUFSCHMIED, P., 1990: The Application of Moment Methods to the Analysis of Fluid Electrical Conductivity Logs in Boreholes, Report NDC-8 of the NAGRA-DOE Cooperative Project. NAGRA Technischer Bericht, 90-42, Nationale Genossenschaft für die Lagerung radioaktiver Abfälle, Baden, Switzerland

MICHALSKI, A., and KLEPP, G.M., 1990: Characterization of Transmissive Fractures by Simple Tracing of In-Well Flow. *Ground Water*, Vol. 28, No.2, pp. 191-198.

MOLZ, F.J., MORIN, R.H., HESS, A.E., MELVILLE, J.G., and GUEVEN, O., 1989: The Impeller Meter for Measuring Aquifer Permeability Variations: Evaluation and Comparison with Other Tests. *Water Resources Research,* Vol. 25, No. 7, pp. 1677-1683.

OSTROWSKI, L.P., and KLOSKA, M.B., 1990: Final Interpretation of Hydraulic Testing at the Siblingen Borehole. NAGRA Technischer Bericht 89-10, Nationale Genossenschaft für die Lagerung radioaktiver Abfälle, Baden, Switzerland.

PAILLET, F.L., HESS, A.E., CHENG, C.H., and HARDIN, E.L., 1987: Characterization of Fracture Permeability with High-Resolution Vertical Flow Measurements during Borehole Pumping. *Ground Water,* Vol. 25, No. 1, pp. 28-40.

PAILLET, F.L., HESS, A.E., and MORIN, R.H., 1990: Estimation of the Relative Permeability Distribution in Fractured Granitic Rocks by Means of Vertical Flow Measurements in the Siblingen Borehole, Switzerland. U.S. Geological Survey, Water Resources Investigations 90-4034, 26 p.

REHFELDT, K.R., HUFSCHMIED, P., GELHAR, L.W., and SCHAEFER, M.E., 1989: The Borehole Flowmeter Technique for Measuring Hydraulic Conductivity Variability. Prepared for the Electrical Power Research Institute (EPRI), Palo Alto, California.

SATTEL, G., and BLUEMLING, P., 1989: Siblingen: Bohrlochgeophysik, Zusammenfassung Rohdaten. NAGRA Interner Bericht, National Genossenschaft für die Lagerung radioaktiver Abfälle, Baden, Switzerland.

STEIGER, H., and STEFFEN, P., 1989: Siblingen: Sampling und Bohrgasmessdienst Tracerservice, Spülungsüberwachung und Bohrstellen-Hydrochemie. NAGRA Interner Bericht, Nationale Genossenschaft für die Lagerung radioaktiver Abfälle, Baden, Switzerland.

THOMPSON, B.M., 1989: KPFLOW - A Program to Analyze Borehole Flowmeter Data, Version 2.0. NAGRA Interner Bericht, Nationale Genossenschaft für die Lagerung radioaktiver Abfälle, Baden, Switzerland.

TSANG, C.F. and HUFSCHMIED, P., 1988: A Borehole Fluid Conductivity Logging Method for the Determination of Fracture Inflow Parameter, NAGRA Technischer Bericht 88-13, Nationale Genossenschaft für die Lagerung radioaktiver Abfälle, Baden, Switzerland.

TSANG, C.F., HUFSCHMIED, P., and HALE, F.V., 1990: Determination of Fracture Outflow Parameters with a Borehole Fluid Conductivity Logging Method. *Water Resources Research,* Vol. 26, No. 4, pp. 561-578.

VOMVORIS, S., MCCORD, J., MCNEISH, J., and LAVANCHY, J.M., 1989: Long-Term Monitoring Investigation Program in the Siblingen Borehole. First Interpretation of Data Collected in the Period June to October 1989. NAGRA Interner Bericht, Nationale Genossenschaft für die Lagerung radioaktiver Abfälle, Baden, Switzerland.

11 NOMENCLATURE

C = concentration (kg/m^3)

C_i = concentration of inflowing fluid from an individual permeable layer i (kg/m^3)

C_{AB} = average inflowing concentration inflowing over the interval confined between depths A and B (kg/m^3)

C_0 = initial concentration in the interval of interest (kg/m^3)

H_i = equivalent fresh-water head of an individual permeable layer/ interval i (m a.s.l.)

K = hydraulic conductivity (m/s)

K_i = hydraulic conductivity of an individual permeable layer/interval i (m/s)

M_n = classical moment of the n^{th} order, dimensions dependent upon order

M_{0+}, M_{0-} = zero classical moment evaluated upstream and downstream, respectively, of an inflow at x_i (kg/m^2)

M_{1t} = time derivation of the first classical moment ($kg/m \cdot s$)

q_i = volumetric flow rate from an individual permeable layer i (m^3/s)

q_{Ri} = flow rate from layer i in response to drawdown D_{Ri} (m^3/s)

q_{si} = flow rate from layer i in response to drawdown D_{si} (m^3/s)

Q_A, Q_B = volumetric flow rate measured at boundary A and boundary B, respectively (m^3/s)

Q_{RW} = Constant rate volumetric flow rate

Q_w = the total injection or production rate for a well (m^3/s)

r_w = radius of the well in the interval of interest (m)

R = radius where pressure is undisturbed during a constant-rate pumping event (m)

R_a = radius of influence for a multi-step pumping test (m)

D_{Ri} = head difference between transmissive interval i and the prepumping average borehole head during a constant rate withdrawal event (m)

D_{si} = head difference between transmissive interval i and the average borehole head under open borehole, no injection no production (static) conditions (m)

D_{RW} = Drawdown in a borehole during a constant-rate event

D_w = drawdown in a well (m)

S_i = storage coefficient for an individual permeable layer/interval i

t_e = effective pumping time for a multi-step pumping test (sec)

T = transmissivity (m^2/s)

T_i = transmissivity of an individual permeable layer/interval i (m^2/s)

V_+, V_- = well-bore velocity upstream and downstream of an inflow at x_i (m/s)

x_i = location as defined by a depth in a borehole (m)

α = proportionality constant between flow rate versus transmissivity of an interval at steady-state conditions (m)

σ = electrical conductivity ($\mu s/cm$)